FRAGILITY BASED SEISMIC VULNERABILITY ASSESSMENT OF
ORDINARY HIGHWAY BRIDGES IN TURKEY

A THESIS SUBMITTED TO
THE GRADUATE SCHOOL OF NATURAL AND APPLIED SCIENCES
OF
MIDDLE EAST TECHNICAL UNIVERSITY

BY

ÖZGÜR AVŞAR

IN PARTIAL FULFILLMENT OF THE REQUIREMENTS
FOR
THE DEGREE OF DOCTOR OF PHILOSOPHY
IN
CIVIL ENGINEERING

JUNE 2009

Approval of the thesis:

**FRAGILITY BASED SEISMIC VULNERABILITY ASSESSMENT OF
ORDINARY HIGHWAY BRIDGES IN TURKEY**

submitted by **ÖZGÜR AVŞAR** in partial fulfillment of the requirements for the
degree of **Doctor of Philosophy in Civil Engineering Department, Middle East
Technical University** by,

Prof. Dr. Canan Özgen   _____
Dean, Graduate School of **Natural and Applied Sciences**

Prof. Dr. Güney Özcebe   _____
Head of Department, **Civil Engineering**

Assoc. Prof. Dr. Ahmet Yakut   _____
Supervisor, **Civil Engineering Dept., METU**

Asst. Prof. Dr. Alp Caner   _____
Co-Supervisor, **Civil Engineering Dept., METU**

Examining Committee Members:

Prof. Dr. Polat Gülkan   _____
Civil Engineering Dept., METU

Assoc. Prof. Dr. Ahmet Yakut   _____
Civil Engineering Dept., METU

Prof. Dr. Murat Dicleli   _____
Department of Engineering Sciences, METU

Assoc. Prof. Dr. M. Altuğ Erberik   _____
Civil Engineering Dept., METU

Dr. Sabahattin Aykaç   _____
Civil Engineering Dept., Gazi University

                                          Date: _____

I hereby declare that all information in this document has been obtained and presented in accordance with academic rules and ethical conduct. I also declare that, as required by these rules and conduct, I have fully cited and referenced all material and results that are not original to this work.

Name, Last Name: Özgür Avşar

Signature   :

ABSTRACT

FRAGILITY BASED SEISMIC VULNERABILITY ASSESSMENT OF ORDINARY HIGHWAY BRIDGES IN TURKEY

Avşar, Özgür

Ph.D., Department of Civil Engineering

Supervisor   : Assoc. Prof. Dr. Ahmet Yakut

Co-Supervisor: Asst. Prof. Dr. Alp Caner

June 2009, 236 pages

Recent devastating earthquakes revealed that bridges are one of the most vulnerable components of the transportation systems. These seismic events have emphasized the need to mitigate the risk resulting from the failure of the bridges. Depending on the seismicity of the bridge local site, seismic vulnerability assessment of the bridges can be done based on the fragility curves. These curves are conditional probability functions which give the probability of a bridge attaining or exceeding a particular damage level for an earthquake of a given intensity level. In this dissertation, analytical fragility curves are developed for the ordinary highway bridges in Turkey constructed after the 1990s to be used in the assessment

of their seismic vulnerability. Bridges are first grouped into certain major bridge classes based on their structural attributes and sample bridges are generated to account for the structural variability. Nonlinear response history analyses are conducted for each bridge sample with their detailed 3-D analytical models under different earthquake ground motions having varying seismic intensities. Several engineering demand parameters are employed in the determination of seismic response of the bridge components as well as defining damage limit states in terms of member capacities. Fragility curves are obtained from the probability of exceeding each specified damage limit state for each major bridge class. Skew and single-column bent bridges are found to be the most vulnerable ones in comparison with the other bridge classes. Developed fragility curves can be implemented in the seismic risk assessment packages for mitigation purposes.

ÖZ

TÜRKİYE'DEKİ TİPİK KARAYOLU KÖPRÜLERİNİN KIRILGANLIK EĞRİLERİ İLE SİSMİK ZARAR GÖREBİLİRLİĞİNİN BELİRLENMESİ

Avşar, Özgür

Doktora, İnşaat Mühendisliği Bölümü

Tez Yöneticisi   : Doç. Dr. Ahmet Yakut

Ortak Tez Yöneticisi: Y. Doç. Dr. Alp Caner

Haziran 2009, 236 sayfa

Geçmişte büyük kayıp ve zarara neden olmuş depremler karayolu ağının zarar görebilirliği en fazla olan parçasının köprüler olduğunu göstermiştir ve dolayısıyla köprü hasarından dolayı meydana gelebilecek riskin azaltılmasının gerekliliğini gün yüzüne çıkarmıştır. Köprünün bulunduğu yerin sismik tehlikesine bağlı olarak, köprü zarar görebilirliği kırılganlık eğrileri ile belirlenebilir. Bu ihtimal eğrileri, belirli bir deprem şiddet seviyesinde köprünün önceden belirlenmiş hasar seviyesine ulaşma ya da aşılma olasılığını verir. Bu tez çalışmasında, 90'lı yıllardan sonra Türkiye'de yapılmış tipik karayolu köprülerinin zarar görebilirliğinin belirlenmesinde kullanılacak kırılgan eğrileri analitik yöntemle elde

edilmiştir. Öncelikle yapısal özelliklerine göre sınıflandırma yapılarak köprü tipleri belirlenmiş ve daha sonra yapısal çeşitliliği hesaba katabilmek için köprü örnekleri oluşturulmuştur. Her bir köprünün kapsamlı üç boyutlu analitik modeli oluşturulmuş ve değişik sismik şiddetteki deprem yer hareketleri altında zaman tanım alanında doğrusal olmayan analizleri yapılmıştır. Köprü bileşenlerinin sismik davranışlarının belirlenmesinde ve eleman kapasiteleri kullanılarak tayin edilen hasar sınır değerlerinin hesaplanmasında bir takım yapısal istem parametreleri kullanılmıştır. Her bir köprü tipi için, belirlenen hasar sınır durumlarının aşılma olasılığı hesaplanarak kırılganlık eğrileri elde edilmiştir. Diğer köprü tipleriyle kıyaslandığında, verev ve tek kolonlu köprülerin zarar görebilirliğinin daha fazla olduğu görülmüştür. Elde edilen kırılganlık eğrileri zarar azaltma amaçlı sismik risk değerlendirme paket uygulamarında kullanılabilirler.

Anahtar Kelimeler: Karayolu Köprüsü, Zarar Görebilirlik, Kırılganlık Eğrisi, Hasar Sınır Durumu, Sismik Şiddet Ölçüdü

To my family…

ACKNOWLEDGEMENTS

TABLE OF CONTENTS

LIST OF TABLES

LIST OF FIGURES

FIGURES

CHAPTER 1

INTRODUCTION

1.1 GENERAL

Earthquake induced damages observed after severe earthquakes (the 1971 San Fernando and the 1994 Northridge earthquakes in US, the 1995 Kobe earthquake in Japan, the 1999 Marmara earthquakes in Turkey and the 1999 Chi-Chi earthquake in Taiwan) occurred in the past at the seismically active regions around the world and in Turkey proved that bridges are the most vulnerable components of the highway transportation systems and the lessons learnt from such big earthquakes revealed the need to mitigate the risk resulting from the seismic damage of the bridges. Seismic vulnerability assessment of the highway bridges located within earthquake prone regions and determination of their performance levels under seismic actions play an important role for the safety of transportation systems. After determining the most unfavorable seismic action level that bridges can be exposed to during their life time using either probabilistic or deterministic approaches, seismic vulnerability assessment of such bridges can be performed based on fragility curves. Using this information, estimations regarding the degree of seismic damage as well as the seismic performance of the bridges can be done for the seismic hazard that the bridge is likely to be exposed to. Fragility curves supply very useful information about the relation between the ground motion intensity at the bridge site and the probability of exceeding a certain damage state for a certain class of bridges. Fragility curves are developed for a certain group of

structures having similar structural characteristic. In this study fragility curves are developed for the ordinary highway bridges in Turkey constructed after the 1990s. These bridges are first classified into different groups exhibiting similar dynamic behavior under the seismic action. Then the fragility curves for each bridge class are developed individually.

The reliability of the seismic vulnerability assessment results is directly dependent on the reliability of the fragility curves. Therefore, the bridge fragility curves that will be used in the assessment procedure should realistically represent the ground motion intensity and the bridge damage. The variability in the structural parameters of the bridges and damage state definitions as well as the uncertainty in the ground motion parameters make the development procedure of the bridge fragility curves a very challenging task. The derived fragility curves are highly sensitive to the choices made for the analysis method, structural idealization, seismic hazard, and damage state definitions. Therefore, fragility curves determined by different researchers can have substantial inconsistency even for the same bridge, local site and seismicity.

The fragility curves are mostly developed using empirical or analytical approach. In the empirical approach, bridge damage due to past earthquakes is examined through site surveys or reconnaissance reports. Damage probability matrix forms representing the relationship between the bridge damage and the ground motion intensity are developed. Then the empirical fragility curves are constructed using the damage probability matrix forms. Although the empirical fragility curves are obtained from the bridge damages due to real earthquakes, their reliability are questionable due to the limited number of observed events during the earthquake. Moreover, subjectivity in the development of damage probability matrix forms through site surveys and the unequal distribution of damage states through different bridge types having diverse properties makes them dubious to be used in the assessment calculations for future events.

The analytical method is the other procedure to develop fragility curves. In this study, fragility curves for certain classes of ordinary highway bridges are determined using analytical method by simulating the bridge responses under

earthquake ground motions having various intensities. The application of analytical method for development of fragility curves is presented in the flow chart shown in Figure 1.1. The given flowchart can be subdivided into three main items each of which has its own variability and uncertainties during the application of the procedure. These three important items considered in the development of fragility curves are as follows;

- Bridge structure sampling and modeling

- Ground motion selection

- Damage state definition

The reliability of the analytically determined fragility curves generally depends on the above mentioned three items. Classification of bridges according to various structural attributes, bridge sampling for each bridge class and their analytical modeling, selection of earthquake ground motions, definitions of the bridge damage limit states with respect to different damage parameters constitute the different phases of the analytical method for the development of fragility curves. These curves are explicitly influenced by the considerations and assumptions made during the application of these stages. The analysis results as well as the reliability of the fragility curves are directly influenced by the assumptions made during the analysis stage and structural modeling. In addition to the several analytical efforts for each item, excessive number of sample bridge simulations under various earthquake ground motions and the complexity involved in the 3D bridge structure modeling make this procedure computationally demanding. Not only the computational time for getting the analysis results, but also the evaluation of the results and the post processing time for arranging the analysis results requires excessive amount of time.

At the end of analytical procedure, analytical fragility curves for each bridge class will be developed. A typical fragility curve for different damage states is presented in Figure 1.2. Using the fragility curve, the probability of exceeding a specific damage state can de determined under an earthquake ground motion considering its seismic intensity measure. Different ground motion intensity measures can be used in the development of fragility curves. While some of the

intensity parameters can be easily determined from ground motion records, some others are computed through equations. The essential point in selecting the appropriate intensity measure is that it should have certain level of correlation with the seismic damage of the bridges. Therefore, selected intensity measure has a considerable effect on the reliability of the bridge fragility curves.
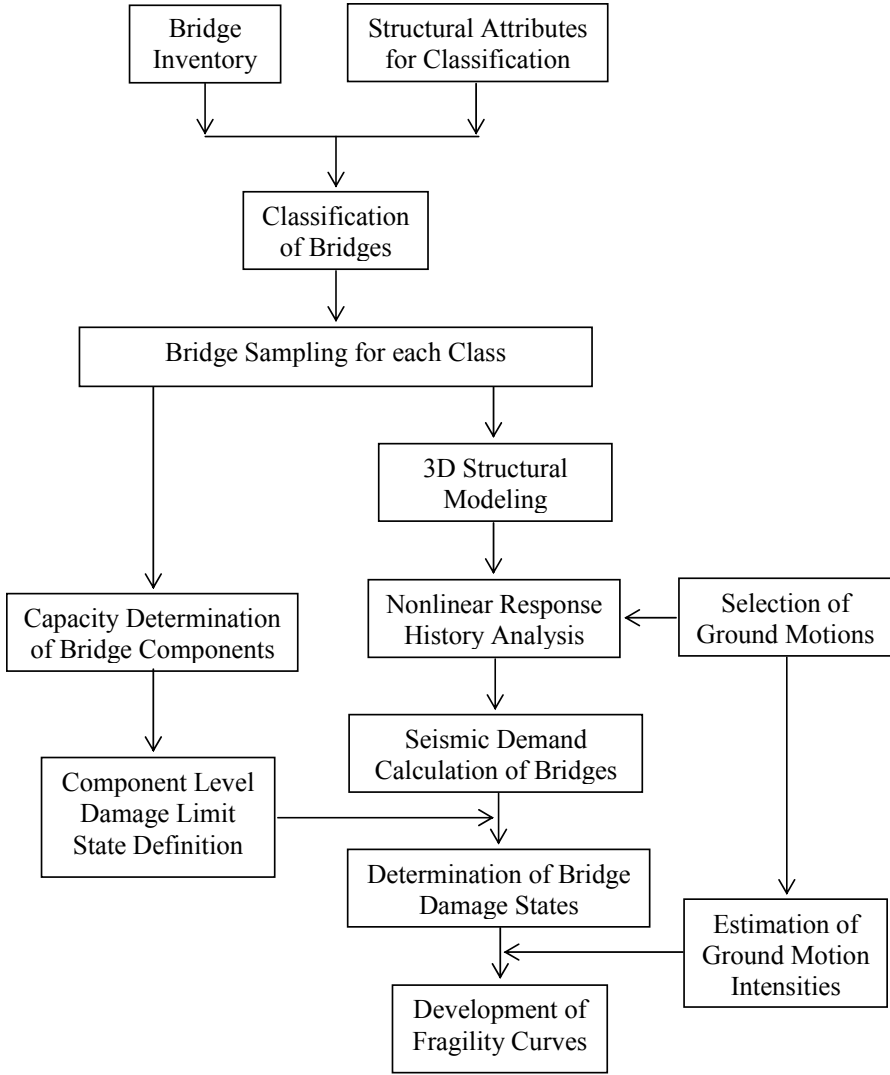
Figure 1.1 Flowchart for the development of bridge fragility curves
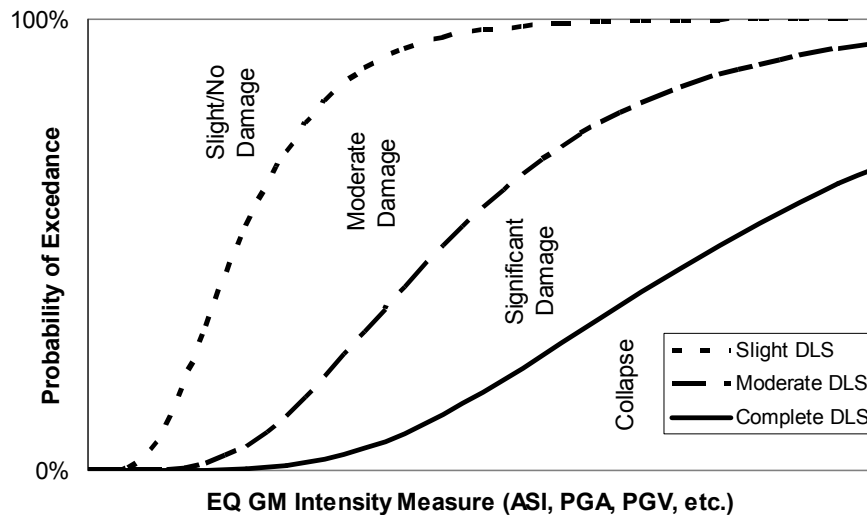
Figure 1.2 A sample fragility curve for different damage limit states

1.2   REVIEW OF PREVIOUS STUDIES

Fragility curve, which is a fundamental component of seismic risk assessment methodologies, is a probabilistic tool used to assess potential seismic damage to highway bridges at a given seismic hazard level. Subject of fragility is a generalized area of structural reliability considering the structural vulnerability conditioned upon some input parameters, which is the ground motion intensity for seismic actions. Application of seismic performance assessment of civil engineering structures using fragility theory became popular in the beginning of 1980s starting with the vulnerability evaluation of nuclear facilities for estimating the structural damage. Fragility curve simply depicts the probability that the seismic demand imposed on the structure (D) is greater than or equal to the capacity of the structure (C). This probability statement is conditioned on a selected seismic intensity measure (IM) representing the level of seismic action for a specific damage limit state (LS). Fragility is defined as the conditional probability of attainment or exceeding of a damage state for a given intensity "x" of ground excitation, as shown in Equation (1.1). Using the formulation given in Equation (1.1), damage level of a

5

bridge under an earthquake with a specific ground motion intensity measures can be determined.

$$P(fragility) = P_{LS}[D \geq C \mid IM = x]$$

(1.1)

There are different ways of obtaining bridge fragility curves considering the bridge response data, which may be obtained from the expert opinions (judgmental), the field observations (post-earthquake bridge damage) or the results of advanced analysis using analytical models. Each data source has associated advantages and disadvantages. Development of bridge fragility curves using experimental data may be taken into account as an alternative solution when the improvements in the big scale testing techniques are considered. However, a parametric study by making big scale experiments through testing of numerous models is neither feasible nor cost-effective when the limitations due to time, material as well as the experimental difficulties are considered. Therefore bridge vulnerability functions may be judgmental, empirical or analytical depending on the type of bridge response data utilized. A combination of more than one of the three above mentioned methods can be used for determining fragility curves, which is then named as hybrid fragility curves. The following sections provide an overview of some of the existing judgmental, empirical, analytical and hybrid methods to perform the assessment of seismic vulnerability of highway bridges.

1.2.1   Judgmental Methods

One of the simplest methods of obtaining fragility curve is judgmental fragility curve, which is based on the bridge response data obtained from expert opinions. Especially, when the available objective information about the recorded data is incomplete or insufficient, it is a good choice to rely on subjective information derived from the opinions of expert engineers and researchers. Expert panels of structural engineers asked to make estimates of the probable bridge

damage distributions for different bridge types when subjected to earthquakes of various intensities. A survey is executed following the Delphi method, in which several rounds of questionnaires are distributed and their answers are updated. Probability distribution functions are fit to the expert predictions to represent the range of bridge damage estimates at each ground motion intensity level. The probability of a specified damage state is derived using the resulting distributions and plotted against the corresponding ground motion intensity level to obtain a set of vulnerability curves for the associated bridge type (Rossetto and Elnashai, 2003).

The most systematic study using this method is conducted by Applied Technology Council in the US and the results of the study are presented at the report of ATC-13 (ATC, 1985) developed for the estimation of earthquake damages to the facilities in California. The ATC organized a panel of more than 70 senior-level experts in earthquake engineering to make estimates of the probable damage distributions for various components of a typical Californian infrastructure for various seismic intensities. However only 5 people were bridge experts and provided information for highway bridges. The questionnaires that were required to answer by the experts on the probability of a bridge being in one of the seven damage states for a given Modified-Mercalli Intensity (MMI) were prepared for only two classes of bridges. These bridges were classified according to their total length as major bridge (spans more than 500 feet) and conventional bridge (spans less than 500 feet). The results were then compiled and reported as the damage probability matrices for bridges in the ATC-13 report. Table 1.1 shows a general form of damage probability matrix defined in ATC-13 (ATC, 1985).

Table 1.1 General form of damage probability matrix in ATC-13

Damage State	Damage Factor Range (%)	Central Factor Range (%)	Probability of Damage in Percent By MMI and Damage State						
			VI	VII	VIII	IX	X	XI	XII
1 - NONE	0	0	95	49	30	14	3	1	0.4
2 - SLIGHT	0 – 1	0.5	3	38	40	30	10	3	0.6
3 - LIGHT	1 – 10	5	1.5	8	16	24	30	10	1
4 - MODERATE	10 – 30	20	0.4	2	8	16	26	30	3
5 - HEAVY	30 – 60	45	0.1	1.5	3	10	18	30	18
6 - MAJOR	60 – 100	80	-	1	2	4	10	18	39
7 - DESTROYED	100	100	-	0.5	1	2	3	8	38

The following definitions can be used as a guideline:

1 - NONE: No damage.

2 - SLIGHT: Limited localized minor damage not requiring repair.

3 - LIGHT: Significant localized damage of some components generally not requiring repair.

4 - MODERATE: Significant localized damage of many components warranting repair.

5 - HEAVY: Extensive damage requiring major repairs.

6 - MAJOR: Major widespread damage that may result in the facility being razed, demolished, or repaired.

7 - DESTROYED: Total destruction of the majority of the facility.

Reliability of judgment-based curves is questionable due to their dependence on the individual experience of the experts consulted. In addition to the subjectivity of the expert opinion involved in the method, the randomness of the ground motion intensity, the uncertainty in the structural response and the coarseness of the bridge classes makes this method disadvantageous in comparison with the other methods.

1.2.2 Empirical Methods

Another way of obtaining fragility information is to investigate the actual bridge damage distributions from the post-earthquake field observations or reconnaissance reports. Fragility curves for different bridge classes can be determined utilizing the observational bridge damage data by statistical analysis. The empirical method is the most realistic approach, because existing state of the damaged bridges is evaluated in detail considering its all structural and non-structural components after an actual earthquake. On the other hand, since the empirical fragility curves are based on observational damage data, the subjectivity

involved in this method is relatively high. During the post earthquake field inspections, bridge damage evaluation differs from one inspector to another depending on their experience and physical conditions during the inspection period. Another difficulty with the development of empirical fragility curves for bridge damage estimation is the inconsistency and discrepancy of bridge damage state definitions between different inspection teams. Besides, the number of damaged bridges and their structural variability, damage states, seismicity of the bridge local site as well as other important components of the fragility curves are limited within the damaged bridge data in hand at the region affected by the earthquake. Consequently the curves are highly specific to a particular region. Also, the observational data tend to be scarce and mostly clustered in the low-damage, low-ground motion severity range. Inadequate number of field observations and detailed reconnaissance reports also influence the results of empirical method due to the insufficient information about the bridge damage distribution during the earthquake. In some cases, to increase the number of observational damage data, bridge damage due to multiple earthquakes may be aggregated and attributed to a single event. This leads to a data scatter in larger scales reducing the reliability of the empirical based fragility curves. Thus, the application of empirical fragility curves is in general very limited.

Following severe earthquakes, empirical bridge fragility curves became more common as a result of more ground motion and bridge damage data. Several researchers used empirical methods considering different earthquakes or combination of several earthquakes and their associated bridge damage data. Basoz and Kiremidjian (1997) used the Loma Prieta and Northridge earthquakes. Shinozuka et al. (2003) and Elnashai et al. (2004) used both Northridge and Kobe earthquakes. Yamazaki et al. (1999) and Shinozuka et al. (2000a) considered only the Kobe earthquake. All the researchers utilized the similar procedures to determine empirical fragility curves. To be used for the damage matrix for highway bridges, generally peak ground acceleration (PGA) is considered for the ground motion intensity measure, which is estimated using shake maps. In Table 1.2 and Table 1.3, bridge damage matrices are given for 1994 Northridge earthquake (Basoz

and Kiremidjian 1997) and 1995 Kobe earthquake (Yamazaki et al., 1999), respectively. In addition to the insufficient bridge damage data for the collapse damage state, damage distribution among the seismic hazard intervals and the number of data for each damage state is not appropriate for the development of reliable vulnerability functions.

Table 1.2 Damage matrix of Basoz and Kiremidjian (1997) – 1994 Northridge earthquake

Observed Damage	PGA (g)										
	0.15-0.2	0.2-0.3	0.3-0.4	0.4-0.5	0.5-0.6	0.6-0.7	0.7-0.8	0.8-0.9	0.9-1.0	>1.0	Total
None	318	502	234	50	34	29	24	29	16	16	1252
Minor	2	10	25	2	6	4	6	1	7	3	66
Moderate	1	15	13	11	10	9	5	4	9	4	81
Major	0	10	2	6	7	3	2	5	11	1	47
Collapse	0	0	1	0	0	0	0	2	2	1	6

Table 1.3 Damage matrix of Yamazaki et al. (1999) – 1995 Kobe earthquake

Observed Damage	PGA (g)										
	0.15-0.2	0.2-0.3	0.3-0.4	0.4-0.5	0.5-0.6	0.6-0.7	0.7-0.8	0.8-0.9	0.9-1.0	>1.0	Total
None	80	34	23	28	12	3	3	1	0	0	184
Minor	0	0	2	1	0	4	0	1	0	0	8
Moderate	0	0	1	3	3	6	0	0	0	0	13
Major	0	0	0	1	0	5	1	0	0	0	7
Collapse	0	0	0	2	0	2	0	0	0	0	4

Using the given damage matrices, damage probability matrices as well as the empirical fragility curves with an appropriate distribution function can be determined.

When the above mentioned limitations are considered for the development of empirical fragility curves, it is almost impossible to obtain good correlation between the data collected and the fragility curves developed using normal or lognormal distributions, or any interpolation functions. Therefore it is essential that empirical vulnerability functions based on field observations needs to be supplemented by

analytically simulated bridge damage data. High level of training inspectors who are entrusted for the bridge damage inspections and the standardization of inspection forms used for the data collection are the essential components to improve the quality of the bridge damage data as well as the reliability of the empirical fragility curves.

1.2.3 Analytical Methods

Analytical fragility curves are the only option for assessing the seismic performance of highway bridges when the actual bridge damage data or any expert opinion is not available. In this method, bridge analytical models are formed and ground motions with various intensity levels are considered for the seismic simulation of the bridge damage by executing numerous analyses. The analysis results are used to develop analytical fragility curves by determining the probability of exceeding a specified damage limit state under a given ground motion intensity. Generally two parameter cumulative log-normal distribution function is employed to define the probability of exceeding a damage state. A fragility curve has the following analytical form according to the lognormal distribution:

$$F(IM) = \Phi\left[\frac{\ln(IM) - \lambda}{\xi}\right] \tag{1.2}$$

F(IM) is the seismic fragility function, IM is the seismic intensity measure (PGA, PGV, etc.), λ and ξ are the mean and standard deviation of natural logarithm of the ground motion intensity and $\Phi[\cdot]$ is the standard normal distribution function.

Analytical fragility curves have the superiority in terms of their reliability in comparison with the judgmental or empirical ones. The reliability of the analytical fragility curves are affected by the modeling assumptions as well as the refinement of the analytical model. Although analytical approaches for vulnerability curve generation is becoming widespread due to its applicability for any type of structure, limitations in modeling capabilities and computational effort required for the

analyses make this approach not also computational and time demanding but also complicated. Also, the damage limit state definitions in terms of meaningful quantities for seismic performance of highway bridges is another important task for the reliability of analytical fragility curves. A variety of analysis procedures have been followed in the development of fragility curves, ranging from the elastic analysis of equivalent single degree of freedom systems to nonlinear response history analysis of 3D bridge models. The choice of analysis procedure and associated structural idealization of highway bridges directly influence the analysis results as well as the bridge damage data necessary for the development of analytical fragility curves.

Elastic spectral method is the simplest and the least time consuming approach for the generation of analytical fragility curves. Using this method, Hwang et al. (2000) and Jernigan and Hwang (2002) developed fragility curves for Memphis bridges. The bridge components that have the potential for being damaged during an earthquake were evaluated to determine their capacity/demand ratios (DCR). For each bridge component capacities were determined according to FHWA (1995) and the seismic demand was determined from an elastic spectral analysis according to the method specified in AASHTO (1996). After the calculation of demands and capacities of each bridge component, DCR is determined and correlated with each damage state for different levels of seismic intensities. The results of all of these calculations were then put together in a bridge damage frequency matrix, which are used to generate fragility curves.

Non-linear static method is an alternative approach, often referred to as capacity spectrum method. This method has been utilized to develop analytical fragility curves of bridges by various researchers (Dutta and Mander, 1998; Mander and Basoz, 1999; Mander, 1999; Shinozuka et al., 2000b; Monti and Nistico, 2002; Banerjee and Shinozuka, 2007). The theoretical background of the bridge damage functions for the generation of bridge fragility curves given in HAZUS (FEMA, 2003) is similar with the ones for Mander and Basoz (1999). In all these studies, they considered a similar methodology that uses the intersection of a capacity spectrum found through non-linear static pushover analysis, and a demand spectrum

found through reduction of the elastic response spectrum as shown in Figure 1.3 (Mander, 1999). In a deterministic analysis, the intersection of the capacity-demand curves result in the expected performance level of the bridge. However, probability distributions are drawn over both the capacity and demand curves to indicate the associated uncertainty in the performance assessment. The probability of failure is determined at the intersection of the demand and capacity distributions. For various levels of selected intensity measure and predefined damage limit state, bridge fragility curves can be generated using these spectra.
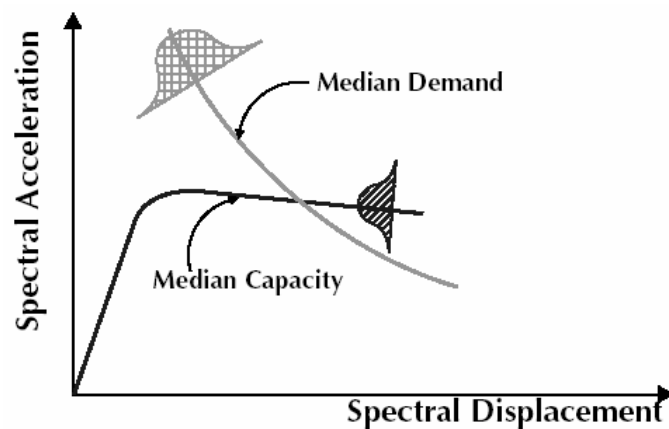
Figure 1.3 Intersection of capacity-demand acceleration-displacement spectra
(Mander, 1999)

Nonlinear response history analysis (NRHA) is believed to be most rigorous method in estimating the inelastic seismic demands of the structures. Although NRHA method has been identified as the most time consuming and computationally demanding, fragility curves developed using this procedure believed to have better reliability in comparison with the ones for above mentioned analytical procedures (Shinozuka et al., 2000b). This method has been utilized in different ways to develop fragility curves by various researchers (Hwang et al., 2001; Karim and Yamazaki, 2003; Elnashai et al., 2004; Choi et al., 2004; Nateghi and Shahsavar, 2004; Mackie and Stojadinovic, 2004). After deciding the major bridge classes,

sample bridges representing the general attributes of the associated bridge class are formed using appropriate sampling techniques, so that uncertainties in the structural and material characteristics for each class can be considered. Different researchers emphasize on different properties of the bridges in uncertainty consideration of highway bridges. Then the analytical models for each bridge sample are constructed by making several assumptions depending on the level of accuracy required to quantify the seismic response of the bridge. Various level of bridge modeling is possible from simple lumped parameter models to comprehensive structural modeling by detailed finite element models. Once the bridge modeling is accomplished with an acceptable level of accuracy in calculating the true seismic response of highway bridges, an appropriate suite of earthquake ground motion records is selected. The reliability of the analytical fragility curves depends on the selected ground motion recordings, which should be representative ground motions for the region of interest. In other words, earthquake source properties of the selected ground motions are supposed to be in accordance with the seismic source properties of the bridge sites. Also the selected ground motions should have equal distribution of seismic intensities covering all levels of intensities for the selected intensity measure. Then, for each bridge sample a nonlinear response history analysis is performed under the effect of the selected ground motions. Maximum responses of the critical bridge components are recorded. Different parts of the bridge structure are considered to be the critical component affecting the seismic performance of the bridge. In the literature, columns are considered to be the critical bridge component that is most frequently utilized in the analysis. On the other hand, the damage limit states defined considering the seismic response of the associated critical bridge components. Damage limit state definitions for each bridge component are based on expert judgment, experimental data, or analytical models. Damage limit state definition, which has a direct influence on the fragility curves, is one of the most essential parts for the development of analytical fragility curves. Finally, using different statistical tools, analytical fragility curves are developed using the NRHA results for each damage limit state. In several steps of this method, various levels of uncertainty are incorporated. Of these steps, analytical modeling

the bridge components, selection of a suite of ground motion records and definition of damage limit states are the most critical ones.

1.2.4 Hybrid Methods

The previously explained three methods have superiority on others at some aspects, while they have some drawbacks at various levels. Therefore, it is not feasible to describe one of the three methods as the best for the generation of fragility curves. Using several of these methods together by making use of their features is a reasonable way of constructing fragility curves. Hybrid vulnerability curves attempt to compensate for the scarcity of observational data, subjectivity of judgmental data and modeling deficiencies of analytical procedures by combining data from different sources (Rossetto and Elnashai, 2003). Although, the judgmental based fragility curves proposed in ATC-13 (ATC, 1985) are mainly based on expert opinion, limited observational data obtained from 1971 San Fernando earthquake has been incorporated. However, in most of the cases, well-suited supplementary data is generally very limited for the generation of hybrid fragility curves. Yet, the consideration of multiple data source is essential for the enhancement of the reliability of the fragility curves.

Some basic features and the limitations of the four methods for the development of fragility curves are summarized in Table 1.4 (Kwon and Elnashai, 2006).

Table 1.4 Categorization of vulnerability curve (Kwon and Elnashai, 2006)

Category		Characteristics
Empirical vulnerability curve	Features	Based on post-earthquake survey Most realistic
	Limitations	Highly specific to a particular seismo-tectonic, geotechnical and built environment The observational data used tend to be scarce and highly clustered in the low-damage, low-ground motion severity range Include errors in structural damage classification Damage due to multiple earthquakes may be aggregated
Judgmental vulnerability curve	Features	Based on expert opinion The curves can be easily made to include all the factors
	Limitations	The reliability of the curves depends on the individual experience of the experts consulted A consideration of local structural types, typical configurations, detailing and materials inherent in the expert vulnerability predictions
Analytical vulnerability curve	Features	Based on damage distributions simulated from the analyses Reduced bias and increased reliability of the vulnerability estimate for different structures
	Limitations	Substantial computational effort involved and limitations in modeling capabilities The choices of the analysis method, idealization, seismic hazard, and damage models influence the derived curves and have been seen to cause significant discrepancies in seismic risk assessments
Hybrid vulnerability curve	Features	Compensate for the scarcity of observational data, subjectivity of judgmental data, and modeling deficiencies of analytical procedures Modification of analytical or judgment based relationships with observational data and experimental results
	Limitations	The consideration of multiple data sources is necessary for the correct determination of vulnerability curve reliability

1.3 OBJECT AND SCOPE

Seismic vulnerability assessment and loss estimation due to earthquake damage for ordinary highway bridges in Turkey are performed considering other available studies or codes, which were developed for other regions especially in the

US and Japan. Therefore in order to perform a reliable seismic vulnerability assessment of the bridges, it is very important to have bridge fragility curves, representing the general attributes of the highway bridge structures as well as the seismic source characteristics of the bridge sites in Turkey. The main objective of the study is to generate fragility curves of the ordinary highway bridges in Turkey constructed after the 1990s for the assessment of their seismic vulnerability. The investigated ordinary highway bridges in the inventory data is dominated by the multi-span simply supported bridges with cast-in-place continuous deck, for which analytical fragility curves are developed. In this study, the key component of the fragility curve development methodology is the quantification of seismic vulnerability of the ordinary highway bridges by developing the relationship between bridge damage and ground motion intensity. The outcome and the limitations of the other studies explained in the literature survey on fragility curve generation are taken into account. Four major bridge types are formed by classifying the highway bridges according to their primary structural attributes. The identified bridge classes represent the majority of the overall inventory for the region. To account for the uncertainty in the structural parameters of the bridges, samples are generated for each major bridge type using the sampling techniques. Three dimensional analytical models for each bridge sample are developed to carry out nonlinear response history analysis under a selected suite of ground motion records. The most important bridge components are identified considering the analysis results and the damage limit states are defined for each critical bridge component. By comparing the seismic demands exerted on the bridge components and the identified damage states, fragility curves are developed using statistical analysis. After obtaining fragility curves for all major bridge types, seismic vulnerability assessment of some bridges located at a specific region of Turkey is performed under several scenario earthquakes.

1.4   ORGANIZATION OF THE DISSERTATION

This thesis is composed of eight main chapters with the brief contents given as follows:

Chapter 1:   General overview of the study and literature survey on the development of bridge fragility curves using different approaches.

Chapter 2:   Investigation of the existing ordinary highway bridges and classification according to their primary structural attributes. Development of bridge samples for each major bridge class using sampling techniques. Identification of the most critical bridge components that affect the seismic response of the bridge.

Chapter 3:   Selection of an appropriate analysis tool and generation of 3D non-linear analytical models of the sample bridge structures using detailed analytical models for its components.

Chapter 4:   Selection of a suite of earthquake ground motion records that are representative of the seismic hazard for the region and deciding the ground motion intensity measure that will be used in the development of fragility curves.

Chapter 5:   Definition of damage limit states for the critical components of the bridge and review of the available damage states definitions in literature.

Chapter 6:   Calculation and presentation of seismic demands from nonlinear response history analysis. Generation of analytical fragility curves for different bridge classes. Comparison of developed fragility curves with those used in the current codes or previous studies.

Chapter 7:   Application of the developed fragility curves through a case study covering different types of bridges in the Marmara Region under the effect of three scenario earthquakes in order to assess their seismic performance.

Chapter 8:   A brief summary and the conclusions are given and recommendations for future studies are provided.

CHAPTER 2

CLASSIFICATION OF BRIDGES

In this study fragility curves will be developed for ordinary highway bridges in Turkey that are constructed after the 1990s. The general understanding of these bridges in terms of their structural attributes as well as their seismic behavior is essential for the generation of fragility curves. Considering each bridge in the inventory data of the specified bridges individually and obtaining its fragility curve is neither feasible nor practical when the total number of bridges is concerned. Each existing bridge has its own characteristics due to its structural properties and hence different seismic behavior. This makes it rather difficult to evaluate the seismic performance of each bridge in a large inventory in detail under an expected earthquake. Although each bridge has its own structural characteristics, they have some similarities at various aspects. Therefore, it is a rational way of classifying bridges into different groups considering their certain structural attributes. The classification is made such that the bridges representing a specific bridge class have some similarities in the basic structural attributes and their seismic response to the same earthquake ground motion is expected to be similar. Classification of the bridges allows us to deal with each bridge class in detail instead of investigating all bridge samples individually. In this approach, it is intended to generate fragility curves for the identified bridge classes not for individual bridges in the inventory data.

The number of bridge classes depends on the structural system variability in the inventory as well as the level of accuracy required for the generation of fragility

curves. If all the structural attributes are taken into consideration through the classification procedure, a very detailed classification can be made and considerable amount of bridge classes can be generated. Meanwhile, it should be kept in mind that it is not possible to include every structural characteristic of a bridge in the classification, nor is practical to specify a large number of bridge classes. The number of bridge classes needs to be as small as possible by considering the most important structural attributes of the bridges only. On the other hand, there should be sufficient number of bridge classes covering every bridge sample in the bridge inventory data. Therefore, the list of bridge classes has to be comprehensive in order to enable the classification of as many bridges as possible and at the same time it has to be simple enough to be manageable and applicable. In this study, a bridge inventory of 52 representative bridge data, whose structural and material properties are known in detail, are collected to develop bridge classes. Detailed information about the associated bridge inventory data is explained in Section 2.2.

2.1   REVIEW OF BRIDGE CLASSIFICATIONS

In order to make the classification, structural attributes that best describe the seismic response of bridges and the parameters affecting their seismic behavior need to be specified for the bridge inventory. Different structural properties of the bridges were used in the previous studies to classify the bridges into groups. ATC-13 (ATC, 1985) considers only two bridge classes according to their total length. Bridges having total length greater than 500 ft and less than 500 ft is classified as major bridge and conventional bridge, respectively. Conventional bridges are further classified into two groups as multiple simple spans and continuous monolithic. This is a very broad classification and neglects various structural characteristics that affect the seismic performance of a bridge, such as material, substructure properties, skewness, etc.

In the classification developed by Basoz and Kiremidjian (1996), bridges are grouped according to number of spans, superstructure type, substructure type and

material, abutment type, and span continuity. Using that classification, bridges damaged in the Northridge and Loma Prieta earthquakes were grouped first by the superstructure type and substructure material. Then, these bridges were further classified into sub-categories based on other structural characteristics, such as number of spans, abutment type, column bent type and span continuity. Empirical damage probability matrices and fragility curves were developed for each of these bridge sub-categories using the damage data from the Northridge and Loma Prieta earthquakes (Basoz and Kiremidjian, 1997). The bridge sub-categories employed in the study of Basoz and Kiremidjian (1997) are given in Table 2.1.

Table 2.1 Description of bridge sub-categories employed by Basoz and Kiremidjian (1997)

Bridge Sub-Category	Abutment Type	Column Bent Type	Span Continuity
Single Span Bridges			
C1S1	Monolithic	Not applicable	Not applicable
C1S2	Non-monolithic	Not applicable	Not applicable
C1S3	Partial integrity	Not applicable	Not applicable
Multiple Span Bridges			
C1M1	Monolithic	Multiple	Continuous
C1M2	Monolithic	Multiple	Discontinuous
C1M3	Monolithic	Single	Continuous
C1M4	Monolithic	Single	Discontinuous
C1M5	Monolithic	Pier wall	Continuous
C1M6	Monolithic	Pier wall	Discontinuous
C1M7	Non-monolithic	Multiple	Continuous
C1M8	Non-monolithic	Multiple	Discontinuous
C1M9	Non-monolithic	Single	Continuous
C1M10	Non-monolithic	Single	Discontinuous
C1M11	Non-monolithic	Pier wall	Continuous
C1M12	Non-monolithic	Pier wall	Discontinuous
C1M13	Partial integrity	Multiple	Continuous
C1M14	Partial integrity	Multiple	Discontinuous
C1M15	Partial integrity	Single	Continuous
C1M16	Partial integrity	Single	Discontinuous
C1M17	Partial integrity	Pier wall	Continuous
C1M18	Partial integrity	Pier wall	Discontinuous

The Federal Highway Administration (FHWA) Recording and Coding Guide (FHWA, 1988) defines bridge types in accordance with their superstructure type, material, and the continuity at supports. Some possible construction materials and construction types are listed in Table 2.2 in the recording and coding guide, which is for National Building Inventory (NBI) in US. FHWA (1988) classification is modified to include the bent and pier information by Hwang et al. (2000).

Table 2.2 Some construction material and construction types in NBI (FHWA, 1988)

Construction Material	Construction Type	
- Concrete - Concrete Continuous - Steel - Steel Continuous - Prestressed Concrete - Prestressed Concrete Continuous - Timber - Masonry - Aluminum, Wrought Iron, or Cast Iron - Other	- Slab - Stringer/Multi-beam or Girder - Girder and Floorbeam System - Tee Beam - Box Beam or Girders – Multiple - Box Beam or Girders – Single or Spread - Frame - Orthotropic - Truss – Deck - Truss – Thru - Arch – Deck	- Arch – Thru - Suspension - Stayed Girder - Movable – Lift - Movable – Bascule - Movable – Swing - Tunnel - Culvert - Mixed Types (applicable only to approach spans) - Segmental Box Girder - Channel Beam - Other

In the study of Nielsen (2005), bridges are assigned to one of 11 bridge classes based on their construction material, construction type and the number of spans. Bridge classes and their corresponding abbreviation defined by Nielsen (2005) are presented in Table 2.3.

Table 2.3 Bridge classes defined by Nielsen (2005)

Bridge Class Name	Abbreviation
Multi-Span Continuous Concrete Girder	MSC Concrete
Multi-Span Continuous Steel Girder	MSC Steel
Multi-Span Continuous Slab	MSC Slab
Multi-Span Continuous Concrete Box Girder	MSC Concrete-Box
Multi-Span Simply Supported Concrete Girder	MSSS Concrete
Multi-Span Simply Supported Steel Girder	MSSS Steel
Multi-Span Simply Supported Slab	MSSS Slab
Multi-Span Simply Supported Concrete Box Girder	MSSS Concrete-Box
Single-Span Concrete Girder	SS Concrete
Single-Span Steel Girder	SS Steel
Others	

HAZUS (FEMA, 2003) has a bridge classification based on the following structural characteristics:

- Seismic Design

- Number of spans: single vs. multiple span bridges

- Structure type: concrete, steel others

- Pier type: multiple column bents, single column bents and pier walls

- Abutment type and bearing type: monolithic vs. non-monolithic; high rocker bearings, low steel bearings and neoprene rubber bearings.

- Span continuity: continuous, discontinuous (in-span hinges) and simply supported.

Classification scheme of HAZUS (FEMA, 2003) incorporates various parameters that affect damage into fragility analysis. In this way, a total of 28 bridge classes (HWB1 through HWB28) are defined as given in Table 2.4.

Table 2.4 HAZUS (FEMA, 2003) bridge classification scheme

Class	State	Year Built	Design	Description
HWB1	Non-CA	< 1990	Conventional	Major Bridge - Length > 150m
HWB1	CA	< 1975	Conventional	Major Bridge - Length > 150m
HWB2	Non-CA	>= 1990	Seismic	Major Bridge - Length > 150m
HWB2	CA	>= 1975	Seismic	Major Bridge - Length > 150m
HWB3	Non-CA	< 1990	Conventional	Single Span
HWB3	CA	< 1975	Conventional	Single Span
HWB4	Non-CA	>= 1990	Seismic	Single Span
HWB4	CA	>= 1975	Seismic	Single Span
HWB5	Non-CA	< 1990	Conventional	Multi-Col. Bent, Simple Support - Concrete
HWB6	CA	< 1975	Conventional	Multi-Col. Bent, Simple Support - Concrete
HWB7	Non-CA	>= 1990	Seismic	Multi-Col. Bent, Simple Support - Concrete
HWB7	CA	>= 1975	Seismic	Multi-Col. Bent, Simple Support - Concrete
HWB8	CA	< 1975	Conventional	Single Col. Box Girder - Continuous Concrete
HWB9	CA	>= 1975	Seismic	Single Col. Box Girder - Continuous Concrete
HWB10	Non-CA	< 1990	Conventional	Continuous Concrete
HWB10	CA	< 1975	Conventional	Continuous Concrete
HWB11	Non-CA	>= 1990	Seismic	Continuous Concrete
HWB11	CA	>= 1975	Seismic	Continuous Concrete
HWB12	Non-CA	< 1990	Conventional	Multi-Col. Bent, Simple Support - Steel
HWB13	CA	< 1975	Conventional	Multi-Col. Bent, Simple Support - Steel
HWB14	Non-CA	>= 1990	Seismic	Multi-Col. Bent, Simple Support - Steel
HWB14	CA	>= 1975	Seismic	Multi-Col. Bent, Simple Support - Steel
HWB15	Non-CA	< 1990	Conventional	Continuous Steel
HWB15	CA	< 1975	Conventional	Continuous Steel
HWB16	Non-CA	>= 1990	Seismic	Continuous Steel
HWB16	CA	>= 1975	Seismic	Continuous Steel
HWB17	Non-CA	< 1990	Conventional	Multi-Col. Bent, Simple Support - Prestressed Concrete
HWB18	CA	< 1975	Conventional	Multi-Col. Bent, Simple Support - Prestressed Concrete
HWB19	Non-CA	>= 1990	Seismic	Multi-Col. Bent, Simple Support - Prestressed Concrete
HWB19	CA	>= 1975	Seismic	Multi-Col. Bent, Simple Support - Prestressed Concrete
HWB20	CA	< 1975	Conventional	Single Col., Box Girder - Prestressed Concrete
HWB21	CA	>= 1975	Seismic	Single Col., Box Girder - Prestressed Concrete
HWB22	Non-CA	< 1990	Conventional	Continuous Concrete
HWB22	CA	< 1975	Conventional	Continuous Concrete
HWB23	Non-CA	>= 1990	Seismic	Continuous Concrete
HWB23	CA	>= 1975	Seismic	Continuous Concrete
HWB24	Non-CA	< 1990	Conventional	Multi-Col. Bent, Simple Support - Steel
HWB25	CA	< 1975	Conventional	Multi-Col. Bent, Simple Support - Steel
HWB26	Non-CA	< 1990	Conventional	Continuous Steel
HWB27	CA	< 1975	Conventional	Continuous Steel
HWB28				All other bridges that are not classified

2.2 STRUCTURAL ATTRIBUTES OF THE INSPECTED BRIDGES

Bridge inventory data is needed to obtain fragility curves for the standard highway bridges constructed after the 1990s in Turkey. However, a detailed bridge inventory data containing the basic properties of each existing bridge such as structural type, basic dimensions, material type of each component, location and its global coordinates, local site conditions, construction year, etc. is not available for the Turkish highway bridges. A group of 52 bridges representing the general characteristics of the ordinary highway bridges constructed after the 1990s in different parts of Turkey are selected. Although the selected bridges do not cover all bridge types, their structural properties reflect general characteristics of most of the highway bridges in Turkey. Detailed information about each bridge is obtained from General Directorate of Highways.

2.2.1 Description of Bridge Inventory

The general attributes of the selected bridges and their distribution are investigated to identify the key components of bridges affecting their seismic response under earthquake ground motion excitation. Schematic drawings of a sample bridge and its components that constitute the general attributes of the bridges are shown in Figure 2.1. Some basic properties of the associated 52 bridges that are considered to be the bridge inventory data to be used in this study are presented in Table 2.5.

The selected 52 bridges are defined as *Ordinary Standard Bridges* as per Caltrans (2006) due to the following properties the bridges possess:

- Span lengths less than 90m
- Constructed with normal weight concrete girder, and column or pier elements
- Horizontal members are supported on conventional bearings

- There are no nonstandard components such as; dropped bent caps, integral bent caps terminating inside the exterior girder, C-bents, outrigger bents; offset columns; isolation bearings or dampers

- Foundations supported on spread footing or pile cap with piles

- Soil that is not susceptible to liquefaction, lateral spreading, or scour.

In this study, fragility curves for ordinary highway bridges will be generated. Some special bridges which do not satisfy the requirements for ordinary standard bridges given in Caltrans (2006), is out of the scope of this dissertation. These type of bridges need to be considered individually. Because their seismic responses due to ground excitation differ at various aspects in comparison with the ordinary highway bridges.

The superstructure is supported by elastomeric bearings, which is placed on the abutments and bent cap beams. There is no connecting device between the elastomeric bearings and the superstructure or substructure. Friction between the bearings and the concrete surfaces are the only resisting force that holds the elastomeric bearing at its place. Several thin metal sheets are provided in the elastomeric bearing to prevent bulging due to the axial loads.
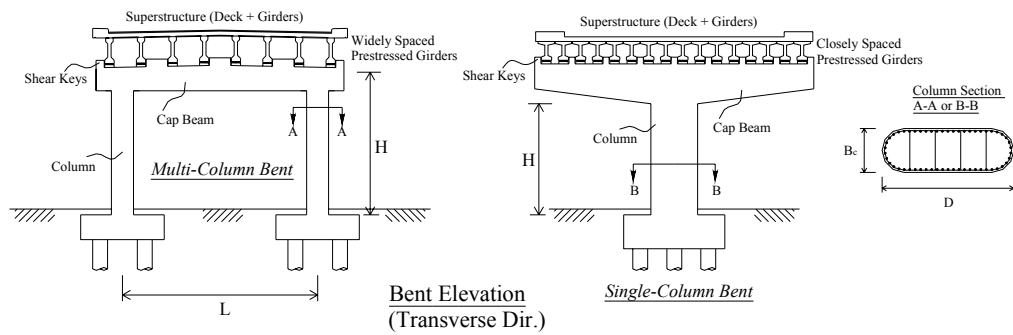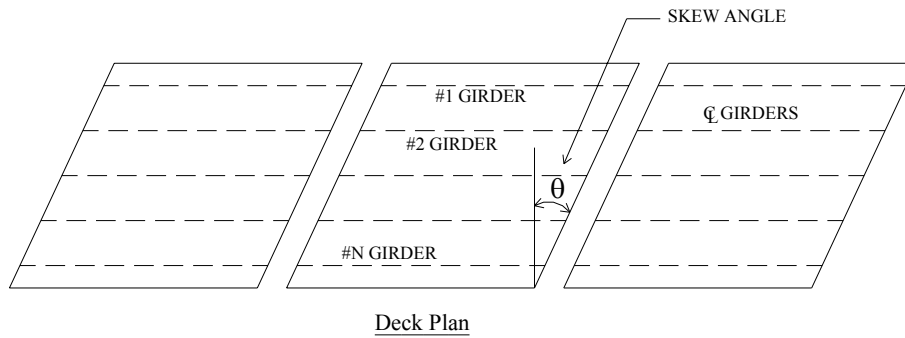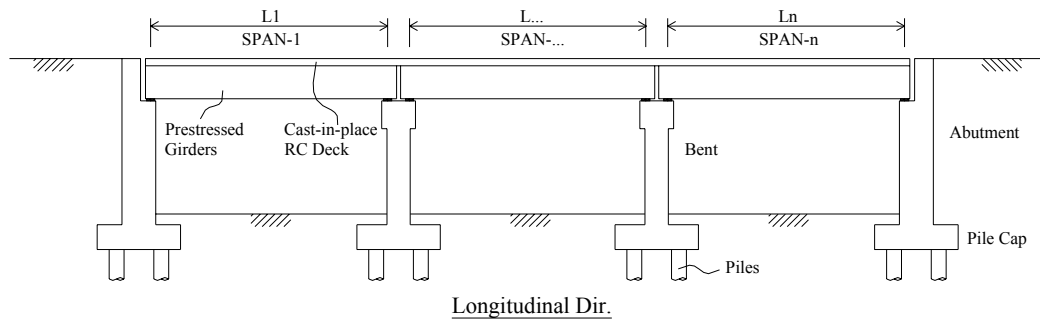
Figure 2.1 General properties of the ordinary highway bridges

Table 2.5 Selected 52 bridges and their structural attributes

No.	Bridge Name	Location	Span No.	Max Span Length (m)	Total Length (m)	Skew Angle (deg)	Number of Columns per Bent	Column Distance center to center (m)	Max Column Height (m)	Total Deck Width (m)	Number of Girders
1	Kirazlı	Bartın	4	19.4	76.8	15.0	2	5.0	8.0	9.0	10
2	GOP Uni. Kavşak	Turhal/Tokat	4	17.9	70.7	41.5	4	5.3	12.0	16.0	19
3	Karasu Çayı	Boyabat/Sinop	3	17.5	51.0	50.0	3	6.6	6.4	13.0	8
4	Çatak Çayı	Boyabat/Sinop	2	17.3	34.6	10.0	2	8.2	5.3	13.0	8
5	Kefenin	Saimbeyli/Adana	3	17.6	44.2	10.0	2	6.9	5.3	13.0	8
6	Sarız	Saimbeyli/Adana	2	20.3	40.7	27.0	2	6.9	5.7	13.0	8
7	Taşköprü	Saimbeyli/Adana	3	17.8	52.5	38.0	3	5.4	9.2	13.0	8
8	Ulusal	Saimbeyli/Adana	3	17.7	44.4	25.0	3	4.7	7.9	13.0	8
9	Aksu Çayı	Denizli	6	36.0	212.8	0.0	2	7.3	13.0	13.8	10
10	Çürüksu Çayı	Denizli	7	38.4	266.8	28.4	2	8.8	5.0	17.5	13
11	Demiryolu Geçişi	Antep-Urfa	3	26.8	55.8	30.1	2	7.5	8.5	17.5	12
12	Çarsak	Boyabat/Sinop	3	17.6	52.2	20.0	2	8.4	2.5	13.7	8
13	Elek Deresi	Boyabat/Sinop	2	20.3	40.6	0.0	3	4.7	4.4	13.7	8
14	Gokırmak	Boyabat/Sinop	4	17.6	64.8	0.0	2	8.4	5.4	12.7	8
15	Alaşehir Çayı	Gölmarmara/Manisa	3	26.7	78.4	58.0	4	7.8	7.0	16.0	12
16	Gediz Çayı	Gölmarmara/Manisa	5	26.0	128.8	40.0	3	7.3	4.8	16.0	12
17	Köprülü Kavşak	Gölmarmara/Manisa	2	29.3	58.6	54.8	4	7.1	5.6	16.3	12
18	Cumayeri Kavşak	Bolu-Düzce	2	20.6	41.1	8.6	2	5.1	6.6	10.9	12
19	Gölkaya Kavşak	Bolu-Düzce	2	22.6	45.1	1.5	2	5.4	6.8	12.0	14
20	Melen	Bolu-Düzce	4	28.6	113.3	0.0	2	8.0	9.1	16.0	12
21	Düzce Çevre Yolu	Bolu-Düzce	2	20.6	41.1	9.7	2	5.4	6.8	10.4	12
22	DBY Üstgeçit-1	Bolu-Düzce	2	20.6	41.1	24.3	2	6.9	6.0	12.5	15
23	DBY Üstgeçit-2	Bolu-Düzce	2	20.6	41.1	7.4	2	6.3	6.0	12.5	15
24	DCY Üstgeçit-1	Bolu-Düzce	2	20.6	41.1	30.7	2	7.3	5.8	12.5	15
25	DCY Üstgeçit-2	Bolu-Düzce	2	20.6	41.1	6.1	2	6.3	6.4	12.5	15
26	DCY Üstgeçit-3	Bolu-Düzce	2	20.6	41.1	16.5	2	6.5	7.2	12.5	15
27	DCY Üstgeçit-4	Bolu-Düzce	2	20.6	41.1	18.0	2	6.5	5.9	12.5	15
28	DCY Üstgeçit-5	Bolu-Düzce	2	20.6	41.1	25.5	2	6.9	6.0	12.5	15
29	DCY Altgeçit-1	Bolu-Düzce	2	17.6	35.1	1.0	2	8.0	6.5	13.3	16
30	Düzce Kavşağı	Bolu-Düzce	2	22.6	45.1	3.7	2	7.5	6.0	15.0	18
31	Asar Suyu	Bolu-Düzce	4	26.1	103.3	13.8	2	8.1	8.2	15.9	12
32	DOBY Üstgeçit-1	Bolu-Düzce	2	20.6	41.1	0.0	2	6.3	5.8	12.5	15
33	Otoyol Kavşak ÜG	Bolu-Düzce	2	25.6	51.1	0.0	2	5.3	5.4	10.6	8
34	DDY Üstgeçit	Sivas	3	18.0	44.0	46.3	3	6.3	7.1	12.8	15
35	Ayaş Yolu Bağlantı	Sincan/Ankara	2	22.8	45.6	0.0	3	7.0	2.3	20.0	24
36	Batıkent-Şaşmaz UG	Ankara	5	36.2	143.6	20.3	2	6.1	5.8	13.5	10
37	Kemalli	Sungurlu-Delice	2	17.5	34.9	40.0	2	9.2	4.3	13.0	15
38	Gürdük Çayı	Akhisar	4	16.3	64.6	20.0	4	3.2	8.7	12.8	9
39	İmbat	Tokat	2	14.2	28.5	0.0	2	8.5	3.2	14.8	12
40	Karakaya	Tokat	2	13.3	26.6	0.0	2	8.5	3.1	14.0	8
41	Çiftlik Kavşağı-Susuz	Ayaş-Ankara	2	30.0	60.0	53.9	3	10.0	5.3	22.3	17
42	Şaşmaz ÜG	Batıkent-Ank	5	36.2	143.6	20.3	2	6.2	5.8	13.5	10
43	Bitlis Çayı-3	Bitlis	3	24.4	64.8	37.0	3	7.0	7.1	14.0	16
44	Bitlis Çayı-11	Bitlis	2	30.9	61.8	53.5	5	7.5	4.0	24.0	18
45	Bitlis Çayı-13_sol	Bitlis	2	23.5	47.0	1.8	2	5.0	6.3	10.5	12
46	Bitlis Çayı-14_sag	Bitlis	2	28.5	52.0	30.0	2	6.0	10.2	10.5	7
47	Bitlis Çayı-16	Bitlis	2	28.7	57.3	43.0	4	8.3	7.8	24.0	18
48	Bitlis Çayı-7	Bitlis	4	24.8	90.4	49.8	3	6.0	10.6	13.7	17
49	Bitlis Çayı-9	Bitlis	3	24.4	64.8	38.0	4	7.5	10.2	24.0	29
50	Bitlis Çayı-17	Bitlis	3	29.8	87.4	53.2	3	6.0	12.0	14.0	10
51	Ulubat-2	Bursa	7	21.4	153.4	0.0	1	-	9.0	12.0	7
52	Canbolu-2	Bursa	9	22.0	187.5	20.0	1	-	7.2	12.0	7

Reinforced concrete is the primary structural material used in the ordinary highway bridges constructed after the 1990s in Turkey. Superstructure girders are the only components which are constructed with prestressed concrete other than the reinforced concrete. Therefore, other material types such as steel, timber, etc. are

not taken into account in the study. C40 concrete class (The characteristic strength is 40 MPa) is used for the prestressed girders and C25 is used for the rest of the reinforced concrete components of the associated bridges. The quality of reinforcement steel is S420 for all RC members. Minimum longitudinal reinforcement ratio of 1% is satisfied for the reinforced concrete columns as per AASHTO (1996). The H_{30}-S_{24} truck loading is considered in the design of all these bridges (KGM, 1982). All the bridges in the inventory data are multiple simple-span composite structures that utilize prestressed concrete girders and a cast-in-place reinforced concrete deck. They have a seat type abutment system and multiple- or single-column bents. Most of these bridges are straight and the curve angle of the curved bridges is in the negligible order that all the bridges in the inventory is assumed to be straight. Hence curve irregularity is not taken into consideration for the generation of fragility curves.

In the current design and construction philosophy of the ordinary highway bridges in Turkey, prestressed girders are delivered from production plants and other components of the bridge are constructed on the site. This method of construction is very rapid and bridge construction can be completed in a very short time period. However, for this construction approach the number of substructure is constraint to the length of the prestressed concrete I-girders that is the most frequently used superstructure beam type in the current applications. Since the feasible length of an I-girder is limited to 40m or less, different ways are sought to decrease the number of substructure in a bridge by engineers. One of the most frequently used methods is designing an inverted T cap beam to increase the span length of the bridge. Although using an inverted T cap beam is very simple, it is not an effective way of increasing the span length as well as decreasing the number of substructure in the bridge. On the other hand, highway bridges with an inverted T cap beam have significant differences in seismic behavior in comparison with the bridges having rectangular cap beam. Due to the occurrence of pounding between the superstructure prestressed girders and the inverted T cap beam in the longitudinal direction due to the longitudinal component of the ground motion; substantial increase in the internal forces of the substructure takes place (Ozkaya

and Caner, 2007). Also as per Caltrans (2006), inverted T cap beams may lead to poor longitudinal seismic response. Since the seismic response of bridges with an inverted T cap beam and with a rectangular cap beam has considerable differences, the two bridges should be considered separately. In this study, bridges with an inverted T cap beam are not investigated and the fragility curves are generated for the bridges with a rectangular cap beam. Although some of the bridges in Table 2.5 have inverted T cap beam, their structural characteristics are similar compared to the bridges with rectangular cap beam. Therefore, not to decrease the number of inventory data, some basic structural attributes of these bridges are used for the bridge classification and sampling stages.

2.2.2 Parameters Influencing Response of Bridges

The statistical distributions of some of the important structural attributes of the bridges are determined considering the associated bridge inventory data. Histograms of the investigated structural attributes are obtained and presented in the following figures. Some of the investigated structural attributes are;

- *Skew Angle:*
Skew angle distribution of the inventory data is presented in Figure 2.2. As shown in Figure 2.1, skew angle is the angle between the line perpendicular to the bridge center line and the center line of the bridge substructure. In general, bridges have skew angle less than 30° varying between 0° and 10°, which means that the number of irregular bridges due to skewness is less throughout the inventory data. But a uniform distribution can be accepted for the skew angle variation. Effect of skewness on the seismic response of bridges is very significant and it should be taken into consideration for estimating the actual seismic behavior of the highway bridges.

- *Span Number:*
All the bridges in the data are multiple-span simply supported bridges. Single span bridges are not taken into account in this study. A single-span (SS) bridge is

comprised of a superstructure supported by two abutments without any intermediate bent system. The reason for neglecting the single-span (SS) bridges is that SS bridges are considered to be less vulnerable in comparison with multiple-span bridges for seismic actions as per AASHTO LRFD (2007) and FHWA (1995). Hence it is mentioned that no detailed seismic structural analysis is required for a single span bridge regardless of seismic zone. Moreover, single span bridge damage due to past earthquakes is very rare in comparison with the multiple-span bridge damage. The distribution of span number for the multiple span bridges is presented in Figure 2.3. More than half of the bridges in the data have 2 spans. The span number has also considerable effect on the seismic response of the bridges.
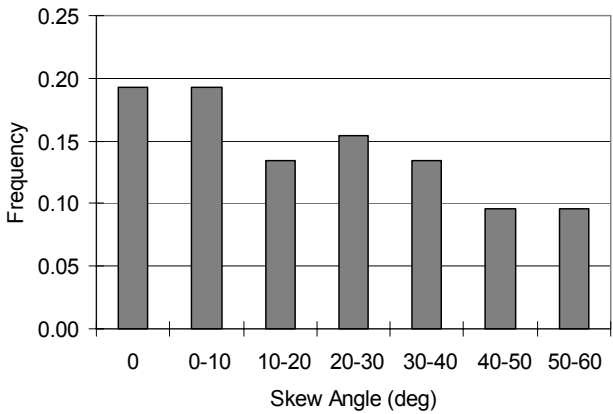
Figure 2.2 Distribution of skew angle
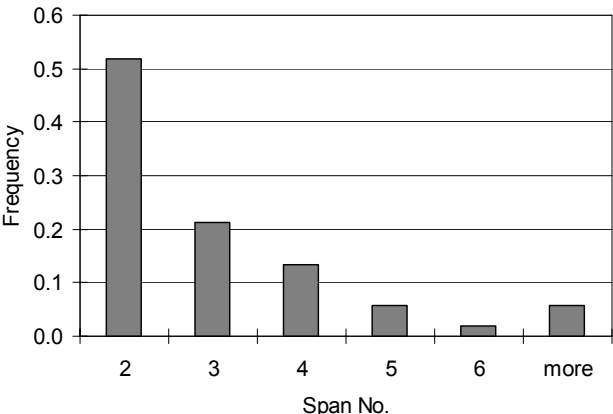
Figure 2.3 Distribution of span number

- Span and Total Length:

The distributions of maximum span length and total bridge length are shown in Figure 2.4 and Figure 2.5, respectively. The maximum span length of the bridges varies between 15m to 30m and its distribution resembles normal distribution. Some of the bridges in the inventory data do not have a constant span length value. As a common application, maximum span length is observed at the intermediate bridge spans. Maximum span length of the bridge has a direct influence on the dynamic behavior of the bridge systems. The longer the maximum span length, the greater the superstructure mass.
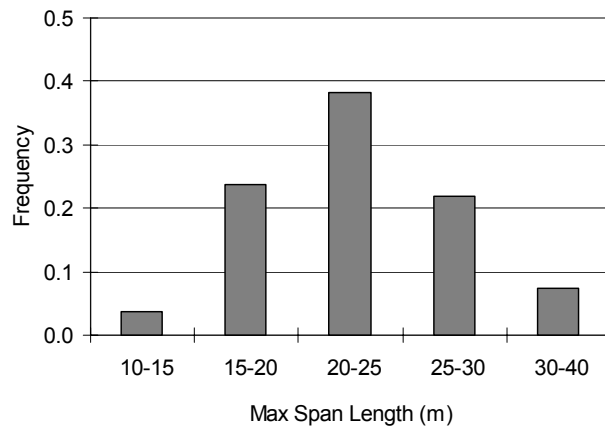
Figure 2.4 Distribution of maximum span length
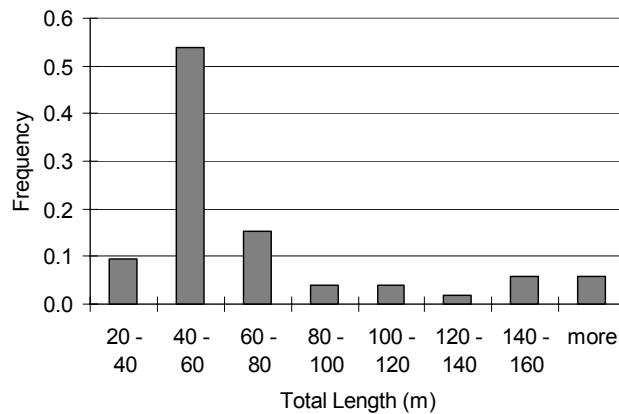
Figure 2.5 Distribution of total length

For the associated bridge inventory data, approximately 85-90 percent of the total mass of the bridge system originates from the superstructure mass. Therefore, seismic response of the highway bridges is affected by the superstructure mass. The total length of the bridges varies between 40m to 200m. However, more than half of the bridges have a total length between 40m to 60m.

- Column Height and Spacing:

Figure 2.6 shows the column height distribution, which varies between 3.0m and 13.0m. Column height is measured from top of the pile cap to the bottom surface of the cap beam. Most of the bridges in the data have column height changing between 6m and 9m. Column spacing for the multiple column bents is considered to be one of the most remarkable structural attributes of the bridge bent. Bent aspect ratio, L/H distribution over the inventory data is given in Figure 2.7. ATC-32 (ATC, 1996) and Priestley et al. (1996) stated that the displacement ductility of the bent system is related to the bent aspect ratio, L/H. Generally L/H ratio varies between 0.5 and 1.25.
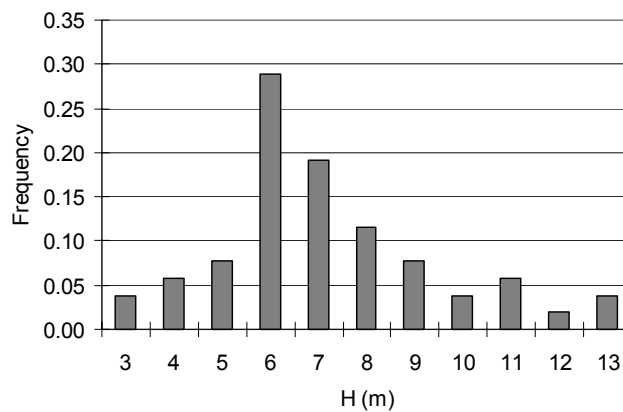
Figure 2.6 Distribution of column height

- Bent Column Number and Column Section Depth:

Multiple-column bents have different number of columns per bent. Figure 2.8 shows that more than 60 percent of the bents have two column bents. In addition to

the column number distribution, column dimensions are also necessary for classifying the bridges with respect to the structural attributes of the bent systems. All the bridge columns have a cross section of a rectangular inner section and two half circles at the rectangle end as shown in Figure 2.1. The great majority of the columns have a width of 1.0m. The distribution for the column section depth in its strong axis is presented in Figure 2.9. The column section depth for the strong axis varies between 2.0m and 3.0m for the multiple-column bent. The joint distribution for the number of columns per bent and column section depth is shown in Figure 2.10. Most of the multiple-column bents have two columns with a section depth of 2.5m in its strong axis.
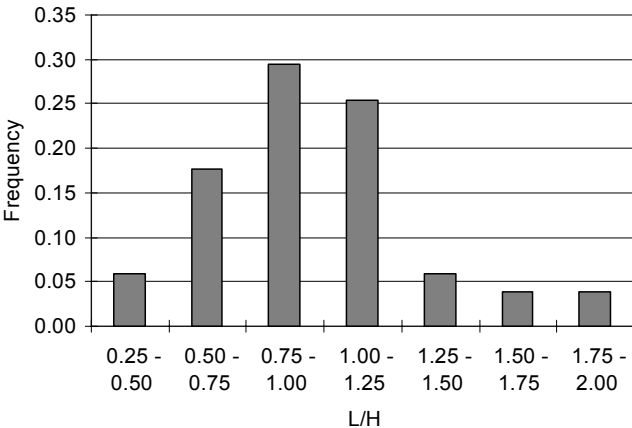
Figure 2.7 Distribution of L/H ratio of the multiple column bents
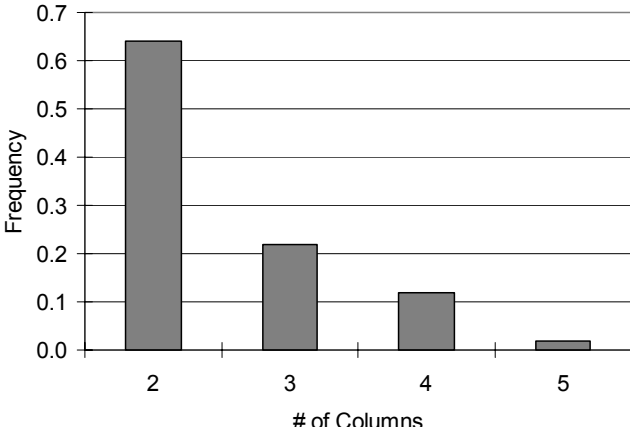
Figure 2.8 Distribution of column number per multiple column bent
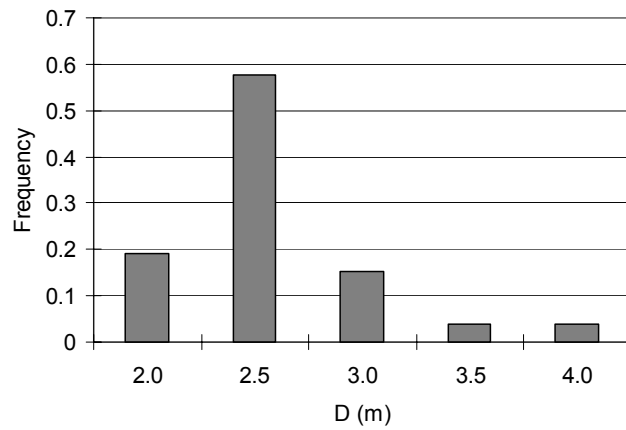
Figure 2.9 Distribution of column section depth
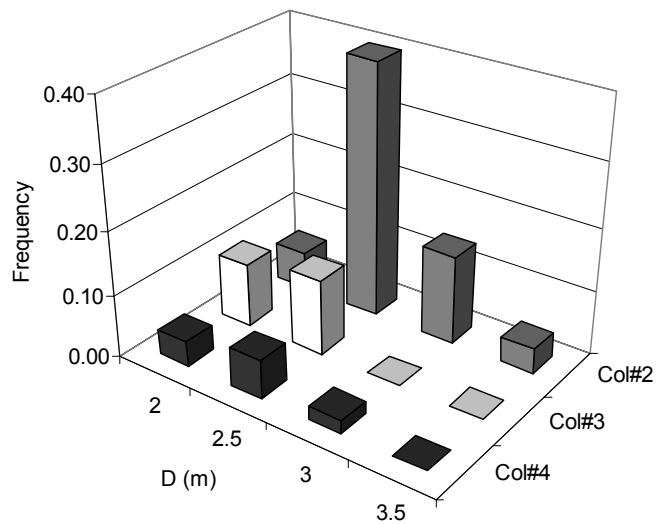
Figure 2.10 Distribution of column section depth and column number

- Cap Beam to Column Inertia Ratio:

According to Caltrans (2006), nonlinearity takes place only at the columns through formation of plastic hinges at the member ends and the rest of the bridge components remain essentially elastic, which is very beneficial and practical for the maintenance and retrofit purposes. That is why in multiple-column bents cap beams are designed to be stronger than columns according to the current design philosophy

of the bridge design practice in the US (ATC-32, 1996). However, this is just the opposite in comparison with the bridge design practice for the Turkish highway bridges that are constructed after the 1990s. As can be seen in Figure 2.11, almost all of the bridges have beam to column inertia ratio less than 0.15, indicating that cap beams are weaker than columns. The effect of cap beam to column inertia ratio on the transverse response of multi column bridge bents has a considerable impact on the seismic behavior of the bridge (Avsar et al., 2008). When the cap beams are weaker than columns, plastic hinges initiate at the cap beams before the column reaches its overstrength capacity. In such cases, seismic damage can localize in the cap beams, which can lead to lower displacement ductility capacity in the transverse direction as well as occurrence of seating problem or even unseating can take place.
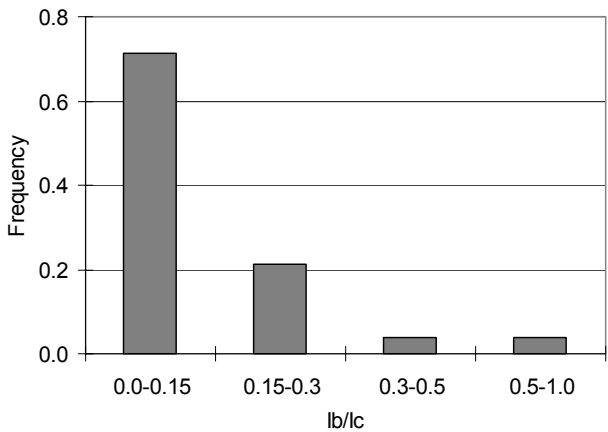
Figure 2.11 Distribution of beam to column inertia ratio

- Seat Length:

The superstructure supports at the abutment or bent cap beams must be of sufficient length to accommodate relative displacements. Minimum seat length requirement given in Equation (2.1) of the AASHTO (1996) for the most unfavorable seismic performance category is examined for the bridges in the inventory data.

$$N = (305 + 2.5L + 10H) \cdot (1+0.000125S^2) \qquad (2.1)$$

N: required minimum seat length [mm]

L: span length, [m]

H: column height, [m]

S: skew angle, [°]

The distribution of seat length and the ratio of required seat length specified in Equation (2.1) to the existing seat length are shown in Figure 2.12. Available seat length of the existing highway bridges are considered as the minimum seat length provided at the abutment or bent cap beams as schematically shown in Figure 2.13. Except for one bridge, adequate amount of seat length is provided with respect to the code requirements for all bridge samples.
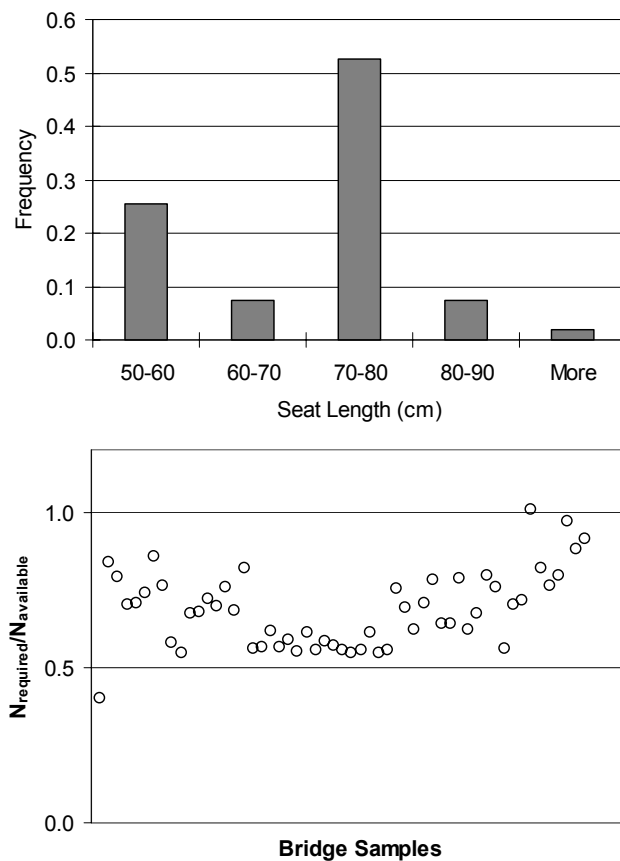
Figure 2.12 Distribution of seat length and the corresponding required to available ratio

38
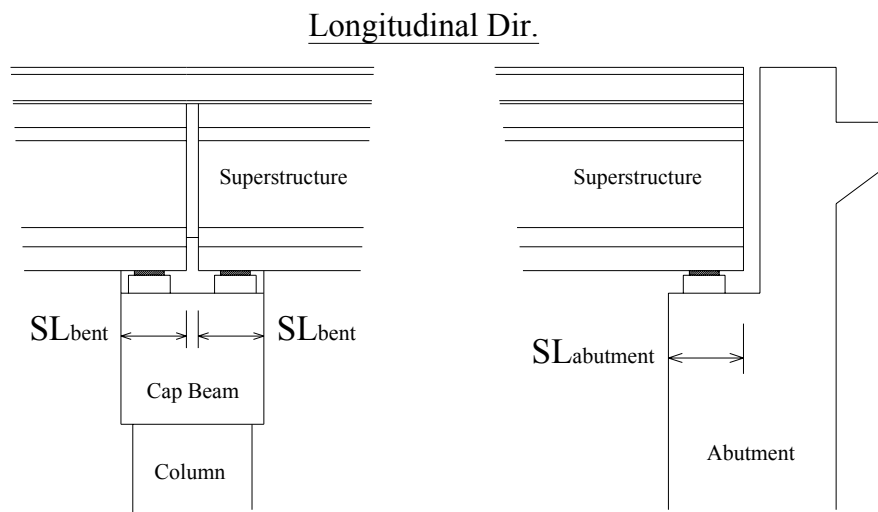
Figure 2.13 Determination of minimum available seat length

- *Superstructure Girder Spacing:*

Finally, in Figure 2.14, the distribution for the type of prestressed girder spacing is given. Two common types of girder spacing are schematically depicted in Figure 2.1, which are either closely spaced or widely spaced. Construction of bridges with closely spaced prestressed girders, which is the most common application, is easier than the widely spaced girders. Diaphragm beams should be constructed at the ends at the bridge site providing a diaphragm effect for the widely spaced prestressed girders. Depending on the span length of the bridge, it is required to apply diaphragm beams at the intermediate locations of the prestressed girders. Although the required prestressed girder depth is less for the closely spaced girders in comparison with the ones for widely spaced girders, the mass placed at the superstructure is more due to the excessive number of prestressed girders.
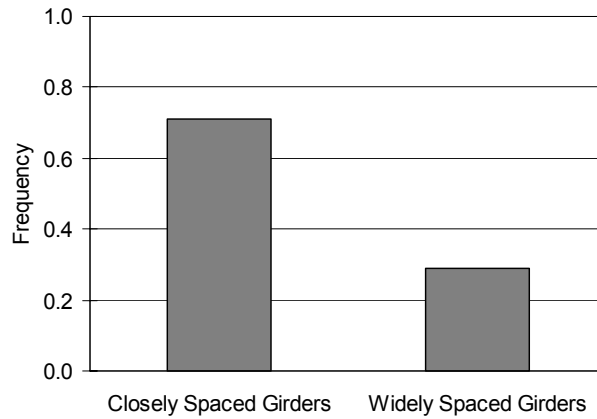
Figure 2.14 Distribution of prestressed girder spacing

- Bridge Deck Width:

The distribution of the total width of the bridge deck is given in Figure 2.15. The bridge deck width is determined with respect to the number of traffic lanes necessary for the highway. More than half of the bridges have a total bridge deck of 13m to 14m.
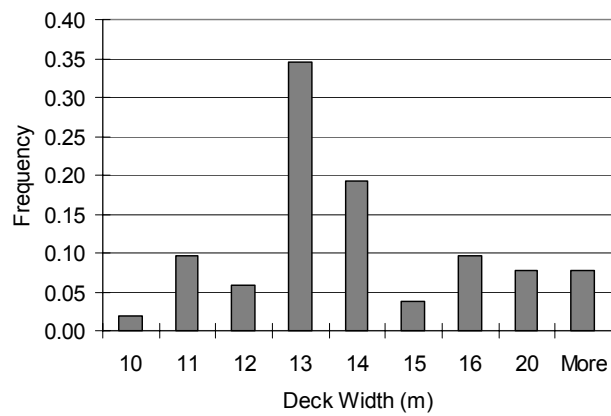
Figure 2.15 Distribution of bridge deck width

2.3   MAJOR BRIDGE CLASSES

Major bridge classes are specified by considering important structural attributes of the highway bridges. When the number of structural attributes explained in the previous section is considered, it is not appropriate to take into account all the structural attributes for generating the major bridge classes. Therefore, the most significant bridge structural attributes, which influence the seismic response of the bridges considerably, need to be determined. Data available from past earthquake reports and previous studies are considered during the selection of the most influential structural attributes. The most important bridge structural attributes such as span number, bent column number and skew angle are designated as the primary structural attributes for the associated bridge inventory data. The rest of the structural attributes are specified as the secondary structural attributes. Major bridge classes are formed using the primary structural attributes of the bridges.

Most of the previous studies such as Basoz and Kiremidjian (1997), HAZUS (FEMA, 2003), Nielsen (2005) take into account the span number as multi-span (MS) or single-span (SS). In the past earthquakes SS bridges performed far better than the MS bridges. As mentioned previously, SS bridges are not taken into account in the study. All the major bridges and their associated samples are MS bridges.

The other most important bridge structural attribute is the bent column number, which is considered as either single-column bent or multiple-column bent in the previous studies of Basoz and Kiremidjian (1997) and HAZUS (FEMA, 2003). Priestley et al. (1996) and ATC-32 (ATC, 1996) investigated the single column bents and multiple-column bents separately and it is mentioned that multiple-column bents can be more susceptible to early damage due to the flexibility of the bent cap beams. Also, Avsar et al. (2008) mentioned that damage initiates at the cap beams first for the multiple-column bents, when the cap beams are designed weaker than columns. On the other hand, column damage is more pronounced for the seismic performance of highway bridges. Since there is no

possibility for the redistribution of seismic forces for single-column bents, any column damage will directly affect the seismic performance of the bridge. Basoz and Kiremidjian (1997) mentioned that, bridges with single column bent performed poorly during the Loma Prieta and Northridge Earthquakes. Also, they stated that the substructure bent column number either single-column or multiple-column play an important role on the damage level that the bridge experiences. In this study, major bridges are classified as either single-column or multiple-column bent according to the bent column number.

Skewness is the last primary structural attribute that is considered for the arrangement of major bridge classes. Skew angle is considered to be a major effect on the performance of bridges and it is agreed that skewed bridges are more vulnerable to seismic effects in various codes and research studies such as FHWA (1995), Basoz and Kiremidjian (1997) and Pamuk et al. (2005). Also, Buckle (1994) illustrated some failed or damaged highway bridges that are associated with large skews during the Northridge Earthquake. In this study two types of highway bridges are formed considering the skewness of the bridges. For the first type, irregularity due to skewness and hence its effect on the seismic response can be neglected for the bridges with small skew angle. For the second type, bridges have greater skew angles and therefore they have considerable irregularity affecting their seismic performance adversely. In order to specify the two bridge types a limiting skew angle value is required, so that the bridges can be classified as skewed or non-skewed using the skewness limit. Bridge irregularity due to skewness is not negligible for the skew angle greater than the specified skewness limit. The skewness limit is specified as 20° by Caltrans (2006), FHWA (1995) and Pezeshk et al. (1993). But in AREMA (1998) and AASHTO (1996) angle of 30° is specified as the limiting skew angle for the irregularity specification of skewed bridges. There is no definite limiting skew angle value, but it varies between 20° and 30° according to codes and previous studies. Since the skew angle variation is between 0°-60° through the sample bridges in the inventory data (Figure 2.2), the median value of 30° is considered as the limit skew angle value for the bridge classification.

Considering the primary structural attributes of the highway bridges, 4 major bridge classes are formed. The four major bridge classes given in Table 2.6 represent the general properties of the bridges in the inventory data. Sample bridges will be formed considering the secondary structural attributes for each major bridge class.

Table 2.6 Major bridge classes

No.	Bridge Classes	Abbreviation
1	Multi Span_Multiple Column_Skewness Less than 30°	MS_MC_SL30
2	Multi Span_Multiple Column_Skewness Greater than 30°	MS_MC_SG30
3	Multi Span_Single Column_Skewness Less than 30°	MS_SC_SL30
4	Multi Span_Single Column_Skewness Greater than 30°	MS_SC_SG30

2.4 BRIDGE SAMPLES FOR THE MAJOR BRIDGE CLASSES

Fragility curves for the major bridges defined in Table 2.6 will be developed for different damage limit states. The curves reflect the probability of exceeding a certain damage state for the sample bridges those are representative of the major bridge classes for which the fragility curve will be developed. It is important that the selected bridge samples, which are used in the calculations of fragility curves, should provide sufficient level of structural variability for the fragility analysis. Therefore selection of sample size has a direct influence on the structural variability and consequently the reliability of the fragility curves. Choosing greater sample size enhances the sensitivity of the fragility curves. On the other hand, modeling and computation effort required for the analysis of too many samples make the development of fragility curves complicated and time demanding. Therefore, it is decided to select the sample size for each major class at a manageable level, but at the same time structural variability could be reflected in the fragility curves. In the studies of Shinozuka et al. (2000a), Hwang et al. (2001) and Choi et al. (2004), a set of 10 nominally identical but statistically different bridge samples were developed

for each bridge type employed in the development of analytical fragility curves. In this study, for each major bridge class 10 bridge samples will be developed considering secondary structural attributes of the bridges.

In some of the previous research studies such as Shinozuka et al. (2000b) and Elnashai et al. (2004), analytical fragility curves for certain bridge types were developed considering representative sample bridges, which were formed by varying only the mechanical and the material properties of the reinforced concrete members. In other words, structural variability in the fragility curves was taken into consideration through the variability in the mechanical and the material characteristics of the bridge components. For instance, the variation in the reinforcement yield strength, compressive strength of concrete or the concrete strain at the peak compressive stress are some of the material variability parameters considered in the modeling. However, variability in the geometry and the configuration of the bridge systems is far more pronounced in the structural variability in comparison with the influence of the mechanical and material variability. Moreover, according to the blueprints for the bridges of the inventory data similar materials are used for the construction of the bridge components. Therefore, material variability is negligible throughout the bridges in the inventory data.

Secondary structural attributes described in the previous sections are considered for the generation of 10 bridge samples for each major bridge class. Although, sample bridges show some structural differences as well as variations in the bridge configuration, they have the similar primary structural attributes representing the corresponding major bridge class. The description of the structural attributes that make the differences between bridge samples and their statistical distributions through the inventory data and the corresponding distribution parameters are shown in Table 2.7 for each major bridge class. Some of the secondary structural attributes of L/H ratio, I_b/I_c ratio, bent column number, column section depth, prestressed girder spacing, deck width, etc. are taken into account implicitly by considering different types of superstructures and substructures. Also,

the total length is related to the span length and number of spans of the bridge, it is not considered explicitly.

Table 2.7 Structural attributes of the sample bridges and statistical distributions

Modelling Parameter	Probability Distribution	MS_MC_SL30 Parameters		MS_MC_SG30 Parameters		MS_SC_SL30 Parameters		MS_SC_SG30 Parameters	
		1	2	1	2	1	2	1	2
Span Length [m]	Normal	μ=23.8	σ=6.1	μ=23.8	σ=6.1	μ=23.8	σ=6.1	μ=23.8	σ=6.1
Col Height [m]	Normal	μ=6.73	σ=2.04	μ=6.73	σ=2.04	μ=6.73	σ=2.04	μ=6.73	σ=2.04
Span No.	Discrete	2-3-4-5		2-3-4-5		2-3-4-5		2-3-4-5	
Skewness [°]	Uniform	l=0	u=30	l=30	u=60	l=0	u=30	l=30	u=60
Superstructure Type	Discrete	Type-1 / Type-2		Type-1 / Type-2		Type-1 / Type-2		Type-1 / Type-2	
Substructure Type	Discrete	Type-1 / Type-2		Type-1 / Type-2		Type-3		Type-3	

Considering the histograms for the structural attributes of span length and the column height given in Figure 2.4 and Figure 2.6, normal distributions are specified with the mean and standard deviations given in Table 2.7. Some of the bridges in the inventory data have variable span length at different spans or variable column height at different bents because of the constraints due to the topography of the bridge site. Generally, end span lengths are shorter than the intermediate span lengths and mid bents have taller columns in comparison with the other bent columns. In this study, it is assumed that each generated sample bridge has a constant value of span length and column height for each span and bent column, respectively. Since a convenient probability distribution function cannot be assigned for the span number variation shown in Figure 2.3, discrete distribution is considered. When the span number distribution and sample size is considered, it is decided to generate 5 samples with 2 spans, 2 samples for each one of 3 and 4 spans and 1 sample with 5 spans of bridges. As mentioned previously, a uniform distribution with the parameters given in Table 2.7 can be considered for the skew angle variation according to Figure 2.2. Uniform distribution of the bridges having skew angle less than 30° (SL30) has the lower and the upper limits of 0° and 30°,

respectively. These limits are taken as 30° and 60° for the bridges having skew angle greater than 30° (SG30).

Two types of superstructures, which are the most frequently utilized, are considered to represent the structural variability for the structural attributes of the superstructures (Figure 2.16). In the first type, 8 prestressed girders are widely spaced under the 22 cm RC deck. Girders are connected to each other with the end diaphragm beams. The second type of superstructure has closely spaced 16 prestressed girders without any diaphragm beams. Type I girders are deeper than the type II girders.
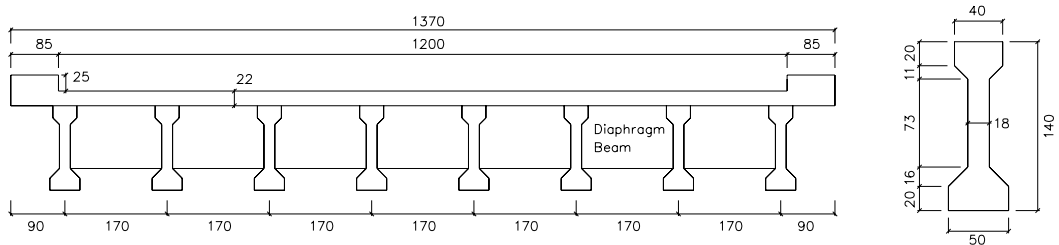
a) Superstructure Type I: Widely Spaced Girders
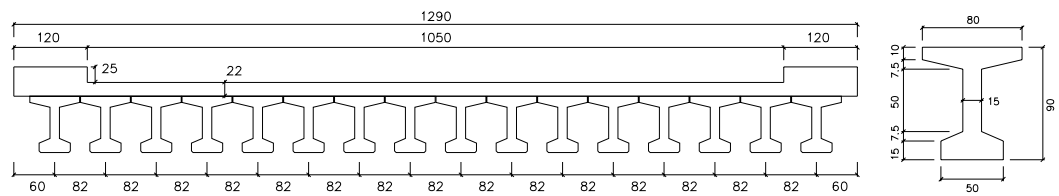
b) Superstructure Type II: Closely Spaced Girders

Figure 2.16 Superstructure types

Finally, structural variability for the structural attributes of the substructures is taken into account by considering the most frequently utilized substructures. For the multiple-column bents two different substructure types are employed (Figure 2.17). Substructure type-I is a three column bent with a column section depth of 2.0m, whereas type-II is a two column bent with a column section depth of 2.5m.

Beam to column inertia ratio of the type-I and type-II substructures are 0.27 and 0.13, respectively. For a single column bent bridge, the structural variability arises only due to the section dimensions of the column and cap beams. In order to simplify the calculations, the most frequently utilized substructure type is employed for the calculations. Although variability for the elastomeric bearing properties is not considered in the sampling procedure explicitly, different elastomeric bearings are employed for each substructure type. The dimensions of the bearings for each substructure type have been included in their drawings in Figure 2.17.
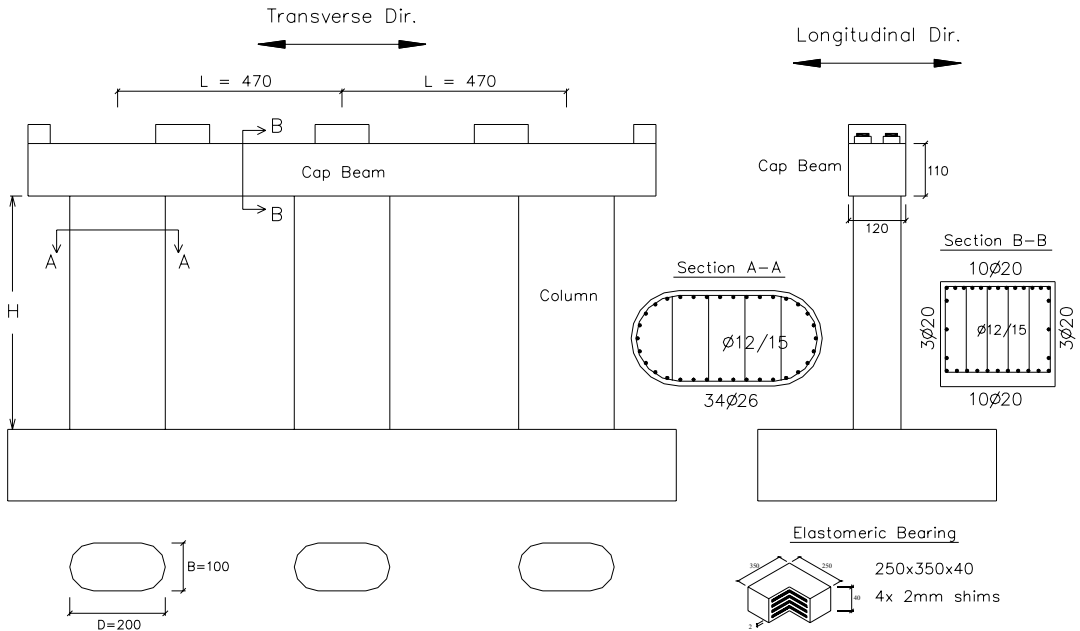
a) Substructure Type-I: Multiple column bent with three columns

Figure 2.17 Substructure types
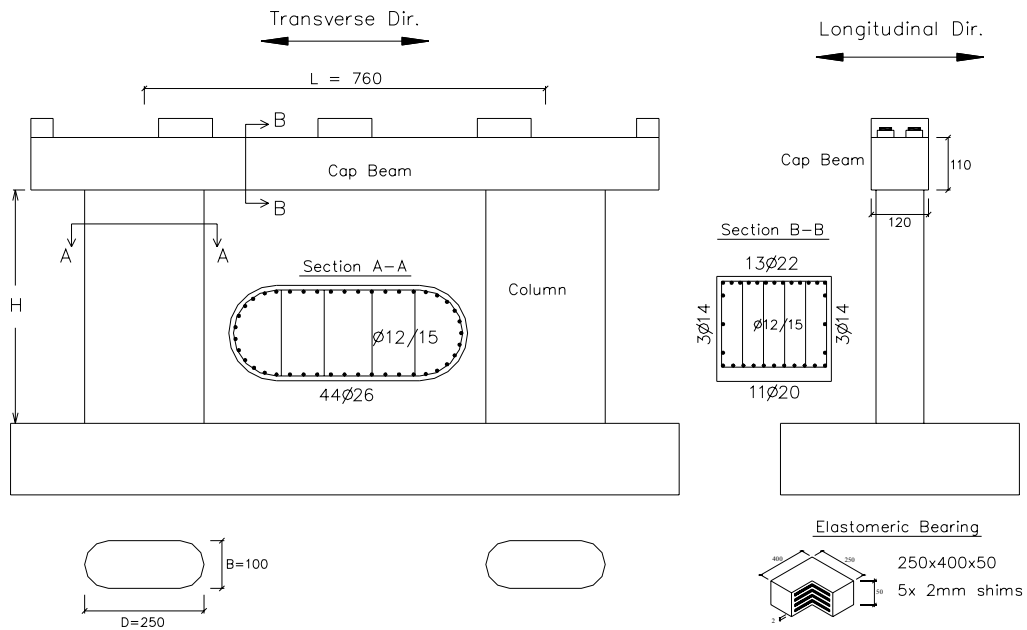
b) Substructure Type-II: Multiple column bent with two columns
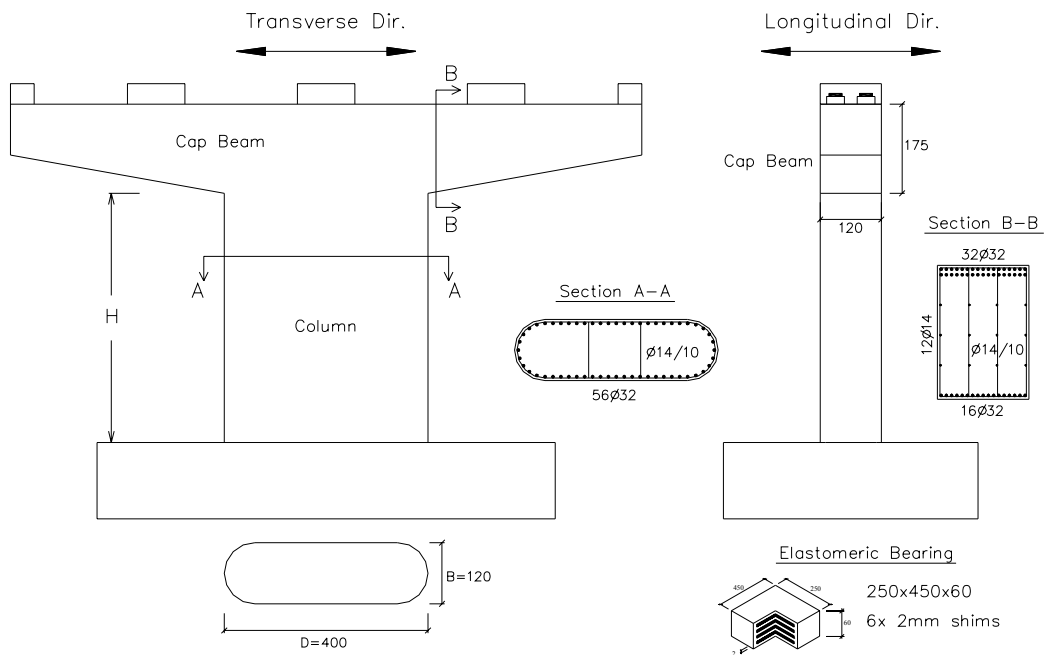
Substructure Type-III: Single column bent

Figure 2.17 Substructure types

2.4.1 Sampling Method

A sampling technique is required for generating a representative group of samples with a manageable number through a large population. By this way the investigated behavior of the population can be estimated by analyzing the representative samples. The Monte Carlo Simulation is the most commonly employed method as a sampling technique. In order to simulate the system of variables with a probability distribution, Monte Carlo method takes randomly generated values into consideration. Although this simulation technique is a straightforward method as well as a powerful sampling tool, a large sample size is needed even for simple systems to satisfy a certain level of accuracy in the estimation. It is neither practical nor feasible to deal with complex systems with a large sample size. As an alternative method, Latin Hypercube Sampling technique is employed in this study. Latin Hypercube Sampling method considers a constrained sampling approach instead of randomly selected samples (Ayyub and Lai, 1989). With the help of this feature, smaller sample size suffices for reliable estimates.

During the sampling process of the major bridge classes, instead of selecting each structural attribute given in Table 2.7 randomly, selection is made in a way that the selected attributes will be consistent with the statistical distribution of the structural attributes. This is achieved by dividing the probability distribution of each structural attribute into the number of selected sample size, so that regions having the same selection probabilities $P(x) = 1/n$, could be generated on the probability distribution function of the structural attributes. A randomly selected value of the structural attribute from each generated region on the distribution function will be used to form the desired number of bridge samples. By using this method, distribution of each structural attribute could be taken into consideration with a relatively small number of samples. The application of the Latin Hypercube Sampling technique on the sampling of span length with a normal distribution and skew angle with a uniform distribution is shown in Figure 2.18 for both on the probability distribution function and cumulative distribution function.
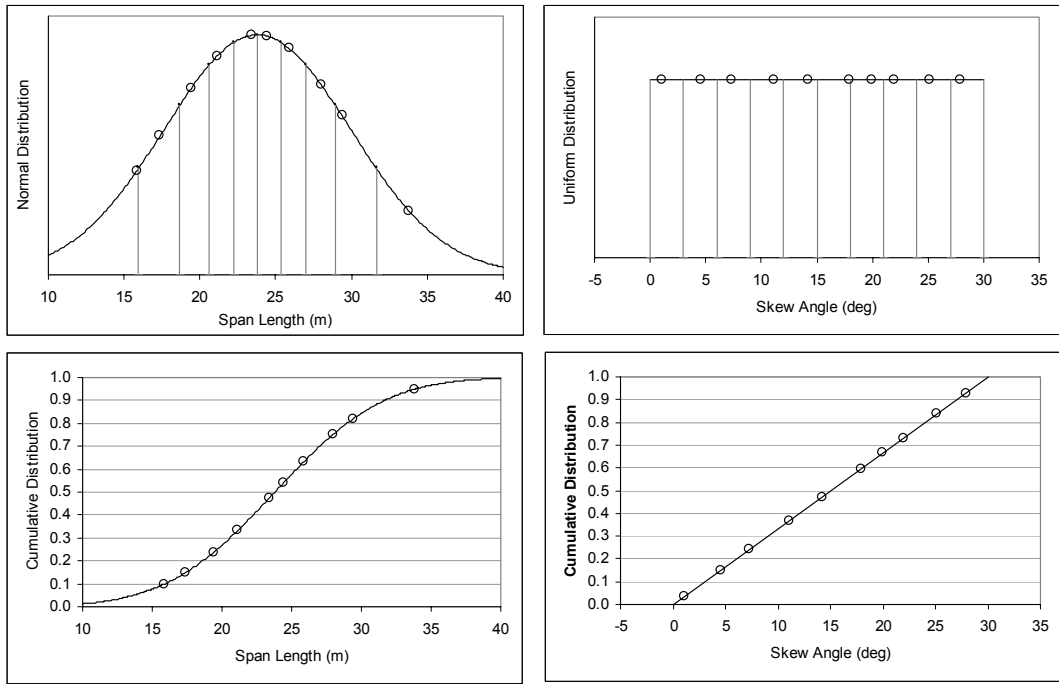
a) Span Length Sampling   b) Skew Angle Sampling

Figure 2.18 Determination of sample bridge attributes using Latin hypercube
sampling technique for a sample size of 10

The selection of the structural attributes of span number, substructure and
superstructure types, which do not have a relevant probability distribution functions,
will be made randomly for sampling. After employing the Latin Hypercube
sampling for the span length and skew angle, uneven results are estimated for these
structural attributes. In order to deal with precise numbers for these attributes, the
estimated results are rounded to the nearest numbers with an order of 5. On the
other hand, after the application of sampling technique, samples of various
structural attributes are calculated with an increasing order. If the arrangement of
the bridge samples will be made in the order of structural attribute samples, bridge
samples with structural attributes all having smaller values or greater values will be
generated. In order to prevent such kind of irrelevant generation of bridge samples,
samples of structural attributes are selected randomly. Finally, structural attributes
of the 10 sample bridges for each major class are specified and presented in Table
2.8.

Table 2.8 Structural attributes for the 10 bridge samples for each major bridge class

a) Multiple-Column Bent Bridges (MS_MC_SL30 and MS_MC_SG30)

Sample ID	Span Length (m)	Number of Spans	Column Height (m)	Superstructure Type	Substructure Type	L/H	MS_MC_SL30 Skew Angle (°)	MS_MC_SG30 Skew Angle (°)
1	20.0	3	7.3	2	2	1.03	5	35
2	35.0	4	8.7	1	1	0.54	25	55
3	15.0	2	4.0	1	1	1.19	20	50
4	20.0	2	5.6	2	2	1.35	10	40
5	30.0	4	7.8	2	1	0.60	20	50
6	25.0	5	9.6	2	2	0.79	15	45
7	20.0	2	6.7	1	1	0.70	20	50
8	25.0	2	6.2	1	2	1.23	30	60
9	30.0	2	4.3	1	1	1.09	0	30
10	25.0	3	7.2	2	2	1.05	5	35

b) Single-Column Bent Bridges (MS_SC_SL30 and MS_SC_SG30)

Sample ID	Span Length (m)	Number of Spans	Column Height (m)	Superstructure Type	Substructure Type	MS_SC_SL30 Skew Angle (°)	MS_SC_SG30 Skew Angle (°)
1	20.0	3	7.3	2	3	5	35
2	35.0	4	8.7	1	3	25	55
3	15.0	2	4.0	1	3	20	50
4	20.0	2	5.6	2	3	10	40
5	30.0	4	7.8	2	3	20	50
6	25.0	5	9.6	2	3	15	45
7	20.0	2	6.7	1	3	20	50
8	25.0	2	6.2	1	3	30	60
9	30.0	2	4.3	1	3	0	30
10	25.0	3	7.2	2	3	5	35

The elastic fundamental periods for the samples of major bridges are calculated by modal analysis (Table 2.9). Since the superstructure is isolated from the substructures by elastomeric bearings, the elastic fundamental period depends on mostly on the stiffness of the elastomeric bearings and the superstructure mass. The minimum and the maximum periods are determined as 0.47s and 0.98s, respectively. These periods will be utilized in the selection process of earthquake ground motions.

Table 2.9 Elastic fundamental periods of the major bridges and their samples

Bridge Sample ID	MS_MC_SL30	MS_MC_SG30	MS_SC_SL30	MS_SC_SG30
1	0.55	0.57	0.53	0.56
2	0.94	0.98	0.93	0.98
3	0.48	0.50	0.49	0.51
4	0.47	0.50	0.47	0.51
5	0.72	0.76	0.71	0.77
6	0.79	0.84	0.76	0.81
7	0.60	0.62	0.60	0.63
8	0.67	0.70	0.67	0.71
9	0.68	0.69	0.69	0.70
10	0.61	0.64	0.59	0.62
min	0.47	0.50	0.47	0.51
max	0.94	0.98	0.93	0.98

CHAPTER 3

ANALYTICAL MODELING OF BRIDGES

Analytical models of the bridge samples need to be formed to calculate their seismic response, which are used in the development of analytical fragility curves. Overall structural displacements, member forces, and local deformations of the bridge samples are analytically determined using mathematical models and analysis tools to quantify the seismic response of the bridges. Analytical bridge models will be developed by making certain assumptions and simplifications during the modeling of the bridge as a whole system and its components. Since the assumptions made during the modeling stage have a direct influence on the analysis results as well as the reliability of the fragility curves, special care is given when simplifications are necessary. Bridge models should be generated in detail with a sufficient level to be manageable and also the analytical model can be controlled easily at every stage when required. Dealing with a very detailed and complicated bridge model is not only computationally demanding but also it can lead to an unrealistic analytical model that is out of control. Therefore, analytical bridge models should be as simple as possible so that the model can be formed easily and the time required for the analysis and evaluation of the results should not be excessive. And finally, the most important criterion during the modeling process is the correct modeling to estimate the actual seismic response of the bridges. As shown in Figure 3.1, Priestley et al. (1996) schematically represent the various levels of modeling for seismic bridge analysis ranging from lumped-parameter models and structural component models to detailed finite-element models.
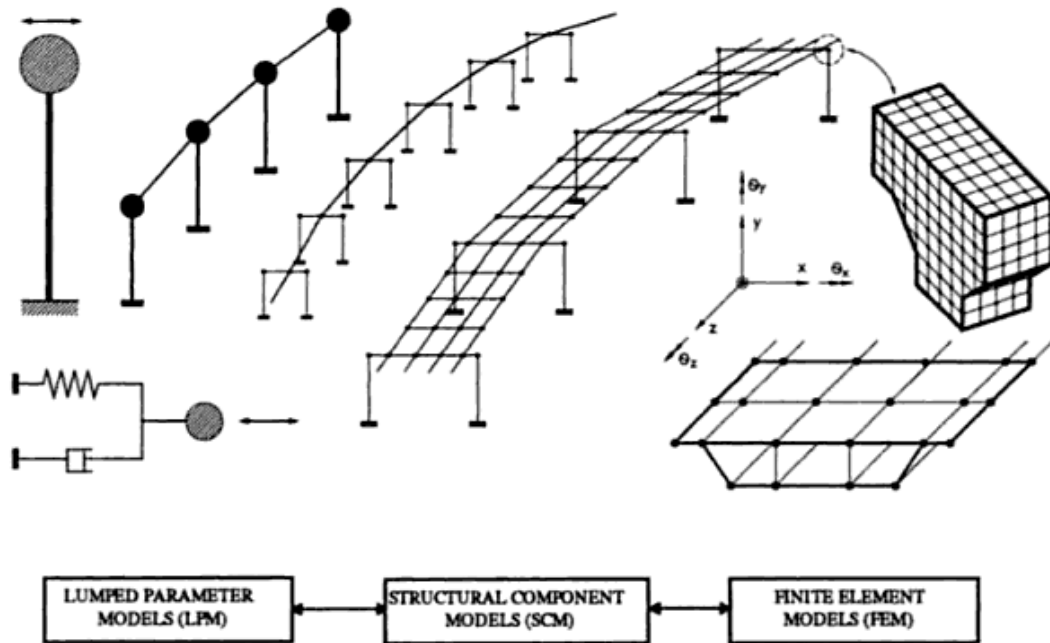
Figure 3.1 Levels of modeling for seismic bridge analysis (Priestley et al., 1996)

Bridge structural properties such as mass, stiffness, and damping are lumped or concentrated at discrete locations for the lumped-parameter models. Although simple mathematical formulations are sufficient for the modeling, significant knowledge and experience is required to represent the true seismic behavior of the bridges. Structural component models are based on idealized structural subsystems and bridge components whose response characterization is specified in the form of member end force-deformation relationships. In the finite-element models, a bridge structure is discretized with a large number of small elements having performance characteristics obtained directly from the constituent structural materials. The geometric discretization effort as well as the time required for the structural analysis increase significantly from the lumped-parameter models to the structural component models and to the finite-element models. On the other hand, the modeling effort in terms of individual member characterization can be automated to a large degree in finite element models but requires significant definition and engineering judgment for structural component and lumped-parameter models. The

54

computation effort as well as the time required for the analysis depends on the selection of analysis tool, which ranges from simple linear elastic analyses to nonlinear dynamic response history analyses for the seismic response quantification of bridges. According to ATC-32 (ATC, 1996), the analytical models are classified into "Elastic Static Analysis", "Elastic Dynamic Analysis", "Inelastic Static Analysis", and "Inelastic Dynamic Analysis". Although nonlinear response history analysis has some shortcomings such as it may suffer from convergence problems or computational stability and require considerable amount of run time and post processing efforts, it is accepted as the most accurate simulation tool combining the nonlinear component characterization and a simulated seismic excitation for a direct estimation of bridge seismic response. In this study, structural component models for the bridge system will be utilized with the nonlinear response history analysis for estimating the seismic response of bridges.

Limitations and applicability of the modeling and analysis tools used for the assessment of bridge seismic response should be investigated whether these analytical models represent the actual seismic behavior of the bridges at a certain level of accuracy. However, due to the lack of instrumented bridges subjected to earthquakes, there is little opportunity to validate these bridge models. Nevertheless, experimental data available for the various bridge components as well as past earthquake experiences allow the development of appropriate bridge component models.

The dimension of the model should be specified at the first step for the analytically modeling of bridges, which is either 2-D or 3-D. 2-D analytical bridge model can be considered to be more attractive in terms of its simplicity as well as its convenience in the modeling and computation effort required. On the other hand, in a 2-D model, the critical bridge direction dominating its seismic response needs to be specified. As shown in Figure 3.2, the longitudinal or transverse direction of the bridge is considered in the modeling depending on the seismic behavior of the bridge. According to some of the previous studies (Rashidi and Ala Saadeghvaziri, 1997; Choi, 2002; DesRoches et al., 2004), bridge response is controlled by longitudinal direction of the bridge. Whereas in some other studies (Cheng et al.,

1998; Wissawapaisal and Aschheim, 2000), it is mentioned that the transverse response of bridges is often critical to their seismic performance. When transverse displacements are large, damage to substructure columns may occur, often in the form of plastic hinges, shear failures, or lap splice failures. However, in some cases, it is not possible to capture the actual seismic response of bridges only considering two dimensional analyses.
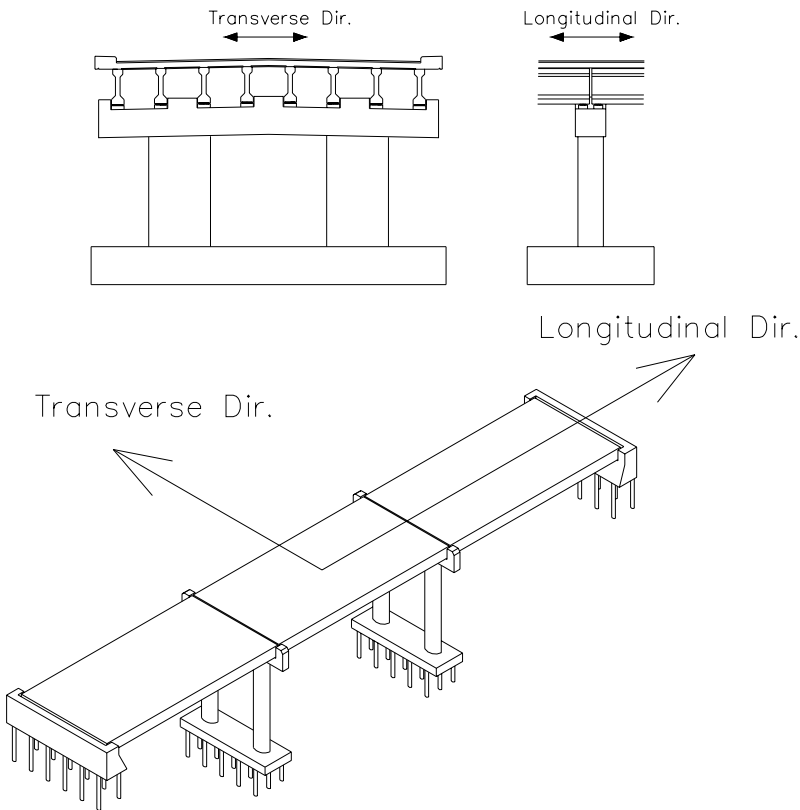
Figure 3.2 Longitudinal and transverse directions in the bridge modeling

Evident from recent severe earthquakes, in addition to the bridge response in longitudinal and transverse directions, rotation of superstructure caused by pounding especially for the skewed bridges has an adverse effect on the bridge response. 3-D bridge models are required to simulate the combined response of the bridge in the longitudinal and transverse directions (Hwang et al., 2000; Nielson,

2005; Zhu et al., 2002). Aviram et al. (2008) mentioned that a three-dimensional model of the structural system is required to capture the response of the entire bridge system and individual components under specific seismic demand characteristics. The interaction between the response in the orthogonal bridge directions and the variation of axial loads in column bents throughout the analysis are captured more accurately in a 3D model. This enables correct evaluation of the capacity and ductility of the system under seismic loads or displacements applied along any given direction, not necessarily aligned with the principal axis of the bridge.

3.1   SELECTION OF ANALYSIS PROGRAM

Development of three dimensional bridge models and performing their nonlinear response history analysis is a very complicated task that it is not possible to do it by simple hand calculations. All the necessary calculations and simulations will be done with the help of an analysis tool. It is required to select the most appropriate analysis tool, which is employed to model the bridge samples quickly under various earthquake ground motions for estimating the seismic response of the bridges as accurate as possible. For this purpose, a very simple analytical model for a bridge sample as shown in Figure 3.3 is generated using 4 different structural analysis software, which are OpenSees, SAP2000, SeismoStruct and LARSA. OpenSees and SeismoStruct are research-based, whereas SAP2000 and LARSA are commercial structural analysis software programs. In order to become familiar with the programs about their modeling and analysis capabilities as well as to make comparisons with each other, a linear elastic analytical model of a bridge sample is developed using each analysis software.

In addition to the modal analysis, linear response history analysis under an earthquake ground motion of the bridge sample is done using each analysis software. As given in Table 3.1, periods of the bridge sample for the first ten modes are calculated almost the same when the results of each software are compared. The longitudinal displacement history for the mid-point of the bridge sample is

presented in Figure 3.4 comparing the results of each software. Linear elastic analysis results revealed that displacement history of the bridge mid point in the longitudinal direction obtained from each program with a response of 10 seconds is almost identical.
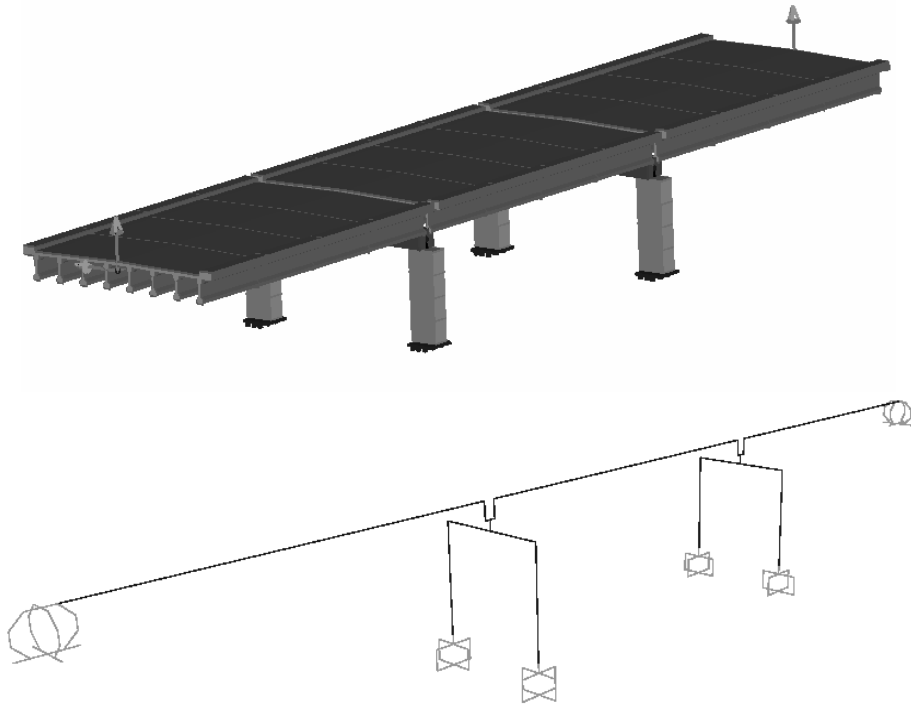
Figure 3.3 Simple analytical model of a 3 span bridge sample

Table 3.1 Modal analysis results of the sample bridge using different programs

	OpenSees	SAP	SeismoStruct	Larsa
Mode#	T (s)	T (s)	T(s)	T(s)
1	0.37218	0.37218	0.37218	0.37172
2	0.14782	0.14782	0.14782	0.14780
3	0.12651	0.12651	0.12651	0.12648
4	0.10140	0.10142	0.10142	0.10127
5	0.10017	0.10017	0.10017	0.10012
6	0.04819	0.04819	0.04819	0.04805
7	0.04512	0.04518	0.04518	0.04509
8	0.04325	0.04325	0.04325	0.04317
9	0.04014	0.04014	0.04014	0.04011
10	0.03933	0.03934	0.03933	0.03931

These results prove that the four analysis softwares used show a good agreement for the linear elastic analysis. However, bridge component models having nonlinear behavior are inevitable to capture the damage at the associated members as well as to estimate the true seismic response of the bridges. In Larsa, there are only lumped plasticity models for the nonlinear modeling of substructure components of column and cap beam, which are believed to behave in the inelastic range. Whereas, for the SeismoStruct, only limited number of cross section types are available for the fiber modeling of nonlinear components. Furthermore, when the two softwares of OpenSees and SAP2000 are compared, it is found out that OpenSees has superiority in the modeling of a large number of bridge samples having certain variable structural parameters. The distributed plasticity of the bridge components, which are expected to experience inelastic deformations, could be modeled through fiber based nonlinear beam-column elements effectively. The material and element library of OpenSees is much more extensive in comparison with the other softwares. Also, it is possible with OpenSees to analyze different bridge models under various number of earthquake ground motions applied in different directions without interrupting the program. Therefore, OpenSees is selected as the analysis software to perform nonlinear response history analyses for the bridge samples to estimate their seismic response under various intensities of seismic input.
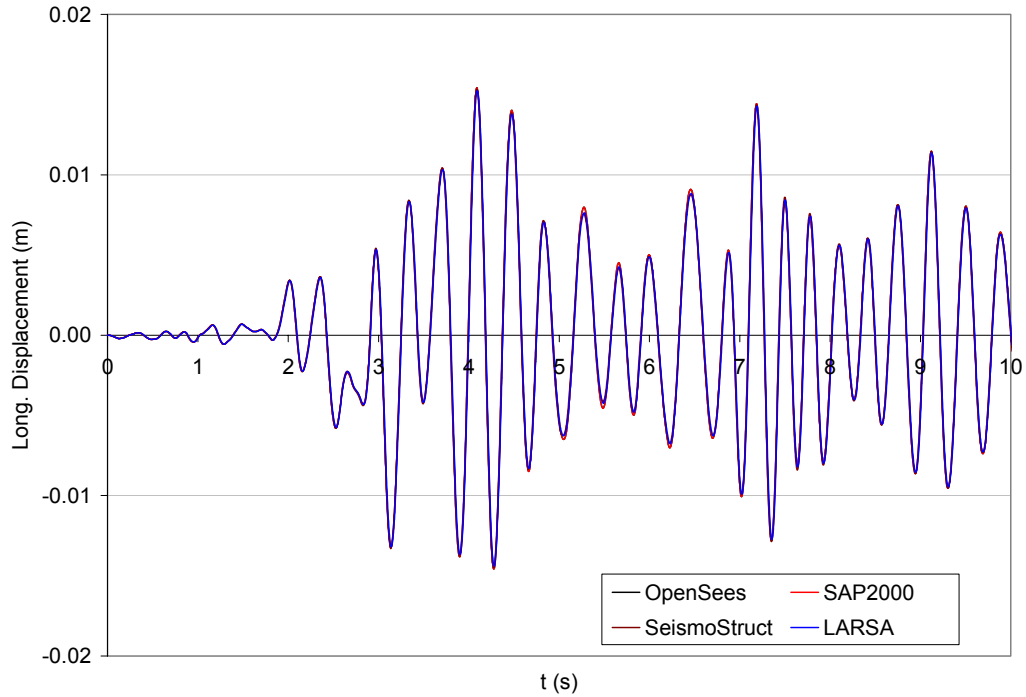
Figure 3.4 Longitudinal displacement of the sample bridge mid point

3.2   MODELING OF BRIDGE COMPONENTS

3-D analytical modeling of the bridges is done by structural component models. The performance of the highway bridges is highly dependent on the performance of individual components as well as the connectivity of these components. Therefore, the accuracy in the estimation of bridge seismic response relies on the bridge component analytical models that should represent the true seismic behavior of the structural components of the bridges. In general, structural components of the bridges can be classified into two groups, which are superstructure and substructure. Precast prestressed concrete girders and cast-in-place reinforced concrete deck constitute the superstructure of the bridge. Substructure is composed of abutments and the bent systems. Elastomeric bearings are placed in between the superstructure and substructure to be used as an isolation unit. Comprehensive analytical models for each of these bridge components will be developed in the OpenSees platform as shown in Figure 3.5 schematically.

60

Elastomeric bearing and the gap between superstructure and the substructure elements are modeled by using appropriate force deformation relationships.
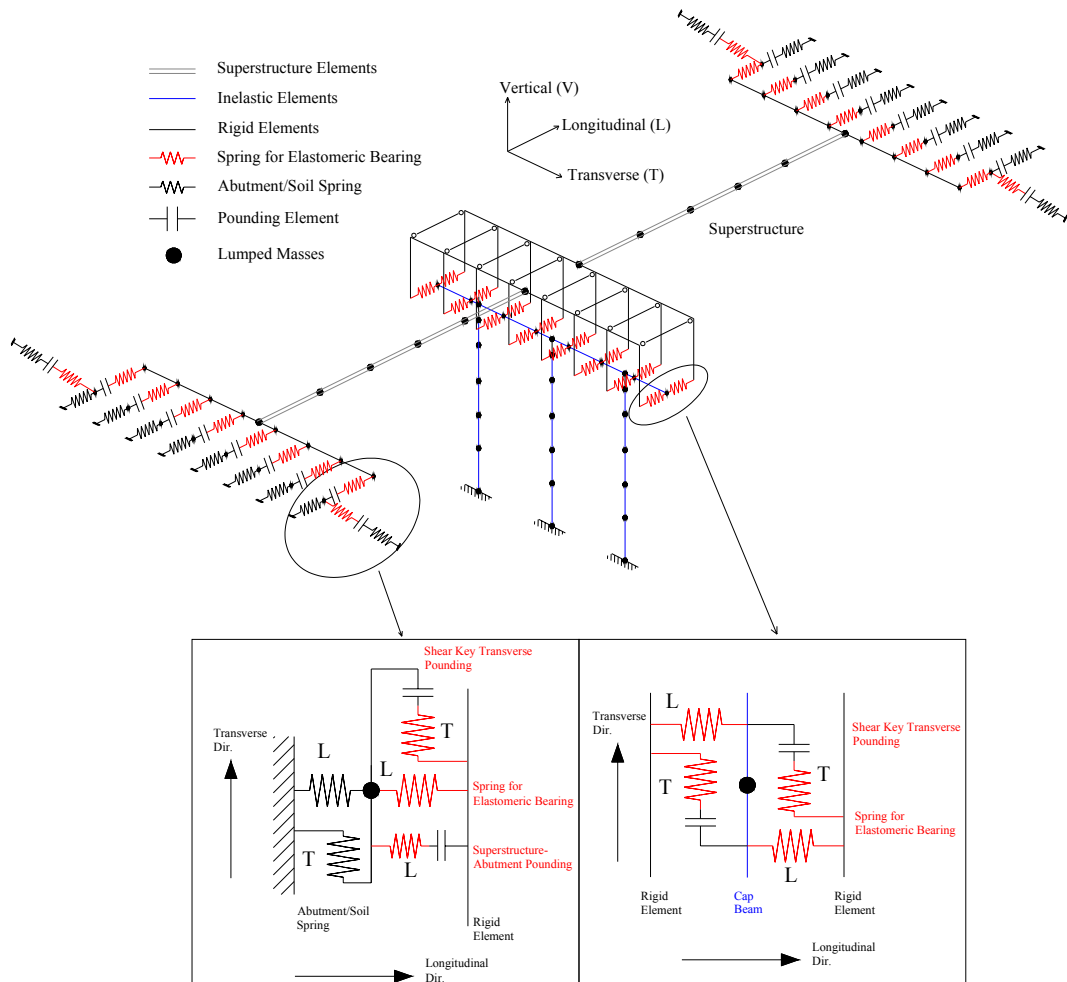
Figure 3.5 Detailed 3-D analytical model of the bridge and its components

Rigid elements are employed at the superstructure ends and at the rigid zones of column and cap beam connections. Great care must be given in selecting a physically realistic value for the stiffness of rigid members. If low stiffness values are specified for the rigid elements, rigid zones cannot be represented accurately in the analytical model. On the other hand, the numerical convergence of the rigid

element can be very slow or even analysis may not converge if a large elastic stiffness is employed. According to Wilson (2002), to minimize numerical problems, the stiffness should not be over 100 times the stiffness of the elements adjacent to the rigid element. Therefore, stiffness of the rigid elements is specified accordingly.

Concrete class of C25 and C40 are used for the members composed of reinforced concrete and prestressed concrete, respectively. Steel grade of S420 is used for the reinforcing bars. Characteristic strength values are used in this study for the associated materials. However, it is possible to encounter reinforcement bars having higher strength values than its characteristic value or the compressive strength of the reinforced concrete components of the existing bridges can be higher due to the aging of concrete. According to Priestley et al. (1996), since concrete continues to gain strength with age, the actual concrete strength when the seismic attack occurs is likely to considerably exceed the specified 28-day strength. Tests in California on concrete cores taken from bridges constructed in the 1950s and 1960s showed between 1.5 and 2.7 times the specified strength, which have considerable influence on the seismic performance of older bridges. In this study since there is no specific information about the concrete strength gain due to aging for the highway bridges in Turkey, increase in the concrete strength is not taken into consideration. Moreover, in the modeling of reinforced concrete components, contribution of the tensile strength of concrete to the member capacity under seismic action is ignored because of its variable nature and the possible influence of shrinkage- or movement-induced cracking (Priestley et al., 1996).

Mass and weight of the bridges are calculated considering the reinforced and prestressed concrete bridge components only. Truck load is not taken into account in the bridge seismic response calculations (AASHTO LRFD, 2007).

Concerning the viscous damping of the bridge structural system under seismic excitations, the damping phenomenon was represented using Rayleigh Damping. The mass and stiffness proportional Rayleigh damping coefficients are determined for the response history analysis of bridges considering the first two modal periods assuming 5% viscous damping ratio. Additional hysteretic damping is developed

through the yielding of bridge components such as bent column and cap beam, which are considered to experience inelastic deformations. P-Δ effects are taken into account in the analyses in order to capture the increase in the bent column seismic demands due to relative displacement between the column top and bottom.

3.2.1 Superstructure

Superstructure is modeled using standard prismatic elastic beam elements with cubic displacement variation along the element length. Superstructure is expected to remain in the elastic range as per Caltrans (2006) without experiencing any seismic damage. End points of the superstructure are connected to the other bridge components using rigid elements. The most important issues in the analytical modeling of superstructure elements are the correct calculation of its elastic properties, mass and weight.

The superstructure is composed of cast in place reinforced concrete deck and prestressed concrete girders working as a composite section having two different materials (Figure 3.6). Modulus of elasticity for normal weight concrete is calculated using Equation (3.1) (AASHTO, 1996; Priestley et al., 1996). Accordingly, E_c of the reinforced concrete deck with C25 and prestressed concrete girders with C40 concrete class are calculated as 23500 and 29725 MPa, respectively. Since the superstructure is modeled using elastic beam elements having a composite section, reinforced concrete deck section is transformed into prestressed concrete by narrowing the width of the deck section with a factor of 23500/29725=0.79. Narrowing of the deck section is applied in a direction parallel to the neutral axis of the section for the considered principal axis, so that a unique value is employed in the calculations for the elastic modulus of the superstructure, which is taken as 29725 MPa. Shear modulus, G_c is calculated using Equation (3.2) for ν=0.2.

$$E_c = 4700\sqrt{f_c} \qquad\qquad (3.1)$$

$$G_c = \frac{E_c}{2 \cdot (1+\nu)} \qquad\qquad (3.2)$$

Transformed sectional properties of the two superstructure types are calculated for each principal axis and presented in Table 3.2. Transformed concrete area is used in the calculation for the axial rigidity of the superstructure. Total area of reinforced and prestressed concrete elements of the superstructure is used in the weight and mass calculations. Since the superstructure does not have a regular cross section, its shear area in both principal axis is assumed be equal to $A_{transformed}$. Torsional rigidity of the superstructure composite section is calculated by LARSA.
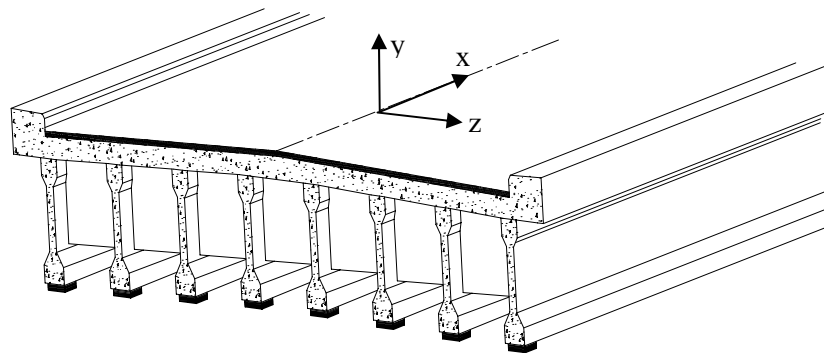
Figure 3.6 Bridge superstructure

Table 3.2 Transformed sectional properties of the superstructure types

Superstructure Type	Concrete Area A (m²)	Transformed Section Properties			
		A (m²)	Izz (m⁴)	Iyy (m⁴)	J (m⁴)
Type-I	6.988	6.209	2.003	103.963	0.1992
Type-II	8.266	7.512	1.091	118.911	0.3555

Mass of the superstructure constitutes 85-90 percent of the bridge total mass. In order to estimate the actual seismic behavior of the bridges, it is very important to calculate the superstructure mass accurately and locate the superstructure mass in the analytical model at its correct place. For this purpose, vertical rigid elements are employed between the superstructure mass and the substructure components. In addition to the mass of the concrete components of the superstructure, mass of the asphalt cover and parapet are taken into consideration. Unit weight of asphalt cover is taken as 20 kN/m^3 (KGM, 1982). In the analytical model, superstructure element is divided into sufficient number of small element segments in order to represent the mass distribution along the element length. Then mass of each segment is lumped at the adjacent nodes considering its tributary area on the superstructure.

3.2.2 Substructure – Bent

Bents are made up of columns and cap beams or only columns depending on the bent column number, which was classified as multiple- or single-column bent. The transverse direction of the bent system is much stiffer than its longitudinal direction. Because the strong axis of the column section is placed in the bent transverse direction and the stiffness contribution of the cap beam is more effective in the transverse direction for the multiple column bents. Cap beam has a contribution from its torsional stiffness to the bridge response in longitudinal direction for the bridges having low skew angle. As the skewness of the bridge increases, the stiffness contribution of the cap beam to the bridge longitudinal axis gets higher by the axial rigidity of cap beams. Substructure components of column and cap beam members, which are expected to display inelastic response under severe earthquakes, are modeled with nonlinear elements. These members are characterized by line elements passing through the cross section center of the members. Rigid end zone matter at the member connection regions is taken into account by using rigid elements. In Figure 3.7, nonlinear elements for column and cap beam and rigid links at the rigid zones are shown schematically. Nonlinear modeling of bent components is made using fiber-based nonlinear elements to

represent the distributed plasticity along the member length at certain control points (Taucer et al., 1991). Fiber modeling of reinforced concrete members has the advantage of considering the interaction between biaxial bending and axial force of the section automatically. Since the analytical modeling of the bridge components are made in 3-D, torsion and shear deformations at the two principal axes should be considered. A linear elastic force-deformation relation is assumed for the reinforced concrete section behavior in shear and torsional response. Shear and torsional elastic rigidity of the section is calculated and aggregated to the fiber section in order to consider the section response for the 6 degrees of freedom.
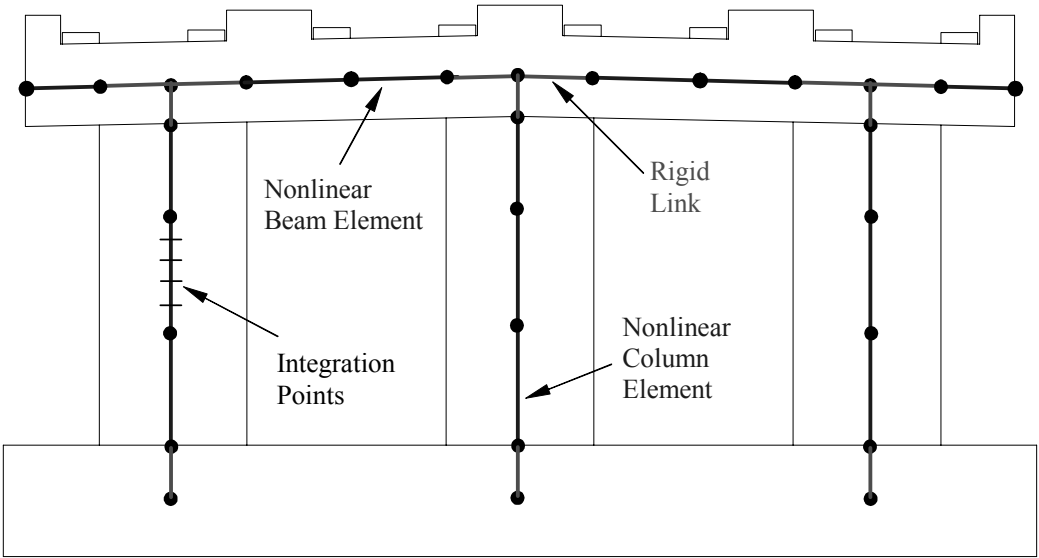
Figure 3.7 Bridge bent model

As shown in Figure 3.8, nonlinear member sections are discretized into longitudinal steel and concrete fibers such that the section force-deformation relation is derived by integrating the uniaxial stress-strain relation of the fibers.

66
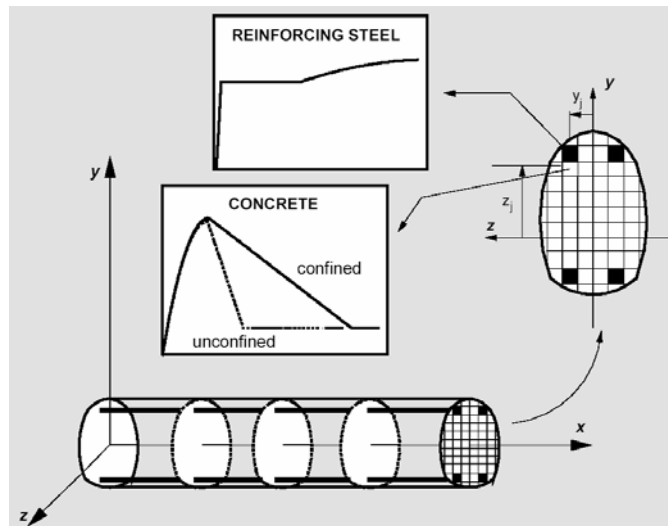
Figure 3.8 Components of a nonlinear fiber element (Taucer et al., 1991)

Several assumptions are made during the application of section fiber modeling. Bond slip is not taken into account and hence a perfect bond is considered between steel and concrete. Also, all the members in the analytical model are based on the assumption that deformations are small and member section remains plane after the application of loads. Moreover, the number of control points or in other words the number of integration points (Figure 3.7) should be specified for the modeling of fiber sections of reinforced concrete members. According to the results of several sensitivity analyses and recommendations, each nonlinear member with fiber section is modeled using 5 integration points along its length.

3.2.2.1 Material Models

Since the nonlinear behavior of the reinforced concrete members is obtained directly from the nonlinear stress-strain relationship of the steel and concrete fibers, reliability of the nonlinear bridge members are highly dependent on the accuracy of the material models utilized. Reinforced concrete sections are composed of three materials, which are unconfined concrete, confined concrete and reinforcement steel.

Reinforcing bars are modeled utilizing the material model of Steel01 in OpenSees. It is a bilinear steel material model with kinematic hardening. Some of the parameters that are used to form the material model of Steel01 are shown in Figure 3.9. For S420 reinforcement steel grade, σ_{sy} is assumed to be 420 MPa with an elastic modulus of 200 GPa. The ultimate strength (σ_{su}) and ultimate strain (ε_{su}) for S420 is given as 550 MPa and 0.1, respectively as per TEC (2007). Strain hardening ratio for this model is determined as 0.0066.

Core concrete, which is confined with transverse reinforcement bars, has a different stress-strain relation in comparison with the unconfined (cover) concrete. Confinement both improves the strength and the ductility of the concrete. For this reason different material models will be employed for the confined and unconfined concrete. Concrete01 Kent-Scott-Park (Kent and Park, 1971 and Scott et al., 1982) material model is used for both confined and unconfined concrete with different parameters. This concrete model has a good balance between simplicity and accuracy. As mentioned previously, tensile strength of concrete members are neglected. For the unconfined concrete no residual stress is considered and concrete strength reaches to zero at a strain value of 0.005. Peak compressive strength of unconfined concrete (σ_{co}) for C25 concrete class is taken as 25MPa at a strain of $\varepsilon_{co}=0.002$. The stress-strain relation of unconfined concrete is presented in Figure 3.10.

According to Figure 3.10, parameters required to develop the confined concrete material model is calculated using Equations (3.3), (3.4) and (3.5). 'K' is a factor which accounts for the increase in the strength and limiting strain of concrete due to the confinement. 'Z' is the strain softening slope; ρ_s is the volumetric ratio of the transverse reinforcement; f_{yh} is the yield strength of transverse bars, $h^{'}$ is the width of core concrete, and s_h is the spacing of transverse bars.

$$K = 1 + \frac{\rho_s f_{yh}}{\sigma_{co}} \tag{3.3}$$

$$\varepsilon_{cco} = 0.002 \cdot K \text{ and } \sigma_{cco} = \sigma_{co} \cdot K \tag{3.4}$$

$$Z = \cfrac{0.5}{\cfrac{3+0.29\sigma_{co}}{145\sigma_{co}-1000}+0.75\rho_s\sqrt{\cfrac{h'}{s_h}}-\varepsilon_{cco}} \qquad (3.5)$$

ε_{cu} is obtained considering the previously calculated parameters and the residual strength of σ_{cu}=0.2·σ_{co}. The ultimate confined concrete strain ε_{cu}^{*} is defined as the limiting strain value at which the core concrete crushing occurs. Although ε_{cu}^{*} is not required to form Concrete01 model for confined concrete, it will be used to determine the ultimate deformation capacity of the reinforced concrete members. The ultimate confined concrete strain is calculated using Equation (3.6) which is suggested by Mander et al. (1988). In the equation, ε_{su} is defined as the ultimate steel strain of the transverse reinforcement, which is specified as 0.1 for S420 as per TEC (2007).

$$\varepsilon_{cu}^{*} = 0.004 + \frac{1.4\rho_s f_{yh}\varepsilon_{su}}{\sigma_{cco}} \qquad (3.6)$$
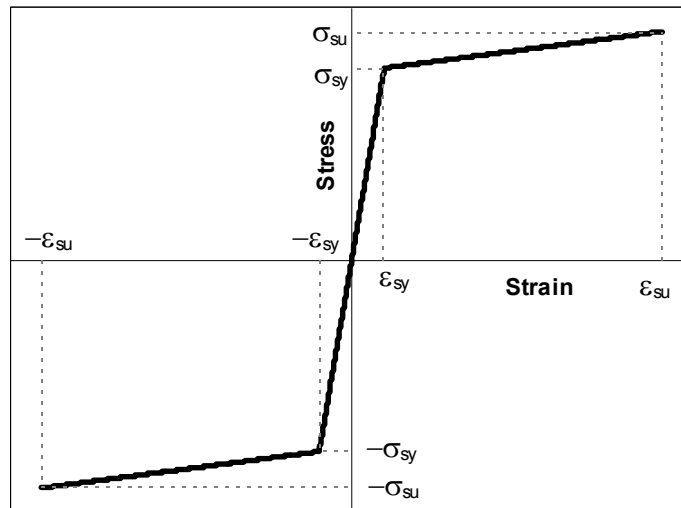
Figure 3.9 Material model for reinforcement steel

a) Unconfined concrete   b) Confined concrete
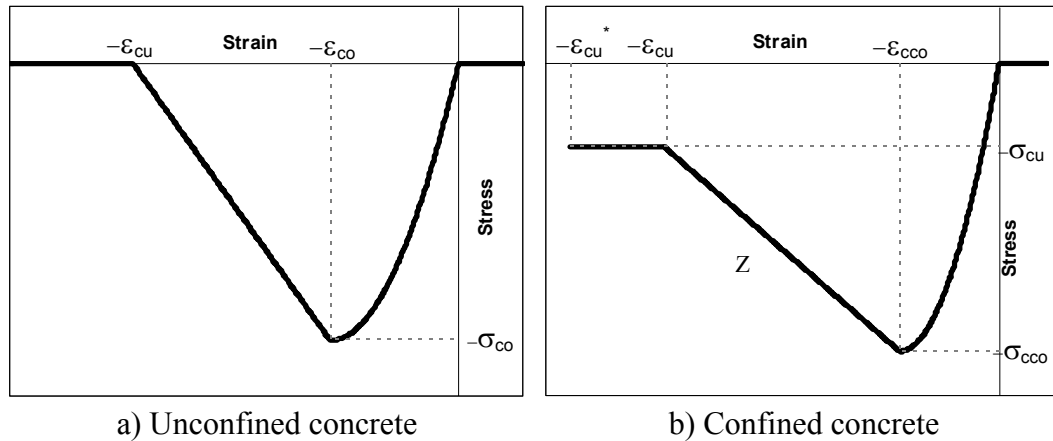
Figure 3.10 Material models for confined and unconfined concrete

Mass of the substructure components constitutes 10-15 percent of the total bridge mass. Masses of the column and cap beam elements are lumped at their adjoining nodes considering their tributary area. Since the boundary condition of the column bottom ends are assumed to be fully restraint, mass of the piles and pile cap is not taken into consideration in the analyses. Considering a fully restrained boundary condition for the bent columns and ignoring the soil-structure interaction for the bridges in this study is accepted to be a major assumption in generating the fragility curves of the highway bridges. As a result, local site conditions of the bridges are considered to be firm soil sites. If the soil flexibility would be taken into account in the analysis, various simplifications and major assumptions need to be done to model the soil flexibility, which requires considerable amount of computational effort and experimental studies for the verification of actual soil behavior. Certain linear/nonlinear spring constants would be specified considering the soil profile and pile groups of the bridges. Since a group of generated bridges representing the ordinary highway bridges constructed after the 1990s in Turkey, are investigated in this study, various soil profiles need to be developed for each bridge sample including additional uncertainties due to the soil conditions. This could lead to unrealistic bridge samples. Because of these reasons, soil flexibility for the bridge samples are not considered in this study.

3.2.3   Substructure – Abutment

Abutments are one of the key components of the highway bridges affecting their seismic response. They provide vertical support to the superstructure as well as lateral restraints depending on the loading direction at the bridge ends. Seat abutment supported by reinforced concrete piles is the most common abutment type through the inspected bridge inventory data. Abutments with wing walls are massive structures and they interact with the earth fill behind the backwall. Therefore, soil-structure interaction becomes important in the abutment modeling. There are many research studies available on the modeling of abutments depending on basic abutment geometric properties to the consideration of actual abutment earthquake response data. Wilson and Tan (1990) proposed analytical models for determining abutment transverse and vertical stiffnesses, which are related to the cross-sectional dimensions and the soil properties of the earth embankment. Ventura et al. (1995) have made research on the abutment stiffness determination using field vibration tests on highway bridges. Goel and Chopra (1997) obtained the capacity and stiffness for the abutment-soil systems of an existing bridge abutment from the ground and structural motions recorded during earthquakes. They investigated the stiffness variation of the abutment during earthquakes and at different abutment displacements. Considering the previous studies, Nielson (2005), utilized multi-linear representation for the force-deformation relationship of the abutments for different directions. However, it is not clear how well the available abutment analytical models represent the complex behavior of abutment-soil system, which is affected by nonlinear soil behavior and soil-structure interaction. Moreover, abutment deformation has a significant influence on the variation of abutment stiffness. That is why stiffness of the abutment depends on the level of shaking. This area still needs further research for the accurate modeling of abutment. Very detailed and complicated abutment models can lead to not only huge computation efforts causing numerical instabilities during the analysis but also due to the uncertainties involved in the abutment-soil systems, the modeling can lead to unrealistic results. Moreover, due to the lack of detailed information about

the backfill soil and abutment for each of the sample bridges generated from bridge inventory data, it is not appropriate to employ detailed models proposed by other researchers. Therefore, effect of abutment and its backfill soil on the bridge system is modeled using a very simple approach based on Caltrans (2006) provisions.

Abutments contribute to bridge stiffness in both transverse and longitudinal directions. In the longitudinal direction, abutments have different stiffness and hence different seismic response in the active and passive pressure directions (Figure 3.11). In the passive direction, abutment resistance is provided by passive pressure of embankment fill and the piles. In the active direction, the contribution of active soil pressure is not taken into consideration to the abutment resistance when it is pulled away from the backfill soil. Therefore, piles are considered to be the only resisting bridge components in the active direction. In the analytical models spring elements are employed in order to represent the force-deformation characteristics of the piles and abutment-embankment soil interaction considering the requirements of Caltrans. A bilinear force-deformation relationship is considered for the passive soil pressure of the embankment fill (Figure 3.12-a). The embankment fill stiffness of K_i=11.5 kN/mm/m is proposed by Caltrans. The given stiffness value is based on passive earth pressure tests and force deflection results from large-scale abutment testing at UC Davis. The abutment stiffness shall be adjusted proportional to the backwall height of the abutment using Equation (3.7).

$$K_{abut} = K_i \times w \times \left(\frac{h}{1.7} \right)$$

(3.7)

Where, w and h are the width and the height of the backwall for seat abutments, respectively. The yielding of the embankment fill for the analytical model is specified considering the maximum passive pressure of 239 kPa given by Caltrans (2006). The maximum passive pressure is based on the ultimate static force developed in the full scale abutment testing conducted at UC Davis. The ultimate soil pressure is amplified by about 50 percent and 368 kPa soil pressure is utilized for dynamic and earthquake loads. The yield force of the analytical model is

calculated using Equation (3.8), by which the height proportionality factor is taken into consideration.

$$F_y = A_e \times 368kPa \times \left(\frac{h}{1.7}\right); \ A_e = h \times w \qquad (3.8)$$
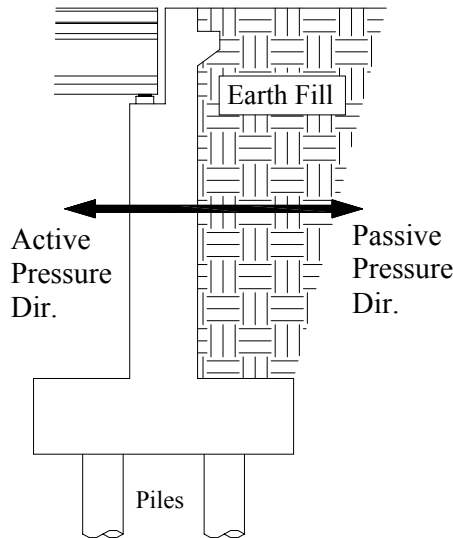
Figure 3.11 Earth pressure types and their directions at the abutment

The abutment piles are assumed to act in both active and passive direction of the abutment. The Caltrans recommendation of 7 kN/mm/pile stiffness with an ultimate strength of 119 kN/pile is accepted for this study (Nielson, 2005). Analytical model for the piles as shown in Figure 3.12-b is developed using the stiffness and strength values of piles given by Caltrans. The analytical models for force-deformation relationship of the embankment soil and piles are developed by spring elements and they are connected in parallel to be utilized in the bridge longitudinal direction.

A conservative approach is used in the modeling of abutment transverse direction response. As per Caltrans, contribution of wing walls is neglected and

abutment response is only characterized by the piles in the transverse direction. In the modeling of abutment transverse direction response, force-deformation relationship for the piles given in Figure 3.12-b is employed.
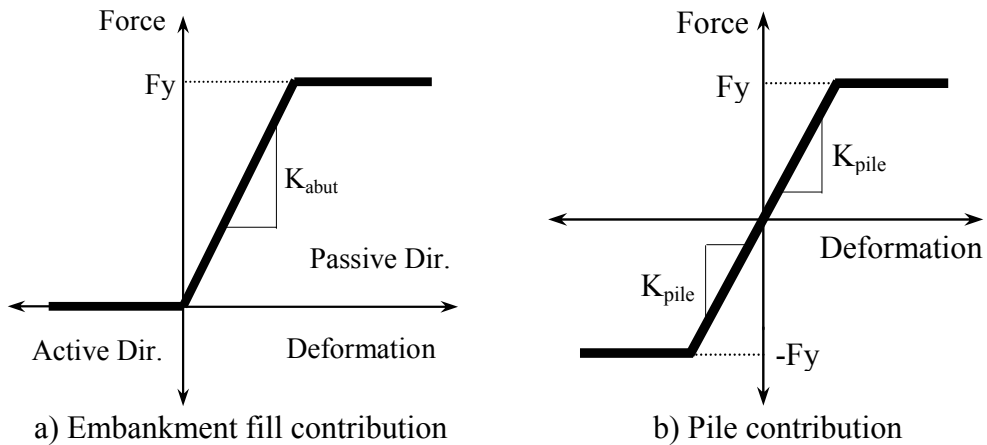
Figure 3.12 Abutment analytical model in longitudinal direction

3.2.4 Elastomeric Bearings

Elastomeric bearings are commonly used between the superstructure and substructure as isolating devices, which are composed of rubber pad and internally placed thin steel reinforcing plates as shown schematically in Figure 3.13. Bearings are placed under each of the prestressed girder of the superstructure. The internal steel plates, referred to as shims, reduce the lateral bulging of the bearing and increase its vertical stiffness considerably. However, horizontal stiffness of the bearings is very low in comparison with the adjoining substructure and superstructure. In the existing highway bridges, elastomeric bearings are simply placed in between the superstructure and substructure components without any connecting device, indicating that the bearings are considered to be free to move. Therefore, no fixity is considered in the modeling of elastomeric bearings. The only resisting force holding the elastomeric bearing at its place against lateral loads is the

friction force between the rubber and concrete surfaces. Therefore, the horizontal force on the bearing increases in proportional with the bearing displacement due to seismic loading until the friction force is exceeded. After this point, it is assumed that no additional horizontal force is carried by the bearings so the force remains constant. The behavior of the elastomeric bearings is characterized by an elastic perfectly plastic model as shown in Figure 3.14.

The initial stiffness of the elastomeric bearing is calculated using the equations given in (3.9). Where G, A and h_{rt} are the shear modulus, area and the total rubber height of the elastomeric bearings, respectively. The shear modulus of elastomeric bearings is specified according to their hardness as per AASHTO (1996). In general, nominal hardness of the elastomeric bearings is 60 on the Shore A scale for the inspected highway bridges. The shear modulus, G of the elastomeric bearings is calculated as 1.1 MPa, which is the average value of the recommended range by AASHTO (1996).
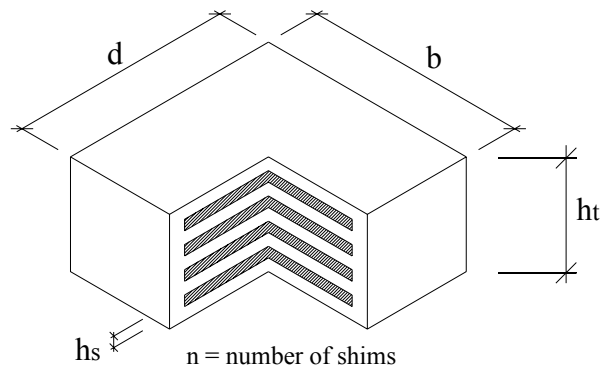
Figure 3.13 A typical elastomeric bearing of a highway bridge

$$K_{bearing} = \frac{G \times A}{h_{rt}}; \ A = d \times b; \ h_{rt} = h_t - n \times h_s \tag{3.9}$$

It is stated by Caltrans (2006) that the lateral shear capacity of the elastomeric bearing pads is controlled by either the dynamic friction capacity between the pad

and the bearing seat or the shear capacity of the pad. Since shear capacity of the pad is less critical, parameters affecting the dynamic friction capacity between the pad and the bearing seat are necessary to determine the ultimate load capacity of the elastomeric bearings. The ultimate shear capacity ($F_{friction}$) depends on the level of axial load on the elastomeric bearings and the dynamic coefficient of friction between the concrete surface and bearings, which is specified as 0.40 by Caltrans (2006). Since the superstructure mass location is higher than the elastomeric bearings, under seismic loadings overturning moments take place at the bearing location causing variable bearing axial forces. Therefore, an iterative approach is necessary to determine the bearing axial force and hence the $F_{friction}$ at each time step to establish the analytical model for the elastomeric bearings as shown in Figure 3.14. Since performing an iterative approach for each elastomeric bearing in the bridge is not a practical way, an average value of bearing axial forces is assumed in the calculations. Axial force of each elastomeric bearing is calculated under the gravity loading, which is assumed to be the average bearing axial force during the seismic loading. Finally, ultimate shear capacity ($F_{friction}$) of the bearings is calculated by multiplying the bearing axial force and the dynamic coefficient of friction.

For ordinary bridges, bearings are considered sacrificial components and they need to be inspected for damage and replaced after a damaging earthquake. Especially, due to lack of connecting devices between the bearing and above and below concrete surface, "walk-out" phenomenon can be observed after severe earthquakes when the friction force is exceeded. An example of dislodgment of bearing systems at Sakarya Viaduct during 1999 Kocaeli Earthquake is presented in Figure 3.15.
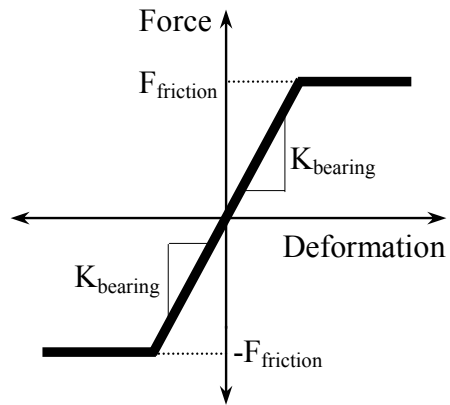
Figure 3.14 Elastomeric bearing analytical model

Figure 3.15 Dislodgment of bearing systems at Sakarya Viaduct (KOERI, 2009)

As mentioned previously, vertical stiffness of the elastomeric bearings is very high when they are under compression and they transmit the vertical loadings in the gravitational directions to the substructure components like a rigid member. However it has no stiffness in the upward direction, because they are not connected to superstructure or substructure. Therefore, when the bearing axial force due to the gravity loading is exceeded by the seismic loadings due to overturning effect, superstructure uplift can take place. Analytical modeling of uplift phenomenon or the contact loss between any members is difficult to simulate due to numerical problems and mostly convergence cannot be satisfied during the analyses. Introducing excessive number of nonlinear components for modeling each bearing in the vertical direction not only affects the numerical stability of the analyses, but also increases the computation time and effort. Moreover, superstructure is modeled with a single elastic beam element causing uneven distribution of bearing compression forces due to the gravity loads. This can lead to unrealistic results in the determination of elastomeric bearing uplift. Therefore, uplift phenomenon is not taken into account in the analytical model and elastomeric bearing end nodes are constrained such that these nodes are forced to displace equally in the vertical direction.

3.2.5 Pounding Elements

Superstructure and substructure components of the highway bridges are not continuous neither in longitudinal nor transverse directions and there exists joints with a certain gap in-between. The opening and closing of expansion joints between bridge components introduce nonlinearities and discontinuities that affect the load path and hence the dynamic response of bridges. Upon the closure of joints, pounding takes place between the adjoining bridge components, which is modeled by pounding elements. The pounding element represents the effect of impact between the superstructure and the abutment backwall in the longitudinal direction, whereas in the transverse direction pounding takes place between the superstructure and the shear keys both at the bents and abutments. Possible pounding locations in

the highway bridges and their analytical model representation are illustrated in Figure 3.16. Pounding effect should be taken into account in the analytical model, because bridge seismic response can be amplified considerably due to the impact of bridge components. As shown in Figure 3.17, shear keys and abutment backwall can experience significant seismic damage due to pounding. Shear keys and abutment backwall are considered to be sacrificial bridge components, which are designed to act as a structural fuse in a bridge system to protect substructure components and foundation systems under severe earthquakes. Because it is much easier and cost-effective to repair upper portion of the substructure than the foundation piles or pile cap.
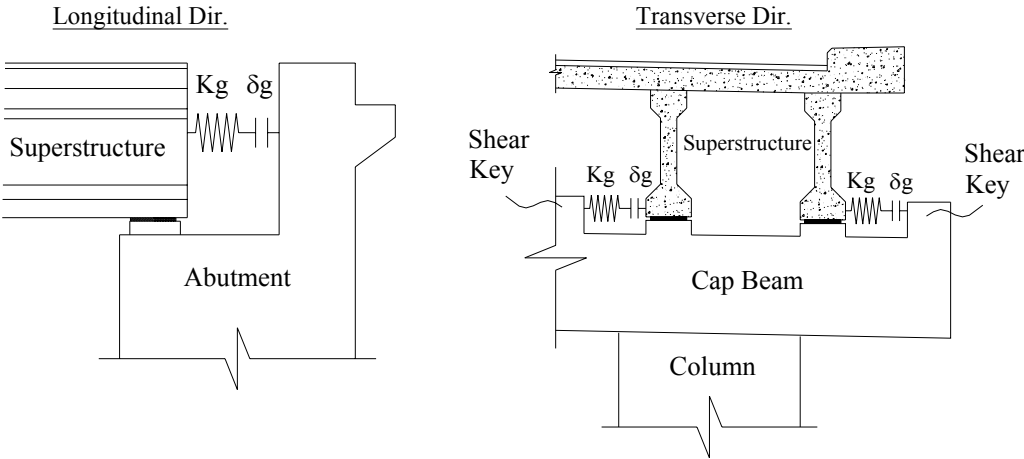
Figure 3.16 Possible pounding locations at the bridge under seismic actions

Figure 3.17 Pounding damage at the abutments in the transverse and longitudinal directions (KOERI, 2009; Kawashima, 2009)

In the analytical model, pounding elements monitor the relative displacement of the nodes at the joints connecting the bridge components at which the pounding can take place. When the calculated relative distance in the closing direction is greater or equal to the specified gap distance, pounding takes place and gap stiffness becomes effective up to a certain value. When the sacrificial bridge components have reached to their ultimate capacity due to pounding, pounding elements in the model do not attract any additional force and it is assumed that pounding element has constant force with the increasing displacement without any increase in the stiffness. Kim and Shinozuka (2003) and Banerjee and Shinozuka (2007) did not consider the yielding of pounding elements, whereas they assumed linear elastic behavior after the closure of gap. In such modeling, unrealistic seismic forces can be developed at the pounding element and very big horizontal forces are

transmitted to the substructure components. However, due to the attainment of ultimate capacity of the sacrificial bridge components at the pounding locations, yielding of pounding element takes place and no additional seismic forces are developed after this point.

The above explained behavior of the pounding element, which is effective when it is under compression, is represented by force-deformation relationship schematically shown in Figure 3.18. The modeling parameters of the pounding element vary according to the location of pounding at the bridge. These parameters are explained and examples for typical pounding elements are given in Table 3.3. Gap distances for the pounding elements in the longitudinal and transverse directions are specified as 50mm and 25mm, respectively. These values are taken from the blue-prints of the inspected highway bridges. However, in the existing bridges expansion joints do not function properly as expected and gap distances change over time due to debris accumulation at the gaps of joints (Caner et al., 2008). Since the level of debris accumulation at gaps is not known exactly, change in the gap distances is not taken into consideration in the analytical models for pounding elements.
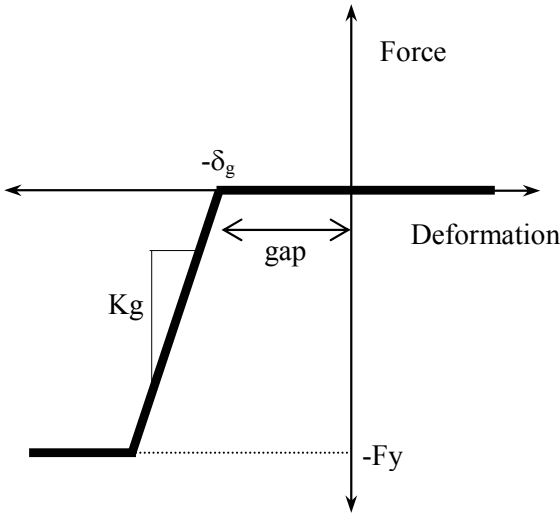
Figure 3.18 Analytical model for pounding element

Table 3.3 Parameters of pounding element analytical model

	Pounding Elements of Bridge Components	
	Superstructure-Abutment Backwall	Superstructure-Shear Keys
Direction	Longitudinal	Transverse
δ_g (mm)	50	25
Kg (kN/m)	Shear and flexural stiffness of abutment backwall (1.5e5)	Shear and flexural stiffness of shear key (3.4e6)
Fy (kN)	Ultimate shear and flexural capacity of abutment backwall (250)	Ultimate shear and flexural capacity of shear key (1600)

Accurate calculation of the ultimate capacity of the sacrificial bridge components due to pounding plays an important role in the modeling of pounding elements. The level of seismic force that the bridge bent columns experience in the transverse direction is directly proportional to the shear force transferred from the shear keys due to pounding. Therefore, shear and flexural capacities of the shear keys and abutment backwall are calculated in detail. In order to provide sacrificial elements to act as a structural fuse in a bridge system to protect substructure components, Caltrans (2006) states that shear key reinforcement shall be located as close to the center of the column as possible to minimize developing a force couple within the shear key reinforcement. However, in the inspected bridges, shear keys are designed so strong that ultimate capacity of the shear keys is calculated very high, which cause excessive seismic force on the bridge bent components. Shear keys are very important to hold the superstructure at its place under minor earthquakes or temperature effects. However, designing very stiff and strong shear keys may cause bridge bent columns more vulnerable in the transverse direction under severe earthquakes.

CHAPTER 4

GROUND MOTION SELECTION

Earthquake ground motions are one of the most influential components for the development of analytical fragility curves. As mentioned in the introduction part, variability in the structural parameters and their analytical models, damage state definitions and seismic hazard parameters are the main sources of uncertainty considered in the fragility curves. Among these items, Kwon and Elnashai (2006) indicated that the effect of randomness in strong-motion characteristics is much more pronounced than the effect of other uncertainties involved. Uncertainty in the seismic hazard is accounted for through the use of suites of earthquake ground motions that are representative for the seismicity of the region where the bridges are located. Therefore, selection of appropriate ground motions is crucial for the reliability of the fragility curves. However, there is not a specific method for selecting the proper ground motion data set for the nonlinear response history analyses. The main purpose in selecting the ground motions is to compile a ground motion database representing wide range of seismic forces that impose various degrees of seismic damage on the bridges. If this can be accomplished, sufficient number of data points can be provided with a uniform distribution along the abscissa of the fragility curve. Otherwise, if the selected ground motions impose similar seismic damage on the bridges, variation in the bridge seismic demands that are calculated from nonlinear response history analyses will be limited. In such case, data points on the fragility curve may accumulate at certain seismic hazard levels.

The seismic hazard level of the earthquake ground motions can be represented by different ground motion intensity measures. Choice of intensity measure also influences the reliability of the bridge fragility curves. The essential point in selecting the appropriate intensity measure is that it should have a certain level of correlation with the seismic damage of bridges. Various ground motion intensity measures are considered in this study for the development of fragility curves.

4.1   EARTHQUAKE GROUND MOTION INTENSITY MEASURES

Fragility curves are conditioned on the seismic intensity measure of the ground motion. The selection of an optimal intensity measure is a challenging task and research still continues on this subject. A specific method is not available for deciding on the optimal intensity measure to be used in the fragility analyses. Several intensity measures are proposed and employed for the development of fragility curves by different researchers. There is lack of agreement among researchers on the most suitable intensity measure to be used for the bridge fragility curves.

In general, existing ground motion intensity measures can be categorized into two groups depending on its computation practice. For the first group, intensity measures can be directly calculated from ground motion records, such as peak ground acceleration (PGA), peak ground velocity (PGV), etc. In the second group, response spectrum of the ground motion is utilized to obtain intensity measures, such as spectral values and spectrum intensity parameters, which can be calculated using response spectrum for certain periods or specific equations are employed in the calculations. Kramer (1996) and Mackie and Stojadinovic (2003) identified various number of intensity measures with their definitions.

The most commonly utilized intensity measure for bridge fragility curves is PGA and to a lesser degree PGV. One of the main reasons for PGA and PGV to be the most common intensity measures is that they can be simply obtained from ground motion records without any additional information about structural

properties to be used in the calculation. Spectral accelerations at certain periods are also employed in previous studies (FEMA, 2003; Nielson, 2005). Several earlier studies were conducted to compare the efficiency of different intensity measures for estimating the seismic damage with a certain level of confidence. According to the results of Akkar et al. (2005), inelastic dynamic response displacements of frame structures are significantly better correlated with PGV than PGA through the structural period range from 0.2s to 1.0s. Dhakal et al. (2006) mentioned that spectral acceleration is a more efficient intensity measure in comparison with PGA. Using spectral acceleration as the intensity measure would give more confidence in the result or would require less number of records to generate results with the same level of confidence. Although PGA is the most commonly used intensity measure, it has some drawbacks when compared with other parameters.

The most important criterion in selecting an appropriate intensity measure is the sufficient level of correlation between the degree of seismic damage sustained by the bridge and the hazard level of the ground motion. Therefore, reliability of the fragility curves is proportional with the level of correlation between seismic damage and the selected intensity measure.

In this study four different intensity measures are considered and their correlation between the seismic damage is investigated. PGA and PGV are the two intensity measures that are considered in the calculations because of their common application in the earthquake engineering. Also, great majority of the available fragility curves are obtained using the two intensity measures. Additionally, PGA/PGV ratio is also regarded as a seismic intensity measure. According to Kramer (1996), dominant frequency and energy content of the earthquake ground motions can be represented by PGA/PGV ratio. Priestley et al. (1996) and Kwon and Elnashai (2006) mentioned that PGA/PGV ratio implicitly accounts for many seismo-tectonic features and site characteristics of earthquake ground motion records. Low PGA/PGV ratios indicate earthquakes with low predominant frequencies, broader response spectra, longer durations and medium-to-high magnitudes, long epicentral distances and site periods. Conversely, high PGA/PGV ratios represent high predominant frequencies, narrow band spectra, short duration

and small–medium magnitudes, short epicentral distance and site periods. These three intensity measures that are PGA, PGV and PGA/PGV ratio can be simply obtained from ground motion records.

The maximum acceleration that the bridges are exposed to during earthquakes, can be determined from elastic response spectrum of the ground motion corresponding to their fundamental periods. Maximum acceleration is proportional to the seismic forces as well as the seismic damage that the bridges experience. Therefore, spectral acceleration of the bridges at their fundamental period can be considered as a good intensity measure for the estimation of seismic damage of the bridges. On the other hand, considering a single spectral acceleration can lead to unrealistic acceleration values that the bridge is expected to experience. Because higher mode effects and the period elongation due to inelastic response of the bridges influence the bridge acceleration level. That is why, it is not convenient to consider a single period to calculate the spectral acceleration. Moreover, fragility curves are developed for a group of bridges whose fundamental periods is not unique among the representative bridge samples. Therefore, instead of dealing with a single period value, considering a period range over response spectra of the ground motions will be more reasonable. The area under the elastic response spectrum (5% damped) within the boundary periods of T_i and T_f is defined as acceleration spectrum intensity (ASI) and can be calculated using Equation (4.1). T_i and T_f are defined as the initial and final periods to be used in the calculation of ASI. The definition of ASI is also presented schematically in Figure 4.1 for the initial and final periods. ASI is considered to be the fourth intensity measure to be utilized in this study.

$$ASI = \int_{T_i}^{T_f} SA(T, \xi) dT \qquad (4.1)$$
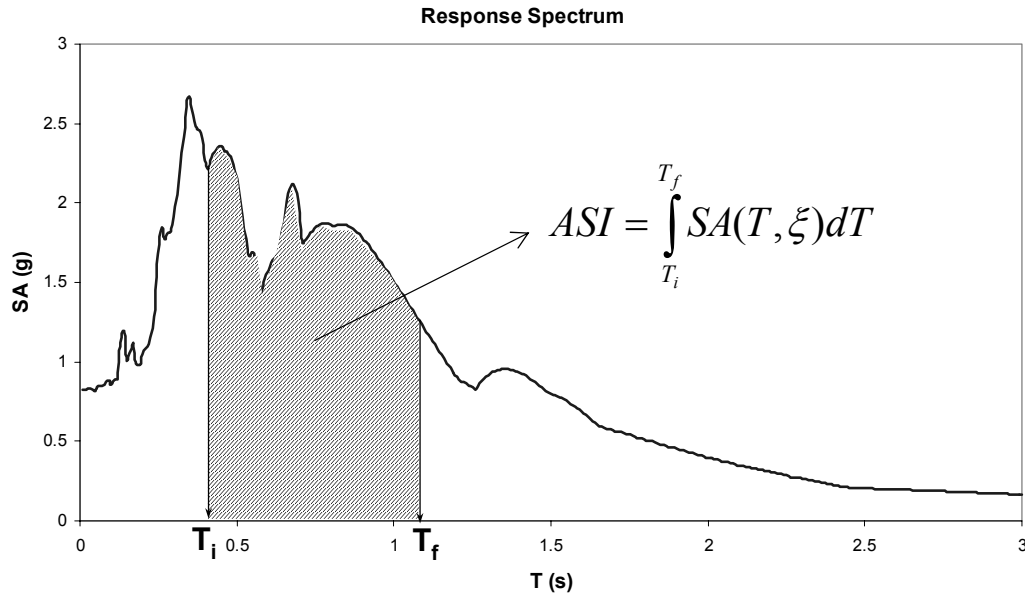
Figure 4.1 Definition of ASI

Von Thun et al. (1988) expressed the ASI as the area under the elastic pseudoacceleration spectrum (5% damped) between the periods of T_i=0.1s and T_f=0.5s. ASI was utilized as an intensity measure for the seismic analysis of concrete dams, which generally have fundamental periods of less than 0.5s. For buildings, Yakut and Yılmaz (2008) mentioned that ASI correlate better with the response of building structures if the period range of T_i=0.1s and T_f=2.0s is employed. It is obvious that the reliability of the ASI is highly dependent on the selection of period ranges T_i and T_f.

According to the modal analyses results of the sample bridges of major bridge classes as presented in Table 2.9, fundamental period values vary between 0.47s and 0.98s. These values are not used for the initial and final periods. In order to consider the higher mode effects a lower value of T_i is selected as 0.40s. After performing some sensitivity analyses, average period elongation of the sample bridges due to their inelastic response to seismic actions is computed as 1.10s on the average, which is then used for T_f. Finally, it is assumed that ASI is determined considering the period range T_i=0.40s and T_f=1.10s for most of the ordinary highway bridges in Turkey.

Both horizontal components of the selected ground motion records will be used in the nonlinear response history analyses. Then the question arises, which horizontal component of the ground motion will be considered in calculating the specified intensity measures? Or any combination of the two horizontal components will be used? Baker and Cornell (2006) mentioned that earth scientists typically use the geometric mean of the intensity measure of the two horizontal components of ground motion for hazard analysis. Similarly, in this study, intensity measure of each ground motion is obtained by calculating the geometric mean of the intensity measures of the two horizontal components of the ground motion.

4.2   SELECTION OF GROUND MOTION RECORDS

Various earthquake ground motion records are investigated and sufficient number of these records is selected to form a ground motion data set for the nonlinear response history analyses. Different ground motions covering a wide range of seismic hazard levels are considered in order to represent the record-to-record variability in the analytical fragility curves. There are several important considerations in selecting the appropriate ground motion records. Fragility curves give information about the level of seismic damage probability with respect to various hazard levels for structures, which belong to a certain region. Therefore, the ground motions that are used in the analyses for constructing fragility curves should be selected from the earthquake ground motions specific to the respective region. However, recorded ground motions at the concerned region may not be adequate or record-to-record variability cannot be represented with the available data. In such cases, spectrum compatible synthetic ground motions were used in the previous studies (Elnashai et al., 2004; Nielson, 2005; Padgett and DesRoches, 2007). Synthetic ground motions can be obtained by generating artificial spectrum compatible records using special purpose programs or by manipulating existing earthquake records to match the design spectrum that is specific to a site. These synthetic records are very attractive in order to obtain ground motions at various levels of seismic hazard. On the other hand, since these synthetic records are forced

to be compatible with the site specific design spectrum, it is highly possible to obtain ground motion recordings having unrealistic energy and frequency contents. Also, synthetic records typically have a longer duration in comparison with real earthquake records (Priestley et al., 2007). Bommer and Acevedo (2004) point out that the real earthquake accelerograms are clearly a viable option for providing input to dynamic analysis of structures, being more realistic than spectrum-compatible artificial records and easier to obtain than synthetic accelerograms generated from seismological source models. Naeim and Lew (1995) mentioned that there are significant potential problems associated with uncontrolled use of synthetic records in seismic design. They can lead to exaggeration of displacement demand and energy input, which in turn can distort the expected performance of the structure when subjected to earthquake ground motions. In order not to come across such problems as well as obtain erroneous analyses results, synthetic ground motions are not employed in this study. Instead, real earthquake ground motions records, which represent the seismic potential of the investigated region, are used.

The recorded ground motions obtained from the past earthquakes in Turkey are not sufficient to be used in the development of bridge fragility curves. Therefore, in addition to the earthquakes in Turkey, recorded ground motions from other regions having similar faulting mechanisms and seismic potential to Turkey are also considered. By this way, the number of earthquake ground motions to be used for the analyses of Turkish highway bridges can be enriched. Most of the recorded ground motions with a damaging potential in Turkey were obtained from the earthquakes occurred at the North and East Anatolian Fault segments, which have strike-slip faulting mechanism. This cannot be generalized for the whole country. But it is assumed that the recorded earthquake ground motions from other regions having strike-slip faulting mechanism can be used for the nonlinear response history analyses of Turkish highway bridges. Therefore, when selecting the earthquake records, all recorded ground motions in Turkey and ground motions obtained from other regions recorded during earthquakes having strike-slip faulting mechanism are considered.

As explained in section 3.2.2, soil flexibility of the bridge foundation is not taken into account in the analytical models and hence a fully restrained boundary condition is assumed for the bridge substructure. In order to be consistent with the analytical model developed in this study, ground motions recorded at the firm soil sites are considered. Shear wave velocity is used to decide on the site conditions. Firm soil site is assumed to be composed of at least dense soil or soft rock according to NEHRP (2000) and it is represented by the site category of C, which has the lower limit for shear wave velocity (Vs) of 360m/s. Therefore, ground motions recorded from soil sites having Vs<360m/s is not taken into account in the selection stage.

The final criterion in the selection of ground motions is the minimum seismic intensity level they have. In order to relate bridge damage and the seismic intensity of the earthquakes, bridges should experience some level of seismic damage under the effect of selected ground motions. It is assumed that the ground motions having PGA less than 0.05g do not produce any damage on the bridge. Therefore, during the ground motion selection phase, ground motions having PGA<0.05g are not taken into account.

In light of the above mentioned information for the ground motion selection criteria, 114 earthquake ground motions are selected satisfying the following conditions:

- All earthquake ground motions recorded in Turkey
- Ground motions recorded from other regions having strike-slip faulting mechanism
- Ground motions recorded from sites having Vs $\geq$ 360 m/s
- Ground motions having PGA $\geq$ 0.05 g

All of the earthquake ground motions are downloaded from strong motion databases of PEER (http://peer.berkeley.edu/smcat/), COSMOS (http://db.cosmos-eq.org/scripts/default.plx), and General Directorate of Disaster Affairs Earthquake Research Department of Turkey (http://angora.deprem.gov.tr/). All the data have been downloaded in March 2008. Most of the available data have already been

corrected. However, for the uncorrected ground motions, their raw data are processed by making appropriate baseline corrections and filtering.

The distribution of ASI versus PGA of the selected 114 ground motions is shown in Figure 4.2. There is not a uniform distribution for the two intensity measures among the selected ground motions. The number of ground motions is higher at the lower intensity values at which the seismic damage imposed on the bridges is limited. Therefore, it is not practical to consider all the selected 114 ground motions for the nonlinear response history analyses.
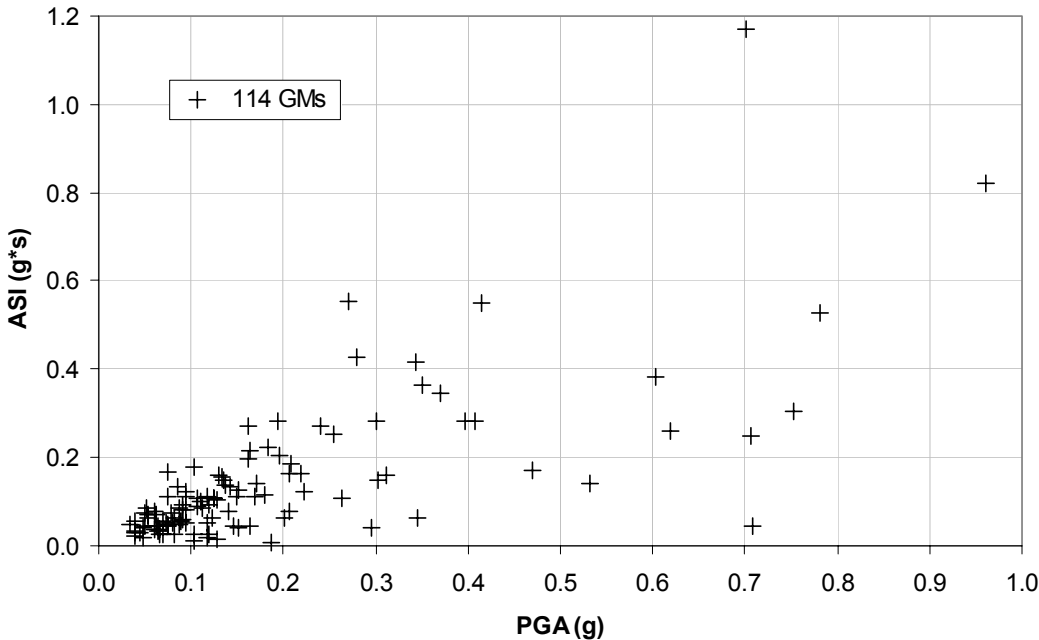
Figure 4.2 ASI versus PGA distribution of the 114 ground motions

According to Dhakal et al. (2006), using many number of EQ records will surely increase the amount of analysis to be done before coming to conclusion, but may not necessarily noticeably enhance the final outcome. Employing all the ground motions in the analyses not only increases the analysis time considerably, but also due to the uneven distribution of the intensity measures, fragility curve data points obtained from analysis results accumulate at certain intensity measures,

which will affect the reliability of the fragility curves in a negative way. Therefore, a certain number of ground motions are further selected among the 114 ground motion data.

Considering different levels of ASI and PGA, a new data set of 33 ground motions are selected for further investigations. Especially, great care is given to ASI when selecting the ground motions. Since ASI has better estimates for the acceleration level imposed on the bridges in comparison with PGA, which implies that ASI is expected to have superior correlation with the seismic damage of the bridges. Therefore, ground motions with smaller ASI levels are discarded in the selection stage. Then 33 ground motions are chosen as shown in Figure 4.3 with circles. It is not a straight forward task to select an appropriate ground motion data set to be used in the development of fragility curves. Because, in the beginning it is not clear to identify the level of seismic damage that the bridge will experience under the effect of earthquake ground motions. In order to overcome this, several sensitivity analyses can be performed before making final decisions in selecting the optimal ground motions. For that reason selected earthquakes are further utilized in the sensitivity analyses considering two bridges having different structural properties. According to the results of sensitivity analyses, bridge damage levels are investigated to compare the effect of each selected 33 ground motions. Bridge damage levels are specified by considering several response parameters such as column and cap beam curvature and shear demands and superstructure relative displacement, which will be explained in detail in Chapter 5. Ground motions having no damaging effects or imposing similar damage on the bridge are specified. Accordingly, 8 additional ground motions are also eliminated from the data set and remaining 25 ground motions are decided to be used in the final analyses.
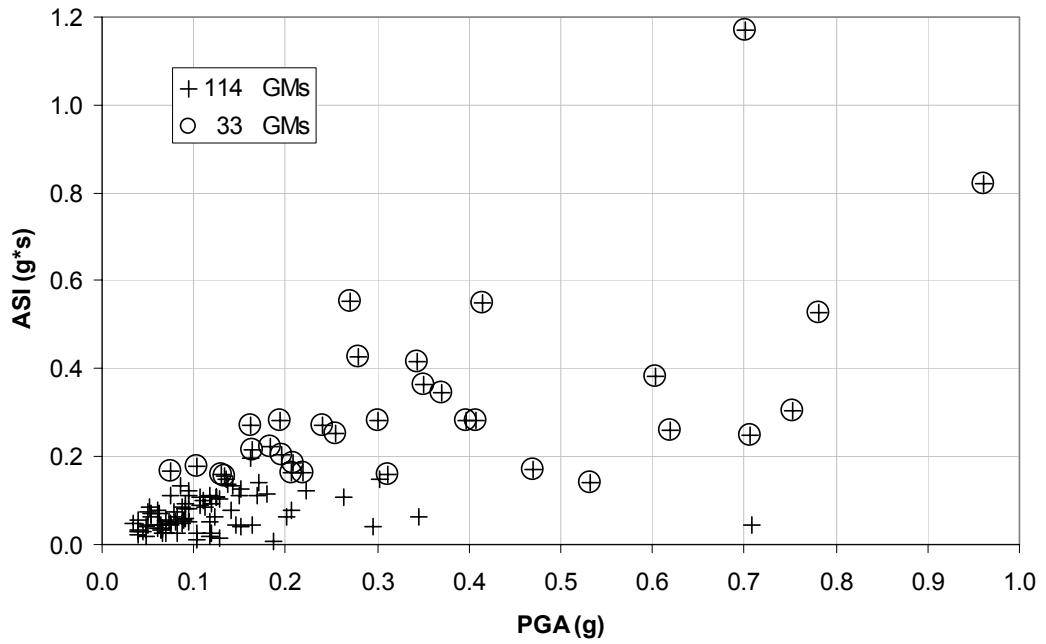
Figure 4.3 Preliminary selection of 33 ground motions

The final selection of 25 earthquake ground motions and their intensity measure distribution in terms ASI and PGA are shown in Figure 4.4. Some of the important features of the earthquakes and several intensity measure parameters of the ground motions are given in Table 4.1. Since earthquake ground motions have two horizontal components, the given values in the table are obtained by simply taking the geometric mean of the two horizontal components. Similarly, response spectrum of each ground motion is calculated by taking the geometric mean of the response spectrum of the two horizontal ground motion components. The response spectra of all the ground motions and their mean are presented in Figure 4.5.
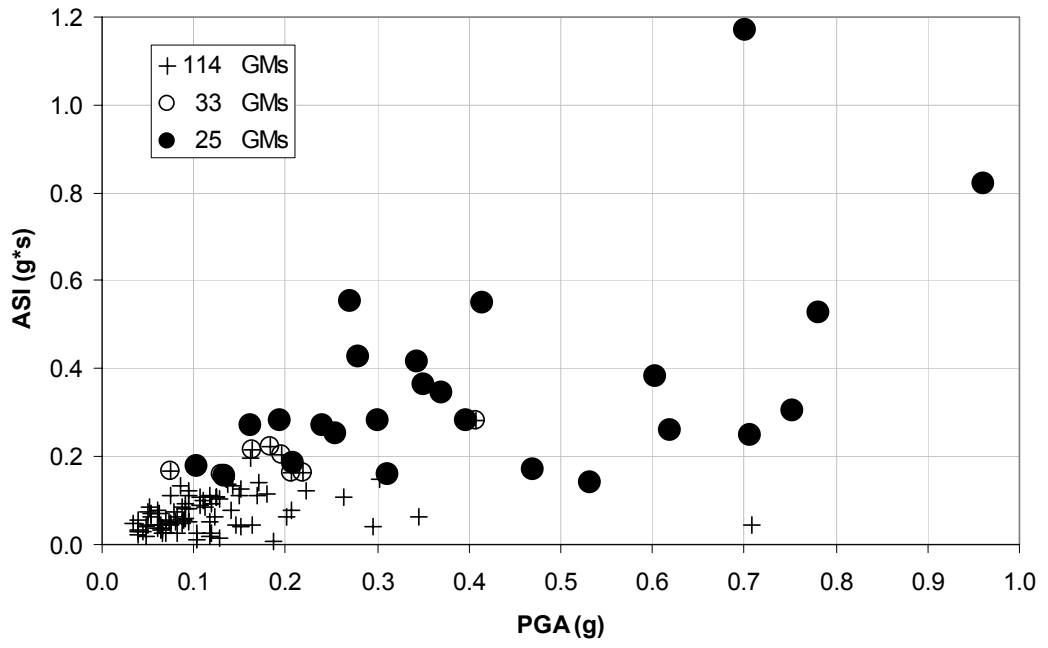
Figure 4.4 Final selection of 25 ground motions
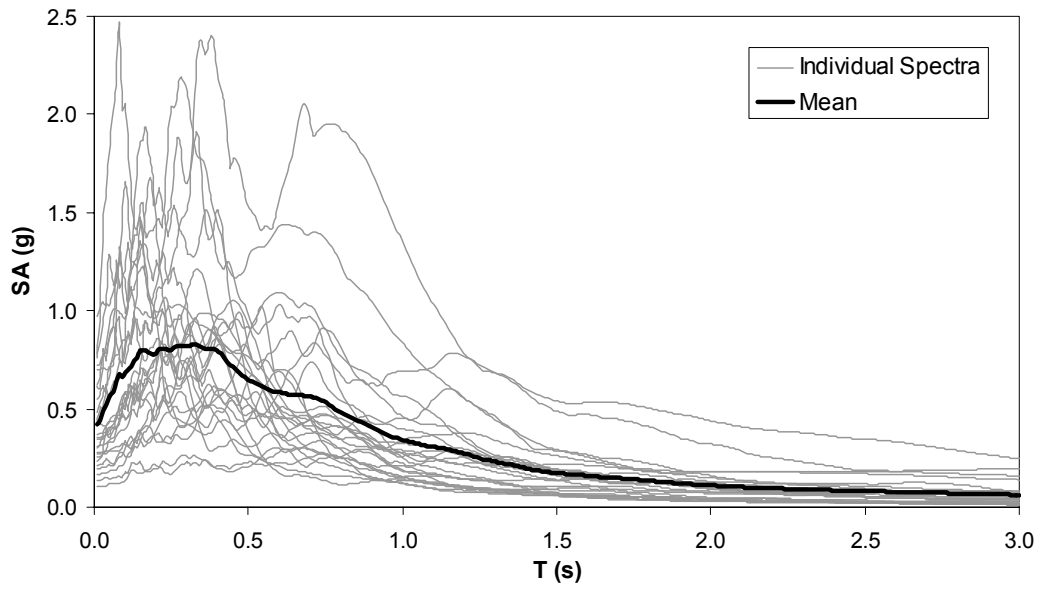
Figure 4.5 Response Spectrum of the selected 25 ground motions

94

Table 4.1 Some important parameters of the selected 25 earthquake ground motions

#	Earthquake, Date	Station	Source	Mw	D (km)	ASI (g*s) Ti=0.4s-Tf=1.1s	PGA (g)	PGV (cm/s)	PGA/PGV (1/s)	Td (s)
1	Parkfield 2004-09-28 17:15:24 UTC	Parkfield, CA - Gold Hill 3W; CSMIP station 36420	COSMOS	6.0	3.9	0.140	0.532	18.71	27.87	20.8
2	Landers 1992/06/28 11:58	23559 Barstow	PEER	7.3	36.1	0.157	0.133	23.77	5.51	40.0
3	Parkfield 1966/06/28 04:26	1438 Temblor pre-1969	PEER	6.1	9.9	0.161	0.312	18.0	17.02	30.3
4	Parkfield 2004-09-28 17:15:24 UTC	Parkfield, CA - Cholame 2E; CSMIP station 36230	COSMOS	6.0	14.5	0.172	0.469	22.51	20.43	20.8
5	Landers 1992/06/28 11:58	33083 Boron Fire Station	PEER	7.3	90.6	0.178	0.103	11.13	9.12	40.0
6	Coyote Lake 1979/08/06 17:05	57217 Coyote Lake Dam (SW Abut)	PEER	5.7	3.2	0.187	0.209	14.81	13.87	28.8
7	Duzce, Turkey 1999/11/12	375 Lamont 375	PEER	7.1	8.2	0.249	0.706	27.15	25.51	41.5
8	Morgan Hill 1984/04/24 21:15	57383 Gilroy Array #6	PEER	6.2	11.8	0.252	0.255	20.45	12.21	30.0
9	Parkfield 2004-09-28 17:15:24 UTC	Parkfield, CA - Cholame 3E; CSMIP station 36450	COSMOS	6.0	14.8	0.260	0.620	25.24	24.08	20.8
10	Landers 1992/06/28 11:58	5071 Morongo Valley	PEER	7.3	19.3	0.270	0.162	18.3	8.69	70.0
11	Parkfield 2004-09-28 17:15:24 UTC	Parkfield, CA - Fault Zone 7; CSMIP station 36431	COSMOS	6.0	1.7	0.271	0.241	19.5	12.10	21.0
12	Westmorland 1981/04/26 12:09	5051 Parachute Test Site	PEER	5.8	24.1	0.282	0.194	32.3	5.88	40.0
13	Denizli, Turkey 1976/08/19	Denizli Directorate of Meteorology	General Dir. of Disaster Affairs/ERD	5.0	67.6	0.283	0.300	19.3	15.23	15.8
14	Bingol, Turkey 2003/05/01	Bingol Directorate of Public Works and Settlement	General Dir. of Disaster Affairs/ERD	6.1	4.9	0.284	0.396	28.37	13.67	23.9
15	Landers 1992/06/28 11:58	24 Lucerne	PEER	7.3	1.1	0.305	0.752	55.80	13.23	48.1
16	Coyote Lake 1979/08/06 17:05	57383 Gilroy Array #6	PEER	5.7	3.1	0.346	0.370	34.72	10.46	27.1
17	Morgan Hill 1984/04/24 21:15	1652 Anderson Dam (Downstream)	PEER	6.2	2.6	0.364	0.350	26.42	12.98	28.3
18	Victoria, Mexico 1980/06/09 03:28	6604 Cerro Prieto	PEER	6.4	34.8	0.383	0.604	25.1	23.62	24.5
19	Landers 1992/06/28 11:58	23 Coolwater	PEER	7.3	2.1	0.416	0.344	32.9	10.24	28.0
20	Landers 1992/06/28 11:58	22170 Joshua Tree	PEER	7.3	11.6	0.425	0.279	34.47	7.94	44.0
21	Superstitn Hills(B) 1987/11/24 13:16	286 Superstition Mtn.	PEER	6.7	4.3	0.528	0.781	37.03	20.68	22.2
22	Superstitn Hills(B) 1987/11/24 13:16	5051 Parachute Test Site	PEER	6.7	0.7	0.549	0.414	70.12	5.79	22.3
23	Parkfield 2004-09-28 17:15:24 UTC	Coalinga, CA - Slack Canyon; Hidden Valley Ranch; CSMIP station 46175	COSMOS	6.0	32.1	0.552	0.271	36.42	7.29	21.3
24	Morgan Hill 1984/04/24 21:15	57217 Coyote Lake Dam (SW Abut)	PEER	6.2	0.1	0.819	0.961	64.57	14.60	30.0
25	Kobe 1995/01/16 20:46	0 KJMA	PEER	6.9	0.6	1.169	0.701	77.72	8.85	48.0

4.3 EFFECT OF VERTICAL COMPONENT OF THE GROUND MOTION

Vertical ground motions may be as important as horizontal components in predicting bridge seismic response in some particular cases. Yet, research still continues on the effect of vertical ground motion on the seismic behavior of the bridges. Current seismic design requirements do not have a direct attempt to account for vertical motion effects. Caltrans (2006) requires an equivalent static vertical load to be applied to the superstructure in the consideration of vertical ground motions for ordinary standard bridges where the site peak rock acceleration is 0.6g or greater. It is not required to perform an analysis for the bridge structure under the combination of vertical and horizontal components of ground motion.

Several earlier studies have been conducted on this subject. Saadeghvaziri and Foutch (1991) showed that varying column axial forces due to vertical excitations results in lower energy-dissipating capacity and influences the column shear capacity. Yu (1996) and Broekhuizen (1996) investigated the effect of vertical motion on several overpasses located close to the epicenter of the 1994 Northridge earthquake. The former study concluded that vertical ground motion has a considerable effect on the column axial load, but its influence on the column longitudinal moment is in the negligible order. Yu (1996) also showed that the effect of vertical ground motion on the horizontal sliding over the bearing seats is not important as long as the vertical acceleration is less than 1 g. Broekhuizen (1996) stated that under high level of vertical accelerations, tensile stresses in the deck could be significantly amplified due to effect of vertical ground motion. According to the post earthquake observations and field investigations of Papazoglu and Elnashai (1996) and Yen et al. (2002), superstructure displacement and substructure damage can be increased due to the combined effects of vertical and horizontal components of the ground motions especially for the near-field earthquakes. Priestley et al. (1996) mentioned that high variation in the vertical load could cause significant variation in the horizontal response of the bearing particularly in the case of near-field earthquakes. In one of the recent studies on the

development of analytical fragility curves for the highway bridges in Central and Southeastern United States (CSUS) by Nielson and DesRoches (2006), vertical ground motions were not considered. Because it is mentioned that vertical ground motions are not necessary for analysis of bridges in the CSUS. Button et al. (2002) conducted a parametric study of the effects of vertical motions on the seismic response of typical highway bridges employing mostly linear response spectrum and linear dynamic analyses. They concluded that the impact of vertical ground motions increases substantially as the bridge site gets closer to the fault. According to their results, including the vertical component of ground motion results in greater seismic demands for the deck shear and moments and column axial forces. Values of horizontal response quantities are not significantly influenced by the vertical component of motion. Analyses results of Kunnath et al. (2008) reveal that vertical ground motions do significantly affect (1) the axial force demand in columns that in turn have an effect on moment demands at the face of the bent cap and shear demands and shear capacity in the columns; and (2) moment demands at the middle of the span.

Past studies have revealed some of the important aspects of the effect of vertical ground motion on the seismic response of the highway bridges. However, there is not a consensus on the vertical ground motion effect on the bridges and it still remains the subject of debate. Further research studies are required and bridge damage potential due to vertical motions needs to be investigated in detail to end up with realistic and consistent conclusions. Several sensitivity analyses are performed to make a decision whether to consider vertical ground motions in the analyses or not in this study. For this purpose 9 ground motions are selected from Table 4.1. Since all the ground motions do not have vertical components, ground motion data set to be used in the sensitivity analyses are formed considering ground motions having vertical components. The ID numbers of the selected ground motions are 6, 7, 9, 14, 16, 17, 20, 23 and 24 in the order of increasing seismic intensity of ASI. Two different bridge samples, which are designated as stiff and flexible bridges, are utilized to take into account the structural variability. Some basic structural features of the bridges are given as follows:

Bridge Type-I (Stiff): 2-span; 3-column bent; span length of 20m; column height of 4.73m. (Figure 4.6-a)

Bridge Type-II (Flexible): 4-span; single-column bent; span length of 30m; column height of 10.0m. (Figure 4.6-b)

a) Stiff bridge   b) Flexible bridge
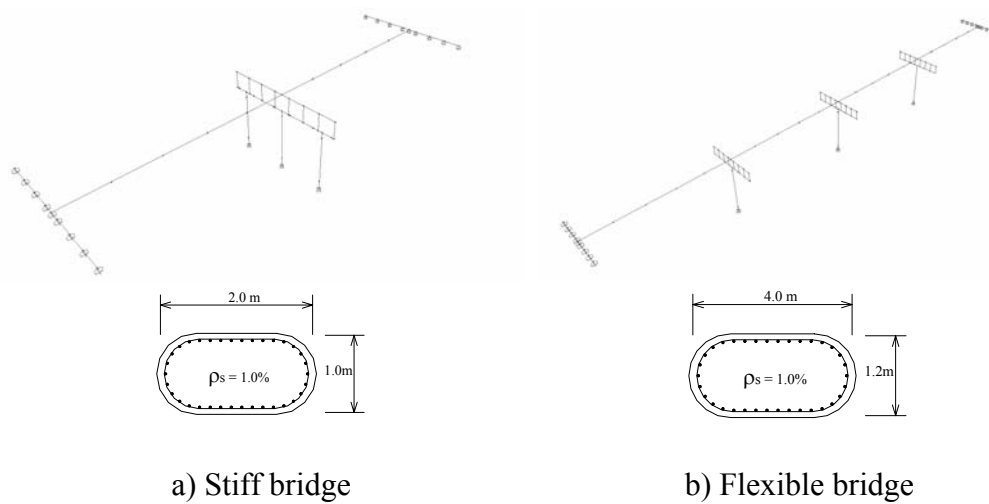
Figure 4.6 Two bridge samples to be used in the sensitivity analyses for the effect of vertical ground motion

In the sensitivity analyses, bridges are investigated for two different cases. In the first case, bridges are analyzed with the selected 9 ground motions for only two horizontal components (L-T). In the second case, in addition to the horizontal components, vertical component of the ground motions are also taken into account (L-T-V). To investigate effect of vertical component, seismic damage of the bridges are considered calculating the bridge demand measures of column curvature in both principal axes, superstructure longitudinal displacement and the column N/No ratio. Seismic demand on the deck is not investigated as it was done in the past studies. Because, it is assumed that the superstructure is expected to remain elastic and it is modeled with elastic beam column element. Analytical models of the bridge samples are developed according to the considerations as explained in CHAPTER 3. Then, nonlinear response history analyses of the bridge samples are performed

under the selected 9 ground motions. The analyses results for two different cases (L-T and L-T-V) and bridge samples are presented in Figure 4.7. According to the analyses results, different levels of seismic damage are imposed on the bridges with the selected ground motions. Except for one ground motion, column curvature demands in both principal axes and the superstructure longitudinal displacement are very close for the two cases (L-T and L-T-V). These findings are consistent with some of the research studies in literature. Values of horizontal response quantities are not significantly influenced by the vertical component of motion. However, effect of vertical motion has a considerable impact on the column axial forces. For most of the ground motions, seismic demand of column axial forces for the (L-T-V) case is greater than the one for the case (L-T). However, for the rest of the ground motions the situation is just the opposite. In other words, calculated max. N/No under the effect of only horizontal components of the ground motions can be greater in comparison with the ground motions when the vertical component is included in the analyses. The reason for this outcome may be the difference in the arrival time of peak vertical and horizontal ground motions.

Due to the variations in the axial load level of the columns for the two cases, column shear capacity will be influenced. However, owing to the bigger column cross-sections, axial capacity of the columns is sufficient to resist any additional demand due to vertical motion.

Although the results of the sensitivity analyses are limited with the selection of ground motions and the bridge samples, it is found out that the effect of vertical ground motion on the seismic damage of the bridges is limited and it is not considered in the final analyses for the development of bridge fragility curves. Moreover, inclusion of vertical motion in the nonlinear response history analyses increases the analyses time by 30 percent on the average. Besides, all ground motions in the data set do not have vertical component. When the vertical motion in the analyses is decided to be considered, some of the ground motions can not be utilized due to lack of their vertical component.
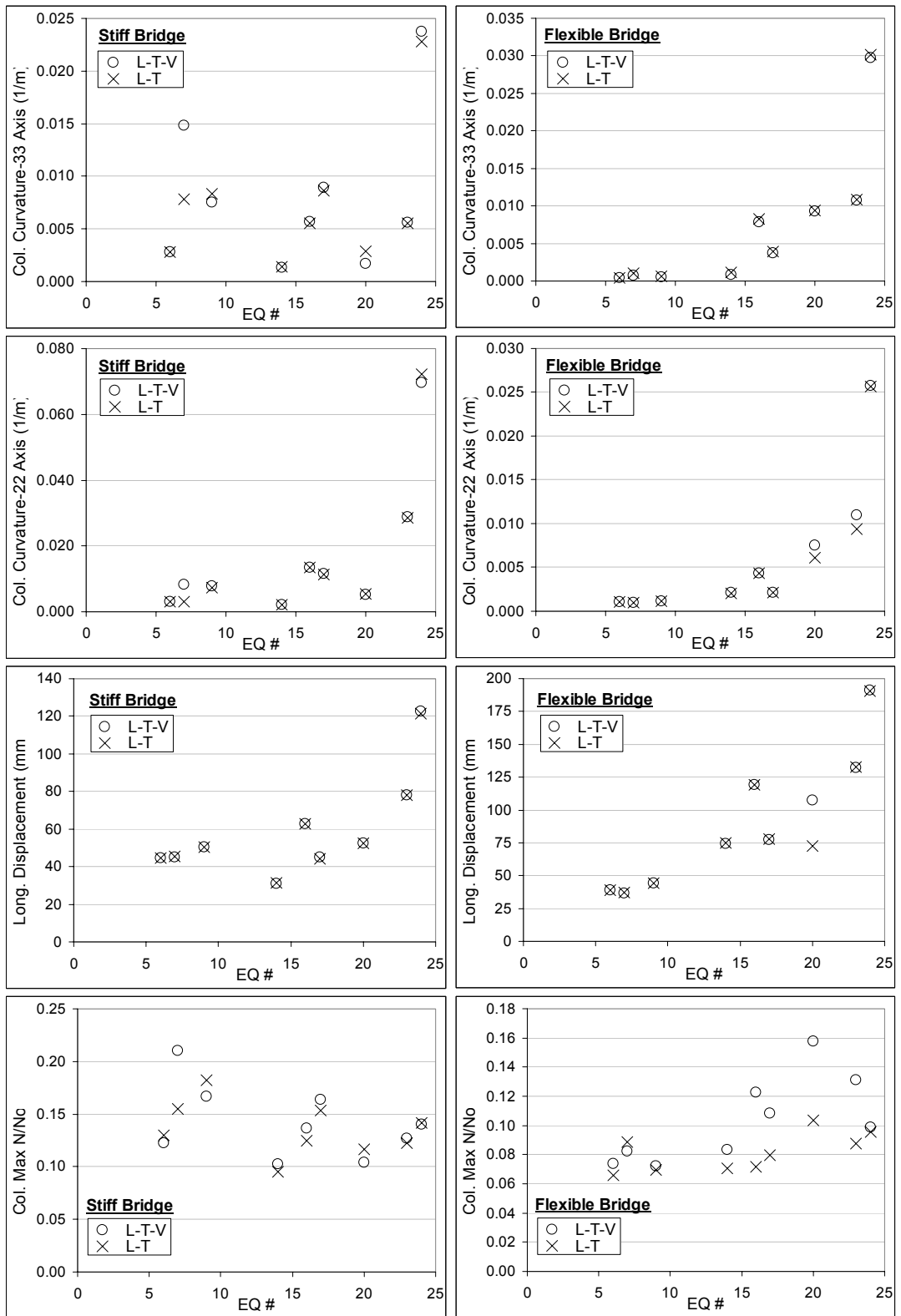
a) Stiff bridge   b) Flexible bridge

Figure 4.7 Results of sensitivity analyses for vertical ground motion effect

4.4 DIRECTIONAL EFFECT OF THE HORIZONTAL COMPONENTS OF THE GROUND MOTION

The selected earthquake ground motions have two horizontal components. Excitation direction of the ground motion components on the bridge samples is arbitrary. As shown in Figure 4.8, two horizontal components of the earthquake ground motions can act on the bridges randomly through an angle θ with respect to the orthogonal bridge directions. One of the main purposes for conducting nonlinear response history analyses is to obtain the maximum seismic responses of the highway bridges. Therefore, ground motion horizontal components should be applied on the bridge samples through the most unfavorable excitation direction with an angle θ in order to attain the maximum seismic responses. However, the critical excitation direction angle, θ is not constant among the bridges and the type of seismic response. Great care should therefore be given when deciding the most critical excitation direction angle, θ. According to Caltrans (2006), earthquake effects are determined from horizontal ground motion applied using two different methods. In the first method, ground motions are applied in two orthogonal bridge directions and the maximum seismic response is calculated using 30% combination rule considering the responses in both orthogonal directions. In the second method, the ground motion shall be applied at a sufficient number of angles to capture the maximum responses of all critical bridge components. The reliability of the first method is questionable for the irregular bridges especially for the bridges having high skew angle. Priestley et al. (1996) mentioned that 30% combination rule, like the other combination rules; apply strictly to structures with linear elastic response. The usefulness of response maxima from individual modes and their subsequent combinations are questionable for inelastically responding bridge systems such as columns and cap beams. Therefore, some sensitivity analyses are performed to capture the maximum responses of all critical bridge components by the application of ground motion components at a sufficient number of angles to the bridges.
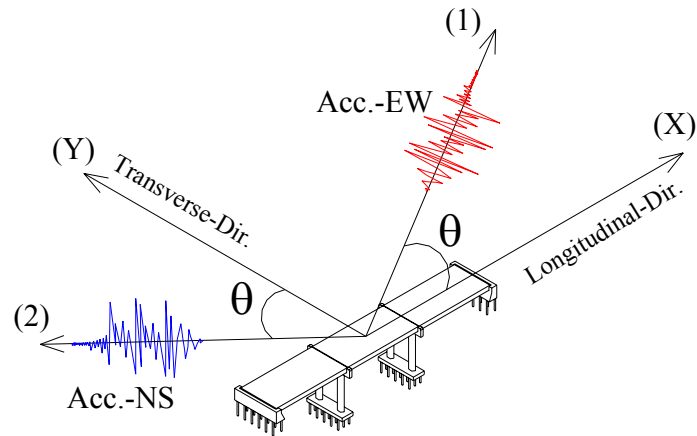
Figure 4.8 Ground motion excitation angle for the maximum bridge response

In order to decide on the most critical excitation direction angle, several sensitivity analyses are conducted considering 2 different bridge types having different skew angles and 7 earthquake ground motions having varying intensities. Two of the sample bridges representing the stiff and the flexible bridges are selected from Table 2.8. A single-column bent bridge having 4 spans with a span length of 35m and column height of 8.7 is selected to represent the flexible bridge in the inventory data. Whereas, a stiff bridge is represented by a sample bridge having a three-column bent with a column height of 4.0m and 2 spans with a span length of 15m. To investigate the effect of bridge skewness on the excitation direction angle and hence maximum bridge seismic response, bridges are analytically modeled with varying skew angles between 0° to 60° with an increment of 10°. Seven earthquake ground motions are selected from Table 4.1. The ID numbers of the selected ground motions are 7, 13, 14, 16, 17, 20, and 21 in the order of increasing seismic intensity of ASI. Horizontal components of all these ground motions are applied to the selected bridges in different directions to capture the maximum seismic response. Excitation direction angle, θ for each ground motion is varied between 0° to 165° with an increment of 15°. Any arbitrary excitation direction should be transformed to the global coordinates to carry out the analyses. For this reason, EQ loading having the directions of '1' and '2' (Figure

4.8) should be transformed to the bridge global coordinates of 'X' and 'Y' using the well known transformation matrix as shown in Equation (4.2) (Khaled et al., 2006).

$$\begin{Bmatrix} a_x(t) \\ a_y(t) \end{Bmatrix} = \begin{bmatrix} \cos\theta & -\sin\theta \\ \sin\theta & \cos\theta \end{bmatrix} \cdot \begin{Bmatrix} a_1(t) \\ a_2(t) \end{Bmatrix}$$

(4.2)

During the analyses of analytical bridge models, column moments in its strong axis (M3) and weak axis (M2) are recorded for the seismic response parameters. Maximum values of the seismic response parameters are determined for each bridge with a specific skew angle under the effect of a ground motion applied in different bridge directions. In order to determine the most critical excitation direction angle for each specific bridge, skew angle and ground motion, maximum column moments for each excitation direction angle are normalized with respect to the maximum column moment values through different excitation directions. This implies that critical excitation angle can be specified among varying excitation angles for a specific bridge, skew angle and ground motion, when the normalized maximum seismic response is calculated to be 1.0. In Figure 4.9, all analyses results are presented together with their mean for different normalized maximum column moments and varying excitation angles. Accordingly, effect of excitation angle on the maximum seismic response of M3 column moment is more pronounced than for the M2 column moment considering their mean values. Maximum M3 moment is determined for the excitation direction angles between 60° to 90°. For the column M2 moment, maximum response variation for different excitation angles is almost negligible.
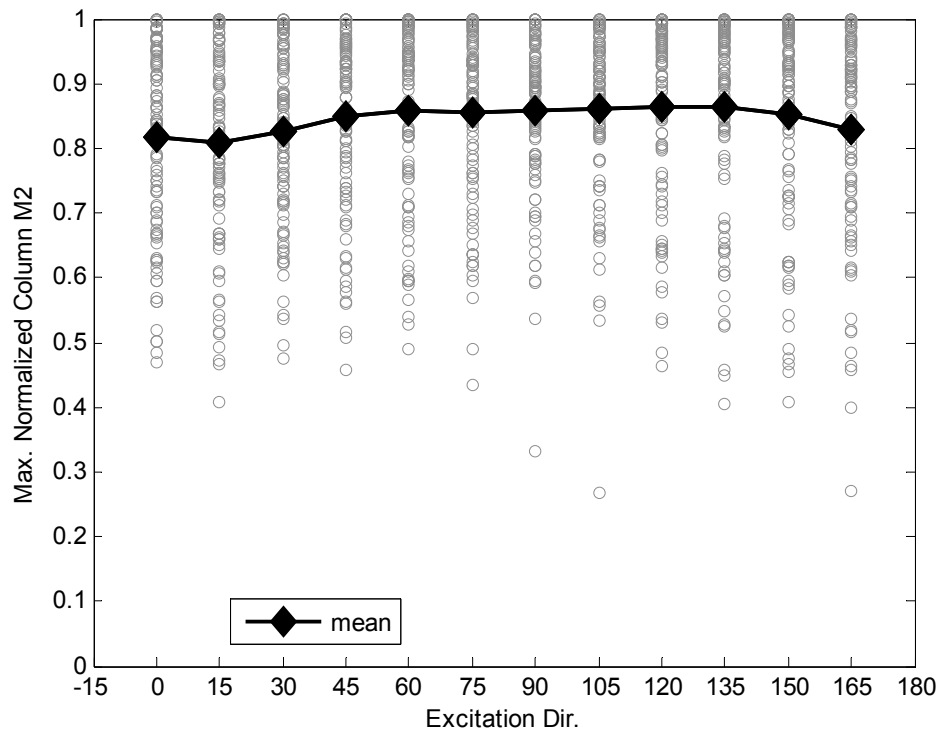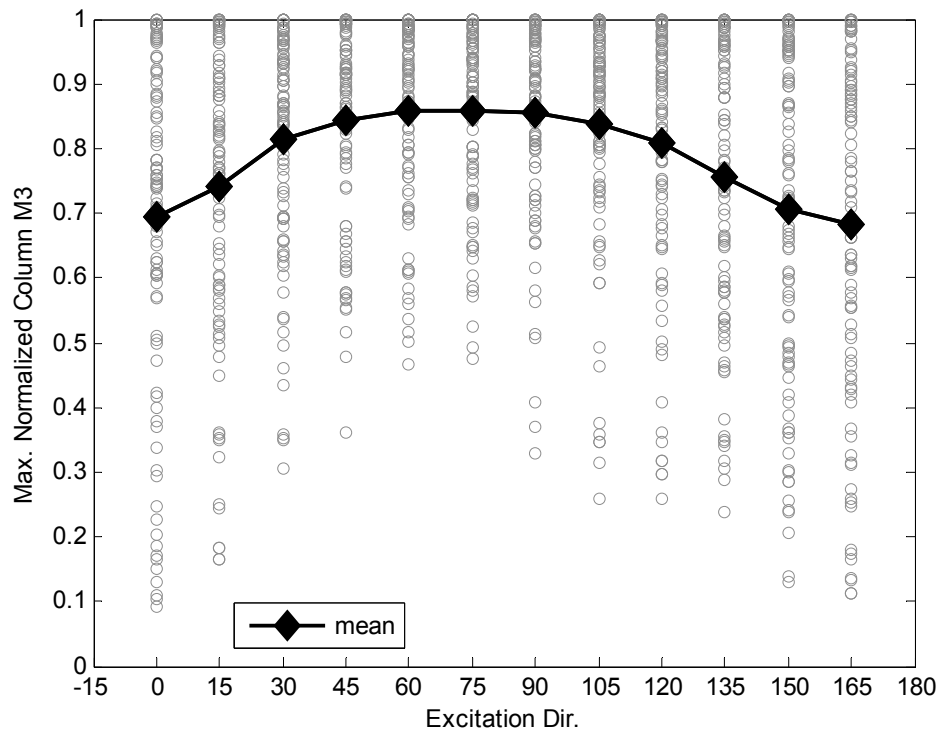
Figure 4.9 Distribution of max normalized column moments (M3 & M2)

Since all the analyses results are presented in Figure 4.9, effect of skewness on the ground motion excitation direction angle can not be examined. To overcome this situation, maximum normalized column moments are determined for each bridge type and for different excitation angles under 7 earthquake ground motions. The mean column moments are calculated among the 7 ground motions in order to investigate the effect of skewness and bridge type on the excitation angle. The results are presented in Figure 4.10 and Figure 4.11 for the stiff and flexible bridges, respectively. Effect of excitation direction angle is more pronounced for M3 column moment than for the M2 column moment considering both stiff and flexible bridges. Although there is not a clear evidence for specifying a general critical excitation direction angle, different excitation angles seem to be critical for different bridge skew angles. As shown in Figure 4.10, mean of the maximum normalized M3 column moments of stiff bridge is greater for the excitation angles between 45° - 90° for all considered skew angles. However, for the M2 column moments, maximum response is obtained for the excitation angles between 90° - 120° for higher skew angles; whereas for lower bridge skew angles, maximum column moments are determined at the lower excitation angles.

The trend between the maximum calculated seismic responses and the excitation angles for different skewness are not similar for stiff and flexible bridges. As shown in Figure 4.11, mean of the maximum normalized M3 column moments of flexible bridge is greater for the excitation angles between 90° - 120° for smaller skew angles. On the other hand, flexible bridges with higher skew angles have seismic response of the maximum normalized M3 column moments during the lower excitation angle values, such as 45° - 60°. However, for the M2 column moments, the difference in the maximum response for various excitation angles is not more than 10 percent. In general maximum response is determined for the excitation angles of 60° - 90°.
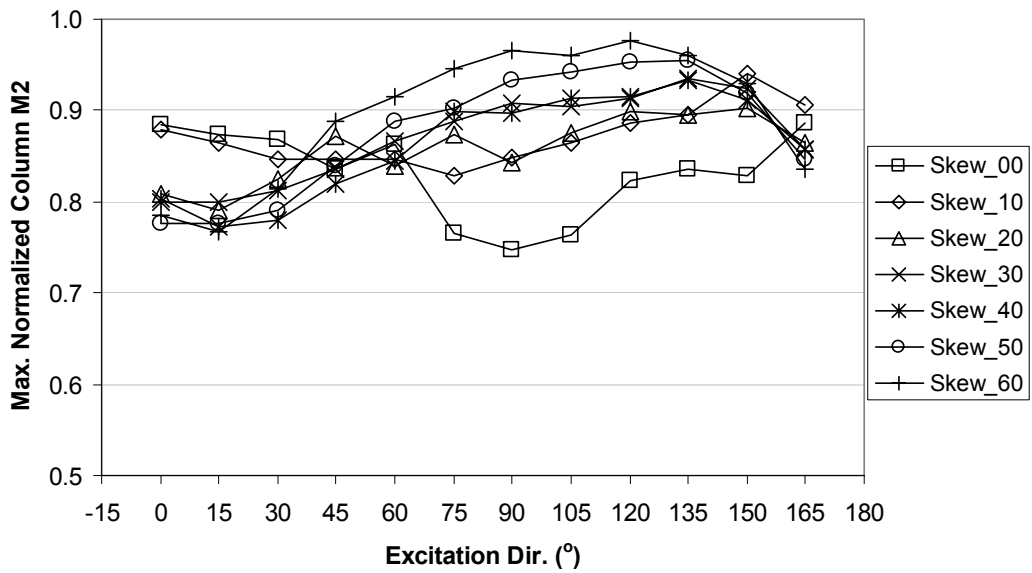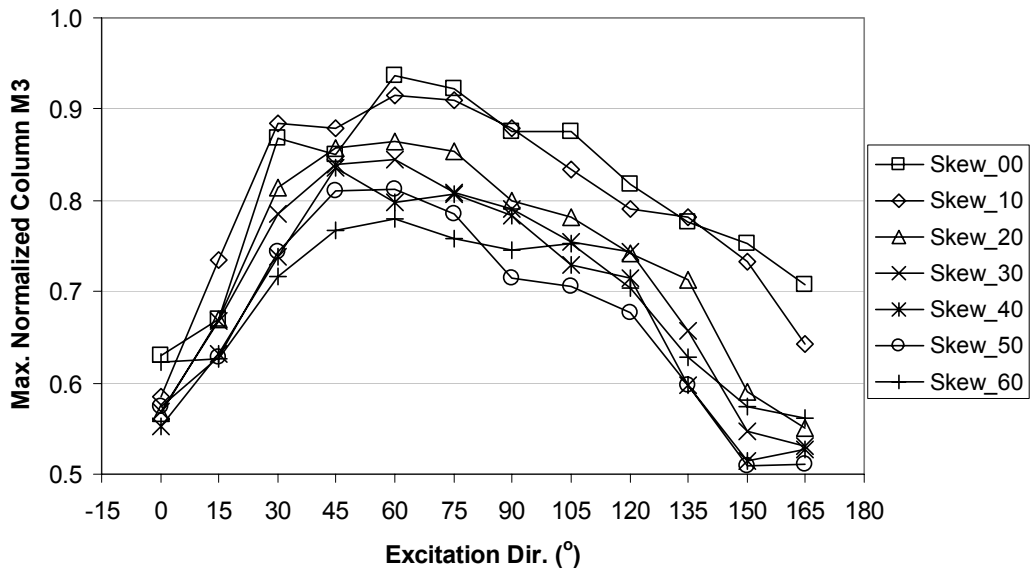
Figure 4.10 Mean of max normalized column moments (M3 & M2) for Stiff
Bridge with varying skewness
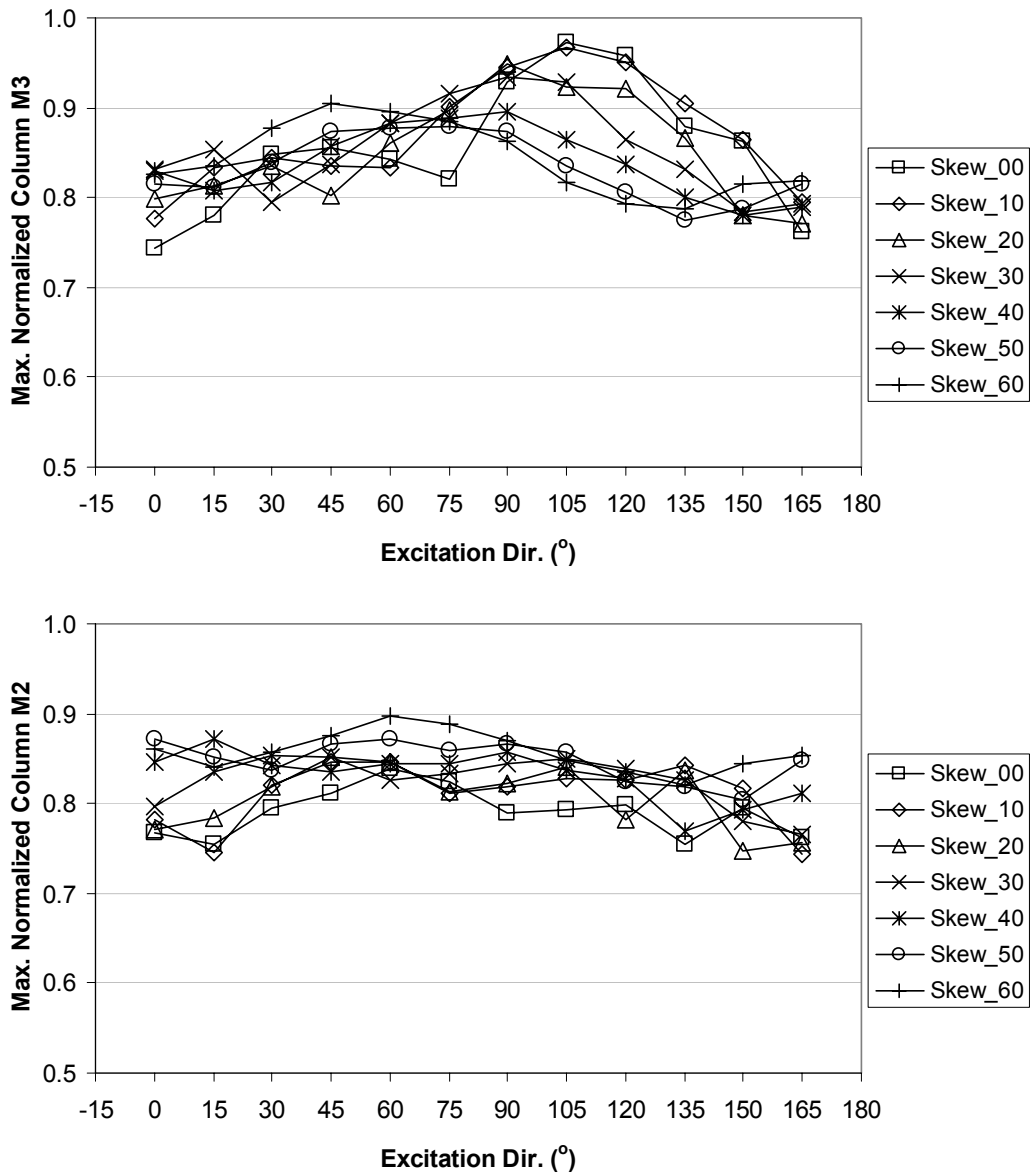
Figure 4.11 Mean of max normalized column moments (M3 & M2) for Flexible
Bridge with varying skewness

According to the results of sensitivity analyses for investigating the critical
ground motion excitation direction angle, in general maximum seismic bridge
responses are obtained when the horizontal components of the ground motion are
applied at the orthogonal bridge directions. In other words, maximum responses can
be obtained when the excitation angles of 0° and 90° are considered. However, it is

still not clear which of the ground motion horizontal component is applied at which bridge orthogonal direction. To solve this problem, all nonlinear response history analyses have been performed for each ground motion twice considering the two cases as schematically depicted in Figure 4.12. In the first case, while one component of the ground motion is applied in the longitudinal direction, the other ground motion component is applied in the transverse direction. In the second case, excitation directions of the ground motion components are interchanged. Finally it is assumed that the maximum seismic response of the bridge under the effect of considered earthquake ground motion is obtained by calculating the maximum seismic responses of the two cases.
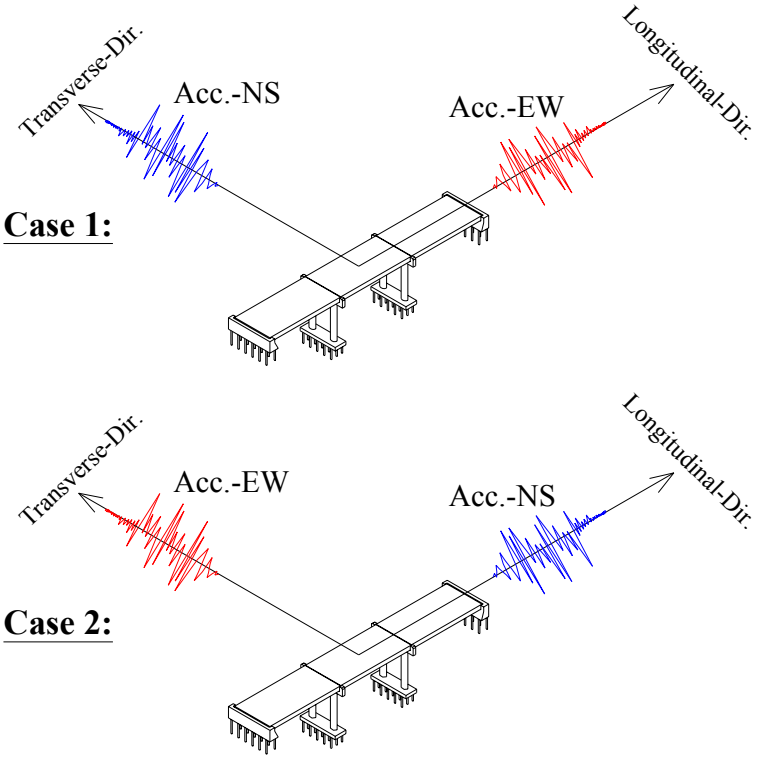
Figure 4.12 Ground motion excitation angle for the maximum bridge response

CHAPTER 5

SEISMIC DAMAGE LIMIT STATES

Determination of bridge damage parameters and their corresponding limit states is one of the significant steps in the development of analytical fragility curves. Bridge damage limit states have a direct influence on the reliability of the fragility curves, which represent the probability of reaching or exceeding a specific damage state under an earthquake ground motion considering its seismic intensity to decide on the performance level of the bridges. Therefore, realistic damage limit states need to be specified to obtain reliable fragility curves and hence to make a reasonable estimate of their seismic performance level. Limit state can be defined as the ultimate point beyond which the bridge structure can no longer satisfy the specified performance level. Moreover, each damage limit state also has functional and operational interpretation. Various qualitative and quantitative limit state definitions for different bridge damage are available in previous studies. Structural damage is related to the deformation of the bridge system and its components. That is why most of the available bridge damage limit state definitions are specified in terms of deformations for the local and global response parameters, which can be expressed as engineering demand parameters. Local engineering demand parameters are utilized for certain structural components whereas global ones are considered for the estimation of overall structural response. Great care should be given to the selection of proper engineering demand parameters for defining the bridge damage limit states to obtain reliable fragility curves. The selected engineering demand parameters should have good correlation with the seismic

damage of bridges. Because seismic damage of the bridge is represented by the bridge seismic response in terms of the selected engineering demand parameter, which is used in the calculation of both capacity and demand of the bridge components.

The physical damage of bridges due to seismic actions should be represented with a sufficient number of damage limit states, which should be quantified by appropriate engineering demand parameters. Although qualitative damage limit state definitions for bridges are available in different codes and studies, widely accepted quantitative damage limit state definitions are not readily available for bridges. Definition of damage limit states for various components of bridges or bridge system as a whole is not a trivial task. Bridge damage state definitions are one of the main sources of uncertainty engaged in the fragility curves due to the subjectivity involved in defining the limit states.

5.1   PREVIOUS STUDIES

Qualitative description of five damage states is defined for highway bridge components by HAZUS (FEMA, 2003). These are the none (ds_1), slight/minor (ds_2), moderate (ds_3), extensive (ds_4) and complete (ds_5) damage states as defined in Table 5.1. Although very detailed qualitative descriptions are defined, quantitative description of these damage states is not given. Each damage state has its own functional and operational interpretation for the bridge components and/or bridge structural system as a whole. As a result, recovery time necessary of the bridges for each damage state differs considerably. As the bridge damage level increases, more recovery time is needed for the bridge to be operational and functional. Restoration functions for each damage state is also specified by HAZUS (FEMA, 2003) as shown in Figure 5.1. These curves are the smooth curves characterized by a cumulative normal distribution function using a mean and standard deviation for each damage state.

Table 5.1 Definitions of damage states by HAZUS (FEMA, 2003)

Damage States	Definitions
None (ds$_1$)	No bridge damage
Slight/Minor (ds$_2$)	Minor cracking and spalling to the abutment, cracks in shear keys at abutments, minor spalling and cracks at hinges, minor spalling at the column (damage requires no more than cosmetic repair) or minor cracking to the deck
Moderate (ds$_3$)	Any column experiencing moderate (shear cracks) cracking and spalling (column structurally still sound), moderate movement of the abutment (<2"), extensive cracking and spalling of shear keys, any connection having cracked shear keys or bent bolts, keeper bar failure without unseating, rocker bearing failure or moderate settlement of the approach.
Extensive (ds$_4$)	Any column degrading without collapse – shear failure - (column structurally unsafe), significant residual movement at connections, or major settlement approach, vertical offset of the abutment, differential settlement at connections, shear key failure at abutments.
Complete (ds$_5$)	Any column collapsing and connection losing all bearing support, which may lead to imminent deck collapse, tilting of substructure due to foundation failure.
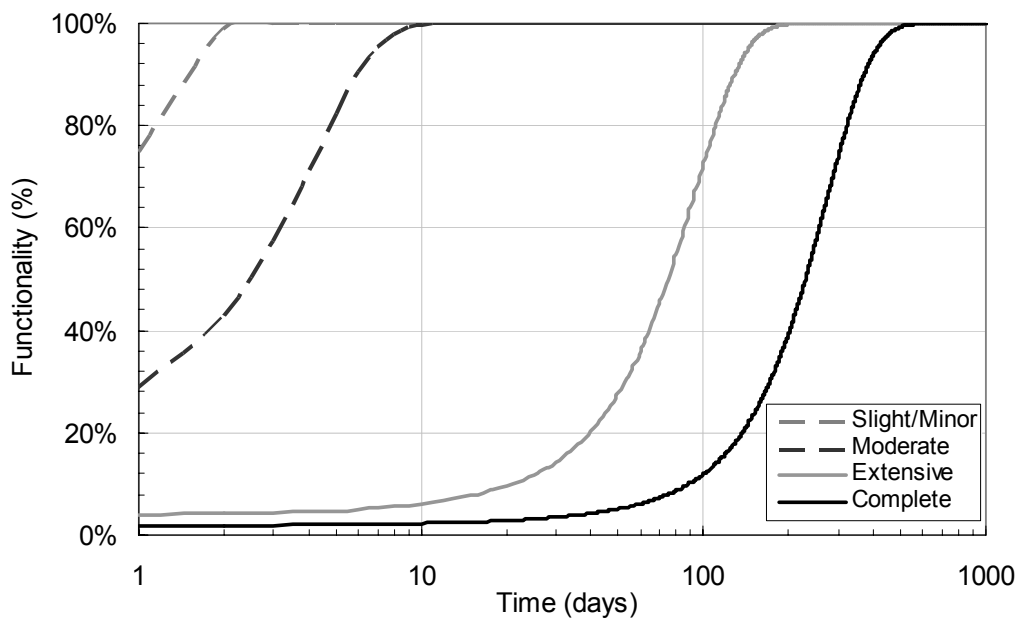
Figure 5.1 HAZUS restoration functions for highway bridges (FEMA, 2003)

In the study of Hwang et al. (2001), two different approaches were considered for the seismic damage assessment and the seismic fragility analysis of bridges. In the first approach, a component-by-component assessment of seismic damage to a bridge was performed by defining damage states for the response parameters of bearings, columns in shear and columns in flexure. Two damage states were defined for the bearings considering their yield and ultimate shear capacity. The second response parameter was the column shear capacity, which is compared with the column shear demand to determine whether columns sustain any shear damage or not. Lastly, four damage states were defined according to the flexural capacity of the columns. Damage description of each damage state and its limit state criteria are given in Table 5.2. M_1 is the column moment at the first yielding of longitudinal bar, whereas M_y is the yield moment at the idealized moment curvature diagram of the column sections. θ_p is the plastic hinge rotation with ε_c equal to 0.002 and 0.004 for the columns with and without lap splices at the bottom of the columns, respectively.

Table 5.2 Seismic damage assessment criteria for columns in flexure (Hwang et al., 2001)

Criterion	Description of Damage	Column Status
$M_1 > M$	No reinforcing steel yielding, minor cracking in concrete	No Damage (OK)
$M_y > M \geq M_1$	Tensional reinforcement yielding and extensive cracking in concrete	Cracking (C)
$M \geq M_y, \theta < \theta_p$	Hinging in column, but no failure of column	Hinging (H)
$M \geq M_y, \theta > \theta_p$	Flexural failure of column	Flexural failure (F)

In the second approach of Hwang et al. (2001), damage limit states were defined to assess the overall seismic damage to bridges for the development of analytical fragility curves. For this purpose, damage states were defined using an

engineering demand parameter of displacement ductility ratio of columns, which is defined by Equation (5.1).

$$\mu_d = \frac{\Delta}{\Delta_{cy1}}$$ (5.1)

Δ is the relative displacement at the top of a column obtained from seismic response analysis, and Δ_{cy1} is the relative displacement of a column when the longitudinal reinforcing bars at the bottom of the column reaches the first yield. Five damage states were defined using demand parameter of displacement ductility ratio of columns, μ_d. The qualitative description of the five damage states is given in Table 5.1, which is defined by HAZUS. The damage states were quantified according to the criteria given in Table 5.3. μ_{cy1} is displacement ductility ratio at the first longitudinal bar yield. Since displacement ductility ratio is defined in terms of the displacement at the first longitudinal bar yield, μ_{cy1} is equal to 1.0. μ_{cy} is yield displacement ductility ratio of the column. μ_{c2} is displacement ductility ratio with $\varepsilon_c=0.002$. μ_{cmax} is the maximum displacement ductility ratio, which is defined as; $\mu_{cmax} = \mu_{c2} + 3.0$.

Table 5.3 Bridge damage states by displacement ductility ratios (Hwang et al., 2001)

Damage States		Criterion
N	No Damage	$\mu_{cy1} > \mu_d$
S	Slight/Minor Damage	$\mu_{cy} > \mu_d > \mu_{cy1}$
M	Moderate Damage	$\mu_{c2} > \mu_d > \mu_{cy}$
E	Extensive Damage	$\mu_{cmax} > \mu_d > \mu_{c2}$
C	Complete Damage	$\mu_d > \mu_{cmax}$

In the study of Hose et al. (2000), five levels of performance and damage states were specified. Seismic damage of the bridges was classified in relation with the socio-economic descriptions at five designated performance levels. Table 5.4 lists the classifications of bridge damage for each of the five levels as well as corresponding damage, repair, and social-economic descriptions.

Table 5.4 Bridge damage assessment (Hose et al., 2000)

Level	Damage Classification	Damage Description	Repair Description	Socio-economic Description
I	NO	Barely visible cracking	NO REPAIR	FULLY OPERATIONAL
II	MINOR	Cracking	POSSIBLE REPAIR	OPERATIONAL
III	MODERATE	Open cracks, onset of spalling	MINIMUM REPAIR	LIFE SAFETY
IV	MAJOR	Very wide cracks, extended concrete spalling	REPAIR	NEAR COLLAPSE
V	LOCAL FAILURE /COLLAPSE	Visible permanent deformation, buckling/rupture of reinforcement	REPLACEMENT	COLLAPSE

To explicitly relate bridge damage to capacity, engineering terms were selected for the performance levels rather than the socio-economic expressions for the five performance levels ranging from concrete cracking and member strength degradation. Qualitative and quantitative performance descriptions corresponding to the five performance levels were given in Table 5.5. The database attempts to explicitly define criteria at each level by providing quantitative guidelines such as crack widths, crack angles, and regions of spalling.

In addition to the quantitative descriptions for each performance level, various engineering demand parameters were investigated for numerical determination of damage limit states using experimental results of several bridge column tests. The investigated engineering demand parameters are steel and concrete strain, curvature and displacement ductility, plastic rotation, principal compression and tension stresses, drift ratio, residual deformation index, equivalent viscous damping ratio and normalized effective stiffness.

Table 5.5 Bridge performance assessment (Hose et al., 2000)

Level	Performance Level	Qualitative Performance Description	Quantitative Performance Description
I	CRACKING	Onset of hairline cracks.	Cracks barely visible.
II	YIELDING	Theoretical first yield of longitudinal reinforcement.	Crack widths < 1mm.
III	INITIATION OF LOCAL MECHANISM	Initiation of inelastic deformation. Onset of concrete spalling. Development of diagonal cracks.	Crack widths 1-2mm. Length of spalled region > 1/10 cross-section depth.
IV	FULL DEVELOPMENT OF LOCAL MECHANISM	Wide crack widths/spalling over full local mechanism region.	Crack widths > 2mm. Diagonal cracks extend over 2/3 cross-section depth. Length of spalled region > 1/2 cross-section depth.
V	STRENGTH DEGRADATION	Buckling of main reinforcement. Rupture of transverse reinforcement. Crushing of core concrete.	Crack widths > 2mm in concrete core. Measurable dilation > 5% of original member dimension.

In the study of Liao and Loh (2004), a total of four damage states were defined for highway bridge components, which are in accordance with the ones defined by HAZUS. The qualitative description of each damage state for bridge components is given in Table 5.6.

Table 5.6 Damage state description for bridge components (Liao and Loh, 2004)

Damage States	Qualitative Descriptions
Slight Damage	Minor cracks and spalling at the column, abutment, girder or deck, cracks at shear key, cracks at expansion joint or approach slab.
Moderate Damage	Column experiencing moderate cracks and spalling, abutment failure without collapse, shear key failure or restrainer failure without unseating.
Extensive Damage	Any column degrading without collapse or shear failure, significant movement at connections, significant offset of abutment.
Complete Damage	Any column collapse or large movement of connections, deck collapse, tilting of substructure due to ground failure.

Liao and Loh (2004) determined analytical fragility curves using the above mentioned damage states, which were quantified in terms of ductility and displacement (Table 5.7). For each damage state, ductility limits were specified for weak pier and strong bearings by considering the design type of the bridge, which is either seismic or conventional design. Whereas, displacement limits were specified for the bridges having weak bearings and strong pier. Available girder seat length is taken into account for the definition of complete damage state. However, in the definition of moderate and extensive damage states, numerical values are given without any physical meaning for the associated damage state.

Table 5.7 Ductility and displacement limits for each damage state (Liao and Loh, 2004)

Ductility limits for weak pier and strong bearings			Displacement limits
			Weak bearings and strong pier
Damage State	Seismic Design	Conventional Design (non-seismic design)	
Slight	$\mu = 2.0$	$\mu = 1.0$	Yield Displacement
Moderate	$\mu = 4.0$	$\mu = \min(1+ (\mu_f-1)/2, 2.0)$	10 cm
Extensive	$\mu = 6.0$	$\mu = \min(\mu_f, 3.0)$	20 cm
Complete	$\mu = 9.0$	$\mu = 4.5$ or pier reach its ultimate capacity	min (40cm, 2N/3)
μ_f: corresponding ductility at occurrence of flexure to shear failure. N: seat length of a girder at the support.			

Kowalsky (2000) considered two damage limit states, which are "serviceability" and "damage control", for circular RC bridge columns. Qualitatively, serviceability limit state implies that repair is not needed after the earthquake, while damage control limit state implies that only repairable damage occurs. Quantitatively, these damage limit states were characterized with respect to concrete compression and steel tension strain limits in Table 5.8.

116

Table 5.8 Quantitative damage limit state definitions (Kowalsky, 2000)

Limit State	Concrete Strain Limit	Steel Strain Limit
Serviceability	0.004	0.015
Damage Control	0.018	0.060

Quantitative descriptions of the limit states were also given by Kowalsky (2000). The serviceability concrete compression strain was defined as the strain at which crushing is expected to begin, while the serviceability steel tension strain was defined as the strain at which residual crack widths would exceed 1 mm, thus likely requiring repair and interrupting serviceability. The damage control concrete compression strain was defined as the compression strain at which the concrete is still repairable. Steel tension strain at the damage control level was related to the point at which incipient buckling of reinforcement occurs. It was mentioned that the proposed strain limits for the serviceability limit states are widely accepted. On the other hand, damage control level strain limits were dependent on the detailing of transverse reinforcement. The given damage control strain limits valid for well detailed systems and they would not be appropriate for assessment of existing columns with insufficient transverse reinforcement.

Five post-earthquake damage states were employed by Elnashai et al. (2004). These are as follows:

- Undamaged;
- Slightly damaged, but usable without repair or strengthening;
- Extensively damaged, but still repairable;
- No collapse, but so severely damaged that must be demolished;
- Collapse.

Four limit states were defined to assess the bridge damage state including both qualitative and quantitative descriptions. Below the first limit state, no damage should take place and the expected response is of small displacement amplitude. This limit state is defined as the point that the first yielding of longitudinal

117

reinforcing bars. Below the second limit state, bridge can experience minor structural damage and it is usable after the earthquake. Member flexural strengths may have been reached and limited ductility developed, provided that concrete spalling in plastic hinges does not occur and that residual crack widths remain sufficiently small. Cover concrete strain ε_c, is employed to identify this limit state. Below the third limit state, significant structural damage is expected. The bridge will be out of service after the earthquake unless significant repair is undertaken. However, repair and strengthening is feasible. Rupture of transverse reinforcement or buckling of longitudinal reinforcement should not occur and core concrete in plastic hinge regions should not need replacement. Below the final limit state extensive damage is expected, but the bridge should not have collapsed. Repair may be neither possible nor cost-effective. The structure will have to be demolished after the earthquake. Beyond this limit state, global collapse endangering life is expected since it corresponds to the inability of the structure to sustain gravity loads. A steel strain of 9% was assumed by Elnashai et al. (2004) to identify the final limit state.

Karim and Yamazaki (2003); Nateghi and Shahsavar (2004) considered five damage states for the development of analytical fragility curves. These are the No, Slight, Moderate, Extensive and Complete damages. Park-Ang damage index based on energy dissipation was employed for the quantification of each defined damage states.

In the study of Basoz and Mander (1999), a total of five damage states were defined for highway bridge components, which are in accordance with the ones defined by HAZUS. Table 5.9 lists these damage states and the corresponding failure mechanisms. Also drift limits were specified to predict the various damage states for non-seismic and seismically designed bridges by Basoz and Mander (1999). These drift limits are applicable to bridges with weak piers and strong bearings. Displacement limits for girder bridges with weak bearings and strong piers increase as the bridge damage state increases. Slight and moderate damage states show initial damage to the bearings. Extensive and complete damage states show incipient unseating (i.e. when the girder seat becomes unstable and is equal to half the width of the girder flange) and collapse (i.e. the bearing topples). The given

drift limits for each damage limit state were further utilized by Banerjee and Shinozuka (2007) to quantify the limit states in terms of rotational ductility of columns.

Table 5.9 Drift and displacement limits for each damage state (Basoz and Mander, 1999)

Damage State	Failure Mechanisms	Drift limits for weak pier & strong bearings		Displacement Limits for Weak Bearings and Strong Pier (m)
		Non-seismic	Seismic	
Slight Damage	Cracking, spalling	0.005	0.010	0.050
Moderate Damage	Bond, abutment backwall collapse	0.010	0.025	0.100
Extensive Damage	Pier concrete failure	0.020	0.050	0.175
Complete Damage	Deck unseating, pier collapse	0.050	0.075	0.300

In the study of Choi et al. (2004), damage states of bridges were defined for column ductility demand, steel fixed and expansion bearing deformations, and elastomeric bearing deformations. The damage state definitions were based on the qualitative descriptions of the damage states as provided by HAZUS. The quantitative definitions of each damage states for the mentioned engineering demand parameters are presented in Table 5.10. Choi et al. (2004) mentioned that the damage states were quantified according to the recommendations from previous studies and experimental test results. The quantified damage states for the columns were described by the column curvature ductility and based on tests of non-seismically designed columns, of which the lap-slices at the base were taken into account. The damage states for the bearings in the pre-stressed concrete girder bridges were based on fracture of the bearing and the displacement necessary for unseating. The problem of instability and unseating is a function of the size of the

bearings and the width of the supports. The displacement at the complete damage limit state was assumed to be δ=255mm by Choi et al. (2004), which accounts for the unseating PSC-girders.

Table 5.10 Definition of damage states for bridge components (Choi et al., 2004)

| Damage State | Engineering Demand Parameters | | | | |
	Columns (μ)	Steel Bearings (δ, mm)	Expansion Bearings (δ, mm)	Fixed Dowels (δ, mm)	Expansion Dowels (δ, mm)
Slight Damage	$1.0<\mu<2.0$	$1<\delta<6$	$\delta<50$	$8<\delta<100$	$\delta<30$
Moderate Damage	$2.0<\mu<4.0$	$6<\delta<20$	$50<\delta<100$	$100<\delta<150$	$30<\delta<100$
Extensive Damage	$4.0<\mu<7.0$	$20<\delta<40$	$100<\delta<150$	$150<\delta<255$	$100<\delta<150$
Complete Damage	$7.0<\mu$	$40<\delta$	$150<\delta<255$	$255<\delta$	$150<\delta<255$

Nielson (2005) utilized bridge damage states described qualitatively by HAZUS. Engineering demand parameters of column curvature ductility, steel fixed and rocker bearing deformations, elastomeric fixed and expansion bearing deformations, and abutment displacements were employed for the quantification of damage states. Column curvature ductility values for each damage limit state were computed using the displacement ductility ratios specified by Hwang et al. (2001).

Priestley et al. (1996) specified limit states for both member and structure response. Qualitative descriptions were given for cracking, first-yield, spalling and ultimate limit states to define the member seismic response. Member limit states are schematically shown on a moment-curvature diagram in Figure 5.2-a. Priestley et al. (1996) considered three structural limit states, which are serviceability, damage-control, and survival limit states. Both qualitative and quantitative limit state descriptions based on an average range of displacement ductility ratios were given. Schematic representation of the three structural limit states as well as the yield point of an idealized force-displacement curve are shown in Figure 5.2-b.

a) member limit state   b) structure limit state
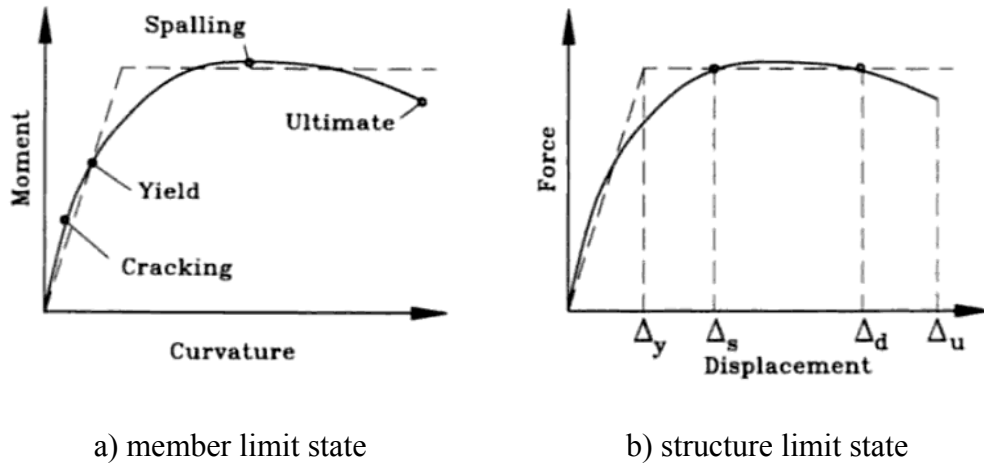
Figure 5.2 Schematic representation of limit states (Priestley et al., 1996)

5.2   DAMAGE PARAMETERS

According to the previous studies, damage states defined by HAZUS are widely accepted among the researchers to be used in the development of fragility curves. Since five damage states were considered, four damage limits should be specified quantitatively to be able to develop analytical fragility curves. Definitions of the first and the last damage limit states, which correspond to the slight and complete damage limit states, have commonly accepted physical meanings. Slight damage limit generally corresponds to the system's yield point beyond which the structure experience inelastic deformations. Complete damage limit state can be specified as the ultimate capacity of the structure, beyond which the structural system is no longer stable and total collapse occurs. On the other hand, intermediate damage limits of moderate and extensive damage limit states correspond to bridge physical damage, which is not commonly defined among the researchers. Defining quantitative measures for the intermediate damage limit states is a subjective task and challenge lies in being able to define these damage limits such that they represent the true physical damage of the bridges. Because of the uncertainties involved in quantifying the intermediate damage limit states, instead of dealing with two intermediate damage limits of moderate and extensive damage limit states, only

121

one intermediate damage limit state is considered in the analyses. This intermediate limit state represents the extreme level of seismic response after which it would not be economically and technically feasible to repair the bridge (FHWA, 1995). Therefore, a total of three damage limits are considered in the development of analytical fragility curves in this study. Damage limits and damage states employed in this study are in accordance with TEC (2007). These three damage limit states are termed as "serviceability" (LS-1), "damage control" (LS-2) and "collapse prevention" (LS-3). Slight/No, moderate, significant, and collapse states are the four corresponding damage states that the bridges can experience under the effect of an earthquake ground motion. The schematic representation of the three damage limits and their corresponding damage states are shown on a force-deformation curve in Figure 5.3.
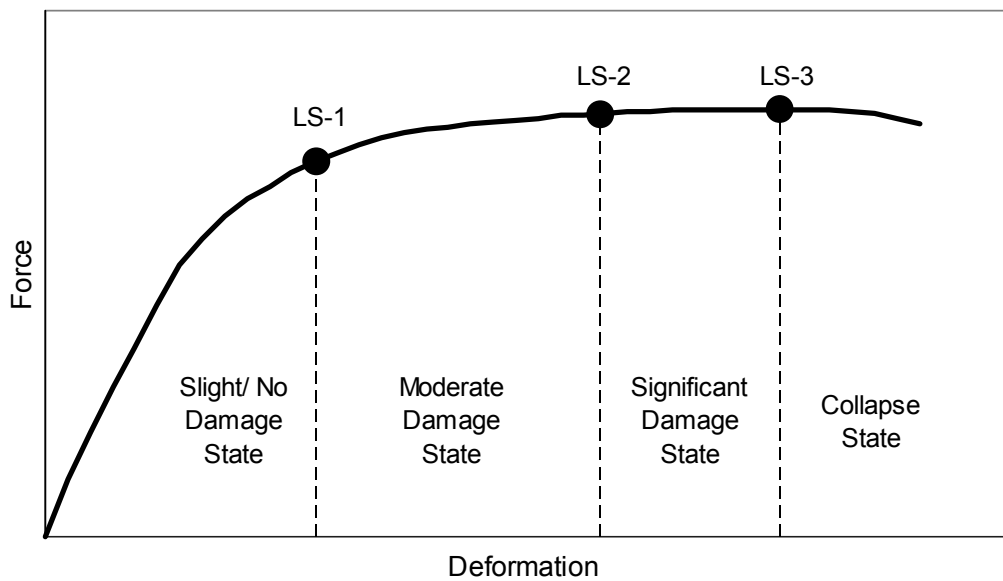
Figure 5.3 Damage states and damage limits on a force-deformation curve

In order to determine analytical fragility curves for highway bridges, it is required to give quantitative descriptions for each damage limit, which represent the

physical seismic damage of the bridges. In the previous studies, quantification of damage limit states is made through consideration of either local or global measures of bridge damage. Selection of damage measure to quantify the damage limit states has a significant influence on the reliability of the analytical fragility curves. Considering a single global damage measure can lead to underestimation of local bridge failures. Moreover, considering local damage of individual bridge components has the advantage of investigating the effect of respective bridge component on the overall seismic response of bridge. Several engineering demand parameters of various bridge components can be considered for the bridge damage assessment. No seismic damage is expected in the superstructure. Because it remains in the elastic range with the help of isolation units employed between the superstructure and substructure. Past earthquakes revealed that the nonlinear elements of bent columns and cap beams are the most susceptible bridge components to seismic damage. Therefore, curvature and shear capacity of the columns and cap beams should be taken into account in the bridge damage assessment. Also deck unseating is one of the most common seismic damage that bridges can experience during damaging earthquakes. For the rest of the bridge components, it is assumed that they do not experience any seismic damage However, in some of the previous studies (Nielson and DesRoches, 2006; Nielson, 2005), abutments are expected to experience seismic damage in the form of backfill soil deformations or structural damage of the abutment. On the other hand, Priestley et al. (1996) mentioned that abutment failure due to seismic loadings is very rare. Moreover, abutments are massive structures in comparison with other bridge components and they are expected to be in the elastic range without any considerable seismic damage under a severe earthquake. Besides, abutment failure due to ground failure is not taken into consideration in the development of fragility curves, because excessive soil deformations and ground failure is out of the scope of this study.

Seismic demands of the bridge components for the interested damage parameters are obtained from nonlinear response history analyses. The demand values will then be compared with the respective capacities specified for each

damage limit state to decide on the damage state of the bridge components. This information will be used in the development of analytical fragility curves. Therefore quantitative damage limits should be specified in detail for each damage parameter. By using the results of the response history analyses, damage state of the relevant bridge components is determined considering the following engineering demand parameters.

- Curvature demands of the RC column and cap beam, which are expected to experience inelastic deformations.
- Shear demand on the RC column and cap beam.
- Superstructure relative displacement for the assessment of deck unseating.

Each damage limit state is quantified considering the above mentioned engineering demand parameters. During this process, several analyses are performed and existing capacities of the bridge components are calculated in detail to obtain reliable damage limits.

5.2.1 Damage Limit States for Curvature Capacity

Column and cap beam curvature is employed as an engineering demand parameter for the quantification of damage limit states of column and cap beam, which are expected to respond in the inelastic range. For this purpose, section analyses are performed to determine the moment-curvature relationship of the column and cap beam RC sections. Material models given in Figure 3.10 for the reinforcement steel, confined and unconfined concrete are utilized in the section analyses. Nonlinear M-K curve is obtained first and then converted to a bilinear representation by the following procedure. Yielding point of longitudinal reinforcement is specified to determine the linear elastic portion and initial slope of the bilinear M-K curve. Ultimate curvature point of the M-K curve is specified when the reinforcement steel or confined concrete extreme fiber has reached its ultimate strain value or when the moment capacity at the M-K curve has decreased

to 80 percent of its maximum attained moment capacity (Priestley et al., 1996). After obtaining the initial slope and the ultimate point of the M-K curve, bilinear M-K curve is determined by applying trial and error calculations in a way that the area under the nonlinear and bilinear curve is equal to each other, which is termed as the equal energy rule.

Section yield point determined from bilinear M-K curve corresponds to the serviceability limit state for the nonlinear bridge components. At this damage limit state, cracks widths should be sufficiently small and the member functionality is not impaired. The intermediate limit state of damage-control limit state is defined as the point at which the concrete cover spalling occurs. According to Priestley et al. (1996), the onset of spalling of cover concrete is considered to be significant damage state, at which the negative stiffness as well as sudden strength loss may take place. Beyond this limit state, bridge may experience significant damage, which can be characterized with several damage indicators such as the fracture of transverse reinforcement, buckling of longitudinal reinforcement and the need for replacement of core concrete in the plastic hinge region. Damage-control limit state is quantified with a curvature limit that is calculated when the extreme fiber of the unconfined concrete attains a compressive strain of 0.003, which is assumed to be the strain limit for the spalling of concrete cover.

Defining the collapse prevention limit state by the ultimate curvature determined from the section M-K curve does not represent the true damage state of the bridge columns. Because the reliability of ultimate curvature is directly influenced by the material models, which involve several assumptions and approximations. Moreover, during the section analyses, perfect bond between concrete and reinforcement is assumed and bond slip is not taken into account in the calculation of ultimate curvature. Therefore, it is more realistic to use the results of experimental data for determining the ultimate curvature that the nonlinear bridge component can experience without occurrence of complete failure. Erduran and Yakut (2004) proposed an empirical equation for the column displacement ductility capacity based on the results of previous column experiments. The given Equation (5.2) for the column displacement ductility has the parameters of ρ_s and N/N_o,

125

which are the amount of transverse reinforcement and axial load level of the columns, respectively. Column displacement ductility of each bridge sample is determined using Equation (5.2). Although axial load level of the columns change during the dynamic analyses of the bridges, an average value is assumed for the column axial load level, which is calculated from gravity analyses.

$$\mu_u = 0.6 \ln\left[\left(\frac{\rho_s}{N/N_o}\right)^2\right] + 7.5 \qquad (5.2)$$

Curvature ductility of the columns can be calculated using the column displacement ductility, the column length, and the plastic hinge length of column using the formulations derived through Equations (5.3) to (5.9) (Priestley et al., 1996). The parameters employed in Equations (5.3), (5.4) and (5.5) are schematically shown in Figure 5.4 for a cantilever column. Plastic hinge length formulation proposed by Priestley et al. (1996) is employed in the calculations as shown in Equation (5.10). Where, d_{bl} is the diameter of the longitudinal reinforcement, f_{ye} is the design yield strength for longitudinal reinforcement, and L is the distance from the critical section of the plastic hinge to the point of contraflexure. L is taken as the total column height for the single column bent. Since the column has a cantilever structural system, development of plastic hinge takes place only at the bottom of the column. This is also valid for the columns in their weak axis at the multi column bents. However, in the column strong axis at the multi column bents, in other words, in the transverse direction of nonskew bridge, cap beams and columns form a frame system. In this system, plastic hinges can develop both at the bottom and top of the column members. Due to the flexibility of the cap beams plastic hinges will be developed at the bottom of the column first and point of contraflexure occurs closer to the column top joint. For simplicity, point of contraflexure is assumed to occur at the mid height of the column for its strong axis and hence distance L to be used in Equation (5.10) is calculated as half of the column clear height.

$$\mu_\Delta = \frac{\Delta_u}{\Delta_y} = \frac{\Delta_p + \Delta_y}{\Delta_y} = 1 + \frac{\Delta_p}{\Delta_y} \tag{5.3}$$

$$\Delta_y = \frac{\Phi_y \cdot L^2}{3} \tag{5.4}$$

$$\Delta_p = (\Phi_u - \Phi_y) \cdot L_p \cdot (L - 0.5 \cdot L_p) \tag{5.5}$$

$$\mu_\Delta = 1 + \frac{(\Phi_u - \Phi_y) \cdot L_p \cdot (L - 0.5 \cdot L_p)}{\dfrac{\Phi_y \cdot L^2}{3}} \tag{5.6}$$

$$\mu_\Delta - 1 = (\frac{\Phi_u - \Phi_y}{\Phi_y}) \cdot \frac{3L_p}{L} \cdot (1 - 0.5 \cdot \frac{L_p}{L}) \tag{5.7}$$

$$\mu_\Delta - 1 = (\mu_\Phi - 1) \cdot \frac{3L_p}{L} \cdot (1 - 0.5 \cdot \frac{L_p}{L}) \tag{5.8}$$

$$\mu_\Phi = 1 + \frac{\mu_\Delta - 1}{\dfrac{3L_p}{L} \cdot (1 - 0.5 \cdot \dfrac{L_p}{L})} \tag{5.9}$$

$$L_p = 0.08L + 0.022 f_{ye} d_{bl} \geq 0.044 f_{ye} d_{bl} \qquad (f_{ye} \, [MPa]) \tag{5.10}$$
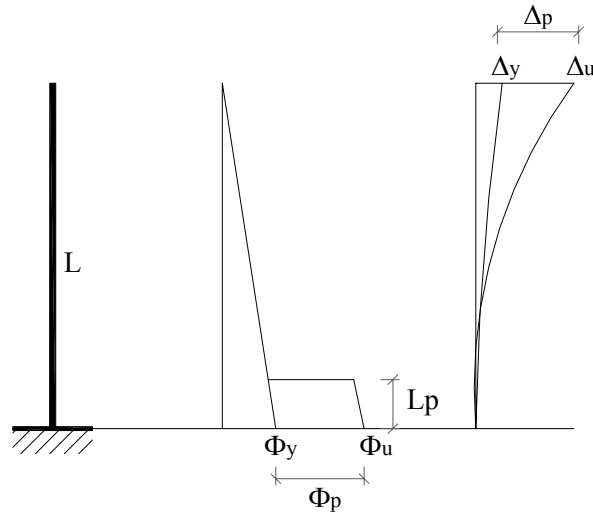
Figure 5.4 Distribution of a cantilever column curvature and displacement

The results of the column ultimate curvature calculations are presented in Table 5.11 and Table 5.12 for the multi-column and single-column bent samples, respectively. In the tables, parameters are given according to their local axis of column sections for 33 (strong axis) and 22 (weak axis). Hwang et al. (2001) specified maximum displacement ductility ratio of 4.76 for a bridge column, which is also utilized in the development of analytical fragility curves by Nielson, (2005). The column displacement ductility specified by Hwang et al. (2001) is in good agreement with the ones calculated using the empirical equation.

Table 5.11 Column curvature calculation results for multi-column bent samples

Sample#	N_{grav} (kN)	N/N_o	ρ_s	μ_Δ	Column Height (m)	L_p-33 (m)	L_p-22 (m)	μ_Φ-33	μ_Φ-22
1	2822	0.049	0.004	4.38	7.3	0.533	0.825	9.35	11.59
2	2824	0.062	0.005	4.10	8.7	0.589	0.938	9.22	11.17
3	1329	0.029	0.005	5.01	4.0	0.480	0.557	7.26	11.22
4	2737	0.047	0.004	4.42	5.6	0.480	0.687	8.25	10.88
5	2773	0.061	0.005	4.13	7.8	0.553	0.866	8.93	10.97
6	3515	0.060	0.004	4.12	9.6	0.623	1.007	9.55	11.45
7	1755	0.039	0.005	4.68	6.7	0.508	0.776	9.74	12.22
8	2954	0.051	0.004	4.33	6.2	0.487	0.734	8.63	10.92
9	2318	0.051	0.005	4.34	4.3	0.480	0.586	6.64	9.81
10	3370	0.058	0.004	4.17	7.2	0.529	0.817	8.78	10.89

Table 5.12 Column curvature calculation results for single-column bent samples

Sample#	N_{grav} (kN)	N/N_o	ρ_s	μ_Δ	Column Height (m)	L_p (m)	μ_Φ
1	5876	0.054	0.004	4.01	7.3	0.881	9.87
2	8308	0.077	0.004	3.60	8.7	0.994	9.06
3	3959	0.037	0.004	4.49	4.0	0.612	9.14
4	5721	0.053	0.004	4.04	5.6	0.743	9.18
5	8202	0.076	0.004	3.61	7.8	0.922	8.85
6	7268	0.067	0.004	3.76	9.6	1.062	9.77
7	5214	0.048	0.004	4.16	6.7	0.832	10.03
8	6172	0.057	0.004	3.95	6.2	0.789	9.22
9	6810	0.063	0.004	3.83	4.3	0.642	7.88
10	6976	0.064	0.004	3.81	7.2	0.873	9.23

Due to the lack of experimental data on the calculation of ultimate curvature or displacement of the cap beams, the ultimate curvature obtained from M-K is considered as the collapse prevention limit state for the cap beams.

Figure 5.5 shows the schematic representation of the three damage limits and their corresponding damage states on a moment-curvature diagram. In some cases, curvatures calculated for damage-control and collapse prevention limit can be very close to each other especially for the weak axis of the single column bent columns. This implies very narrow interval for the significant damage state affecting the reliability of the fragility curves. In this case, ultimate curvature calculated using empirical equations for the collapse prevention limit state is modified by considering the curvature specified for the damage-control limit state, which is a commonly accepted damage limit for the concrete cover spalling. According to Eurocode 8 - Part3 (2005), the chord rotation capacity corresponding to significant damage may be assumed to be 3/4 of the ultimate chord rotation. In a similar way, ultimate curvature capacity for the collapse prevention limit state is updated with a factor of 4/3 of the calculated curvature for the damage-control limit state. Therefore, curvature capacity for the collapse prevention limit state is obtained by the maximum value of the curvature calculated with Equation (5.9) employing the empirical formulation for displacement ductility and the curvature corresponding to the 4/3 of the limiting curvature for damage-control limit state, which is calculated for the compressive strain of 0.003 at the unconfined concrete.
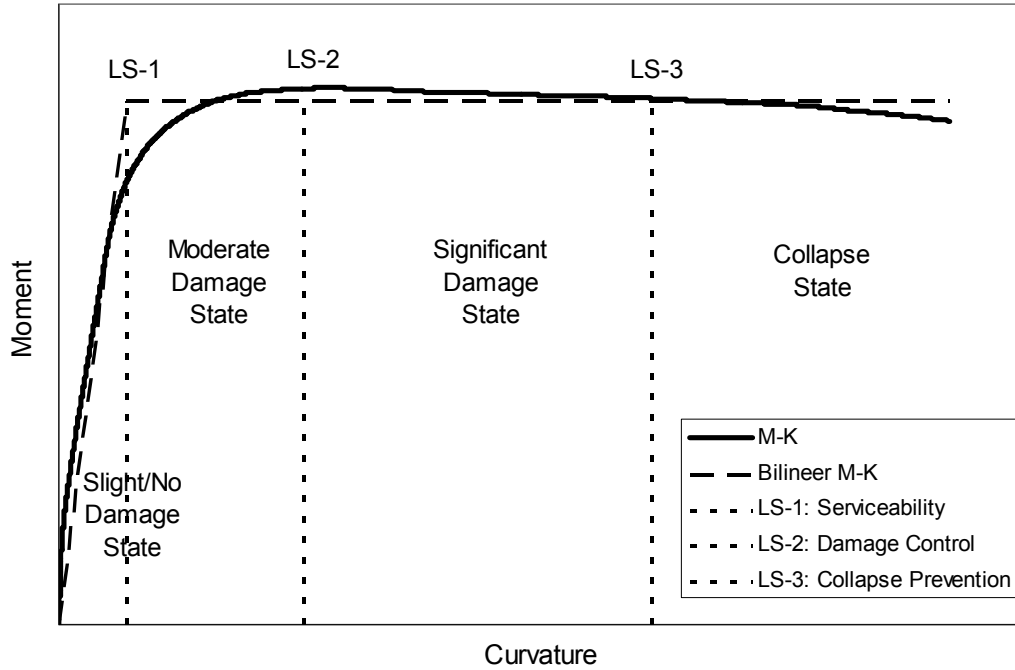
Figure 5.5 Damage limits defined for column and cap beam curvature

5.2.2 Damage Limit States for Shear Capacity

Column and cap beam shear capacity is considered to be another engineering demand parameter for the quantification of damage limit states. Shear failure is a brittle type of failure mode resulting in a sudden collapse of the RC members. There is no distinction between the damage limit states for brittle type of failure mode and hence an identical capacity level is considered for all damage limit states. Since total collapse occurs when the shear capacity is exceeded by the seismic shear demand, only collapse prevention limit state is defined for the shear capacity of columns and cap beams in both principal axes. RC members shear strength is calculated using the equation proposed by Priestley et al. (1996), which is presented in Equation (5.11).

$$V_{total} = V_c + V_s + V_p \tag{5.11}$$

130

where V_c is the shear carried by concrete shear resisting mechanism, V_s is the shear carried by transverse reinforcement shear resisting mechanism, and V_p is the shear strength provided by axial force in columns.

The shear strength provided by concrete, V_c is calculated as

$$V_c = k\sqrt{f_c}\,A_e \tag{5.12}$$

where A_e is the effective shear area of cross section that is equal to $0.8A_{gross}$. f_c is compressive strength of unconfined concrete. "k" is expressed as a factor defining the relationship between ductility and strength of concrete shear resisting mechanism. A constant value of 0.29 MPa is assumed for the calculations, which corresponds to the initial shear strength of the RC members.

Shear strength contribution of transverse reinforcement for rectangular RC sections is determined with Equation (5.13);

$$V_s = \frac{A_{sw}f_y D'}{s}\cot\theta \tag{5.13}$$

where A_{sw} is the area of transverse reinforcement in the direction of applied shear force, f_y is the yield strength of transverse reinforcement, D' is the core dimension in the direction of applied shear force, "s" is the spacing of transverse reinforcement, θ is the angle of the critical inclined flexure shear cracking to the member axis, which is taken as 30° (Priestley et al., 1996).

Shear strength contribution provided by axial force in columns is calculated by Equation (5.14), where P is the axial force and α is the angle formed between the column axis and the strut from the point of load application to the center of the flexural compression zone at the column plastic hinge critical section.

$$V_p = P\tan\alpha \tag{5.14}$$

Shear capacity of the RC sections is compared with the shear demand obtained from nonlinear response history analyses to decide whether the member attains the collapse prevention limit state or not.

5.2.3 Damage Limit States for Superstructure Displacement

Superstructure displacement in both orthogonal axes of the bridge is considered to be final engineering demand parameter for the quantification of damage limit states. Due to the movement of the superstructure, bridge can experience different levels of seismic damage. FHWA (1995) described qualitative damage states due to the displacement of bearings and superstructure. It is mentioned that settlement and vertical misalignment of a span due to an overturned bearing may be a minor problem, resulting in only a temporary loss of access which can be restored. Collapse may occur due to loss of support resulting from large relative transverse or longitudinal movement at the support in vulnerable structures. Moreover, it is stated that "walk out" phenomenon may occur under severe shaking due to inadequate fastening of the bearings.

As mentioned in chapter-3, there is no fastener or connecting device between the elastomeric bearings and the superstructure and substructure components. Therefore, friction force developed between the concrete surfaces and the bearings is the only resisting force that holds the elastomeric bearing at its place. When the seismic demand for the superstructure displacement exceeds the friction force, which depends on the axial load level of the bearings and the friction coefficient, bearings will be no longer stable and superstructure starts to make permanent displacements leading to minor problems at the bridge. Displacement capacity of the bearings, beyond which the friction force is exceeded by the seismic forces, is accepted as the ultimate bearing displacement for defining the serviceability limit state. This displacement capacity is determined for each bridge sample based on the level of axial load on the elastomeric bearings and the dynamic coefficient of friction between the concrete surface and bearings, which is specified as 0.40 by Caltrans (2006).

Pedestals are constructed over the cap beams and abutments with different heights to position the vertical alignment of the superstructure girders as shown in Figure 5.6. Under extreme seismic events, superstructure girders may experience large horizontal displacements and fall over the pedestal and rests on the cap beam directly. This could cause excessive damage on the asphalt disturbing the traffic flow and affecting the functionality of the bridge. Damage control limit state is specified for the displacement when the superstructure falls over pedestal on the cap beam as depicted by LS-2 in Figure 5.6. Finally, when the superstructure displacement exceeds the available seat length provided by the cap beam, it will fall over the bent and total collapse occurs. Therefore, this damage limit state is defined as the collapse prevention limit state (LS-3 in Figure 5.6), beyond which the bridge is no longer stable. Although the displacement limits for the limit states of LS-2 and LS-3 are very variable among the existing highway bridges in Turkey, constant values are assumed for these limit states for simplicity.
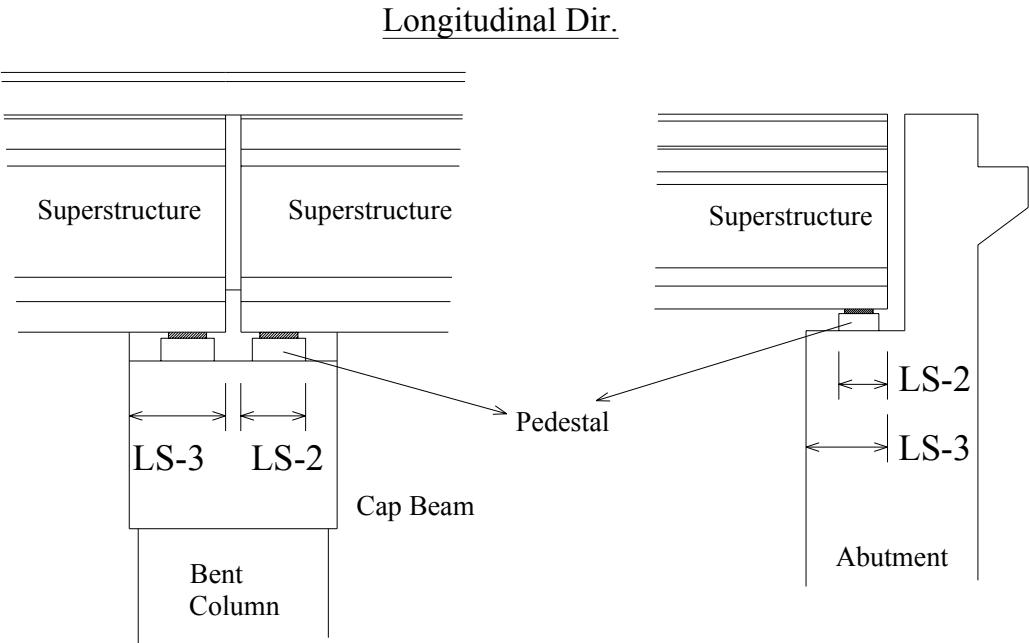

Figure 5.6 Superstructure seat length at the bent and abutment

The possible bridge damage parameters and their corresponding damage limits are presented in Table 5.13 altogether for the three damage limit states. These damage limits will be utilized in the development of analytical fragility curves for highway bridges in Turkey.

Table 5.13 Damage parameters of the bridge components and damage limits

a) Multi column bent bridge samples

Damage Parameters	Damage State	Bridge Sample #									
		1	2	3	4	5	6	7	8	9	10
Col K33 (rad/m)	LS-1	0.00175	0.00217	0.00218	0.00176	0.00217	0.00175	0.00218	0.00175	0.00217	0.00175
Col K33 (rad/m)	LS-2	0.00665	0.00810	0.00959	0.00668	0.00812	0.00629	0.00908	0.00656	0.00851	0.00637
Col K33 (rad/m)	LS-3	0.01649	0.01996	0.01594	0.01458	0.01932	0.01661	0.02111	0.01507	0.01433	0.01539
Col K22 (rad/m)	LS-1	0.00397	0.00405	0.00405	0.00397	0.00405	0.00397	0.00404	0.00397	0.00404	0.00397
Col K22 (rad/m)	LS-2	0.02908	0.02461	0.02983	0.02935	0.02481	0.02724	0.02822	0.02873	0.02639	0.02762
Col K22 (rad/m)	LS-3	0.04606	0.04537	0.04537	0.04329	0.04456	0.04531	0.04932	0.04326	0.03961	0.04330
Cap K22 (rad/m)	LS-1	0.00286	0.00296	0.00296	0.00286	0.00296	0.00286	0.00296	0.00286	0.00296	0.00286
Cap K22 (rad/m)	LS-2	0.04655	0.05550	0.05550	0.04655	0.05550	0.04655	0.05550	0.04655	0.05550	0.04655
Cap K22 (rad/m)	LS-3	0.09024	0.10804	0.10804	0.09024	0.10804	0.09024	0.10804	0.09024	0.10804	0.09024
Col V2 (kN)	LS-3	6039.8	4673.2	4691.4	6235.0	4719.3	6004.3	4580.8	6214.4	4991.8	6192.2
Col V3 (kN)	LS-3	5855.9	5252.5	5257.1	5894.9	5264.1	5848.8	5229.4	5890.8	5332.2	5886.4
Cap V3 (kN)	LS-3	4921.0	4921.0	4921.0	4921.0	4921.0	4921.0	4921.0	4921.0	4921.0	4921.0
Deck Disp. (mm)	LS-1	15.7	47.3	20.3	15.7	23.5	19.6	27.0	33.8	40.5	19.6
Deck Disp. (mm)	LS-2	425.0	425.0	425.0	425.0	425.0	425.0	425.0	425.0	425.0	425.0
Deck Disp. (mm)	LS-3	550.0	550.0	550.0	550.0	550.0	550.0	550.0	550.0	550.0	550.0

b) Single column bent bridge samples

Damage Parameters	Damage State	Bridge Sample #									
		1	2	3	4	5	6	7	8	9	10
Col K33 (rad/m)	LS-1	0.00104	0.00103	0.00105	0.00104	0.00103	0.00103	0.00104	0.00104	0.00103	0.00103
Col K33 (rad/m)	LS-2	0.00468	0.00418	0.00523	0.00475	0.00418	0.00438	0.00487	0.00462	0.00448	0.00445
Col K33 (rad/m)	LS-3	0.01078	0.00978	0.01037	0.01016	0.00957	0.01053	0.01103	0.01015	0.00878	0.01011
Col K22 (rad/m)	LS-1	0.00311	0.00313	0.00313	0.00312	0.00313	0.00312	0.00312	0.00311	0.00312	0.00312
Col K22 (rad/m)	LS-2	0.02936	0.02510	0.03782	0.02981	0.02526	0.02683	0.03210	0.02876	0.02761	0.02733
Col K22 (rad/m)	LS-3	0.03915	0.03346	0.05043	0.03974	0.03367	0.03577	0.04280	0.03835	0.03682	0.03644
Cap K22 (rad/m)	LS-1	0.00214	0.00214	0.00214	0.00214	0.00214	0.00214	0.00214	0.00214	0.00214	0.00214
Cap K22 (rad/m)	LS-2	0.01431	0.01431	0.01431	0.01431	0.01431	0.01431	0.01431	0.01431	0.01431	0.01431
Cap K22 (rad/m)	LS-3	0.03640	0.03640	0.03640	0.03640	0.03640	0.03640	0.03640	0.03640	0.03640	0.03640
Col V2 (kN)	LS-3	15216.7	15439.4	15511.8	15547.8	15583.5	15149.6	15179.1	15512.7	16373.6	15462.1
Col V3 (kN)	LS-3	9961.4	10028.2	10049.9	10060.7	10071.4	9941.2	9950.1	10050.2	10308.4	10035.0
Cap V3 (kN)	LS-3	7453.0	7453.0	7453.0	7453.0	7453.0	7453.0	7453.0	7453.0	7453.0	7453.0
Deck Disp. (mm)	LS-1	15.7	47.3	20.3	15.7	23.5	19.6	27.0	33.8	40.5	19.6
Deck Disp. (mm)	LS-2	425.0	425.0	425.0	425.0	425.0	425.0	425.0	425.0	425.0	425.0
Deck Disp. (mm)	LS-3	550.0	550.0	550.0	550.0	550.0	550.0	550.0	550.0	550.0	550.0

In the previous sections, damage limit states are specified for highway bridge components to be used in the development of fragility curves. These are the "Serviceability", "Damage Control" and "Collapse Prevention" damage limit states. Slight/No, moderate, significant, and collapse are the four corresponding damage states that the bridges can experience under the effect of an earthquake ground motion. Both qualitative and quantitative descriptions are given for the three damage limit states. Several engineering demand parameters of various bridge components are considered for the quantitative definitions of each damage limit state. Curvature and shear capacities of the RC column and cap beam members in both principal axes and the superstructure relative displacement for assessing the deck unseating are the investigated engineering demand parameters in defining the damage limit states of the highway bridges.

CHAPTER 6

DEVEPOLMENT OF ANALYTICAL FRAGILITY CURVES

Fragility curves are one of the most important components in the seismic loss estimation of structures. These curves are very valuable tools in estimating the bridge damage likely to occur during a seismic event. As described in Chapter-1, fragility is described as the probability of exceeding a particular damage level under a certain seismic hazard level designated by relevant intensity measures. The mathematical expression of a fragility function for a specific damage limit state is given in Equation (1.1). In the development of analytical fragility curves, seismic response of critical bridge components, which are expected to experience certain level of seismic damage, are estimated in terms of certain engineering demand parameters. In order to decide the damage state of the bridge, the seismic demands of the bridge components are compared with the damage limits specified in accordance with the corresponding engineering demand parameters. If the seismic demand is greater than or equal to the specified damage limit, then the bridge is considered to be in the corresponding damage state. By repeating the same procedure for all bridges samples under different seismic actions, damage state of each individual bridge sample is determined. For this purpose, numerous nonlinear response history analyses are conducted to determine the seismic response of the bridge components. Bridge analytical models are formed and ground motions with various intensity levels are considered for the seismic simulation of the bridge damage by executing numerous analyses. Maximum seismic demands of the critical

components of the sample bridges are recorded under the effect of each earthquake ground motion to be used in the development of fragility functions.

6.1   SEISMIC DEMAND CALCULATION OF BRIDGE COMPONENTS

Seismic response of the bridge components are determined by performing nonlinear response history analysis (NRHA), which is believed to be the most rigorous method in estimating the inelastic seismic demands of the structures. Although NRHA may suffer convergence problems and excessive amount of run time and post-processing efforts are required, its capability in simulating inelastic seismic behavior is far more superior in comparison with the other analysis methods. Detailed analytical models of the bridge components are developed according to Chapter-3 using OpenSees (2005). Nonlinear dynamic analyses of the bridge models are performed under the effect of selected ground motion records with two horizontal components. Earthquakes can affect the bridges in any direction. Therefore, in order to determine the most unfavorable response of the bridge components, each ground motion record is analyzed twice as explained in Chapter-4. The free-field ground motion is assumed to be uniform over the bridge site; therefore the effects of spatial variation of ground motion are not addressed in this study (Fenves and Ellery, 1998). The dynamic analyses are followed after the application of gravity loads, which are compatible with the masses specified for the bridge components. Any other type of loading such as; truck, wind, snow loads, etc. are not taken into account in the calculations.

Fragility curves are developed for each bridge class, which is represented by 10 bridge samples. For the NRHA, a total of 25 recordings are employed as the ground motion data set. Since each ground motion record is analyzed twice to obtain the maximum response, a total of 500 analyses are performed for one bridge class. In Chapter-2, bridge inventory in Turkey is classified into four main bridge classes to be considered in this study. Therefore, the total number of analyses performed for the development of fragility curves is 2000. The maximum seismic response of each bridge sample under the effect of each ground motion recording is

calculated by post processing the analyses results using Matlab (2004). Seismic response of the bridge components are determined in terms of several engineering demand parameters, which are employed in specifying the damage limits discussed in Chapter-5. These engineering demand parameters are the column and cap beam curvature and shear demands in the principal directions of the RC sections and the longitudinal displacement of the superstructure.

Maximum response of the bridge components are calculated by taking the absolute maximum of the response time history of the corresponding engineering demand parameters, which is obtained from the NRHA results. A schematic representation for determining the maximum response of the bridge components in terms of different engineering demand parameters are shown in Figure 6.1. As seen in the figure, maximum response of each engineering demand parameter can take place at different time steps of the response history.
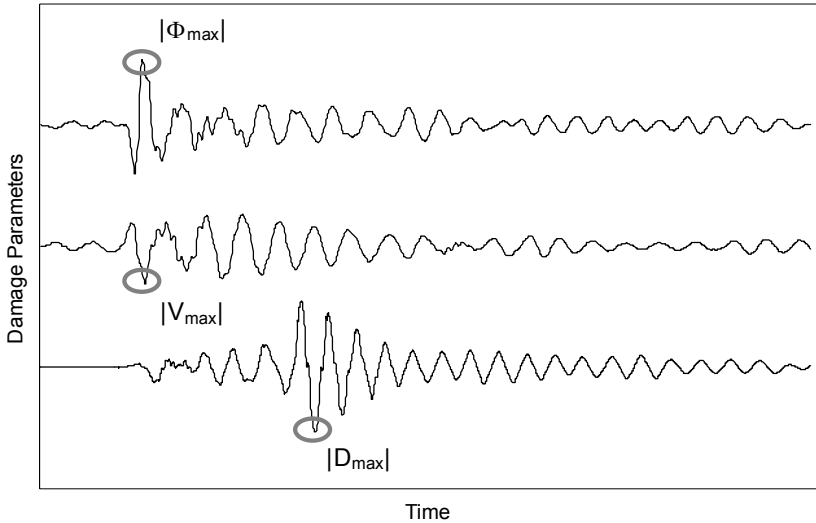

Figure 6.1 Maximum seismic response of different damage parameters

Maximum response of each bridge sample is determined for each ground motion record. These results are used to specify the damage states of the bridges under various levels of seismic excitations. As an initial step, the maximum

response results are compared and evaluated to identify the suitable ground motion intensity measures that have better correlation with the seismic damage. The comparisons are made using the results of the bridge samples that represent the same bridge class and to be consistent, results of the same engineering demand parameters are considered for each comparison. Since each bridge sample has its own damage limits for different damage states, it is reasonable to compare the maximum response results of all bridge samples in the same graph. Therefore, all the results are normalized with respect to certain parameters to make rational comparisons and evaluations. For the maximum responses of the curvatures of the bent members and the longitudinal displacement of the superstructure, the results are normalized with respect to the corresponding damage limits specified for the Serviceability Damage Limit State (LS-1). For the shear demand of the bent members, the results are normalized with respect to the corresponding damage limits specified for the Collapse Prevention Damage Limit State (LS-3).

In Appendix-A from Figure A.1 to Figure A.28, normalized maximum seismic responses of the bridge components of each bridge class are presented with respect to four different earthquake ground motion intensity measures of ASI, PGV, PGA, and PGA/PGV. The intensity measures are calculated by taking the geometric mean of the two horizontal components of the ground motions. Therefore, it is not possible to choose a ground motion data set having a uniform distribution among the investigated intensity measures at the same time. It is inevitable that some of the intensity measures accumulate at certain values, while there exist fewer data points at the other values of intensity measures. In spite of the uneven distribution for the intensity measures of ASI and PGV, they have a better correlation with the maximum seismic response of the bridge components especially for the engineering demand parameters of column curvature and shear demands and superstructure longitudinal displacement. Damage parameters of the cap beam curvature and the shear demands are found to have the worst correlation with the investigated intensity measures (Figures A.5, A.6, A.12, A.13, A.19, A.20, A.26, A.27). With the increasing values of PGA/PGV, there is not any explicit trend with seismic response of any of the bridge component. Therefore, intensity measure of

PGA/PGV is not taken into account in the development of fragility curves. Although PGA does not have good correlation with the bridge seismic response as does the ASI or PGV, PGA has some level of tendency with the seismic damage of bridge components. In a similar way, Akkar et al. (2005) found that PGV has a better correlation than PGA in terms of the inelastic dynamic response displacements of frame structures through the structural period range from 0.2s to 1.0s. In the previous studies, most of the fragility curves were given with respect to PGA and to a lesser degree PGV, which can be easily obtained by calculating the peak values of the acceleration and velocity time series of the ground motion. In addition to PGA and PGV, ASI is also utilized as the ground motion intensity measures in the development of analytical fragility curves in this study.

In the definition of ASI in Chapter-5, T_f was specified as 1.10s according to the results of some sensitivity analyses. Period elongation of the sample bridges due to their inelastic response and hence system softening is taken into account in deciding the T_f. Therefore, elongation in the fundamental period of the sample bridges is investigated. In Figure 6.2, variation between the elastic and elongated inelastic periods of the sample bridges due to their inelastic response under each ground motion is given for each major bridge class. In most of the cases, inelastic period of the sample bridge is elongated in comparison with its elastic period. However, in a few cases, especially for the bridge samples of MS_MC_SL30 bridge class, inelastic period of the bridge samples is less than its elastic period. This situation can be explained by the engagement of the superstructure with the abutments at the last step of the NRHA. At this step, the system stiffness is increased by the additional abutment stiffness after the closure of gap between the abutment and the superstructure. The increase in the system stiffness results in a lower system period.

In Table 6.1, the mean values of the elongated period of the bridge samples for each bridge class are tabulated. The maximum of the mean elongated period values for each bridge class varies between 1.06s and 1.13s. Therefore, T_f=1.10s in calculating the ASI is accepted as a reasonable value for ordinary highway bridges in Turkey, which represents the final period in the calculations.
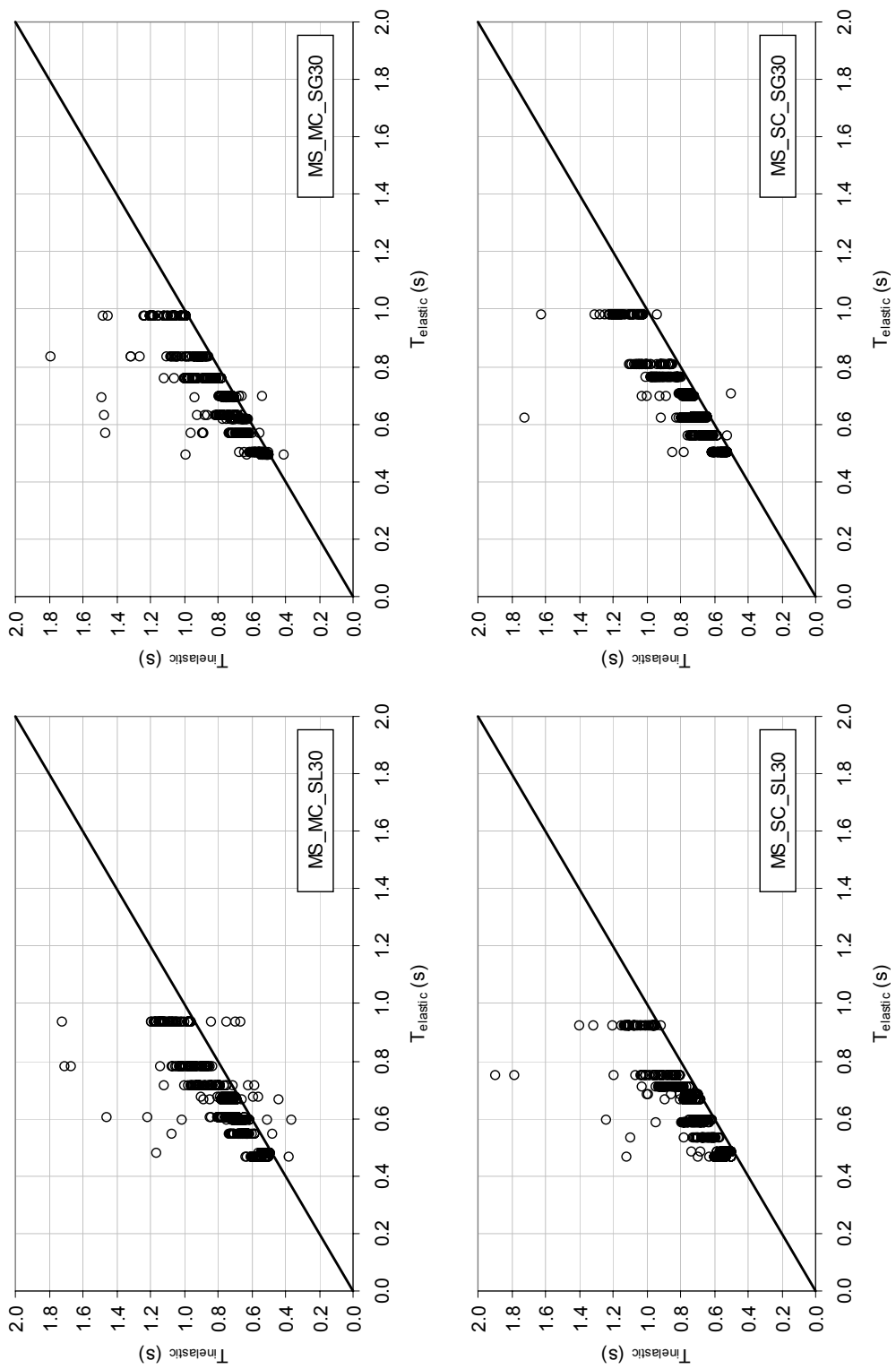
Figure 6.2 Period elongation of the bridges due to inelastic response

141

Table 6.1 Mean elongated periods of the major bridges and their samples

Bridge Sample ID	$T_{inelastic}$ (s)			
	MS_MC_SL30	MS_MC_SG30	MS_SC_SL30	MS_SC_SG30
1	0.66	0.69	0.65	0.66
2	1.06	1.11	1.06	1.13
3	0.52	0.52	0.53	0.55
4	0.55	0.57	0.57	0.58
5	0.86	0.89	0.86	0.89
6	0.97	0.98	0.96	0.95
7	0.67	0.67	0.69	0.68
8	0.73	0.74	0.74	0.76
9	0.73	0.75	0.75	0.77
10	0.76	0.76	0.73	0.76
min	0.52	0.52	0.53	0.55
max	1.06	1.11	1.06	1.13

6.2   FRAGILITY CURVE DEVELOPMENT METHODOLOGY

Any point on the fragility curve of a particular bridge class indicates the probability of attaining or exceeding a certain damage limit state due to an earthquake ground motion, which is represented by an appropriate intensity measure on the fragility curve. The maximum seismic responses obtained from NRHA results for each engineering demand parameters of the bridge components are assumed to represent the seismic damage of the investigated bridge samples. Seismic damage thresholds of the bridge components in terms of certain engineering demand parameters have already been specified for each damage limit state in Chapter-5. Seismic damage state of the bridge components under each ground motion can be specified by comparing the corresponding threshold values of the damage limit states and the maximum seismic response of the bridge components. Seismic damage state of a bridge as a whole cannot be specified directly by identifying the damage state of its components. Since there does not exist any specific method that relates the bridge damage with the damage state of its components, a simple assumption is made for identifying the bridge damage state. If any of the bridge components attains or exceeds a damage limit state, bridge system as a whole is assumed to be in the same damage state regardless of the damage states of the rest of the bridge components. An example for the damage state

142

assessment of a sample bridge is presented in Table 6.2. Damage state of the bridge is calculated for different earthquakes and limit states by inspecting the component level damage states. If the bridge component has reached or exceeded a certain damage limit state, then the score of the bridge component for that limit state is assumed to be 1, otherwise 0. According to the assumption made in identifying the bridge damage state, if any of the bridge component has the score of 1, then the bridge is assumed to be in that damage state with the score of 1. In the first two damage limit states only 4 damage parameters are taken into account in the seismic performance assessment of the sample bridges. Whereas in the Collapse Prevention limit state, in addition to the previous damage parameters column and cap beam shear demands are also included in the assessment. As mentioned in the previous chapter, since shear failure is a brittle type of failure resulting in a sudden collapse of the RC members, only collapse prevention limit state is defined for the shear capacity of cap beams and columns in both principal axes.

Table 6.2 Determination of the damage state of the bridges

EQ#	Intensity Measure (ASI, PGV, PGA)	Serviceability Limit State (LS-1)				
		Col. K33	Col. K22	Cap K33	Deck Disp.	**OverAll**
EQ-1	IM-i	1	1	0	1	**1**
EQ-2	IM-i	0	1	1	1	**1**
-	-	-	-	-	-	**-**
-	-	-	-	-	-	**-**
EQ-N	IM-i	1	0	1	1	**1**

EQ#	Intensity Measure (ASI, PGV, PGA)	Damage Control Limit State (LS-2)				
		Col. K33	Col. K22	Cap K33	Deck Disp.	**OverAll**
EQ-1	IM-i	1	0	0	0	**1**
EQ-2	IM-i	0	0	0	0	**0**
-	-	-	-	-	-	**-**
-	-	-	-	-	-	**-**
EQ-N	IM-i	0	0	1	0	**1**

EQ#	Intensity Measure (ASI, PGV, PGA)	Collapse Prevention Limit State (LS-3)							
		Col. K33	Col. K22	Cap K33	Col. V2	Col. V3	Cap V2	Deck Disp.	**OverAll**
EQ-1	IM-i	1	0	0	1	0	0	0	**1**
EQ-2	IM-i	0	0	0	0	0	0	0	**0**
-	-	-	-	-	-	-	-	-	**-**
-	-	-	-	-	-	-	-	-	**-**
EQ-N	IM-i	0	0	0	0	0	0	0	**0**

0 = NOT Attained the Specified Damage Limit State
1 = Attained the Specified Damage Limit State

Damage states of each bridge sample of the four bridge classes are identified under the effect of selected ground motions. When the performance assessment results of each earthquake are investigated individually, the number of bridge samples that reached or exceeded the specified damage limit state can be obtained. The ratio of the number of sample bridges, which reached or exceeded the specified damage limit state, to the total number of sample bridges gives the probability of exceeding the corresponding limit state of the bridge class for the investigated earthquake. After performing the same operations for each earthquake ground motion data set and for the three specified damage limit states, probability of exceeding the damage limit states is obtained for each earthquake. Since fragility curves are developed for bridge classes, evaluation of the results of bridge samples is made for each bridge class separately.

When earthquake ground motions are represented with an appropriate seismic intensity measure, distribution of exceeding probabilities with respect to the selected intensity measure is obtained as schematically shown in Figure 6.3-a. In this graph, x-axis is the seismic intensity measure of the earthquake; y-axis is the probability of exceedance of a certain damage limit state. In the seismic loss estimation studies, continuous functions of fragility curves are required in the calculations. Therefore, a mathematical expression is utilized to characterize the jaggedly varying exceedance probability points to achieve smooth fragility curves for a specific damage limit state and bridge class. A representative sketch is shown Figure 6.3-b illustrating a function that is the best fit for the exceedance probability points. In the most recent studies, the probability of exceeding a certain damage limit states is generally modeled as a cumulative lognormal probability distribution (HAZUS, 2003; Karim and Yamazaki, 2003; Elnashai et al., 2004; Nielson, 2005; Banerjee and Shinozuka, 2007). In this study, fragility curves for all bridge classes are modeled as lognormally-distributed functions that give the probability of reaching or exceeding different damage states for a given level of ground motion. Each fragility curve is characterized by a median value and an associated dispersion factor (lognormal standard deviation) of ground motion, which is represented by seismic intensity measures.
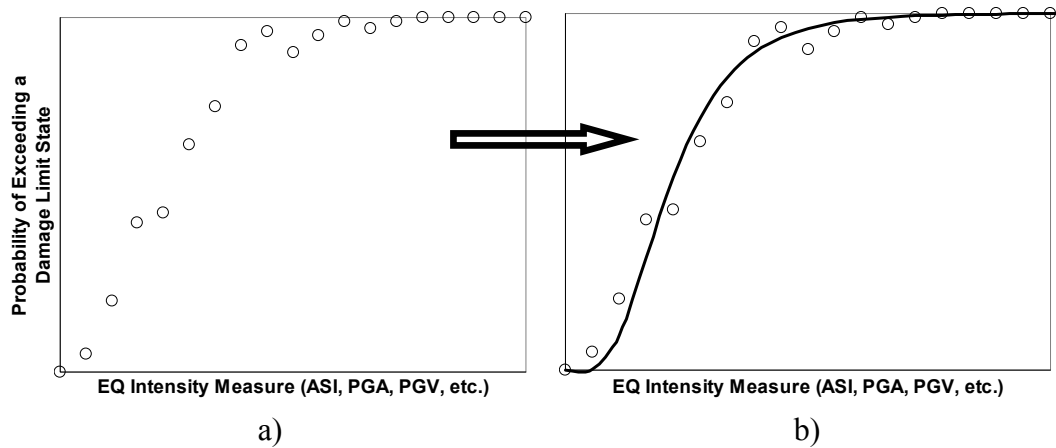
Figure 6.3 Schematic representation of a fragility curve

The median and the dispersion values of the cumulative lognormal probability distribution function are determined by employing the least squares technique to the exceedance probability points. The evaluation of the fragility function, which is characterized by a two parameter cumulative lognormal distribution, how closely it represents the exceedance probability points is made through graphical examination of the data points and the estimated curve. Moreover, evaluations have been quantified by computing the coefficient of determination (R^2) using the probability points and the estimated fragility functions to investigate the correlation in between. R^2 is an indicator varying between 0 and 1 that reveals how closely the estimated values by fragility functions correspond to the actual data of the probability points. The closer the R^2 value to 1, the more reliable the estimated fragility curves.

Fragility functions of each bridge class are developed for the intensity measures of ASI, PGV, and PGA by employing the above mentioned procedure. The median and dispersion values of the cumulative lognormal probability distribution functions that are utilized to develop fragility curves are determined for each damage state of bridge classes and for different intensity measures (Table 6.3). Besides, to investigate correlation between the exceedance probability points and the developed fragility curves, R^2 is computed for each individual fragility curve. When the coefficient of determination values calculated for each intensity measure

145

is investigated, it is found out that ASI has the highest and PGA has the lowest R^2 values. This implies that fragility curves developed using ASI has a better correlation with the corresponding exceedance probability points in comparison with the other intensity measures. Whereas, PGA has the least correlation with the data points. Therefore, the reliability of the developed fragility curves with ASI is higher than the ones with PGV. And the reliability of the fragility curves with PGV is higher than the ones with PGA. This result is consistent with the correlation of bridge damage state and the intensity measures. It was mentioned in the previous section that, ASI and PGV has better correlation with the maximum seismic response of the bridge. Fragility curves of four bridge classes for three different damage limit states are given in Figure 6.4 to Figure 6.9 with respect to the intensity measures of ASI, PGV, and PGA.

Table 6.3 Fragility curve parameters of the bridge classes

MS_MC_SL30									
Intensity	LS-1: Serviceability			LS-2: Damage Control			LS-3: Collapse Prevention		
Measure	Median	Disp.	R^2	Median	Disp.	R^2	Median	Disp.	R^2
ASI (g*s)	0.121	0.401	0.758	0.592	0.290	0.748	0.693	0.308	0.902
PGV (cm/s)	11.238	0.454	0.299	59.678	0.573	0.569	72.287	0.628	0.619
PGA (g)	0.117	0.400	0.121	0.693	0.280	0.296	0.869	0.316	0.361

MS_MC_SG30									
Intensity	LS-1: Serviceability			LS-2: Damage Control			LS-3: Collapse Prevention		
Measure	Median	Disp.	R^2	Median	Disp.	R^2	Median	Disp.	R^2
ASI (g*s)	0.137	0.366	0.843	0.497	0.272	0.777	0.623	0.309	0.721
PGV (cm/s)	10.914	0.423	0.235	49.109	0.532	0.501	62.887	0.570	0.469
PGA (g)	0.094	0.500	0.128	0.583	0.350	0.176	0.756	0.380	0.205

MS_SC_SL30									
Intensity	LS-1: Serviceability			LS-2: Damage Control			LS-3: Collapse Prevention		
Measure	Median	Disp.	R^2	Median	Disp.	R^2	Median	Disp.	R^2
ASI (g*s)	0.133	0.381	0.779	0.438	0.389	0.846	0.593	0.368	0.937
PGV (cm/s)	11.083	0.354	0.307	44.434	0.486	0.602	57.340	0.529	0.643
PGA (g)	0.110	0.450	0.131	0.577	0.400	0.144	0.741	0.480	0.207

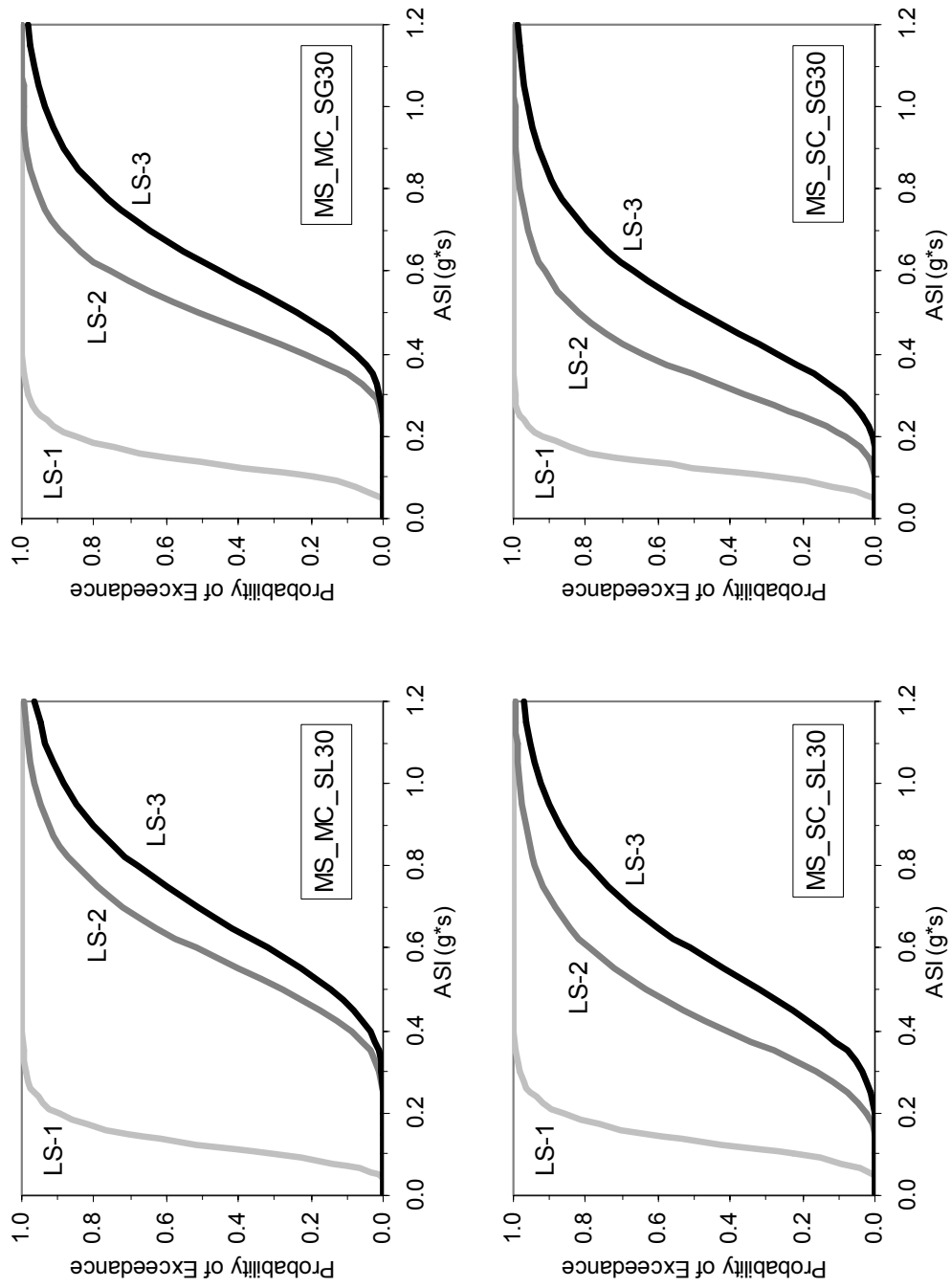| MS_SC_SG30									
Intensity	LS-1: Serviceability			LS-2: Damage Control			LS-3: Collapse Prevention		
Measure	Median	Disp.	R^2	Median	Disp.	R^2	Median	Disp.	R^2
ASI (g*s)	0.123	0.346	0.804	0.347	0.400	0.826	0.508	0.385	0.900
PGV (cm/s)	10.090	0.386	0.323	33.049	0.444	0.655	47.656	0.535	0.740
PGA (g)	0.100	0.420	0.124	0.482	0.360	0.223	0.613	0.400	0.218

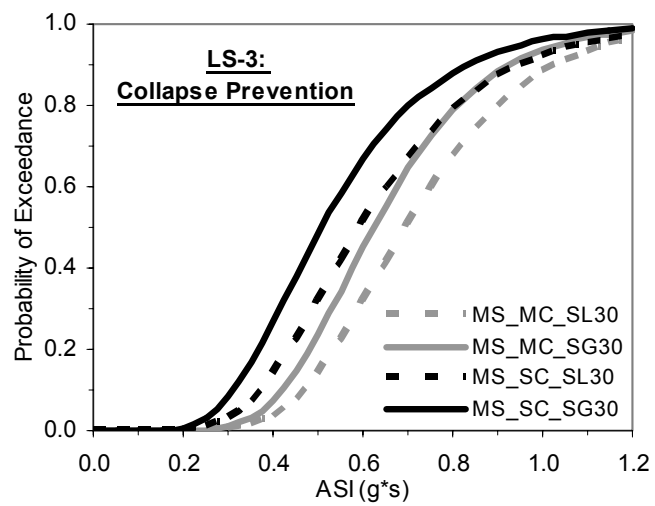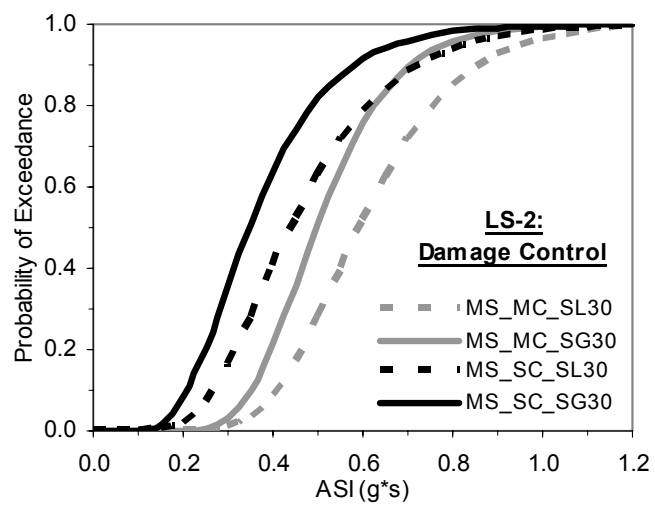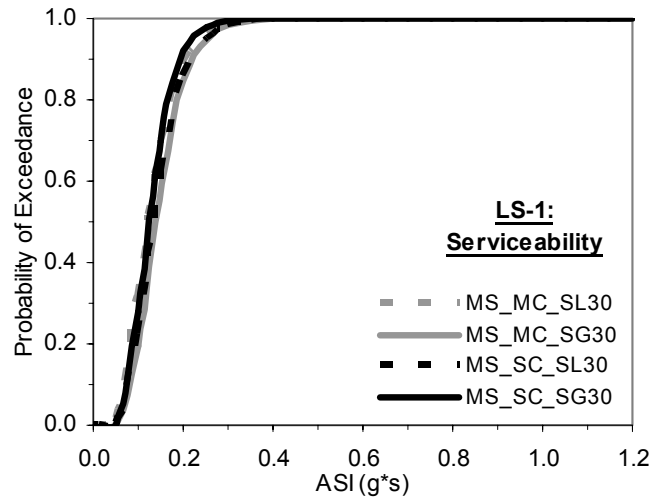Figure 6.4 Fragility curves for different bridge classes (ASI)

147

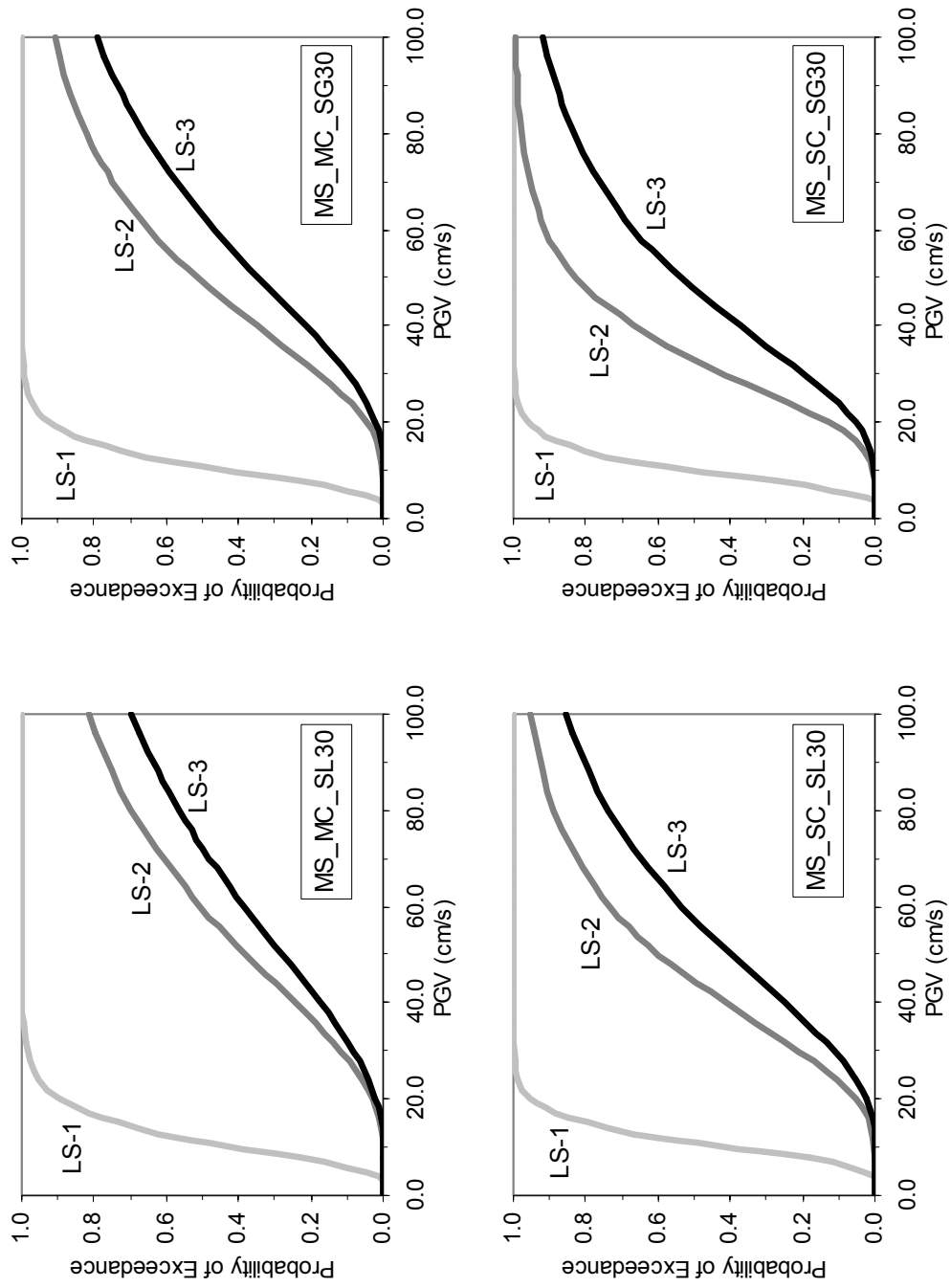Figure 6.5 Fragility curves for different damage limit states (ASI)

Figure 6.6 Fragility curves for different bridge classes (PGV)
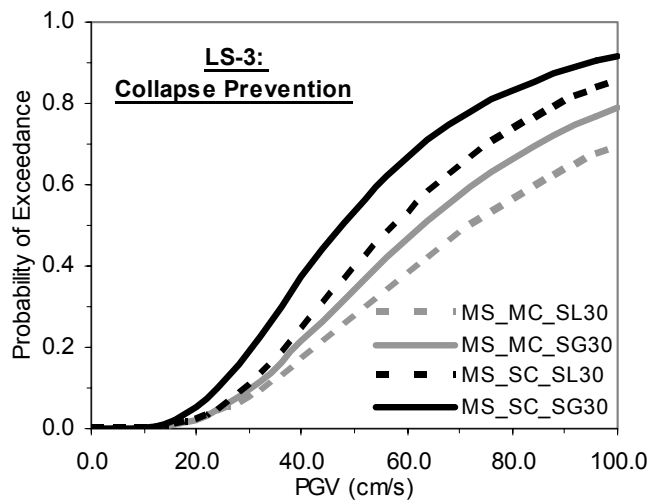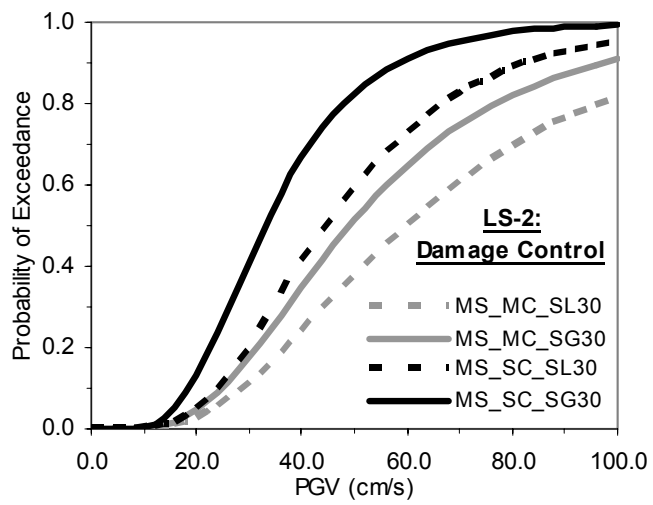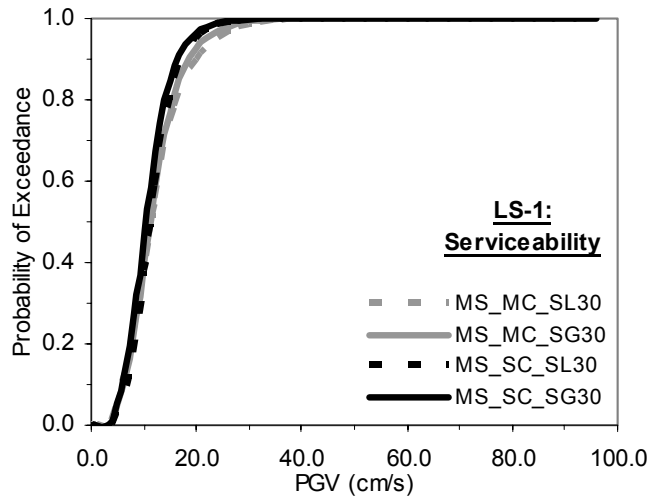
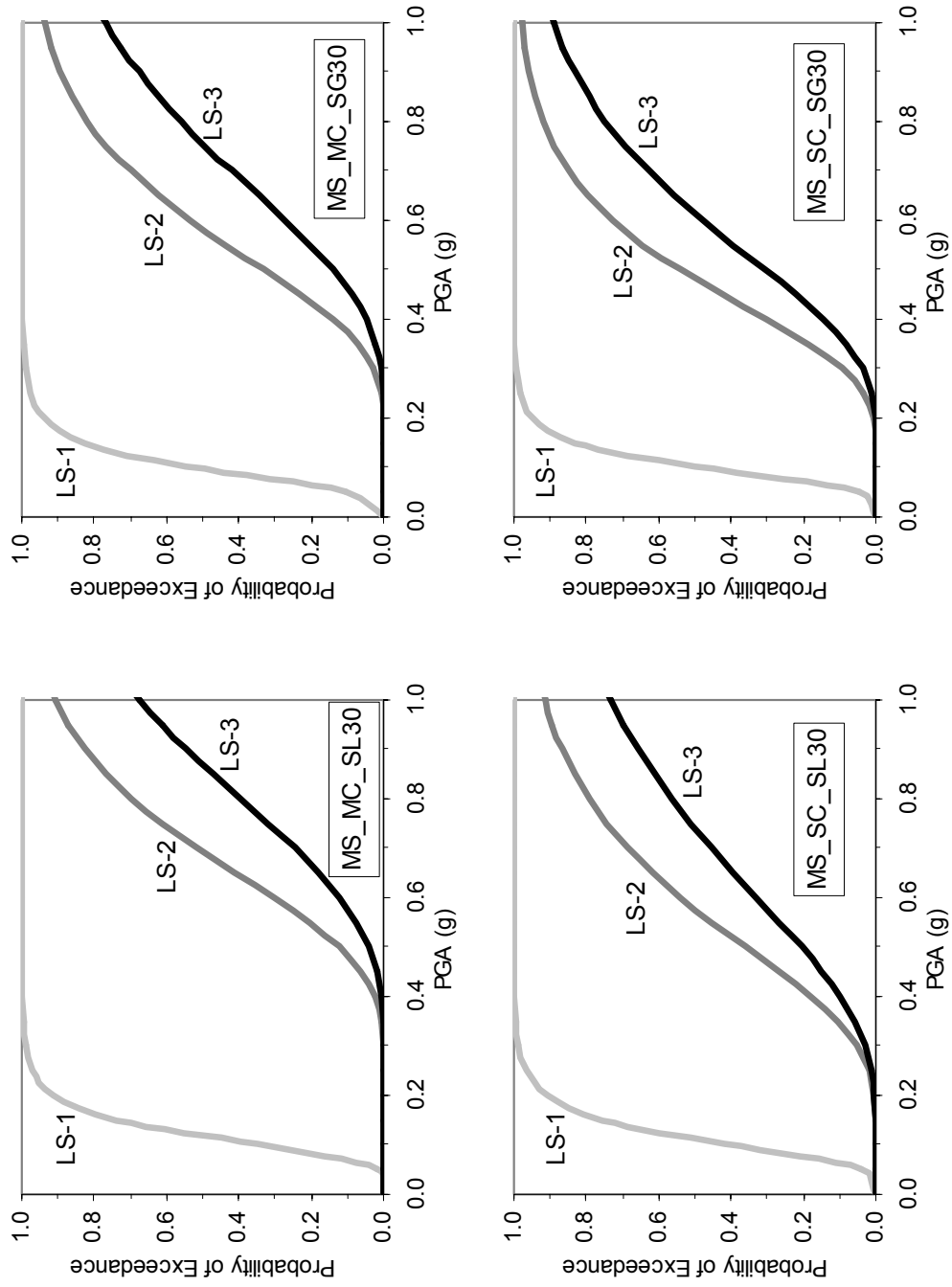Figure 6.7 Fragility curves for different damage limit states (PGV)

Figure 6.8 Fragility curves for different bridge classes (PGA)
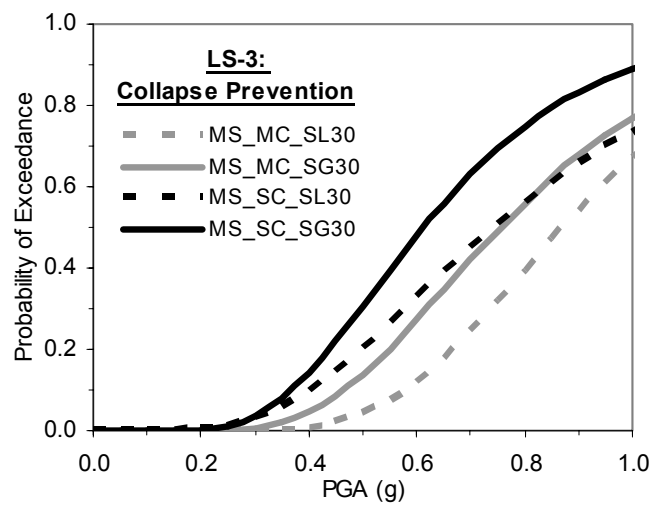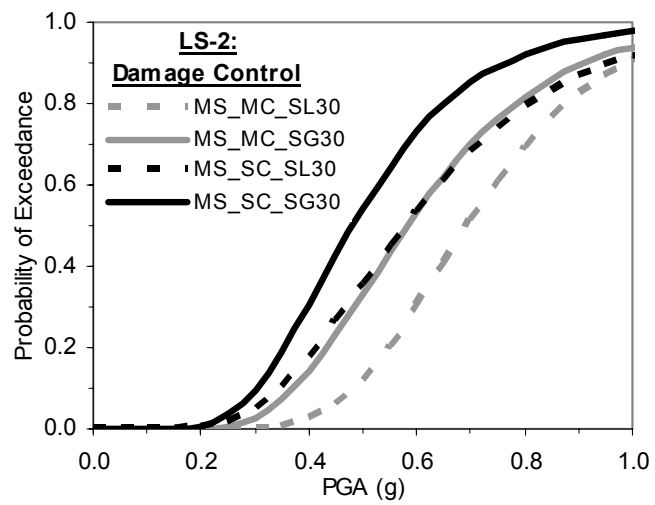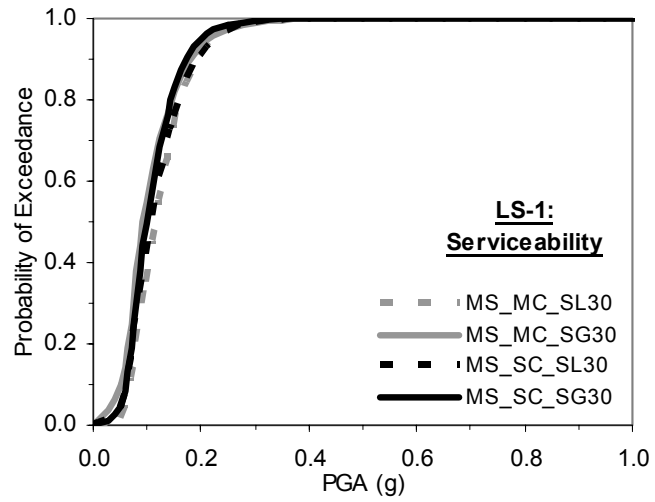
151

Figure 6.9 Fragility curves for different damage limit states (PGA)

In the plots of Figure 6.4, Figure 6.6 and Figure 6.8, fragility curves of four bridge classes are shown for the intensity measures of ASI, PGV and PGA, respectively. The three curves in each figure represent the probability of exceeding the LS-1 (serviceability), LS-2 (damage control) and LS-3 (collapse prevention) damage limit states from left to right. These curves are further grouped separately in Figure 6.5, Figure 6.7 and Figure 6.9 for the three damage limit states, to compare the effect of different bridge classes on the fragility curves.

Bridge classes with larger skewness are more vulnerable than the bridges with small skew angles. Bridges that fall into the bridge classes of skewness greater than 30° (SG30) have the fragility curve resulting higher probability of exceeding values in comparison with the fragility curves of bridge classes for skewness less than 30° (SL30). This outcome is consistent with the response of the bridges observed in the Loma Prieta and Northridge Earthquakes (Buckle,1994; Basoz and Kiremidjian, 1997). In various codes and research studies such as Buckle (1994), FHWA (1995), Basoz and Kiremidjian (1997), Pamuk et al. (2005), skew angle is considered to be a major effect on the performance of bridges and it is agreed that skewed bridges are more vulnerable to seismic effects. Bent column number also has a considerable effect on the fragility curves. Single-column bents are found to be more vulnerable compared to the multiple column bents. This finding is in accordance with the performance of bridges during the Loma Prieta and Northridge Earthquakes. Basoz and Kiremidjian (1997) mentioned that, bridges with single-column bent performed poorly during these earthquakes. They stated that the substructure bent column number either single-column or multiple-column play an important role on the damage level that the bridge experiences.

The difference between the fragility curves of all the bridge classes for the serviceability damage limit state is negligible regardless of the intensity measure considered. Reaching or exceeding the serviceability damage limit state mostly occurs when the superstructure displacement exceeds the specified displacement limit, at which the friction force between the bearings and concrete surfaces can no longer hold the elastomeric bearing at its place. Therefore, contribution of the bridge skew angle or the bent column number on the fragility curve for

serviceability limit state is found to be insignificant. A single fragility curve can be utilized for all bridge classes for the serviceability limit state. This finding is in good agreement with the HAZUS, (FEMA 2003) applications of the fragility curves. In HAZUS, a modification factor is employed for the skewness of the bridges in the determination of fragility curves for the moderate, extensive, and complete damage limit states. Whereas, for the slight damage limit state no modification factor is considered. Namely, same fragility curve is considered for the fragility curve of slight damage limit state of the bridges having different skew angles.

Fragility curves for the damage control (LS-2) and the collapse prevention (LS-3) damage limit states are mostly dominated by the column and cap beam curvature demands. The main reason for exceeding the column and cap beam curvature capacities for the two damage limit states is the high shear forces transferred from superstructure to the substructure by shear keys. Since shear keys of the investigated existing bridges have been designed so strong that they transfer considerable amount of seismic forces to the substructure due to the pounding of superstructure with the shear keys in the bridge transverse direction.

The difference between the fragility curves for LS-2 and LS-3 damage limit states is relatively small. One of the main reasons for the small difference is the acceptance criteria definitions of the corresponding damage limit states. The other reason is the number of engineering demand parameters defined for the LS-2 and LS-3 damage limit states. Any shear damage on the bridge components is specified only for the collapse prevention damage limit state. Therefore, number of engineering demand parameters defined for collapse prevention damage limit state is more than the others. Although column and cap beam curvature dominates the LS-2 and the LS-3 damage limit states, columns and cap beams of several bridge samples experience shear failure. This increases the probability of exceedance for the collapse prevention damage limit state, which causes smaller difference between the fragility curves for LS-2 and LS-3 damage limit states.

6.3   COMPARISON OF FRAGILITY CURVES

The proposed fragility curves for the ordinary highway bridges in Turkey are compared with various bridge fragility curves developed in other studies. The fragility curves developed in this study are mostly not suitable for making comparisons with the previously developed analytical or empirical fragility curves. Because, the attributes of the bridges, damage limit state definitions, input ground motion characteristics, the analyses methods and modeling techniques considered for the developed fragility curves in this study do not exactly match with the ones considered to obtain previously developed fragility curves. On the other hand, making comparisons at least gives an idea about the level of discrepancies as well as the similarities between the fragilities of the investigated bridges. Most of the available fragility curves were developed in terms of PGA and some of them were given with respect to PGV. However, in the previous section it was mentioned that the proposed fragility curves with PGA are less reliable than the ones for ASI or PGV, which have a better correlation with the bridge seismic damage. Since there does not exist an available fragility curve in terms of ASI, great care is given for the fragility curves with PGV. Although proposed fragility curves with PGA are less reliable, comparisons are still made to give some reference points with the available fragility curves given in terms of PGA.

In the previous studies, fragility curves were developed for various damage limit states and for different types of bridges. Therefore, when making the comparisons, the bridge types having certain level of similarities with the bridge classes employed in this study are considered. In the comparison of fragility curves, LS-1, LS-2, and LS-3 correspond the damage limit states of serviceability, damage control, and collapse prevention, respectively for the proposed fragility curves in this study. Damage limit states of the fragility curves of the previous studies are generally in accordance with the ones defined in HAZUS (FEMA, 2003). Therefore, available fragility curves were generally given with four damage limit states, which are slight, moderate, extensive, and complete.

i) Yamazaki et al. (1999): In the study of Yamazaki et al. (1999) empirical fragility curves were developed by utilizing the bridge damage data obtained after the 1995 Kobe earthquake in Japan. The fragility curves are based on the actual damage data of 216 bridge structures on 4 routes. The two parameters of the probability distributions were determined by the least squares method on the cumulative log-normal distribution. Empirical fragility curves were constructed considering four damage limit states for three different intensity measures of PGA, PGV, and JMA (Japan Meteorological Agency) intensity measure. Since these fragility curves are not classified in terms of structural attributes for the investigated bridges, the comparisons are made with the average of the proposed fragility curves for different bridge classes considered in this study. As shown in Figure 6.10 and Figure 6.11, proposed fragility curves result in higher probability of exceedance values for the same seismic intensity level when compared with the fragility curves developed by Yamazaki et al. (1999). The disparity between the two sets of curves is more pronounced with the intensity measure of PGV.
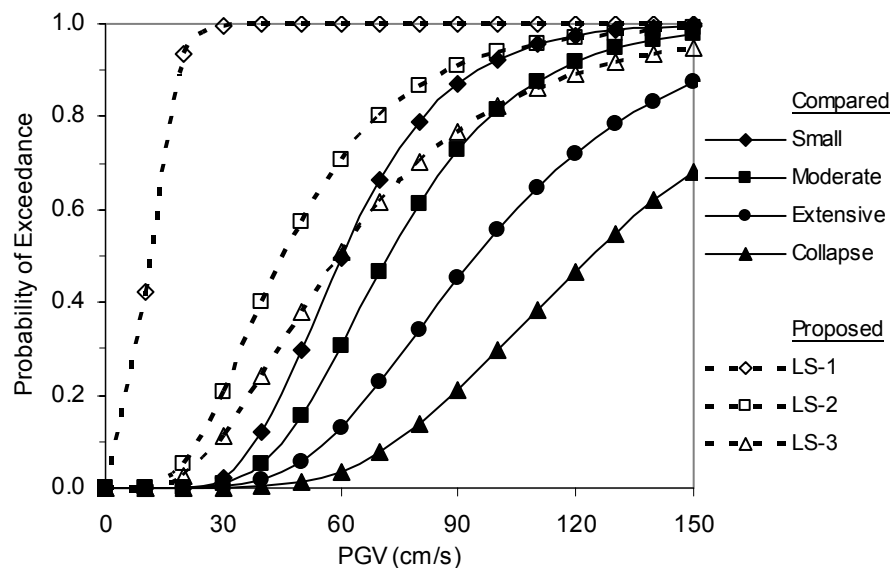

Figure 6.10 Comparison of proposed and Yamazaki et al. (1999) fragility curves for PGV
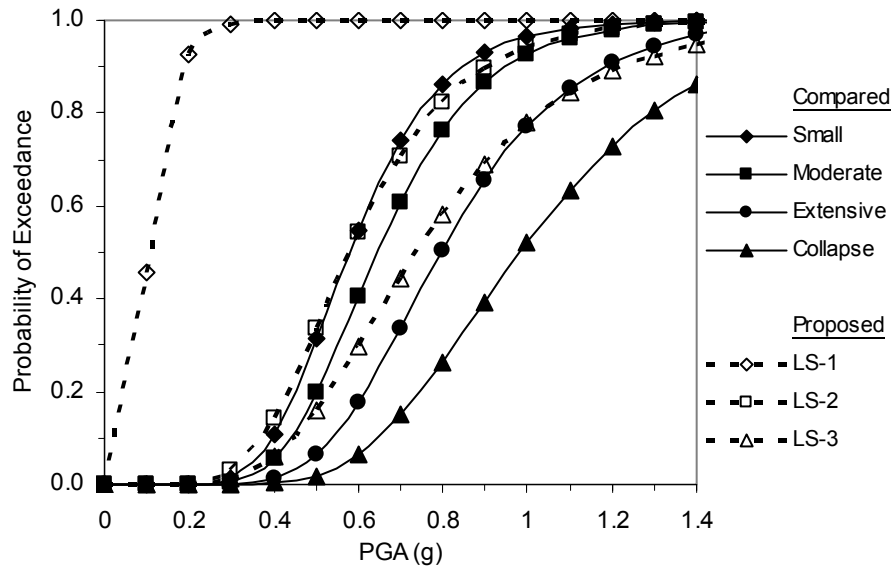
Figure 6.11 Comparison of proposed and Yamazaki et al. (1999) fragility curves
for PGA

ii) Shinozuka et al. (2000a): Shinozuka et al. (2000a) presented empirical fragility
curves that are constructed on the basis of a sample of 770 single-support RC
columns along two stretches of viaduct, one in the HEPC's Kobe Route and the
other in the Ikeda Route with a total of 40 km. Damage limit states of the fragility
curves were classified as minor, moderate, and major.

The two parameters of the probability distributions were determined by the
maximum likelihood method on the cumulative log-normal distribution with the
intensity measure of PGA. To be consistent in comparing the two sets of fragility
curves, the average of the proposed fragility curves for the bridge classes of single-
column bents is considered. As shown in Figure 6.12, proposed fragility curves
result in higher probability of exceedance values for the same seismic intensity level
when compared with the fragility curves developed by Shinozuka et al. (2000a).
The difference between the two sets of curves is more pronounced for the LS-1
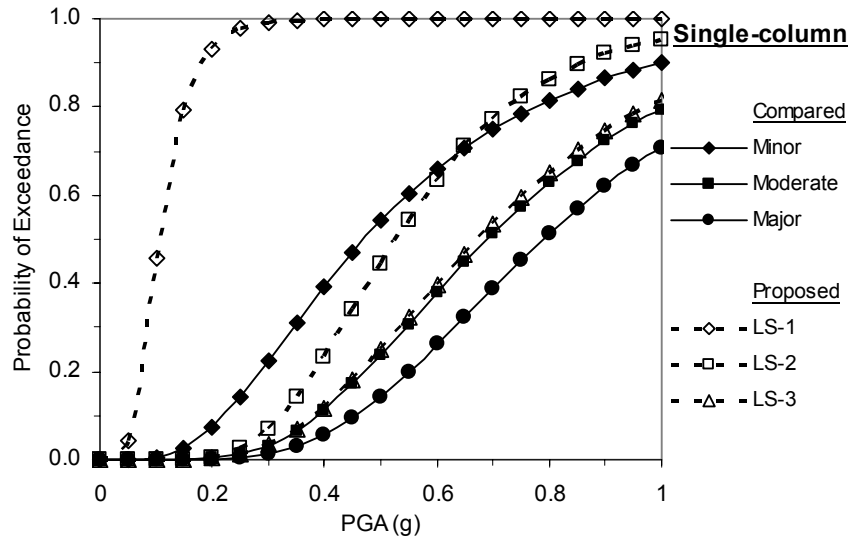damage limit state.

Figure 6.12 Comparison of proposed and Shinozuka et al.(2000a) fragility curves

iii) HAZUS, FEMA (2003): Fragility curves are given for 28 standard highway bridge classes, which are classified according to their various structural attributes and design considerations such as; total length, span number, design date and type, bent column number, material type, superstructure form, etc. as shown in Table 2.4. Among these 28 bridge classes, HWB7 and HWB19 are the ones that have similarities with the bridge types considered in this study. Since these two bridge classes have the multiple-column bents, the comparisons are conducted with the MS_MC_SL30 and MS_MC_SG30 bridge types considered in this study. Same median and dispersion values are given for the two bridge classes in HAZUS. Therefore, only one fragility curve is developed for the damage limit states, which is determined using the median and dispersion values considering modification factors for the skewness and the number of spans according to the Equations (6.1) and (6.2). In order to make comparisons, the parameters in Equations (6.1) and (6.2) need to be specified to obtain HAZUS fragility curves. Span number is assumed to be 3. Two different skew angle values are assumed to compare the effect of skewness with the bridge classes MS_MC_SL30 and MS_MC_SG30 separately. Average values of 15° and 45° are assumed, respectively.

158

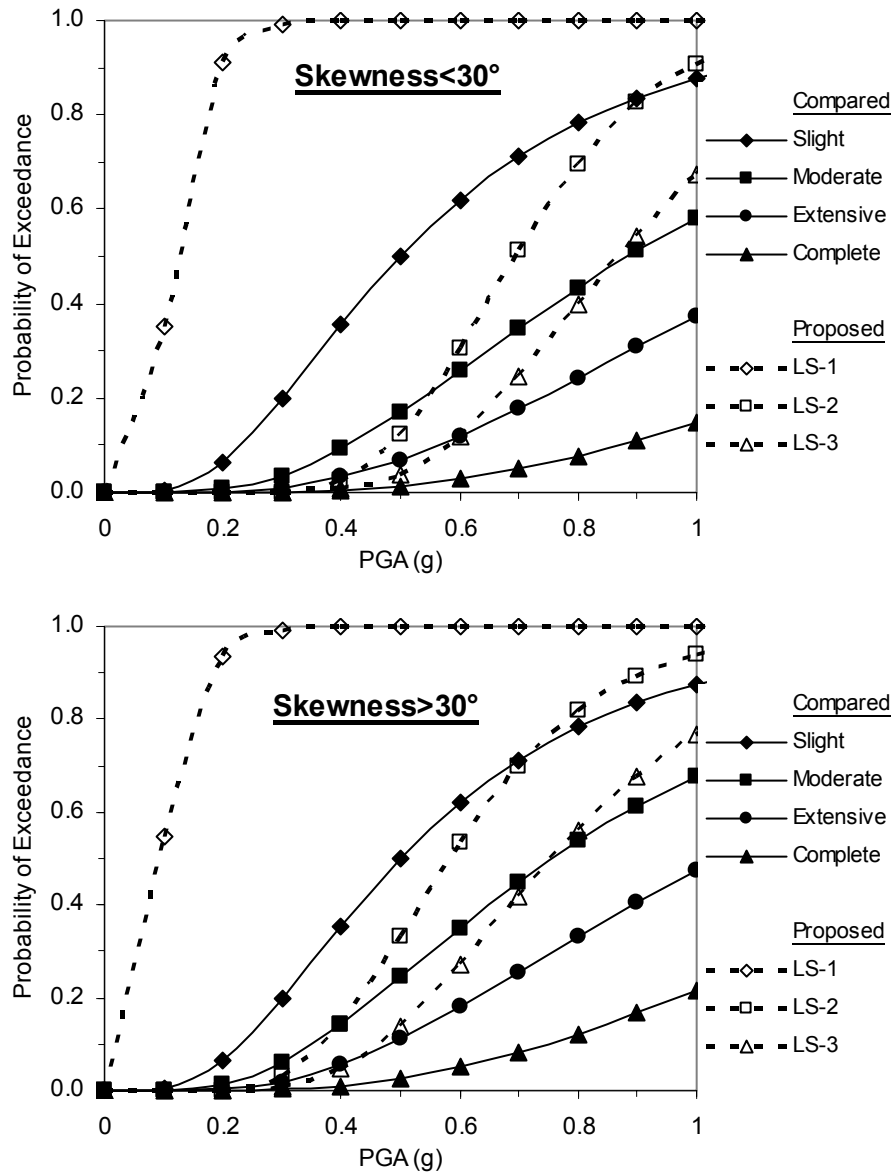Figure 6.13 Comparison of proposed and HAZUS (FEMA, 2003) fragility curves

$$K_{pskew} = \sqrt{\sin(90 - \theta)} \; ; \theta \text{ is the skew angle in degrees} \qquad (6.1)$$

$$K_{3D} = 1 + \frac{0.25}{N-1} \; ; N \text{ is the number of spans} \qquad (6.2)$$

Nielson (2005) mentioned that the fragility curves given in HAZUS were developed by Mander and Basoz (1999). In the work of Mander and Basoz (1999),

the developed fragility curves were given in terms of median PGA. However, the same values are reported as median spectral accelerations at one second (S_{a-1}) in HAZUS. The motive behind this shift is not altogether clear but is likely based on assumption that the PGA is an approximation of S_{a-1}. Therefore, in this study, fragility curves given in HAZUS by S_{a-1} are considered as PGA. In Figure 6.13, comparisons of the proposed and the HAZUS fragility curves are shown for two different skewness levels. The difference between the two sets of fragility curves is apparent, especially for the slight damage limit state. Proposed fragility curves result in higher probability of exceedance values for the same seismic intensity level when compared with the HAZUS fragility curves.

iv) Elnashai et al. (2004): In the study of Elnashai et al. (2004), both analytical and empirical fragility curves for RC bridges were developed. Analytical fragility curves were obtained by considering four bridge samples having the similar structural attributes. The superstructure and the bent columns of the sample bridges have a monolithic connection. Since the sample bridges do not fit any of the bridge classes considered in this study, analytically developed fragility curves are not compared with the proposed fragility curves. Empirical fragility curves for RC bridges were also developed in the work of Elnashai et al. (2004) by considering the actual damage data obtained after the 1994 Northridge and 1995 Kobe earthquakes with a sample size of 1668 bridges. In order to describe the damage condition of bridges, 5 post-earthquake categories were considered: no damage, minor damage, moderate damage, major damage and collapse. Empirical fragility curves were obtained using PGA as the parameter representing the ground motion intensity. Although both cumulative normal and lognormal distribution functions were employed for the empirical fragility curves, to be consistent only the ones with cumulative lognormal distribution functions are used to make the comparisons with the proposed fragility curves. Bridge samples that are used in the development of empirical fragility curves cannot be represented with a certain bridge class considered in this study. Therefore, for the comparisons average of the proposed fragility curves of all the bridge classes are considered. As presented in Figure 6.14,

proposed fragility curves for damage limit states of LS-2 and LS-3 are in good agreement with the counter parts of the empirical fragility curves. On the other hand, the difference between the LS-1 of proposed fragility curve and its empirical counter part is evident.
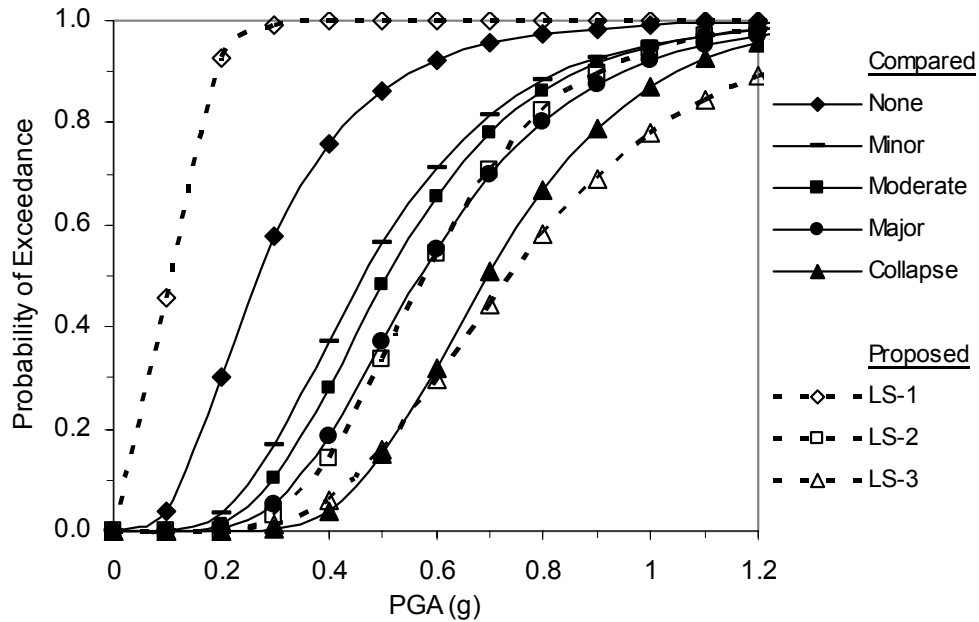

Figure 6.14 Comparison of proposed and Elnashai et al. (2004) fragility curves

v) Liao and Loh (2004): In the study of Liao and Loh (2004), analytical fragility curves were developed for various bridge classes on the south-north freeway in Taiwan considering the seismic intensity measure of PGA. Damage limit states considered for the fragility curves are in accordance with the ones defined in HAZUS. Bridges were classified according to several structural considerations such as span number, superstructure type, pier type, design type of the bridges. Among the 8 different bridge classes, type 2 and 3 can be represented with the bridge classes having the single-column and multiple-column bents, respectively. Therefore, for the comparison purposes, average values for the proposed fragility curves of MS_MC_SL30 and MS_MC_SLG0 are assumed for the multiple-column bent bridges and average values for the proposed fragility curves of MS_SC_SL30

161

and MS_SC_SLG0 are assumed for the single-column bent bridges. On the other side, Liao and Loh (2004) defined two different fragility curves for both type 2 (single-column) and 3 (multiple-column) bridge classes. The difference lies in the design type, which is either conventional or seismic. In a similar way, for the comparison purposes, average values of the fragility curves for the conventional and seismic design type are assumed for the type 2 and type 3 bridge classes. The comparisons of the two sets of fragility curves for the two types of the bridge classes are given Figure 6.15. Proposed fragility curves for damage limit states of LS-2 and LS-3 are in good agreement with the fragility curves given by Liao and Loh (2004) for extensive and complete damage limit states, respectively.

According to the fragility curves of Liao and Loh (2004), single-column bent bridges are more vulnerable to seismic damage than multiple-column bent bridges, which is in good agreement with findings in this study. Similarly, Liao and Loh (2004) specified the same median values for the two bridge classes for the slight damage limit state, which is the case for the proposed fragility curves for LS-1. As mentioned in the previous section, proposed fragility curves of different bridge classes for LS-1 are almost identical.

vi) Nielson (2005): In the study of Nielson (2005), a total of 9 bridge classes were formed to be used in the development of analytical fragility curves. Of these bridge classes, MSSS (multi span simply supported) concrete is the most convenient bridge class that fits the bridge classes considered in this study. Since this bridge class covers all the multi span simply supported concrete bridges regardless of the bent column number and skew angle, average values of all the proposed fragility curves are considered in the comparison of fragility curves. As shown in Figure 6.16, proposed fragility curves results in higher probability of exceedance values for the same seismic intensity level when compared with the fragility curves developed by Nielson (2005). The disparity between the two sets of curves is more pronounced for the higher PGA values for the damage states of LS-2 and LS-3 of the proposed fragility curves.
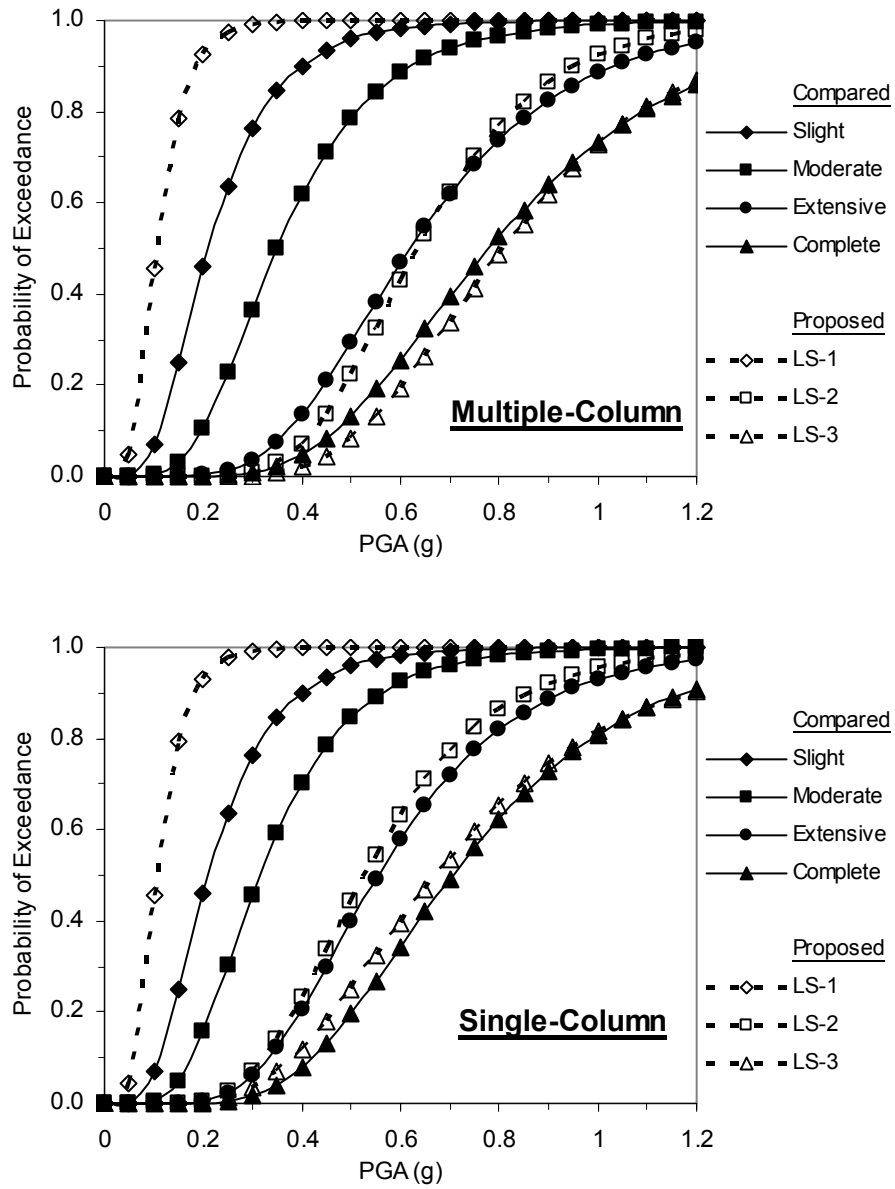
Figure 6.15 Comparison of proposed and Liao and Loh (2004) fragility curves
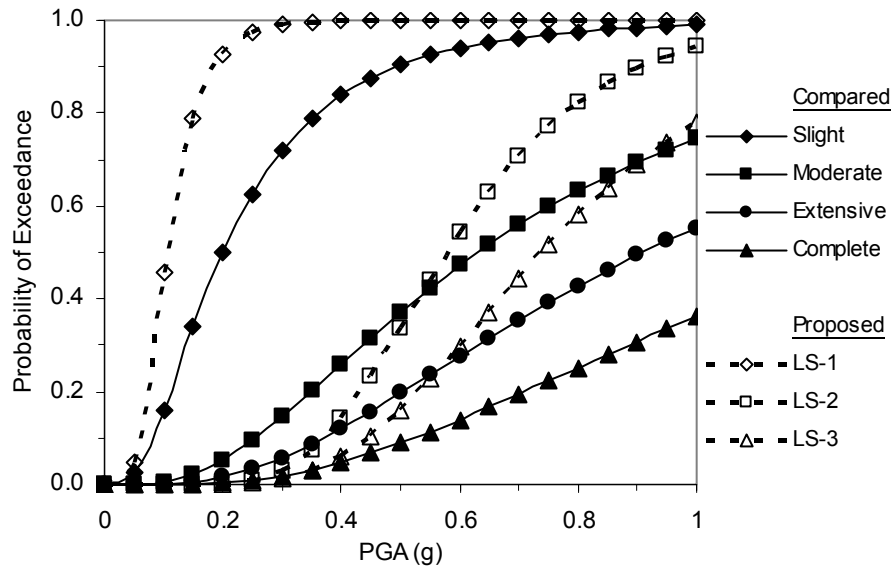
Figure 6.16 Comparison of proposed and Nielson (2005) fragility curves

Several comparisons are made between the proposed analytical fragility curves and the previously developed analytical and empirical fragility curves for various damage limit states. Since there are major differences in the development of fragility curves, it is not suitable to use the previously developed fragility curves to validate or invalidate the proposed analytical fragility curves. But these comparisons provide useful information to acquire a general idea if relatively big discrepancies exist between the fragility curves. For instance, proposed fragility curves for the damage limit state of LS-1 results in higher probability of exceedance values for the same seismic intensity level in comparison with the previously developed fragility curves. The reason for this obvious difference is the deficiency in the connection of the superstructure and the substructure components. Since there is no connecting device between the elastomeric bearings and the concrete components of the superstructure and the substructure, even at lower levels of seismic input, friction force between the bearings and concrete surfaces can be exceeded easily with the movement and becomes inadequate to hold the elastomeric bearings at their place and unseating takes place. This can cause permanent displacement of the superstructure and may affect the functionality of the bridge.

However, bridges considered in the previous studies mostly have monolithic connection between superstructure and substructure. Or in some cases, bolts are utilized to connect the elastomeric bearings to the concrete members. These connecting devices provide additional strength to the system preventing the permanent displacement of the superstructure at lower levels of seismic input. On the other hand, it should be kept in mind that introducing these connecting devices results in higher seismic forces transmitted to the substructure components.

In some cases, proposed fragility curves for the damage limit states of LS-2 and LS-3 are in good agreement with corresponding fragility curves given in the previous studies. This provides some level of confidence with the proposed fragility curves. However, actual damage data of the highway bridges in Turkey is necessary to validate the proposed curves.

CHAPTER 7

CASE STUDIES

Seismic risk assessment of some existing highway bridges around the Marmara Region (northeast part of Turkey) is performed using the developed fragility curves. In this application, deterministic approach is applied for the seismic hazard assessment of the bridge sites. For the case study 105 bridge samples were selected, whose structural attributes are in accordance with the ones considered in Chapter-2. In other words, the selected bridge samples can be classified as being one of the 4 major bridge categories, of which the fragility curves are developed. Some important features of these bridges are given in Table 7.1. As shown in Figure 7.1, MS_MC_SL30 (Multi Span_Multi Column_Skew Angle Less than 30°) bridge type dominates the selected sample.
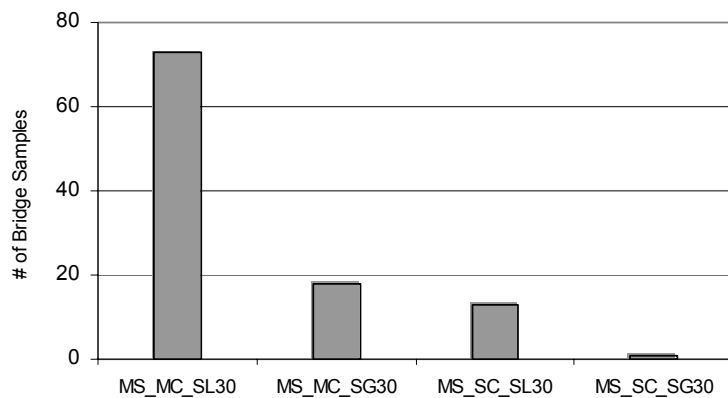

Figure 7.1 Bridge type distribution among 105 sample bridges

Table 7.1 Some important parameters of 105 bridge samples

#	GDH No.[1]	Name of Bridge	Province	Longitude	Latitude	Skew Angle (°)	Span #	Max Span L. (m)	Total L. (m)	Bent Column #	Hcol (m)	Bridge Type	D_surface to Scenario EQ Faults (km)		
													Bursa	Düzce	Marmara
1	1496	KARABÜK KAVŞAK	KARABÜK	41.1950	32.6242	16	2	29.8	60.2	2	7.90	MS_MC_SL30	279.88	109.46	272.84
2	1470	MURATLI KAVŞAK	TEKİRDAĞ	41.1628	27.4925	33	2	20.6	42.0	2	8.32	MS_MC_SG30	143.47	293.53	45.38
3	1458	ÜNİVERSİTE ÖNÜ KAVŞAK	TEKİRDAĞ	40.9892	27.5775	21	2	17.3	35.3	2	6.58	MS_MC_SL30	123.59	284.54	25.59
4	1461	SOĞANLI	KARABÜK	40.9928	32.5967	10	4	31.0	98.8	1	13.88	MS_SC_SL30	268.16	99.69	267.50
5	1448	DEMİRYOLU	BİLECİK	39.9208	30.0011	0	2	20.0	40.9	4	6.48	MS_MC_SL30	26.68	123.90	100.82
6	1453	MODERN SANAYİ ÜG	SAKARYA	40.7386	30.4139	5	2	24.0	48.6	2	5.60	MS_MC_SL30	101.67	45.26	82.40
7	1415	KOCASU	BURSA	39.9319	28.9717	0	3	22.0	67.2	1	5.48	MS_SC_SL30	26.75	191.70	91.15
8	1421	UMURBEY	BURSA	40.4050	29.1358	0	2	17.2	32.5	2	5.93	MS_MC_SL30	24.71	158.42	36.77
9	1404	VALİDE	BURSA	40.6086	29.5622	0	3	20.0	61.2	2	7.38	MS_MC_SL30	55.88	118.34	16.21
10	1398	ÖMERLİ	İSTANBUL	41.0819	29.3233	0	3	16.0	49.2	2	7.51	MS_MC_SL30	102.55	141.01	39.71
11	1399	GELİNDERESİ-8	BALIKESİR	39.5675	27.2378	30	2	15.7	32.1	2	4.98	MS_MC_SG30	117.95	342.45	127.69
12	1403	SARIMSAKCI	ÇANAKKALE	39.7933	26.3392	30	6	15.7	97.2	2	6.63	MS_MC_SG30	182.05	405.75	131.75
13	1378	ÇAYAĞZI	ZONGULDAK	41.0967	31.2144	0	5	20.3	103.9	2	4.43	MS_MC_SL30	176.36	33.37	155.21
14	1353	ÇAYCUMA	ZONGULDAK	41.4261	32.0875	0	11	23.4	251.0	2	6.00	MS_MC_SL30	255.75	90.54	235.72
15	1355	UMURBEY	ÇANAKKALE	40.2661	26.5933	20	2	24.0	48.6	3	6.93	MS_MC_SL30	158.01	372.38	78.85
16	1356	MUSAKCA	BALIKESİR	40.2828	27.6011	20	4	15.7	64.6	2	7.31	MS_MC_SL30	74.31	288.10	52.93
17	1360	YALAKDERE(sağ köprü)	YALOVA	40.6031	29.5622	0	3	13.0	40.2	2	5.68	MS_MC_SL30	55.30	118.44	16.68
18	1342	BÜYÜK MELEN	DÜZCE	40.8417	30.9950	34	3	29.6	82.0	3	6.68	MS_MC_SG30	143.73	7.62	131.94
19	1346	MENGEN	BOLU	40.9372	32.0708	10	2	23.7	48.0	2	4.68	MS_MC_SL30	225.53	55.59	222.97
20	1351	ÇOBANÇEŞME	İSTANBUL	40.9939	28.8197	30	3	22.2	58.0	2	4.78	MS_MC_SG30	89.71	180.81	15.33
21	1341	KÜÇÜKBOSTANCI	BALIKESİR	39.5869	27.9286	0	4	31.9	111.8	2	5.18	MS_MC_SL30	71.00	288.31	132.15
22	1321	HAVRAN	BALIKESİR	39.5533	27.0856	20	7	15.8	114.2	2	7.60	MS_MC_SL30	130.14	355.01	130.57
23	1312	İVRİNDİ	BALIKESİR	39.5978	27.4914	0	3	17.5	53.7	2	6.75	MS_MC_SL30	97.75	321.29	125.05
24	1313	GÜLÜÇ	ZONGULDAK	41.2522	31.4281	30	7	21.0	151.2	2	8.83	MS_MC_SG30	201.23	51.33	177.38
25	1314	MUDURNU	SAKARYA	40.6411	30.6128	0	3	30.0	91.4	2	3.78	MS_MC_SL30	104.82	31.75	99.58
26	1289	GEYİKKIRI DRENAJ KANALI	ÇANAKKALE	40.3142	27.1181	0	2	24.0	48.6	2	6.11	MS_MC_SL30	114.91	327.64	47.54
27	1238	GEREDEÇAYI(HAMAMLIÇAY)	KARABÜK	40.8672	32.5956	20	4	21.4	80.6	2	5.78	MS_MC_SG30	262.85	97.16	266.43
28	1227	KARASU-6	ZONGULDAK	41.0156	32.0792	45	3	20.0	61.6	2	8.48	MS_MC_SG30	230.20	59.67	224.65
29	1208	GEBZE ŞEKEPINAR ÜG	KOCAELİ	40.8631	29.3836	18	2	26.0	52.6	5	7.78	MS_MC_SL30	79.35	132.21	15.74
30	1189	TROMPET KAVŞAĞI	BİLECİK	39.9222	30.0047	10	2	26.6	53.9	3	5.98	MS_MC_SL30	26.92	123.58	100.83
31	1180	KULACA KAVŞAĞI	BURSA	40.0647	29.5672	25	2	18.0	36.7	1	5.40	MS_SC_SL30	3.76	140.80	73.56
32	1180	PAZARYERİ KAVŞAĞI	BURSA	40.0592	29.5839	0	2	16.5	33.7	2	5.75	MS_MC_SL30	3.54	139.98	74.40
33	1181	DOMANİÇ KAVŞAĞI	BURSA	40.0425	29.5922	5	2	16.5	33.7	2	6.00	MS_MC_SL30	1.94	140.47	76.35
34	1181	YENİKÖY KAVŞAĞI	BURSA	39.9822	29.6581	0	2	18.5	37.7	1	5.70	MS_SC_SL30	3.05	140.07	84.03
35	1183	OSMANİYE KAVŞAĞI	BURSA	39.9428	29.7100	0	2	16.5	33.7	1	6.45	MS_SC_SL30	6.42	139.53	89.35

Table 7.1 Some important parameters of 105 bridge samples (continued)

#	GDH No.[1]	Name of Bridge	Province	Longitude	Latitude	Skew Angle (°)	Span #	Max Span L. (m)	Total L. (m)	Bent Column #	Hcol (m)	Bridge Type	D_surface to Scenario EQ Faults (km)		
													Bursa	Düzce	Marmara
36	1184	MURATDERE KAVŞAĞI	BURSA	39.8919	29.8961	0	2	16.5	33.7	1	5.70	MS_SC_SL30	20.21	132.21	99.86
37	1186	BULDAN(BEYCUMA)	ZONGULDAK	41.3283	31.9689	30	2	17.5	35.6	2	4.01	MS_MC_SG30	241.30	75.93	222.98
38	1168	FILYOS-2	ZONGULDAK	41.2283	31.9628	0	15	21.9	327.5	2	9.38	MS_MC_SL30	234.36	66.83	219.52
39	1175	FILYOS-1	ZONGULDAK	41.3050	32.1039	0	14	21.9	305.0	2	6.18	MS_MC_SL30	248.90	81.04	233.09
40	1175	KARAPÜRÇEK	BALIKESİR	39.9875	28.1992	25	3	19.5	59.9	2	4.68	MS_MC_SL30	23.45	248.63	88.72
41	1129	ÇAYAĞZI	DÜZCE	41.0969	31.2206	0	5	20.0	103.6	2	4.00	MS_MC_SL30	176.76	33.32	155.72
42	1129	ALAPLI	DÜZCE	41.1075	31.2636	0	9	22.0	205.2	3	4.18	MS_MC_SL30	180.20	34.07	159.50
43	1131	AKÇIN	ÇANAKKALE	39.6061	26.4142	20	3	24.0	73.2	2	5.28	MS_MC_SL30	181.07	406.26	145.11
44	1133	KÜÇÜK AGONYA(AKPINAR)	ÇANAKKALE	40.3356	26.7069	0	2	14.7	30.0	2	7.28	MS_MC_SL30	149.58	361.60	66.51
45	1110	YENİKÖY ÜG	YALOVA	40.6967	29.4953	40	4	17.6	70.0	2	6.48	MS_MC_SG30	63.82	122.81	5.54
46	1110	ŞAHİNDERE	BALIKESİR	39.5694	26.7539	35	2	23.5	47.8	3	4.28	MS_MC_SG30	155.15	380.54	135.97
47	1111	BAHÇECİK KAVŞ. ÜG	KOCAELİ	40.7131	29.9244	17	2	18.0	36.6	3	5.88	MS_MC_SL30	81.38	86.60	41.14
48	1114	HASANPAŞA(ÇANDIR)	BURSA	40.0542	29.6064	15	4	28.3	115.3	2	7.08	MS_MC_SL30	3.52	138.73	75.29
49	1099	SOĞUCAK BAĞLANTI YOLU ÜG	YALOVA	40.5936	29.2814	0	2	21.0	42.6	3	6.28	MS_MC_SL30	48.19	142.02	14.72
50	1100	GÖLCÜK-1 BAĞLANTI YOLU ÜG	KOCAELİ	40.7147	29.8094	0	2	18.0	36.6	4	5.98	MS_MC_SL30	79.36	96.26	31.45
51	1100	GÖLCÜK-2 BAĞLANTI YOLU ÜG	KOCAELİ	40.7164	29.8175	1.5	2	21.0	42.6	3	5.98	MS_MC_SL30	79.72	95.57	32.12
52	1102	HİSAREYN BAĞLANTI YOLU ÜG	KOCAELİ	40.7053	29.8522	13.5	2	21.0	42.6	3	5.18	MS_MC_SL30	79.32	92.74	35.08
53	1066	TABAKHANE	DÜZCE	40.9083	31.1425	31	2	16.2	33.1	2	5.81	MS_MC_SG30	158.01	13.87	145.12
54	1053	AKÇAY DERESİ	SAKARYA	40.6656	30.3581	0	2	16.0	32.6	2	4.38	MS_MC_SL30	92.34	51.17	77.93
55	1057	YAHYAKÖY-2	BALIKESİR	39.9786	28.1833	20	9	28.4	260.4	2	11.18	MS_MC_SL30	25.11	250.25	89.60
56	1052	KAYNARCA	SAKARYA	41.0325	30.3067	0	2	17.0	34.6	2	6.04	MS_MC_SL30	125.50	61.50	81.06
57	1052	OTOYOL	SAKARYA	40.7081	30.3756	39	3	27.5	77.9	2	6.58	MS_MC_SG30	97.02	48.85	79.17
58	1037	BURHANİYE KAVŞAK	BALIKESİR	39.5031	26.9692	0	2	20.0	40.6	2	6.18	MS_MC_SL30	141.58	366.40	137.88
59	1038	KARABÜK KAVŞAK	KARABÜK	40.8714	32.5789	16	4	17.0	60.2	2	6.98	MS_MC_SL30	261.70	95.82	265.05
60	1024	İHSANİYE	İZMİT	40.7114	29.8417	4	4	18.0	73.8	2	6.48	MS_MC_SL30	79.74	93.58	34.17
61	1026	SAMANLI DERE	YALOVA	40.6497	29.2400	37	2	16.0	32.8	2	2.26	MS_MC_SG30	54.09	144.72	8.72
62	1026	KULLAR DERESİ	İZMİT	40.7350	29.9556	0	6	18.0	111.0	2	5.14	MS_MC_SL30	84.38	83.83	43.79
63	1027	BAŞİSKELE KÖPRÜLÜ KAVŞ.	İZMİT	40.7206	29.9392	7.5	4	18.0	61.8	4	7.13	MS_MC_SG30	82.48	85.31	42.37
64	1028	YENİKÖY ÜG	İZMİT	40.7069	29.8817	40	4	19.4	70.0	2	6.48	MS_MC_SG30	79.96	90.25	37.55
65	1011	ÇAYCUMA DDY ÜG	ZONGULDAK	41.4161	32.0950	0	3	20.0	61.2	2	8.43	MS_MC_SL30	255.57	90.03	235.96
66	1012	KAVUKKAVLAĞI	ZONGULDAK	41.1175	31.3006	30	3	15.6	48.2	2	6.40	MS_MC_SG30	183.23	35.20	162.78
67	1013	K2 KANDIRA-İZMİT KAVŞAK	İZMİT	41.0706	30.1472	0	4	17.0	69.8	2	12.13	MS_MC_SL30	124.70	75.33	71.42
68	1021	ÇİFTLİKKÖY KAVŞAK	YALOVA	40.6644	29.3231	0	4	19.4	64.0	2	6.38	MS_MC_SL30	56.56	137.59	6.64
69	1010	MUDURNU	SAKARYA	40.6581	30.5953	0	3	25.0	76.2	2	7.08	MS_MC_SL30	105.03	32.31	97.94
70	1011	TAŞKÖPRÜ KAVŞAK	YALOVA	40.6783	29.3892	15	4	15.4	56.0	2	6.83	MS_MC_SL30	59.60	131.89	4.74

Table 7.1 Some important parameters of 105 bridge samples (continued)

#	GDH No.[1]	Name of Bridge	Province	Longitude	Latitude	Skew Angle (°)	Span #	Max Span L. (m)	Total L. (m)	Bent Column #	Hcol (m)	Bridge Type	$D_{surface}$ to Scenario EQ Faults (km) Bursa	Düzce	Marmara
71	992	KAYTAZDERE KAVŞAĞI	YALOVA	40.6919	29.5403	0	4	18.0	61.2	2	6.68	MS_MC_SL30	64.18	119.07	9.25
72	992	YENİKÖY DERESİ	BİLECİK	40.1203	30.0467	0	3	18.0	55.2	2	5.70	MS_MC_SL30	31.92	105.06	84.25
73	996	KOCABAŞ-2	ÇANAKKALE	40.2375	27.2403	10	4	22.0	89.8	2	8.08	MS_MC_SL30	103.17	319.09	53.41
74	980	GÖYNÜK DERESİ-1	SAKARYA	40.5083	30.2967	0	2	16.0	32.6	2	3.98	MS_MC_SL30	75.52	62.25	76.29
75	981	GÖYNÜK DERESİ-2	SAKARYA	40.5061	30.3208	15	3	16.0	49.2	2	10.53	MS_MC_SL30	76.72	60.57	78.31
76	983	YEŞİLÇAY DERESİ	KOCAELİ	41.1281	29.8553	33	3	15.0	46.6	2	3.78	MS_MC_SG30	118.62	100.23	57.53
77	988	SUBAŞI KAVŞAK	YALOVA	40.6928	29.4783	5	2	20.3	41.3	3	6.58	MS_MC_SL30	63.12	124.27	4.57
78	960	İSTANBUL-EDİRNE Yolu (A Yolu)	İSTANBUL	41.0297	28.4578	0	7	22.0	157.6	2	6.48	MS_MC_SL30	99.46	211.43	22.67
79	951	KAVŞAK	SAKARYA	40.4342	30.4261	0	2	19.3	39.4	2	6.95	MS_MC_SL30	77.89	57.78	89.38
80	955	TOPÇULAR KAVŞAK	YALOVA	40.6875	29.4325	8	4	18.0	61.8	2	5.50	MS_MC_SL30	61.60	128.17	3.49
81	956	CEYLANKENT KAVŞAK	YALOVA	40.6819	29.3608	0	4	18.0	61.8	2	7.90	MS_MC_SL30	59.33	134.24	4.49
82	957	BALABANDERE	YALOVA	40.6581	29.2914	0	2	13.0	26.6	2	2.23	MS_MC_SL30	55.40	140.31	7.52
83	927	KARACABEY(ALT GEÇİT)	BURSA	40.1825	28.3581	28	2	20.0	40.7	3	8.58	MS_MC_SL30	12.29	228.68	69.50
84	910	ÜSKÜBÜ-MELEN	BOLU	40.8919	31.1678	20	5	21.4	109.4	2	7.18	MS_MC_SL30	158.52	11.55	146.99
85	898	ALT GEÇİT (Belveren)	BOLU	41.0797	31.1036	39	3	27.0	55.6	2	7.58	MS_MC_SG30	168.38	33.24	145.76
86	898	ALT GEÇİT (fındıklık)	BOLU	41.0817	31.1031	5	3	27.0	55.4	2	7.98	MS_MC_SL30	168.50	33.47	145.77
87	902	KARASU-18	BİLECİK	40.1403	29.9794	1	3	20.0	61.2	1	12.88	MS_SC_SL30	28.00	107.81	79.06
88	902	KURUDERE	BİLECİK	40.2044	29.9747	1	3	20.0	61.2	1	7.68	MS_SC_SL30	32.22	103.61	73.11
89	903	GÜVENCERDERE	BİLECİK	40.1956	29.9703	0	3	20.0	61.2	1	8.88	MS_SC_SL30	31.25	104.52	73.66
90	883	BURSA KAVŞAĞI 5NOLU KÜG	BİLECİK	40.1744	29.9711	21	4	17.0	69.8	3	5.61	MS_SC_SL30	29.73	105.92	75.57
91	885	KÜTAHYA KAVŞAĞI 4NOLU KÜG	BİLECİK	39.8964	30.0919	30	4	17.0	70.4	3	4.40	MS_MC_SG30	34.89	121.22	107.01
92	885	TROMPET KAVŞAĞI KÜG	BİLECİK	39.9222	30.0036	10	4	22.0	75.8	2	6.88	MS_MC_SL30	26.83	123.64	100.78
93	886	SARAYCIK KAVŞAĞI KÜG	BİLECİK	39.9067	30.0344	25	4	22.0	75.8	3	5.68	MS_MC_SL30	29.89	123.31	103.56
94	886	SANAYI KAVŞAĞI KÜG	BİLECİK	40.1706	29.9764	6	4	15.0	61.8	3	5.58	MS_MC_SL30	29.80	105.84	76.18
95	886	SAHİL YOLU KAVŞAĞI	BİLECİK	40.1492	29.9767	22	6	15.0	93.0	3	5.58	MS_MC_SL30	28.37	107.35	78.12
96	867	ULUBAT-2	BURSA	40.2056	28.4333	0	7	21.4	153.4	1	9.00	MS_SC_SL30	12.73	221.82	68.04
97	869	KOCASU KÖPRÜSÜ	BURSA	39.9319	28.9717	0	3	22.0	67.2	1	4.88	MS_SC_SL30	26.75	191.70	91.15
98	873	GÖÇMEN KONUTLARI KAVŞAĞI ÜG	BURSA	40.2206	28.8261	20	2	22.0	44.6	1	7.35	MS_SC_SL30	5.57	189.63	66.70
99	837	DARICA DDY ÜG	KOCAELİ	40.7833	29.4131	24	3	13.5	41.9	3	8.23	MS_MC_SL30	71.46	129.41	7.04
100	832	DEĞİRMENBOĞAZI (ikileme)	BALIKESİR	39.6975	27.9658	30	2	22.0	44.8	1	6.33	MS_SC_SG30	59.54	279.87	120.11
101	835	LİMAN YOLU ÜG	BALIKESİR	40.3497	27.9444	17	2	22.0	44.6	2	6.08	MS_MC_SL30	50.91	258.10	47.63
102	816	BİGADİÇ AYR. KAVŞ. ÜG	BALIKESİR	39.6014	27.9106	0	2	22.0	44.6	4	5.58	MS_MC_SL30	70.71	288.92	130.43
103	823	CANBOLU-2	BURSA	40.1964	28.3519	20	9	22.0	192.4	1	7.20	MS_SC_SL30	13.87	228.72	67.88
104	812	HAVAALANI ÜG	BALIKESİR	39.6358	27.9131	25	3	22.0	67.4	2	6.48	MS_MC_SL30	67.66	286.97	126.63
105	812	KEPSUT ÜG	BALIKESİR	39.6542	27.9364	25	4	22.0	90.1	2	6.58	MS_MC_SL30	64.81	284.27	124.74

[1] Bridge No. at the General Directorate of Highways

In the deterministic seismic hazard assessment for the bridge sites, 3 earthquake scenarios are taken into account in the Marmara region. These are the Marmara Earthquake scenario (Mw7.4) with a fault rupture at the Marmara Sea, the 1999 Düzce Earthquake (Mw7.2) and the Bursa Earthquake scenario (Mw7.0) with a rupture of 3 fault segments at the Bursa province. The detailed information for these scenario earthquakes and the corresponding analysis results are given in the following sections. Various ground motion seismic intensity measures due to these scenario earthquakes are calculated considering three different attenuation relationships, which are expressed as a function of distance, magnitude, local site classification and faulting type. The formulations and important parameters of the three attenuation relationships are as follows:

i) Boore et al. (1997): The following attenuation relationship is proposed by David M. Boore, William B. Joyner and Thomas E. Fumal (1997). The equation parameters are explained briefly and the coefficients, which depend on the period of interest, are given in the relevant publication.

$$\ln Y = b_1 + b_2 (M_w - 6) + b_3 (M_w - 6)^2 + b_5 \ln r + b_v \ln(V_S / V_A) \qquad (7.1)$$

where

$$r = \sqrt{r_{jb}^2 + h^2} \qquad (7.2)$$

$$b_1 = \begin{cases} b_{1SS} & \text{for strike - slip earthquakes} \\ b_{1RS} & \text{for reverse - slip earthquakes} \\ b_{1ALL} & \text{if mechanism is not specified} \end{cases} \qquad (7.3)$$

Y : ground motion parameter (PGA, SA), [g]

M_w : moment magnitude

r_{jb} : the closest horizontal distance to the vertical projection of the rupture, [km]

V_s : average shear wave velocity to 30 m, [m/sec]

h : fictitious depth, [km]

V_A : fictitious velocity, [m/sec]

ii) Kalkan and Gülkan (2004): The following attenuation relationship is proposed by Erol Kalkan and Polat Gülkan (2004). The equation has the same general form as the equation proposed by Boore et al. (1997). The equation parameters are explained briefly and the coefficients, which depend on the period of interest, are given in the relevant publication.

$$\ln Y = b_1 + b_2(M_w - 6) + b_3(M_w - 6)^2 + b_5 \ln r + b_v \ln(V_S / V_A) \qquad (7.4)$$

where

$$r = \sqrt{r_{jl}^2 + h^2} \qquad (7.5)$$

Y : ground motion parameter (PGA, SA), [g]

M_w : moment magnitude

r_{jl} : the closest horizontal distance to the vertical projection of the rupture (or Joyner-Boore distance), [km]

V_s : average shear wave velocity to 30 m, [m/sec]

h : fictitious depth, [km]

V_A : fictitious velocity, [m/sec]

When using Kalkan and Gülkan (2004) and Boore et al. (1997) attenuation relationships, intensity measures of PGA and ASI are estimated for each bridge site. The calculation of ASI from the pseudo spectral acceleration is made using the procedure explained in detail in Chapter-4 for the relevant initial period (T_i) and final period (T_f) specific for the associated bridge type. When using this attenuation relationship, some limitations are taken into consideration as given in Table 7.2.

ii) Akkar and Bommer (2007): The following attenuation relationship is proposed by Sinan Akkar and Julian J. Bommer (2007). Derived equations are used to estimate PGV for both the larger and the geometric mean of the horizontal components. Since the fragility curves developed in this study are for the geometric mean of the two horizontal components, the attenuation relationship equations for the geometric mean of PGV is used to assess the seismic hazard of the bridge sites.

The equation parameters are explained briefly and the coefficients are given in the relevant publication.

$$\begin{aligned}
\log(\text{PGV}_{GM}) = b_1 + b_2 M + b_3 M^2 + (b_4 + b_5 M)\log\sqrt{R_{jb}^2 + b_6^2} \\
+ b_7 S_S + b_8 S_A + b_9 F_N + b_{10} F_R
\end{aligned}$$
(7.6)

where

PGV_{GM} : geometric mean of peak ground velocity, [cm/s]

M : moment magnitude

R_{jb} : the closest horizontal distance to the vertical projection of the rupture (or Joyner-Boore distance), [km]

S_A and S_S : dummy variables representing the influence of site class, taking values of 1 for stiff and soft soil sites, respectively, and zero otherwise.

F_N and F_R : dummy variables for the influence of style-of-faulting, taking values of 1 for normal and reverse ruptures, respectively, and zero otherwise.

Using Akkar and Bommer (2007), intensity measure of mean PGV is estimated for each bridge site. When using this attenuation relationship, some limitations are taken into consideration as given in Table 7.2. The closest distance limitations and the intensity measures calculated using these three attenuation relationships are presented in Table 7.2.

Table 7.2 Considered attenuation relationships and their limitations

Attenuation Relationships	Calculated IMs	Mw Range	Distance Range
Kalkan and Gülkan (2004)	PGA, ASI	4.0 - 7.5	up to 250km
Boore et al. (1997)	PGA, ASI	5.5 - 7.5	up to 80km
Akkar and Bommer (2007)	PGV	5.0 - 7.6	5km to 100km

Kalkan and Gülkan (2004) and Boore et al. (1997) are the most suitable and well known attenuation relationships for estimating PGA as well as spectral accelerations for Turkey. Therefore, in some studies combination of these two attenuation relationships were used for estimating PGA for a specific site. However, in this study, each sample bridge has its own closest distance to the seismic source, which varies between 2 km to 406 km. When the distance range limitation for each attenuation relationship is concerned, it is not appropriate to use the combination of the two relationships. So, calculated results of each attenuation relationship are considered to be used individually in the deterministic seismic hazard analysis.

The earthquake databases that are employed during the development process of the selected attenuation relationships, represent the typical characteristics of the earthquakes occurred in Turkey. This is the main reason for selecting these attenuation relationships. For ASI and PGA intensity measures, two different attenuation relationships are used (Kalkan and Gülkan, 2004 and Boore et al., 1997). Kalkan and Gülkan (2004) equation results in lower estimates for ASI and PGA in comparison with Boore et al. (1997). The statistical tools and numerical methods used for the formulation of these relationships are out of the scope of this study.

When using the attenuation relationships, type of faulting is considered to be strike-slip in order to be consistent with the development of fragility curves. Similarly, due to the lack of information about the bridges' local site condition, an average value of 350m/s is assumed for the shear wave velocity in the calculations. Each attenuation relationship uses the similar definition for the shortest distance to the fault, which is adopted as the closest horizontal distance between the bridge local site and the point on the vertical projection of the fault rupture on the earth's surface. The data pertinent to bridges are collected and implemented as a data-base using geographic information system (GIS) software, ArcView GIS. The bridge locations and the ruptured fault segments due to scenario earthquakes are shown in Figure 7.2. The coordinates of the closest point on the scenario earthquake ruptured fault to the bridge site is calculated using ArcView.
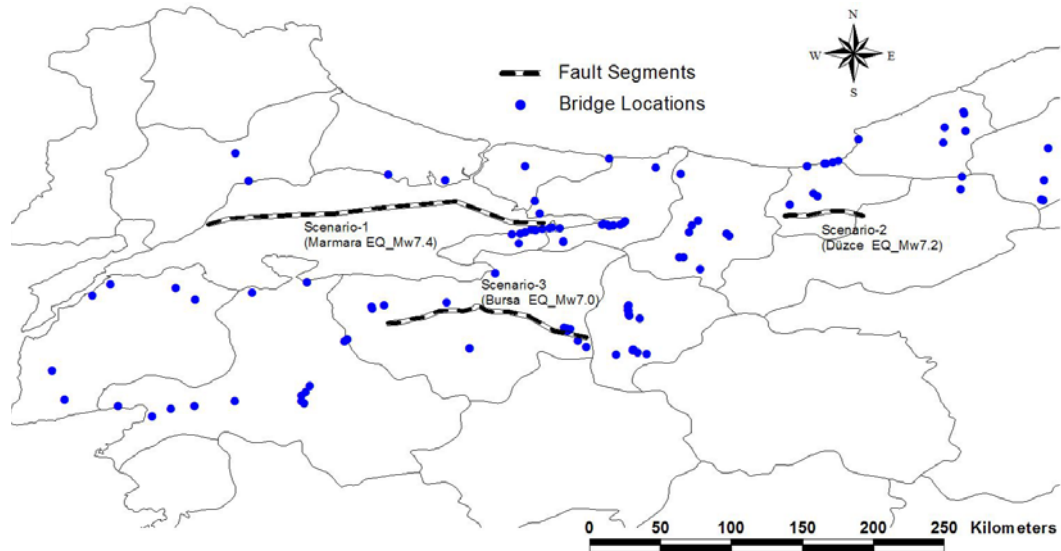
Figure 7.2 105 sample bridge locations and the fault segments for the 3 scenario earthquakes

The distance between the bridge and the closest point on the fault line can be calculated according to the formulations given in Equations (7.7), (7.8) and (7.9) using Figure 7.3 and Figure 7.4. In the given equations, R is the term denoting the radius of the earth. Although the radius of the earth changes according to the geological characteristics of the site, a constant value of 6371km is assumed in the calculations. The closest distances between the bridge and the ruptured fault segment for the three scenario earthquakes are calculated and presented in the last three columns of Table 7.1. When the closest distance results are investigated, some of them are out of the limits specified for the attenuation relationships given in Table 7.2. Seismic hazard of the bridge site is not taken into consideration, when the closest distance of the bridge to the fault segment is greater than the upper limit specified for the interested attenuation relationship. Moreover, a lower limit is specified for the closest distance by Akkar and Bommer (2007) attenuation relationship for estimating PGV. In this case, when the closest distance is less than the lower limit value, then the calculations were done with respect to the specified lower limit for the closest distance.
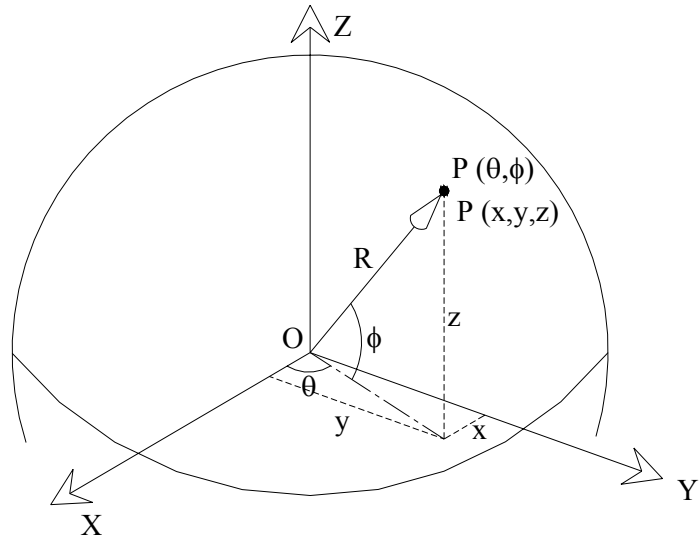
Figure 7.3 Spherical coordinates (θ, Φ) converted to 3D Cartesian coordinates (x, y, z)
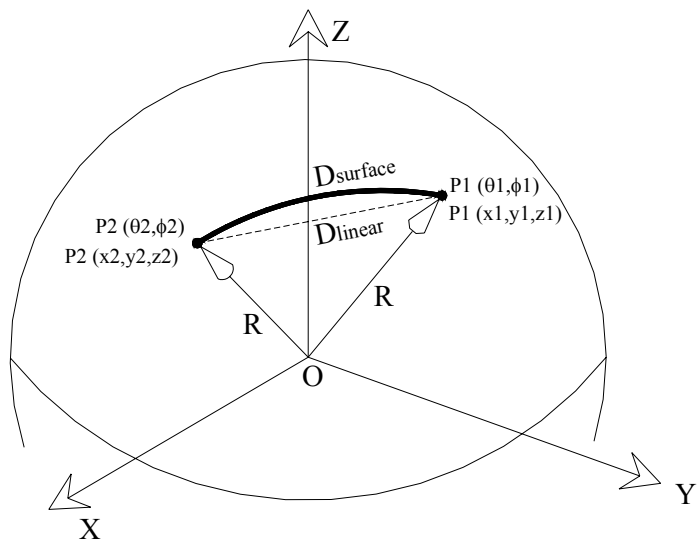
Figure 7.4 Linear and surface distances between two points on the earth

$$x = R \cdot \cos(\phi) \cdot \cos(\theta), \quad y = R \cdot \cos(\phi) \cdot \sin(\theta) \quad \text{and} \quad z = R \cdot \sin(\phi) \tag{7.7}$$

$$D_{linear} = \sqrt{(x_2 - x_1)^2 + (y_2 - y_1)^2 + (z_2 - z_1)^2} \tag{7.8}$$

$$D_{surface} = R \cdot \left[2 \cdot \sin^{-1}(D_{linear}/2R) \right] \tag{7.9}$$

7.1   DETERMINATION OF THE BRIDGE PERFORMANCE STATES

Damage state of each 105 sample bridge when exposed to scenario earthquakes is determined using the developed fragility curves and the selected attenuation relationships. The methodology employed for the damage state calculations is represented schematically in Figure 7.5. Accordingly, different ground motion intensity measures are estimated using previously defined attenuation relationships with respect to the closest distance to the fault segment, Magnitude (Mw) of scenario earthquakes, bridge local site conditions and the faulting mechanism. Using the estimated seismic intensity measure value, cumulative probability of exceeding a certain damage limit state is calculated by the developed fragility curve that is specific for the type of the bridge sample. Discrete probability of being in a certain damage state can be simply calculated for each damage state. Namely, each damage state has its own probability that the bridge is being in the corresponding damage state.

The important task is to decide the bridge performance level using the calculated probabilities for each damage state. This is a subjective task depending on the judgment of the decision makers or the bridge owners. According to Hwang et al. (2000), three damage states, which are no/minor, repairable and significant damage were considered for the calculation of expected damage of bridges in Memphis. They considered the following rule for determining the expected damage to each bridge based on the probabilities of damage states. If the probability of no/minor damage or the probability of significant damage of a bridge is greater than 50 percent, then the bridge is expected to sustain no/minor damage or significant damage, respectively. Otherwise, the bridge is expected to sustain repairable damage. Although 4 bridge damage states are considered in this study, similar approach is applied for deciding the expected bridge damage due to scenario earthquakes. If the probability of the any damage state is greater than 50 percent, then the bridge is expected to sustain the corresponding damage. Otherwise, three damage states having the highest probabilities of being in that damage state are taken into consideration. Then the expected damage state that the bridge sustains is

determined by considering the average of the three damage states. To illustrate this condition, a bridge sample whose discrete probabilities being in each damage state are 5, 30, 40 and 25 percent for the damage states of slight/no, moderate, significant and collapse, respectively is considered. Since none of the damage state probability is greater than 50 percent, damage states of moderate, significant and collapse having the highest probabilities are taken into consideration. The average of the three damage states is considered as significant damage, which is in-between the moderate and collapse damage states. Therefore, the damage state of the sample bridge is decided to be significant damage.
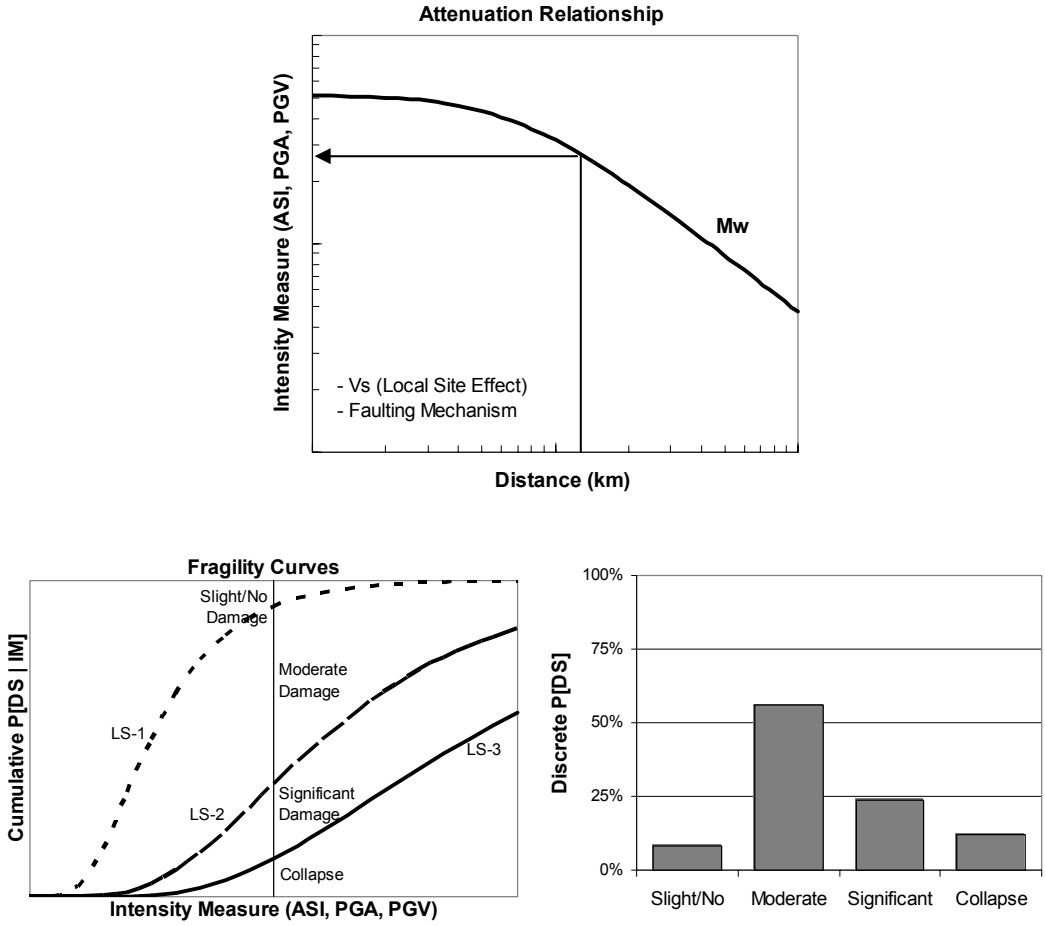
Figure 7.5 Schematic representation of damage state determination of bridges

7.1.1 Scenario-1: Marmara Earthquake_Mw7.4

The faults that extend in the east-west direction along the Marmara Sea are believed to be one of the main sources affecting the seismic hazard of the selected bridge sites. These fault segments constitute the extensions of the North Anatolian Fault Zone at the Marmara Sea region. They are composed of 7 fault line segments having a total length of 179 km. The coordinates and some of the important parameters of the Marmara Sea fault segments were given in literature (Yücemen et al., 2005 and Yücemen et al., 2006). Although various earthquake magnitudes corresponding to the largest earthquakes that are likely to occur were assigned for each fault segment, it is assumed that the scenario earthquake used in the deterministic analysis is believed to trigger these fault segments causing an earthquake of M_w=7.4. The location of the Marmara fault segments and the sample bridges are shown in Figure 7.2.

After calculation of the closest distances (the last three columns of Table 7.1) from the bridge sites to the Marmara fault segments, seismic hazard intensity parameters are calculated using the selected attenuation relationships given in Table 7.2. Then the calculated intensity measure (IM) value is used as the abscissa of the fragility curve corresponding to the bridge type considered. For each damage state cumulative probability of exceedance as well as the discrete probabilities of the bridge being in each damage state are determined. Finally, under the effect of scenario earthquake, damage state of the bridge is decided according to the above explained procedure.

The damage state calculations for the sample bridges are made according to different attenuation relationships and seismic intensity measures. Therefore, calculations are repeated five times with respect to the attenuation relationships and intensity measures of; Boore et al. (1997) for ASI, Boore et al. (1997) for PGA, Kalkan and Gülkan (2004) for ASI, Kalkan and Gülkan (2004) for PGA and Akkar and Bommer (2007) for PGV. The bridge damage distributions determined for different attenuation relationships and intensity measures are presented in Figure 7.6.
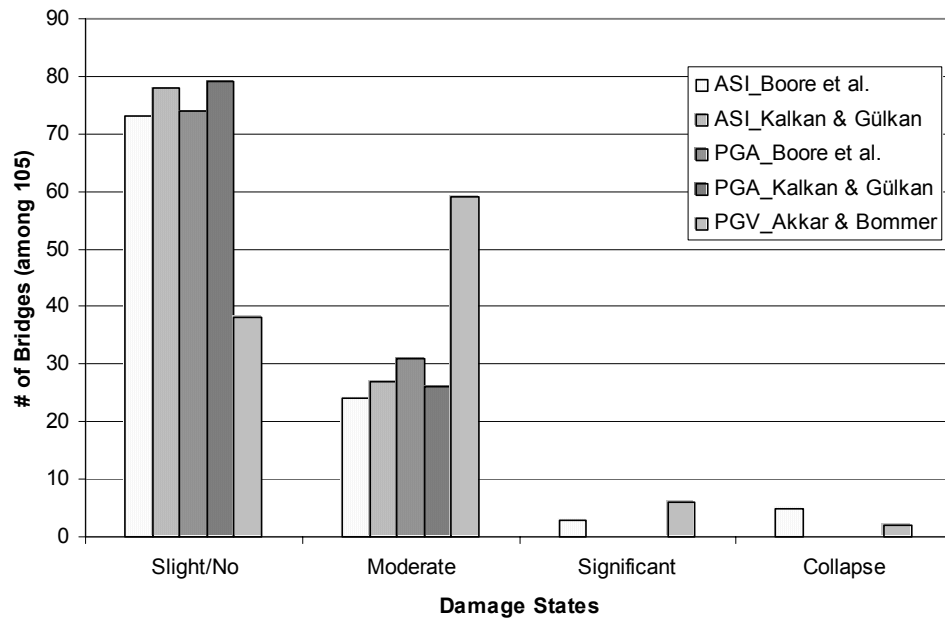
Figure 7.6 Bridge damage distribution for Marmara Scenario EQ (Mw7.4)

As can be seen in Figure 7.6, under the effect of Marmara Scenario EQ (Mw7.4), most of the bridges are in the slight/no damage state and to a lesser degree in the moderate damage limit state. Very few bridges, which are very close to the fault segments, are in the significant damage or collapse state with respect to the Boore et al. (1997) for ASI and Akkar and Bommer (2007) for PGV. The damage state distributions of 105 sample bridges due to the Marmara scenario earthquake are presented through Figure 7.7 to Figure 7.11.
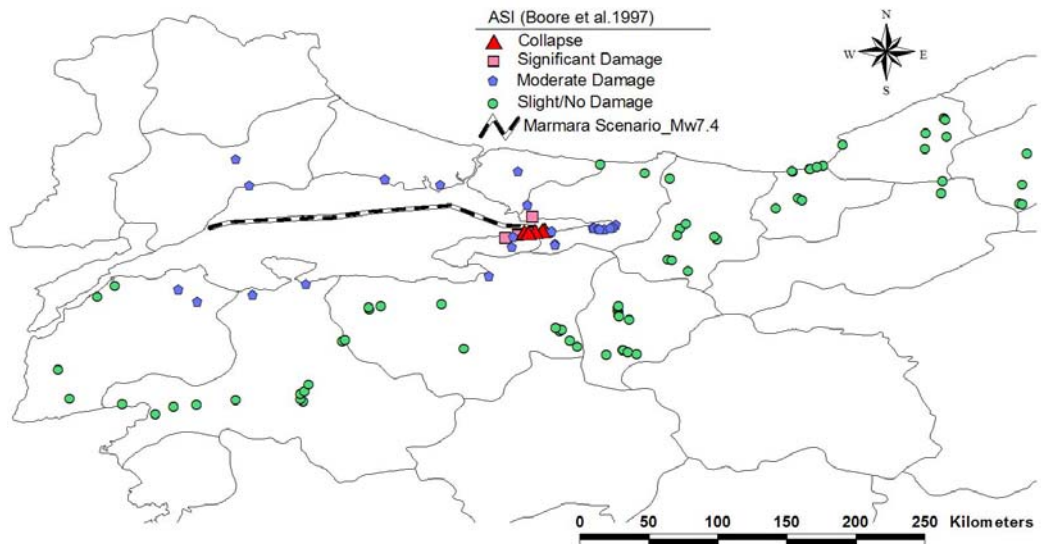
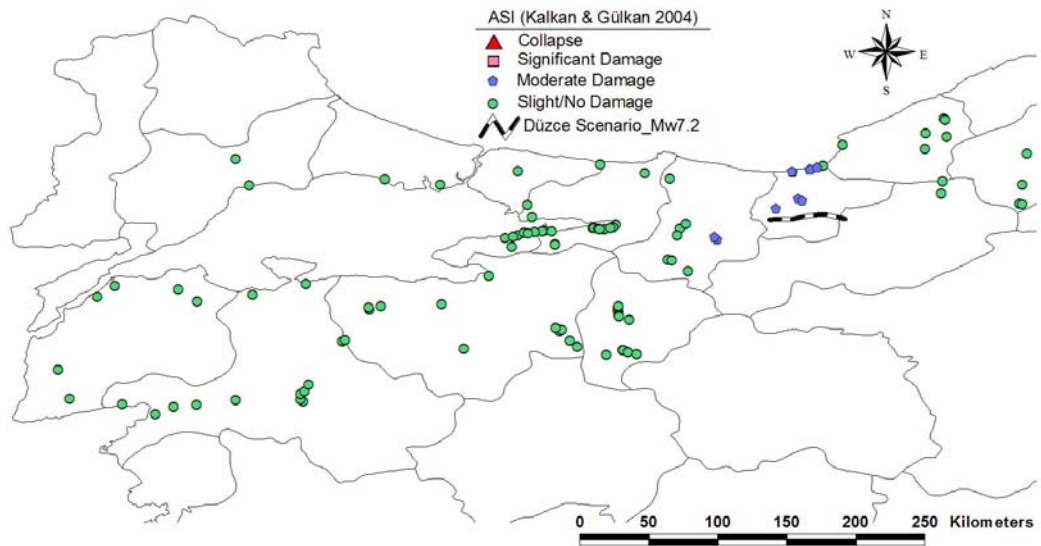Figure 7.7 Marmara scenario EQ damage distribution (ASI_Boore et al., 1997)
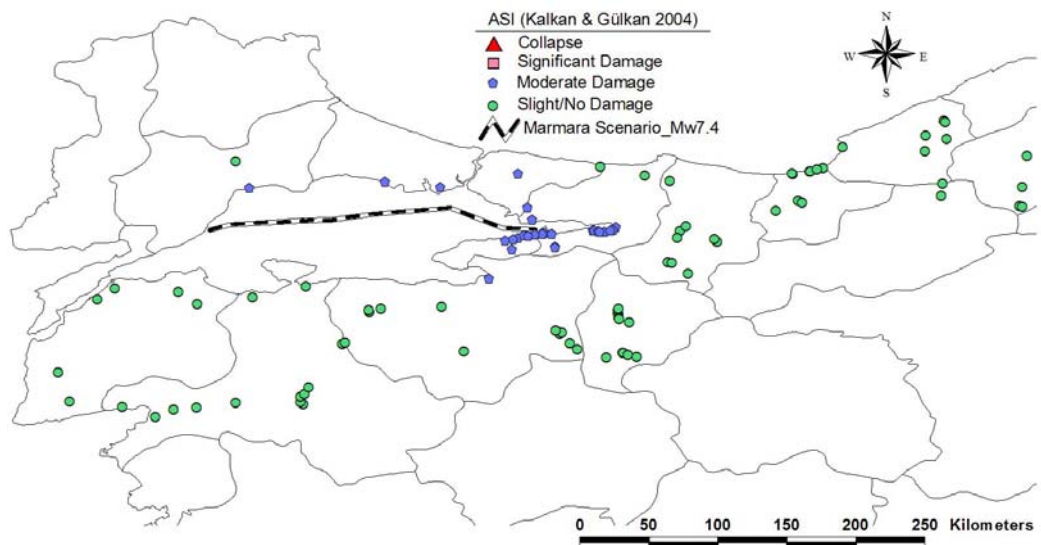
Figure 7.8 Marmara scenario EQ damage distribution (ASI_Kalkan and Gülkan, 2004)
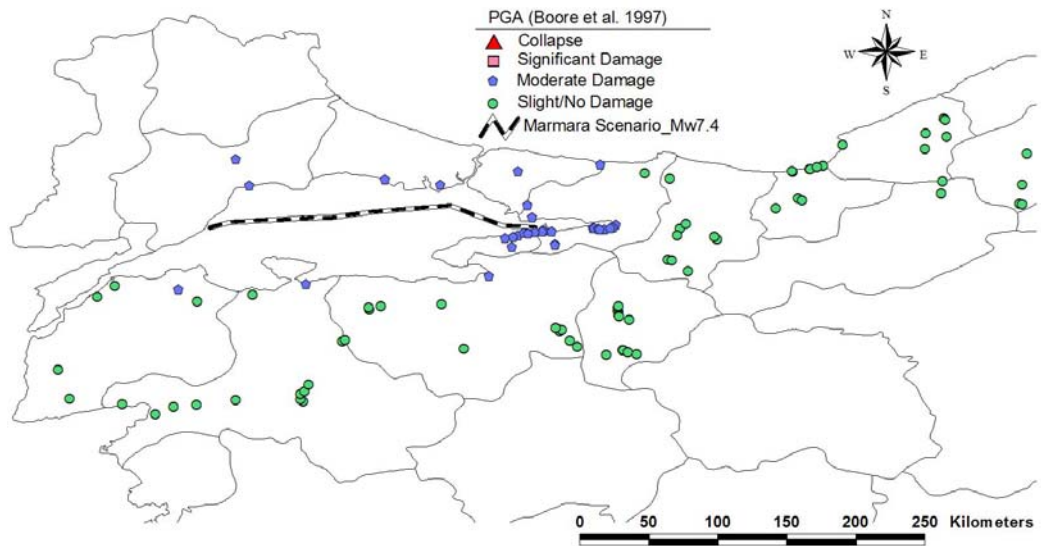
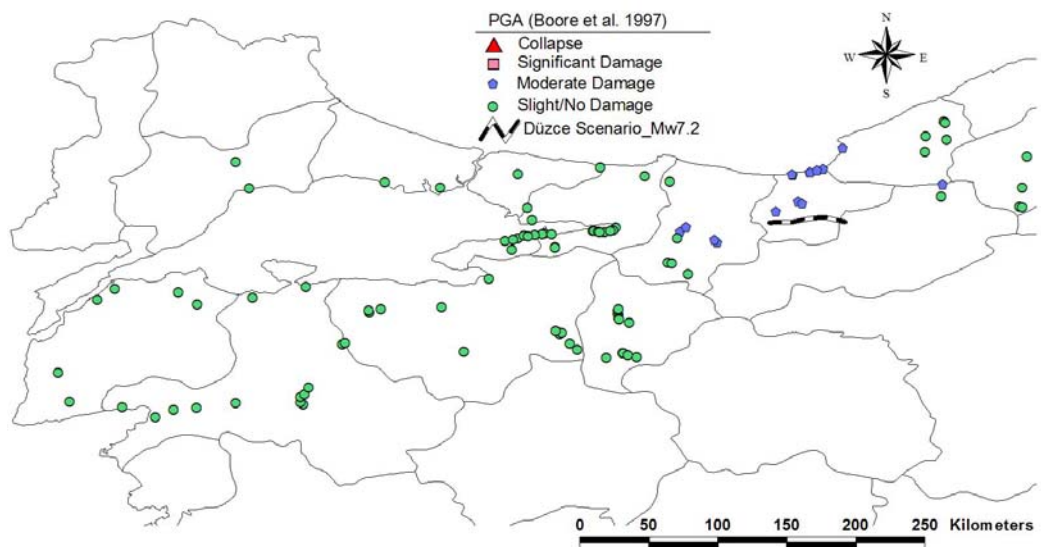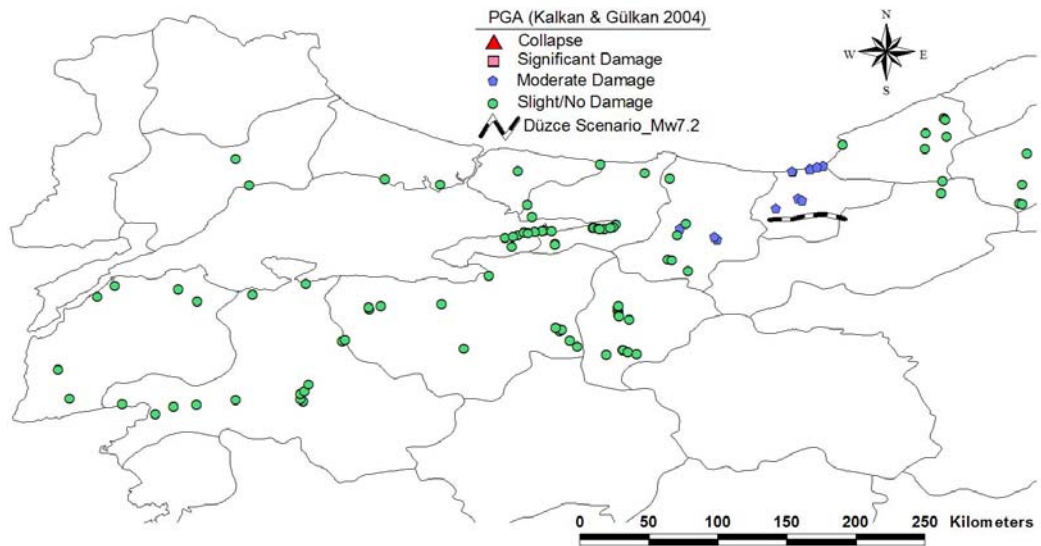Figure 7.9 Marmara scenario EQ damage distribution (PGA_Boore et al., 1997)
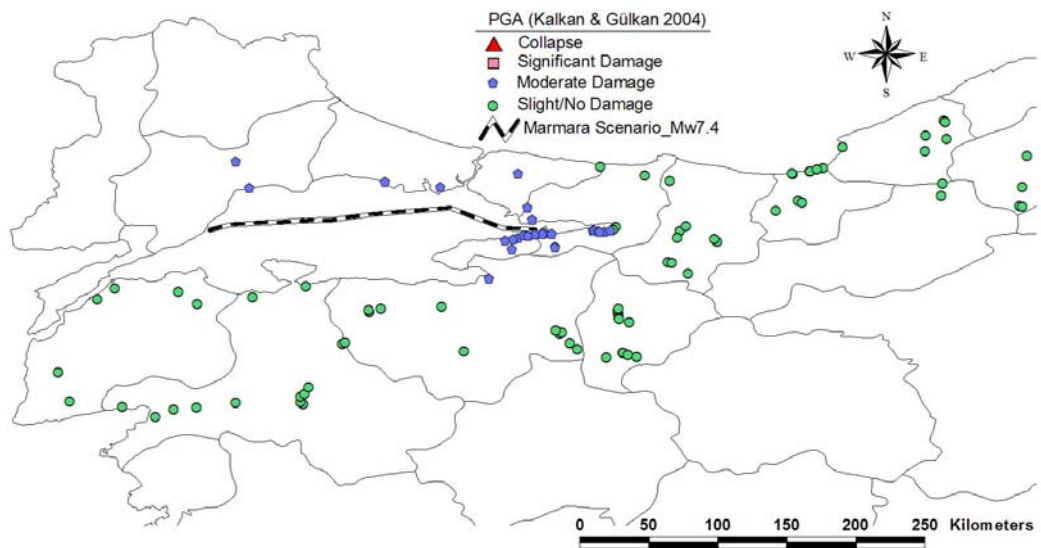
Figure 7.10 Marmara scenario EQ damage distribution (PGA_Kalkan and Gülkan, 2004)
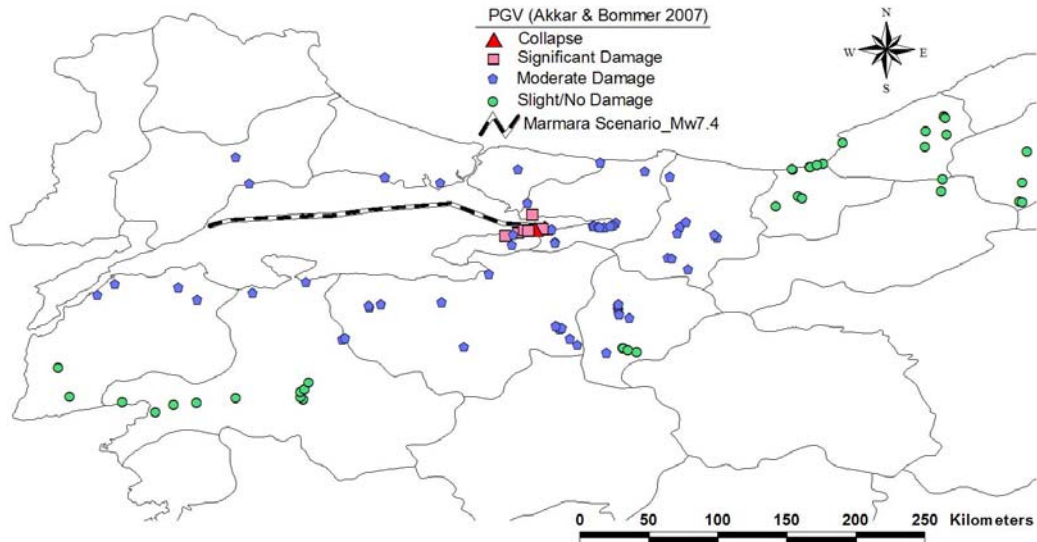
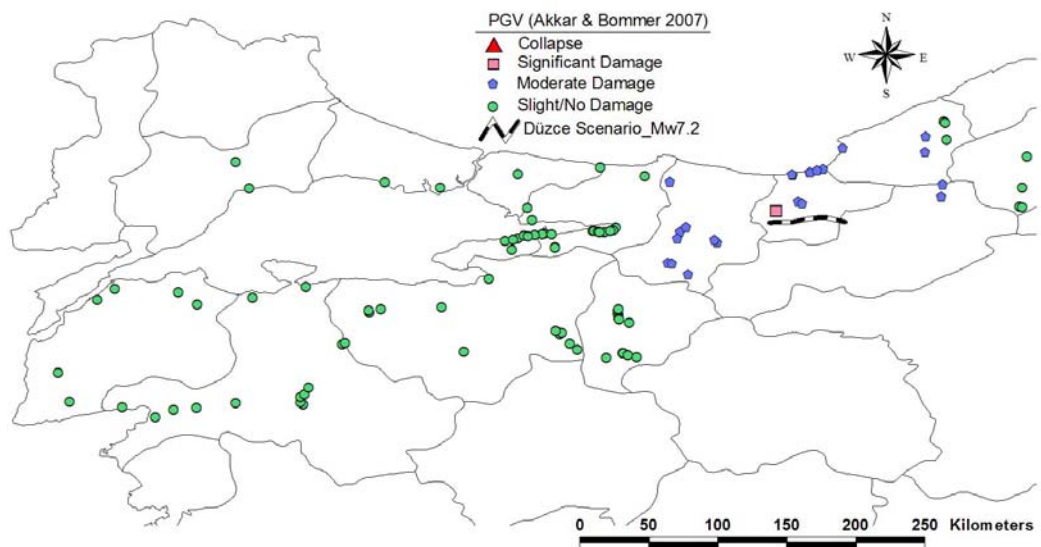Figure 7.11 Marmara scenario EQ damage distribution (PGV_Akkar and Bommer, 2007)

7.1.2 Scenario-2: Düzce Earthquake_Mw7.2

In the second case study, fault system causing the 12 November 1999 Düzce Earhquake (Mw7.2) is considered to be another important seismic source affecting the seismic hazard of the selected bridge sites. According to the report by Emre et al. (1999), 43km length of the Düzce fault segment was ruptured during the Mw7.2 Düzce Earthquake. As can be seen in Figure 7.12, surface ruptures were observed starting east of Gölyaka, passing from the south of Lake Efteni, then crossing Kaynaşlı and finally disappearing around the Bolu Tunnel. The location of the ruptured segment of the Düzce fault and the sample bridges are shown in Figure 7.2.

The number of sample bridges closer to the fault segments of Düzce scenario earthquake is less than the ones for other scenario earthquakes. Therefore, the effect of Düzce scenario earthquake on the sample bridges can be regarded as less influential in comparison with the other scenario earthquakes. However, it should be emphasized that the bridge damage levels depend not only on the seismic hazard level, but also the proximity of the bridge sites to the seismic sources. After

deterministic seismic hazard assessment of the bridge sites are made for the Düzce earthquake, damage states of the sample bridges are calculated using the relevant fragility curves.
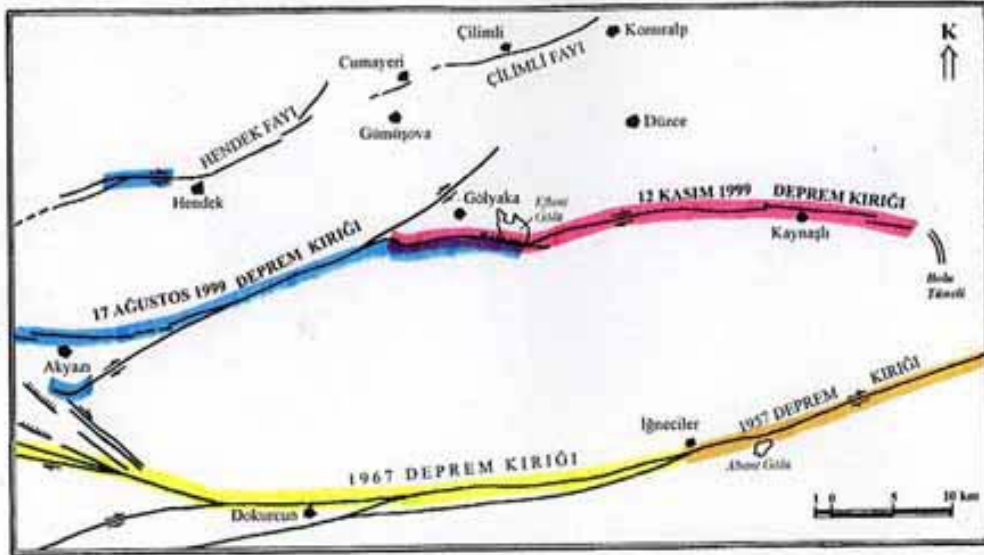
Figure 7.12 November 1999 Düzce earthquake fault rupture (red line)

The bridge damage distributions determined for different attenuation relationships and intensity measures are presented in Figure 7.13. Under the effect of Düzce Scenario EQ (Mw7.2), vast majority of the bridges are in the slight/no damage state and the rest of the bridges are in the moderate damage limit state. Only one bridge is in the significant damage with respect to the Akkar and Bommer (2007) for PGV. The damage state distributions of 105 sample bridges due to the Düzce scenario earthquake are presented through Figure 7.14 to Figure 7.18. It is clear that the bridges closer to the fault segments are likely to be in the higher damage limit states. Since the Düzce fault segment is relatively far away from the sample bridges and its fault length is shorter in comparison with the fault segments belonging to the other scenario earthquakes, seismic effect of the Düzce scenario earthquake on the sample bridges is generally negligible.
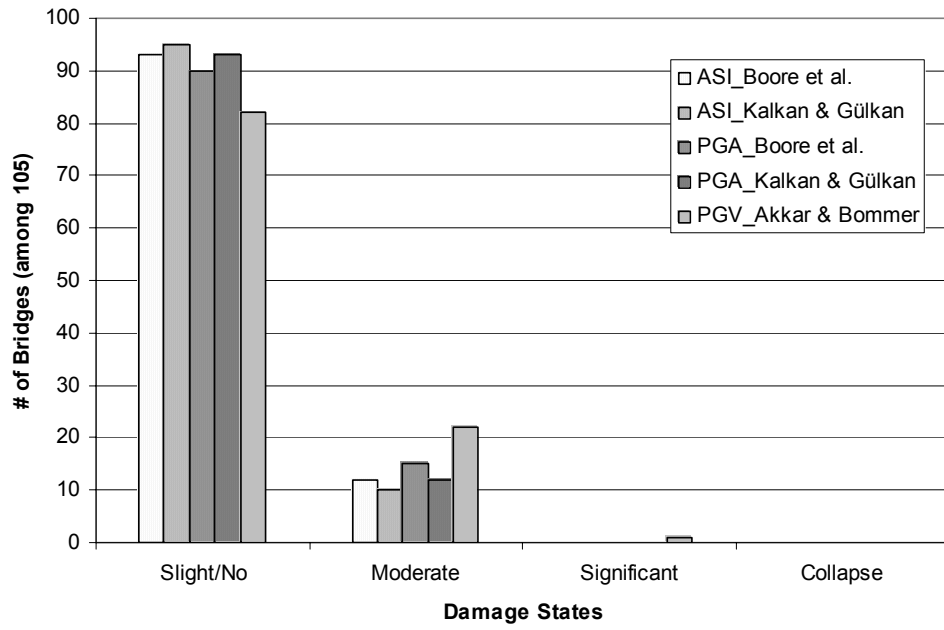
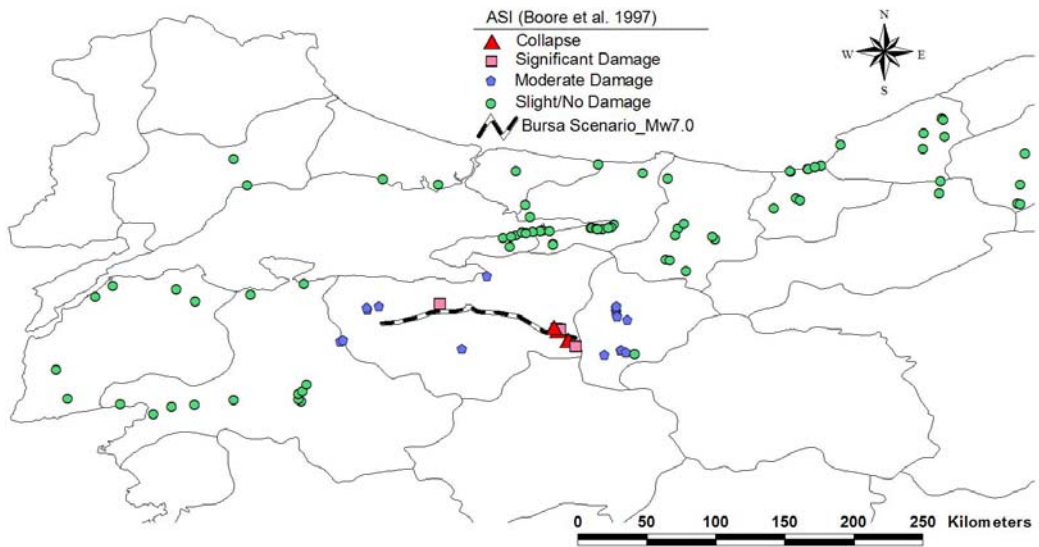Figure 7.13 Bridge damage distribution for Düzce Scenario EQ (Mw7.2)
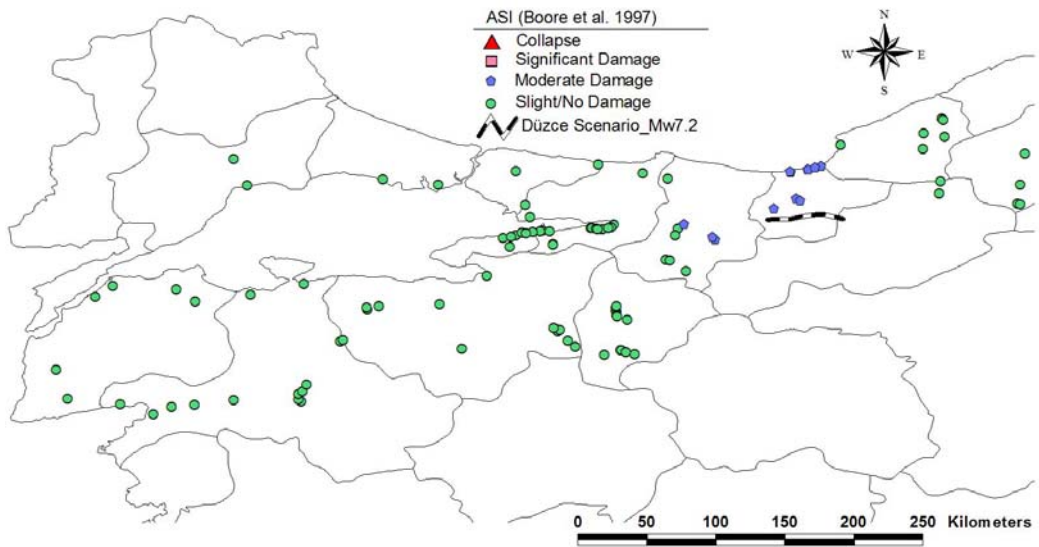
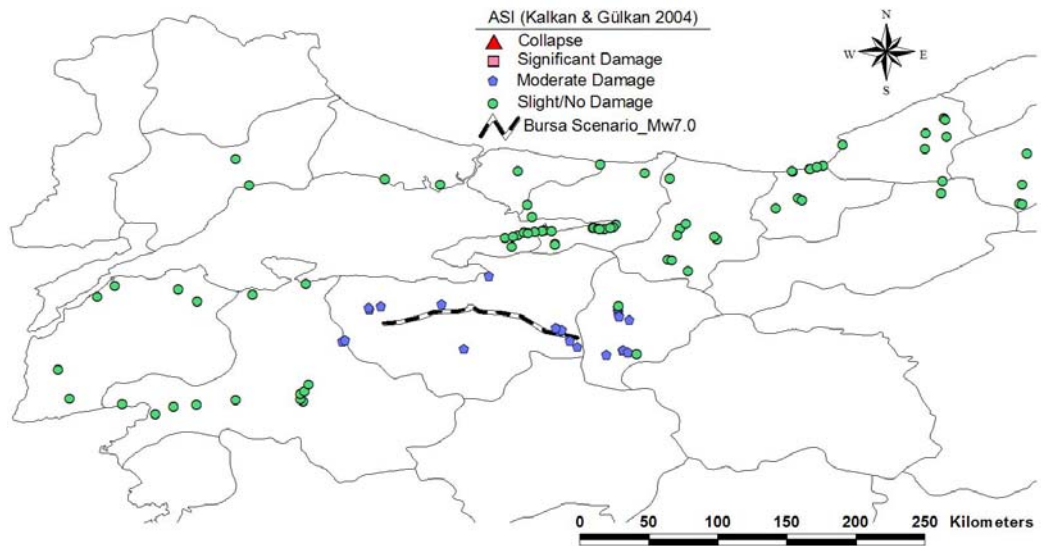Figure 7.14 Düzce scenario EQ damage distribution (ASI_Boore et al., 1997)

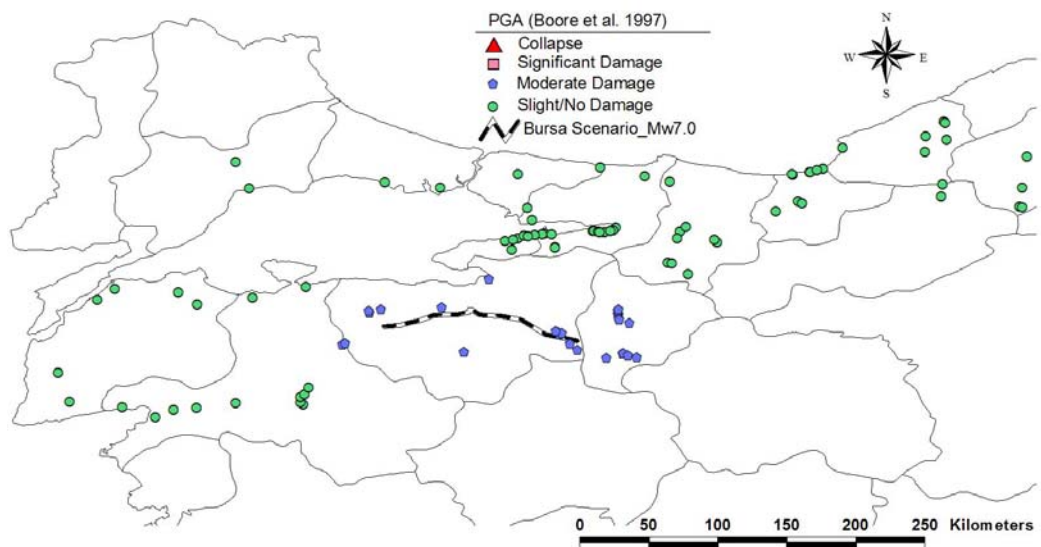Figure 7.15 Düzce scenario EQ damage distribution (ASI_Kalkan and Gülkan, 2004)

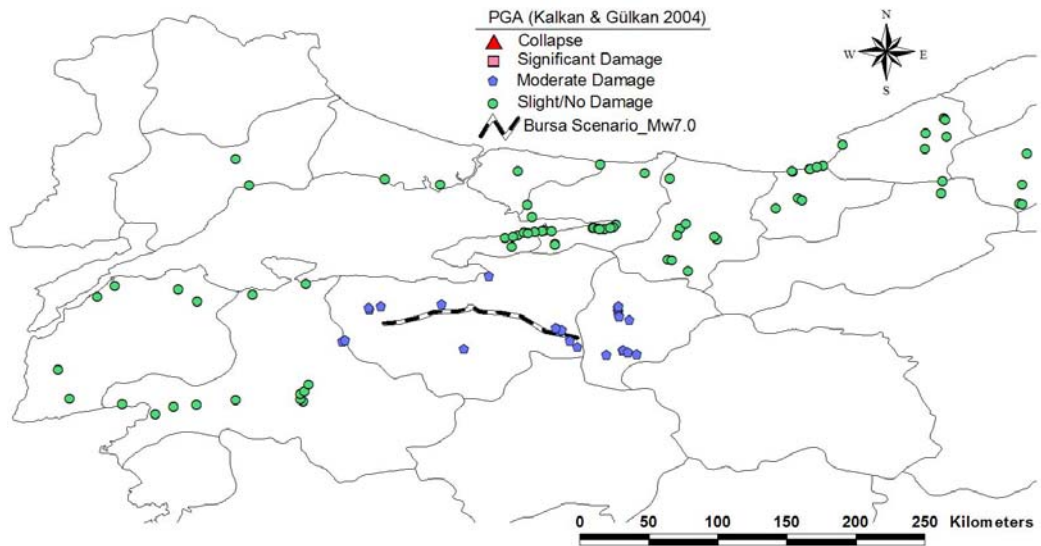Figure 7.16 Düzce scenario EQ damage distribution (PGA_Boore et al., 1997)

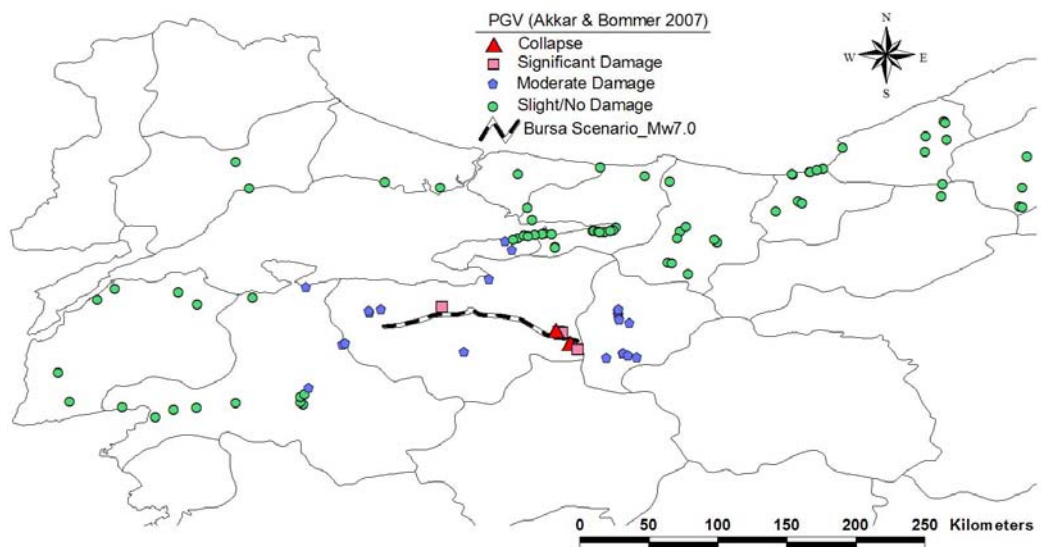Figure 7.17 Düzce scenario EQ damage distribution (PGA_Kalkan and Gülkan, 2004)

Figure 7.18 Düzce scenario EQ damage distribution (PGV_Akkar and Bommer, 2007)

7.1.3   Scenario -3: Bursa Earthquake_Mw7.0

The fault segments located at the Bursa city and near vicinity are considered to be the seismic sources that are likely to affect the seismic hazard of the sample bridge sites. At the Bursa region, there are more than 40 fault segments having different seismic activities. The coordinates and some of the important parameters of the fault segments at the Bursa region were given in literature (Yücemen et al., 2006). Although various peak earthquake sizes and the return intervals that are likely to occur were assigned for each fault segment, when a relatively big earthquake occurs, it is believed that this earthquake triggers only some of these fault segments. Therefore, for use in the deterministic analysis, it is assumed that a Bursa scenario earthquake that triggers only three fault segments of Bursa, Çalı and Ayaz Faults causes a moment magnitude of Mw7.0 earthquake. The total length of the three fault segments are 107 km. The location of the Bursa scenario earthquake fault segments and the sample bridges are shown in Figure 7.2.

The bridge damage distributions determined for different attenuation relationships and intensity measures are presented in Figure 7.19. As can be seen in Figure 7.19, under the effect of Bursa Scenario EQ (Mw7.0), most of the bridges are in the slight/no damage state and to a lesser degree in the moderate damage limit state. Very few bridges are in the significant damage or collapse state with respect to the Boore et al. (1997) for ASI and Akkar and Bommer (2007) for PGV. The damage state distributions of 105 sample bridges due to the Düzce scenario earthquake are presented through Figure 7.20 to Figure 7.24.
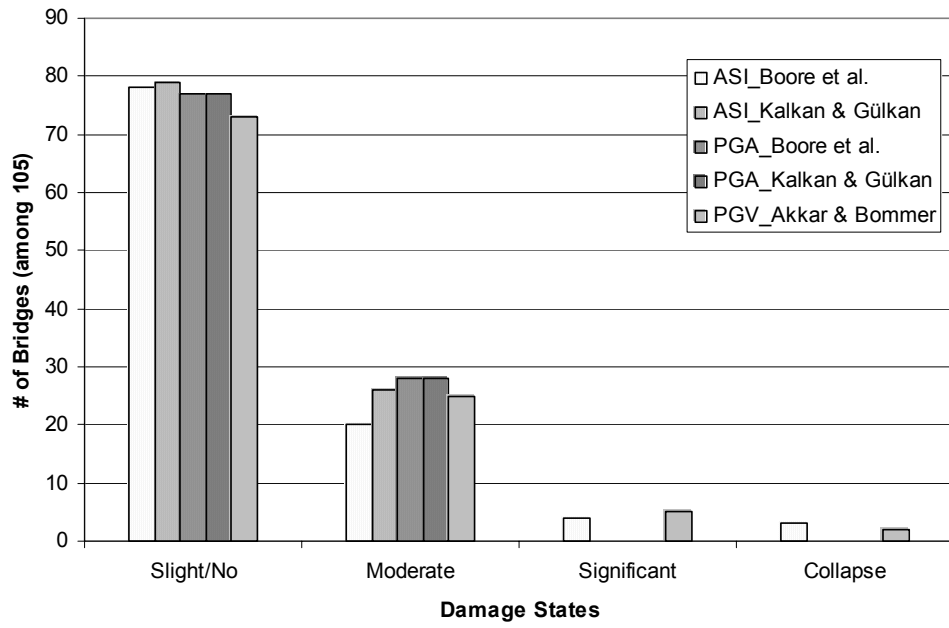
Figure 7.19 Bridge damage distribution for Bursa Scenario EQ (Mw7.0)

Figure 7.20 Bursa scenario EQ damage distribution (ASI_Boore et al., 1997)

Figure 7.21 Bursa scenario EQ damage distribution (ASI_Kalkan and Gülkan, 2004)

Figure 7.22 Bursa scenario EQ damage distribution (PGA_Boore et al., 1997)

Figure 7.23 Bursa scenario EQ damage distribution (PGA_Kalkan and Gülkan, 2004)

Figure 7.24 Bursa scenario EQ damage distribution (PGV_Akkar and Bommer, 2007)

When all the three case studies are examined, it can be said that the sample highway bridges considered in this study generally experience very low level damage under the effect of severe earthquakes. However, highway bridges that are very close to the earthquake seismic source can experience significant damage or even collapse can take place.

As mentioned in Chapter 6, fragility curves developed with respect to the intensity measure of ASI is the most reliable, whereas, PGA is the least reliable one in comparison through the intensity measures of ASI, PGV and PGA. Since the fragility curves are the main tools in determining the seismic vulnerability of the highway bridges, damage state calculations of the bridges using the fragility curves for ASI are more reliable than the results of other intensity measures. Other than the fragility curves, attenuation relationships have a considerable effect on the results of the seismic vulnerability assessment. Therefore, it should be kept in mind that seismic damage assessment of the highway bridges is highly dependent on the accuracy of the selected attenuation relationships.

CHAPTER 8

CONCLUSIONS AND RECOMMENDATIONS

8.1   SUMMARY

In this dissertation, analytical fragility curves are developed for the ordinary highway bridges in Turkey constructed after the 1990s to be used in the assessment of their seismic vulnerability. A representative data set of 52 bridge samples is selected to investigate the general characteristics of these bridges. The general attributes of the bridges and their distribution are investigated to identify the key components of bridges. Bridge classification is made by considering the primary structural attributes, which are defined as the span number, skewness, and the bent column number. Since seismic vulnerability of single span bridges are negligible in comparison with multi span bridges, single span bridges are not investigated in this study. A total of four major bridge classes are formed and fragility curves are determined for each bridge class separately. Skew angle less than or greater than 30° and single-column or multiple-column bent for multi span bridges are considered in the formation of major bridge classes. Variations in several secondary structural attributes such as span length, column height, superstructure and substructure types and variation in the skewness and the span number are employed in the formation of bridge samples for each bridge class. Latin Hypercube Sampling method is used in the formation of bridge samples to account for the uncertainty in the structural input parameters.

Detailed 3-D analytical model of each bridge sample is generated for conducting nonlinear response history analyses. A data set of recorded earthquake ground motions is formed to be used in the analyses covering a wide range of seismic hazard level to represent the record-to-record variability in the analytical fragility curves. The employed ground motions are selected in a way that they have similar faulting mechanisms and seismic potential that are in accordance with Turkey. The analyses are repeated twice for each ground motion to obtain the maximum seismic response of the bridges. The two orthogonal horizontal components of the ground motion are applied on both bridge orthogonal directions.

Damage limit states are defined for different bridge components in terms of several engineering demand parameters such as column and cap beam curvature and shear, and superstructure longitudinal displacement. The engineering demand parameters are also considered in calculating the maximum seismic response of the corresponding bridge components that are obtained from the results of the nonlinear response history analyses. Damage state of the bridge components as well as the bridge system as a whole is decided by comparing the maximum seismic response and the damage limit state. Probability of attaining or exceeding a particular damage limit state is determined by considering the damage state of each bridge sample under each ground motion record, which is represented by the intensity measures of ASI, PGV, and PGA. The probability of exceeding a certain damage limit state is modeled by a cumulative lognormal probability distribution function to obtain the fragility curves for each major bridge class. The coefficients of determination are computed for each curve fit of the fragility curves in terms of the investigated intensity measures. The developed fragility curves are compared with the relevant empirical or analytical fragility curves given in the previous studies.

Final part of the study is devoted to the application of a case study for the seismic vulnerability assessment of several existing highway bridges in the Marmara Region in Turkey. The bridges are grouped with respect to major bridge classes, whose fragility curves are employed in the calculations. Seismic hazard assessment of the bridge sites is performed using deterministic approach for three different earthquake scenarios. Various ground motion seismic intensity measures

due to these scenario earthquakes are calculated considering three different available attenuation relationships. After calculating the seismic intensity levels that the bridge is expected to experience during the scenario earthquake, probability of exceeding each damage limit state is obtained by using the relevant fragility curves. Finally, damage distribution of the investigated bridges is calculated for each scenario earthquake.

8.2 CONCLUSIONS

The following conclusions are reached according to the results obtained in this study.

- The most significant contribution of this study is the development of fragility curves for certain bridge classes common in the highway transportation system in Turkey. These fragility curves are very valuable tools to be used in the seismic vulnerability assessment of bridges as well as in the loss estimation studies for pre-earthquake preparedness plans and post earthquake emergency response plans. They can be used to determine the seismic risk associated with existing ordinary highway bridges in Turkey.

- Fragility curves of the highway bridges are developed for three damage limit states. Fragility curve for the Serviceability damage limit state (LS-1) is mostly governed by the superstructure relative displacement. Whereas, curvature demands of the column and cap beam dominate the fragility curves for the Damage Control and Collapse Prevention damage limit states. Developed fragility curves are original for the Turkish highway bridges in terms of the applied methodology as well as the acceptance criteria employed in the calculation procedure.

- Classification and sampling of bridges, 3-D analytical modeling of bridge components and structural idealization, selection of analysis method, selection of earthquake ground motions, definition of bridge damage limit states, and generation of fragility functions are some of the important stages in the development of analytical fragility curves. Different levels of uncertainties are involved in the application of these stages, which may affect the reliability of the fragility curves considerably. Earthquake ground motion selection and definition of bridge damage limit states are found to be the more influential stages among the others on the reliability of fragility curves.

- Deciding the most critical ground motion excitation direction is crucial to obtain the maximum seismic response of the bridge components. In general, for ordinary highway bridges in Turkey, it is found that maximum seismic response occurs when the horizontal components of the ground motion are applied in the orthogonal bridge directions. Therefore, each earthquake ground motion should be analyzed twice for two different cases. In the first case, two horizontal components of the ground motion are applied in the two bridge orthogonal directions. In the second case, application direction of the horizontal components has been interchanged with respect to the first case. Finally, maximum seismic response is obtained by taking the maximum of the results of the two cases for each ground motion.

- Shear keys of the investigated existing bridges have been designed so strong that they transfer considerable amount of seismic forces to the substructure due to the pounding of superstructure. They are expected to perform like a fuse to prevent the excessive seismic force transfer to the substructure components. However, due to the high capacity of the shear keys, higher seismic forces are transferred to the substructure columns and cap beams, which may experience seismic damage exceeding the damage control or even collapse prevention damage limit states.

- In addition to PGA and PGV, acceleration spectrum intensity (ASI), which is defined as the area under the 5% damped elastic response spectrum within the boundary periods of T_i and T_f, is also used as the seismic intensity measure in the development of analytical fragility curves. It was found that T_i=0.4s and T_f=1.1s resulted in good correlation thus are proposed as the boundary periods of ASI for ordinary bridges employed in this study.

- Among the investigated ground motion intensity measures (ASI, PGV, PGA, and PGA/PGV) ASI and PGV appear to be the ones that have better correlation with the seismic damage of the bridge components. Therefore, the generated fragility curves based on ASI or PGV are found to be more realistic in the estimation of damage state of the bridges. PGA/PGV is not considered in the development of fragility curves due to its poor correlation with the seismic damage. The coefficient of determination value of each fragility curve is determined for different intensity measures to investigate the correlation between the probability of exceeding values and the proposed fragility functions in terms of cumulative lognormal probability distribution. It is found that the ASI has the strongest correlation with the analytical fragility curves. Therefore, reliability of the developed fragility curves with ASI is higher in comparison with other intensity measures.

- When the fragility curves of the major bridge classes are investigated, it is found that the skew and single-column bent bridges experience higher level seismic damage compared to the non-skew and multiple-column bent bridges. This result is in accordance with the past earthquake experiences.

- The difference between the fragility curves of all the bridge classes for the serviceability damage limit state (LS-1) is negligible regardless of the intensity measure considered. Effect of bridge skew angle or bent column

196

number on the fragility curve for serviceability limit state is found to be insignificant. Therefore, a single fragility curve can be utilized for all bridge classes for the serviceability damage limit state.

- Proposed fragility curves for the serviceability damage limit state result in higher probability of exceedance values for the same seismic intensity level in comparison with the previously developed fragility curves because of the deficiency in the connection of superstructure and substructure components. Connection between the elastomeric bearings and the superstructure and substructure is provided with the friction force between the bearings and concrete surfaces only. When the horizontal component of the seismic force is greater than the friction force, which is the case even at lower ground motion intensities, "walk-out" phenomenon takes place and superstructure starts to move. This can cause permanent displacement of the superstructure affecting the functionality of the bridge.

- Proposed analytical fragility curves are compared with the previously developed fragility curves in spite of the several differences in the development of fragility curves. However, proposed fragility curves for the damage control and collapse prevention damage limit states were found to be in good agreement with the ones generated in some of the previous studies.

8.3 RECOMMENDATIONS FOR FUTURE STUDIES

In the light of the studies conducted in this dissertation, the following recommendations can be made towards future research on the subject.

- Soil structure interaction should be taken into account using reliable analytical models in order to investigate the effect of bridge local site on the

seismic response of bridges. To be consistent, ground motion data should be formed accordingly representing the characteristics of bridge local site.

- Nation wide highway bridge inventory needs to be generated in order to increase the reliability of the bridge classification. This database of the bridge inventory should contain at least the basic information about each bridge such as location and its coordinates, structural type of the bridge and the material type of each component, geometric properties, local site conditions, the construction year, etc.

- Reliability of the developed analytical fragility curves should be investigated as the new earthquakes occur and new bridge damage data is available for calibration purposes.

- Other types of bridges such as bridges with inverted T cap beams or pier wall column bent type should be investigated for the development of fragility curves.

- Other types of bridge irregularities should be considered such as curved bridges, uneven distribution of bridge column heights or differences in the column cross sections cause stiffness and strength variations for multi-span bridges.

- Superstructure uplift due to overturning effects or vertical component of ground motion should be taken into consideration with appropriate analytical models. Due to unseating phenomenon, dislodgement can take place even unseating can occur when the vertical and horizontal components of the ground motion are combined in an unfavorable way especially for the near-field excitations.

REFERENCES

AASHTO, 1996, "AASHTO Guide Specifications for LRFD Seismic Bridge Design", American Association of State Highway and Transportation Officials 16th Ed. with 2001 Interims, Washington D.C.

AASHTO LRFD, 2007, "Standard Specifications for Highway Bridges", Subcommittee for Seismic Effects on Bridges, prepared by Roy A. Imbsen, Imbsen Consulting.

Akkar S., Sucuoğlu H. and Yakut A., 2005, "Displacement–Based Fragility Functions for Low and Mid–Rise Ordinary Concrete Buildings", Earthquake Spectra, Volume 21, No. 4, pp. 901–927.

Akkar S. and Bommer J.J., 2007, "Empirical Prediction Equations for Peak Ground Velocity from Strong-Motion Records from Europe and Middle East", Bulletin of Seismological Society of America, Volume 97, No. 2, pp. 511-530.

Applied Technology Council (ATC), 1985, "Earthquake Damage Evaluation Data for California", Report No. ATC-13, Redwood City, California.

Applied Technology Council (ATC), 1996, "Improved Seismic Design Criteria for California Bridges: Provisional Recommendations", Report No. ATC-32, Redwood City, California.

ArcView GIS 3.2, 1999, Environmental Systems Research Institute, Inc., Redlands, Calif.

AREMA, 1998, "Manual for Railway Engineering", American Railway Engineering and Maintenance of Way Association, Washington, D.C.

Aviram A., Mackie K.R. and Stojadinovic B., 2008, "Guidelines for Nonlinear Analysis of Bridge Structures in California", PEER Report 2008/03, Pacific Earthquake Engineering Research Center, University of California, Berkeley, California.

Avsar O., Caner A. and Yakut A., 2008, "Effect of Cap Beam to Column Inertia Ratio on Transverse Seismic Response of Multi Column Bridge Bents", 14th World Conference on Earthquake Engineering, Paper No. 06-0024, Beijing, China.

Ayyub B.M., and Lai, K–L., 1989, "Structural Reliability Assessment Using Latin Hypercube Sampling", Proceedings of ICOSSAR'89, the 5th International Conference on Structural Safety and Reliability, Part II. pp. 1177–1184, ASCE: San Francisco, CA.

Baker J. and Cornell C.A., 2006, "Which Spectral Acceleration Are You Using?", Earthquake Spectra, Volume 22, No. 2, pp. 293–312.

Banerjee S. and Shinozuka M., 2007, "Nonlinear Static Procedure for Seismic Vulnerability Assessment of Bridges", Computer-Aided Civil and Infrastructure, Vol. 22, pp. 293-305.

Basoz N., and Kiremidjian A.S., 1997, "Evaluation of Bridge Damage Data from The Loma Prieta and Northridge, CA Earthquakes", Technical Report No. 127, John A. Blume Earthquake Engineering Center, Stanford, CA (also Technical Report MCEER-98-004).

Basoz N.I. and Kiremidjian A.S., 1996, "Risk Assessment for Highway Transportation Systems", Technical Report, J. A. Blume Earthquake Center, Report No. 118.

Basoz N. and Mander J., 1999, "Enhancement of the Highway Transportation Lifeline Module in HAZUS", National Institute of Building Sciences.

Bommer J.J. and Acevedo A.B., 2004, "The Use of Real Earthquake Accelerograms as Input to Dynamic Analysis", Journal of Earthquake Engineering, Volume 8, Special Issue 1, pp. 43-92.

Boore D.M., Joyner W.B. and Fumal T.E., 1997, "Equations For Estimating Horizontal Response Spectra and Peak Acceleration From Western North American Earthquakes: A Summary of Recent Work", Seismological Research Letters, Volume 68, No. 1, pp. 128-153.

Broekhuizen D.S., 1996, "Effects of Vertical Acceleration on Prestressed Concrete Bridges", Master's Thesis, University of Texas at Austin, Texas, US.

Buckle I.G., 1994, "The Northridge, California Earthquake of January 17, 1994: Performance of Highway Bridges", Technical Report NCEER-94-0008.

Building Seismic Safety Council, 2000, "NEHRP Recommended Provisions for Seismic Regulations for New Buildings & Other Structures", FEMA 368, Washington, DC.

Button M.R., Cronin C.J. and Mayes R.L., 2002, "Effect of Vertical Motions on Seismic Response of Highway Bridges", ASCE Journal of Structural Engineering, Volume 128, No.12, pp. 1551-1564.

Caltrans, 2006, "Seismic Design Criteria Version 1.4.", California Department of Transportation, Sacramento, CA.

Caner A., Yanmaz A.M., Yakut A., Avsar O. and Yilmaz T., 2008, "Service Life Assessment of Existing Highway Bridges with No Planned Regular Inspections", ASCE Journal of Performance of Constructed Facilities, Volume 22, No. 2, pp. 108-114.

Cheng F.Y., Lou K.Y. and Sheng L.H., 1998, "Collapse Studies of Freeway Bridges During the Northridge Earthquake", 6th US National Conference on Earthquake Engineering, Seattle, WA. EERI.

Choi E., 2002, "Seismic Analysis and Retrofit of Mid-America Bridges", PhD Thesis, Georgia Institute of Technology.

Choi E., DesRoches R. and Nielson B., 2004, "Seismic Fragility of Typical Bridges in Moderate Seismic Zones", Engineering Structures, Volume 26, No. 2, pp. 187-199.

Computers and Structures, Inc., 2005. SAP 2000 Nonlinear, Version 10.0.1, Structural Analysis Program, Berkeley, CA.

DesRoches R., Choi E., Leon R.T., Dyke S.J. and Aschheim M., 2004, "Seismic Response of Multiple Span Steel Bridges in Central and Southeastern United States I: As Built", ASCE Journal of Bridge Engineering, Volume 9, pp. 464-473.

Dhakal R.P., Mander J.B. and Mashiko N., 2006, "Identification of Critical Ground Motions for Seismic Performance Assessment of Structures", Earthquake Engineering and Structural Dynamics, Volume 35, pp. 989-1008.

Dutta A. and Mander J.B., 1998, "Seismic Fragility Analysis of Highway Bridges", INCEDE-MCEER Center-to-Center Workshop on Earthquake Engineering Frontiers in Transportation Systems, 311-25, Tokyo, Japan.

Elnashai A.S., Borzi B. and Vlachos S., 2004, "Deformation–Based Vulnerability Functions for RC Bridges", Structural Engineering and Mechanics, Volume 17, No. 2, pp. 215-244.

Emre Ö., Duman T.Y., Doğan A., Ateş Ş., Keçer M., Erkal T., Özalp S., Yıldırım N., Güner N., 1999, "12 Kasım 1999 Düzce Depremi Saha Gözlemleri ve Ön Değerlendirme Raporu", http://www.mta.gov.tr/deprem/dzc.html, 15/12/2008.

Erduran E. and Yakut A., 2004, "Drift Based Damage Functions for Reinforced Concrete Columns", Computers and Structures, Volume 82 pp. 121-130.

European Committee for Standardization, Eurocode 8, 2005, "Design of Structures for Earthquake Resistance Part 3: Assessment and Retrofitting of Buildings", European Standard EN 1998-3:2005, Brussels.

Federal Highway Administration (FHWA), 1988, "Recording and Coding Guide for the Structure Inventory and Appraisal of the Nation's Bridges", Rep. No. FHWA-ED-89-044, Ofc. of Engrg., Bridge Division, Washington, D.C.

Federal Highway Administration (FHWA), 1995, "Seismic Retrofitting Manual for Highway Bridges", Report No. FHWA-RD-94-052, McLean, VA

FEMA, 2003, HAZUS-MH MR1: Technical Manual, Vol. Earthquake Model. Federal Emergency Management Agency, Washington DC.

Fenves G.L. and Ellery M., 1998, "Behavior and Failure Analysis of A Multiple-Frame Highway Bridge in The 1994 Northridge Earthquake", PEER Report 1998/08, Pacific Earthquake Engineering Research Center, University of California, Berkeley, California.

Goel R.K. and Chopra A.K., 1997, "Evaluation of Bridge Abutment Capacity and Stiffness during Earthquakes", Earthquake Spectra, Volume 13, No. 1, pp. 1–23.

Hose Y., Silva P. and Seible F., 2000, "Development of a Performance Evaluation Database for Concrete Bridge Components and Systems under Simulated Seismic Loads", Earthquake Spectra, Volume 16, No. 2, pp. 413–442.

Hwang H., Liu J.B. and Chiu Y.H., 2001, "Seismic Fragility Analysis of Highway Bridges", Report No. MAEC RR-4, Center for Earthquake Research Information.

Hwang H., Jernigan J.B. and Lin Y., 2000, "Evaluation of Seismic Damage to Memphis Bridges and Highway Systems", ASCE Journal of Bridge Engineering, Volume 5, No. 4, pp. 322–330.

Jernigan J.B. and Hwang H., 2002, "Development of Bridge Fragility Curves", 7th US National Conference on Earthquake Engineering, EERI, Boston.

Kalkan E. and Gülkan P., 2004, "Site-Dependent Spectra Derived from Ground Motion Records in Turkey", Earthquake Spectra, Volume 20, No. 4, pp. 1111-1138.

Kandilli Observatory and Earthquake Research Institute (KOERI), 2009, Istanbul, Turkey. Av: http://www.koeri.boun.edu.tr/depremmuh/eqspecials/kocaeli/kocaeli_eq.htm, 25/04/2008.

Karim K.R. and Yamazaki F., 2003, "A Simplified Method of Constructing Fragility Curves for Highway Bridges", Earthquake Engineering and Structural Dynamics, Volume 32, pp. 1603-1626.

Kawashima Research Group, 2009, Department of Civil Engineering, Tokyo Institute of Technology, Tokyo, Japan, Av: http://seismic.cv.titech.ac.jp/en/, 26/11/2008.

KGM, Karayolları Genel Müdürlüğü, 1982, "Yol Köprüleri İçin Teknik Şartname", Yayın No.: 207 T.C. Bayındırlık Bakanlığı, Ankara.

Kent D.C. and Park R., 1971, "Flexural Members with Confined Concrete", Journal the Structural Division, American Society of Civil Engineers, New York, Volume 97, (ST7) pp. 1969-1990.

Khaled A., Tremblay R. and Massicotte B., 2006, "Assessing the Adequacy of the 30% Combination Rule in Estimating the Critical Response of Bridge Piers under Multi-Directional Earthquake Components", 7th International Conference on Short&Meduim Span Bridges, Paper No. SD-014-1, Montreal, Canada.

Kim S.H. and Shinozuka M., 2003, "Effects of Seismically Induced Pounding at Expansion Joints of Concrete Bridges", ASCE Journal of Engineering Mechanics, Volume 129, No. 11, pp. 1225-1234.

Kowalsky M.J., 2000, "Deformation Limit States for Circular Reinforced Concrete Bridge Columns", ASCE Journal of Structural Engineering, Volume 126, No. 8, pp. 869-878.

Kramer S.L., 1996, "Geotechnical Earthquake Engineering", Prentice-Hall, Englewood Cliffs, N.J.

Kunnath S.K., Erduran E., Chai Y.H. and Yashinsky M., 2008, "Effect of Near-Fault Vertical Ground Motions on Seismic Response of Highway Overcrossings", ASCE Journal of Bridge Engineering, Volume 13, No. 3, pp. 282-290.

Kwon O.S. and Elnashai A.S., 2006, "The Effect of Material and Ground Motion Uncertainty on the Seismic Vulnerability Curves of RC Structure", Engineering Structures, Volume 28, pp. 289–303.

LARSA Inc., 2006, LARSA 4D user's manual, New York.

Liao W.I. and Loh C.H., 2004, "Preliminary Study on the Fragility Curves for Highway Bridges in Taiwan", Journal of the Chinese Institute of Engineers, Volume 27, No. 3, pp. 367-375.

Mackie K. and Stojadinovic B., 2004, "Fragility Curves for Reinforced Concrete Highway Overpass Bridges", 13th World Conference on Earthquake Engineering, Paper No. 1553, Vancouver, B.C. Canada.

Mackie K. and Stojadinovic B., 2003, "Seismic Demands for Performance-Based Design of Bridges", PEER 2003/16. Pacific Earthquake Engineering Research Center, University of California, Berkeley, California.

Mander J.B., Priestley M.J.N. and Park R., 1988, "Observed Stress-Strain Behavior of Confined Concrete", Journal of Structural Engineering, Volume 114, No. 8, pp. 1827–1849.

Mander J.B., 1999, "Fragility Curve Development for Assessing the Seismic Vulnerability of Highway Bridges", Technical Report, MCEER Highway Project/FHWA.

Mander J.B. and Basoz N., 1999, "Seismic Fragility Curve Theory for Highway Bridges", 5th US Conference on Lifeline Earthquake Engineering (ASCE), Seattle, WA, USA.

Monti G. and Nistico N., 2002, "Simple Probability-Based Assessment of Bridges under Scenario Earthquakes", ASCE Journal of Bridge Engineering, Volume 7, No. 2, pp. 104-114.

Naeim F. and Lew M., 1995, "On the use of Design Spectrum Compatible Time Histories", Earthquake Spectra, Volume 11, No. 1, pp. 111-127.

Nateghi F. and Shahsavar V.L., 2004, "Development of Fragility and Reliability Curves for Seismic Evaluation of a Major Prestressed Concrete Bridge", 13th World Conference on Earthquake Engineering, Paper No. 1351, Vancouver, B.C. Canada.

Nielson B.G. and DesRoches R., 2006, "Seismic Fragility Methodology for Highway Bridges Using a Component Level Approach", Earthquake Engineering and Structural Dynamics, Volume 36, pp. 823-839.

Nielson B.G., 2005, "Analytical Fragility Curves for Highway Bridges in Moderate Seismic Zones", PhD Thesis, Georgia Institute of Technology. Atlanta, Georgia.

OpenSees, 2005, "Open System for Earthquake Engineering Simulation", Version 1.7.3, Pacific Earthquake Engineering Research Center, http://opensees.berkeley.edu, 15/03/2007.

Ozkaya C. and Caner A., 2007, "Sismik İzolasyonlu ve Ters T Başlık Kirişli Standart Karayolu Köprülerinin Deprem Davranışının Belirlenmesi", 1. Köprü ve Viyadükler Sempozyumu , Antalya, Türkiye.

Padgett J.E. and DesRoches R., 2007, "Sensitivity of Seismic Response and Fragility to Parameter Uncertainty", ASCE Journal of Structural Engineering, Volume 133, No. 12, pp. 1710-1718.

Pamuk A., Kalkan E. and Ling H.I., 2005, "Structural and Geotechnical Impacts of Surface Rupture on Highway Structures during Recent Earthquakes in Turkey", Soil Dynamics and Earthquake Engineering, Volume 25, pp.581–589.

Papazoglu A.J. and Elnashai A.S., 1996, "Analytical and Field Evidence of the Damaging Effect of Vertical Earthquake Ground Motion", Earthquake Engineering and Structural Dynamics, Volume 25, pp. 1109-1137.

Pezeshk S., Chang T.S., Yiak K.C. and Kung H.T., 1993, "Seismic Vulnerability Evaluation of Bridges in Memphis and Shelby Country, Tennessee", Earthquake Spectra, Volume 9, No. 4, pp. 803–816.

Priestley M.J.N., Seible F. and Calvi G.M., 1996, "Seismic Design and Retrofit of Bridges", John Wiley & Sons, Inc., New York, NY.

Priestley M.J.N., Calvi G.M. and Kowalsky M.J., 2007, "Displacement-Based Seismic Design of Structures", IUSS Press, Pavia, Italy.

Rashidi S. and Ala Saadeghvaziri M., 1997, "Seismic Modeling of Multi-Span Simply-Supported Bridges Using ADINA", Computers and Structures, Volume 64, No. 5/6, pp. 1025-1039.

Rossetto T. and Elnashai A.S., 2003, "Derivation of Vulnerability Functions for European Type RC Structures Based on Observational Data", Engineering Structures, Volume 25, No. 10, pp. 1241-1263.

Saadeghvaziri M.A. and Foutch D.A., 1991, "Dynamic Behavior of R/C Highway Bridges under the Combined Effect of Vertical and Horizontal Earthquake Motions", Earthquake Engineering and Structural Dynamics, Volume 20, pp. 535–549.

Scott B.D., Park R. and Priestley M.J.N., 1982, "Stress-Strain Behavior of Concrete Confined by Overlapping Hoops at Low and High Strain Rates", ACI Structural Journal, Volume 79, No. 1, pp. 13-27.

SeismoSoft, 2005, "SeismoStruct - A computer Program for Static and Dynamic Non-linear Analysis of Framed Structures", Online. Available from URL: http://www.seismosoft.com, 15/11/2006.

Shinozuka M., Feng M.Q., Kim H., Uzawa T. and Ueda T., 2003, "Statistical Analysis of Fragility Curves", Report No. MCEER-03-0002, MCEER.

Shinozuka M., Feng M.Q., Lee J. and Naganuma T., 2000a, "Statistical Analysis of Fragility Curves", ASCE Journal Of Engineering Mechanics, Volume 126, No. 12, pp. 1224-1231.

Shinozuka M., Feng M.Q., Kim H.K. and Kim S.H., 2000b, "Nonlinear Static Procedure for Fragility Curve Development", ASCE Journal of Engineering Mechanics, Volume 126, No. 12, pp. 1287-1295.

Taucer F.F., Spacone E. and Filippou F.C., 1991, "A Fiber Beam-Column Element for Seismic Response Analysis of Reinforced Concrete Structures", Report No. UCB/EERC-91/17, Earthquake Engineering Research Center, College of Engineering, University of California, Berkeley.

The Mathworks Inc., 2004, Matlab, Version 7.0.

Turkish Earthquake Code, TEC, 2007, "Specification for Structures to be Built in Disaster Areas", Ministry of Public Works and Settlement Government of Republic of Turkey.

Ventura C.E., Finn W.D.L. and Felber A.J., 1995, "Ambient Vibration Study of the Painter Street Overpass", 7th Canadian Conference on Earthquake Engineering, Montreal, pp. 787-794.

Von Thun J.L., Rochim L.H., Scott G.A. and Wilson J.A., 1988, "Earthquake Ground Motions for Design and Analysis of Dams", Earthquake Engineering and Soil Dynamics II - Recent Advances in Ground-Motion Evaluation, Geotechnical Special Publication, Volume 20, pp. 463-481.

Yakut A. and Yılmaz H., 2008, "Correlation of Deformation Demands with Ground Motion Intensity", ASCE Journal of Structural Engineering, Volume 134, No. 12, pp. 1818-1828.

Yamazaki F., Onishi J. and Tayama S., 1999, "Earthquake Damage Assessment of Expressway Structure in Japan", Asian-Pacific Symposium on Structural Reliability and its Applications, pp. 1-10.

Yen W.P., Ghasemi H. and Cooper J.D., 2002, "Lessons Learned from Bridge Performance of the 1999 Turkish & Taiwan Earthquakes", Technical Note of National Institute for Land and Infrastructure Management, Volume 41, pp. 113-120.

Yu C.P., 1996, "Effect of Vertical Earthquake Components on Bridge Responses", PhD Thesis, University of Texas at Austin, Texas, US.

Yücemen M.S., Koçyiğit A., Yakut A. and Gencoğlu S., 2005, "Determination of Guidelines for the Development of Seismic Hazard Map and a Pilot Study", Appraisal Report No. 1, Technical Report prepared for the General Directorate of Disaster Affairs, Ankara.

Yücemen M.S., Koçyiğit A., Yakut A. and Gencoğlu S., 2006, "Guidelines for the Development of Seismic Hazard Maps", Technical Report prepared for the General Directorate of Disaster Affairs, Ankara.

Wilson J.C. and Tan B.S., 1990, "Bridge Abutments: Formulation of Simple Model for Earthquake Response Analysis", Journal of Engineering Mechanics, ASCE, Volume 116, No. 8, pp. 1828-1837.

Wilson E.L., 2002, "Three Dimensional Static and Dynamic Analysis of Structures", Computers and Structures, Inc., Berkeley, Calif.

Wissawapaisal C. and Aschheim M., 2000, "Modeling the Transverse Response of Short Bridges Subjected to Earthquakes", Mid-America Earthquake Center, CD Release 00-05.

Zhu P., Abe M. and Fujino Y., 2002, "Modeling Three Dimensional Non-linear Seismic Performance of Elevated Bridges with Emphasis on Pounding of Girders", Earthquake Engineering and Structural Dynamics, Volume 31, pp. 1891-1913.

APPENDIX A

SEISMIC RESPONSE OF BRIDGE COMPONENTS
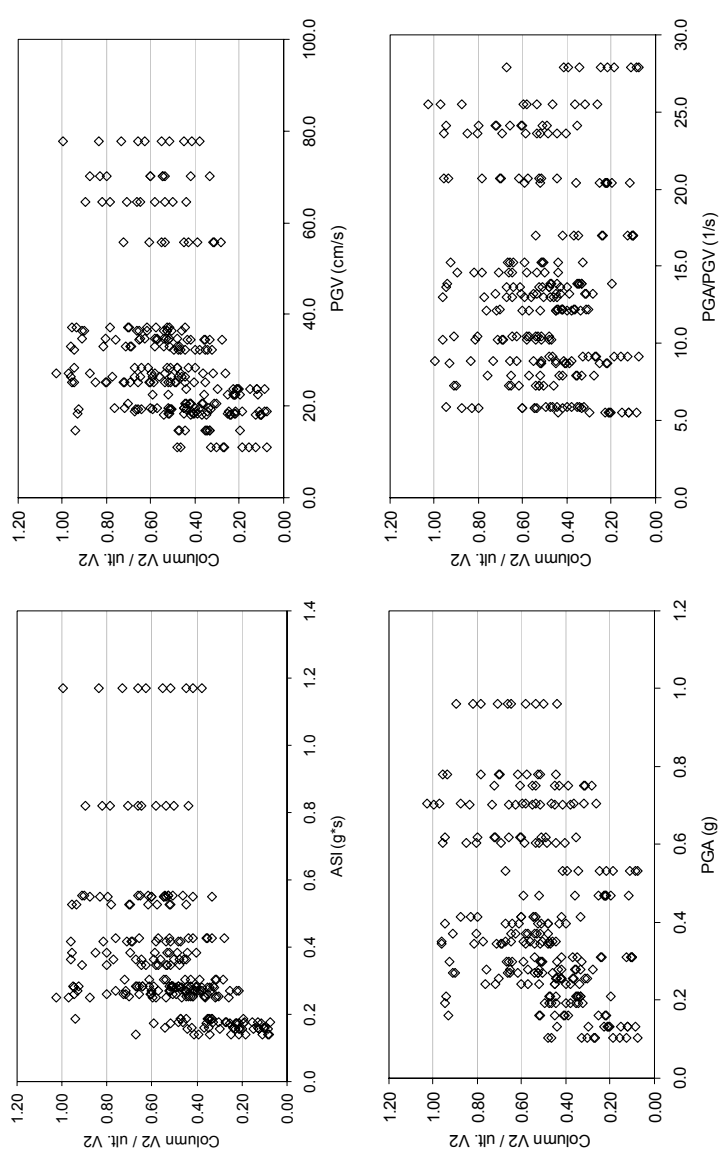
Figure A.1 Normalized column shear-2 demand for MS_MC_SL30
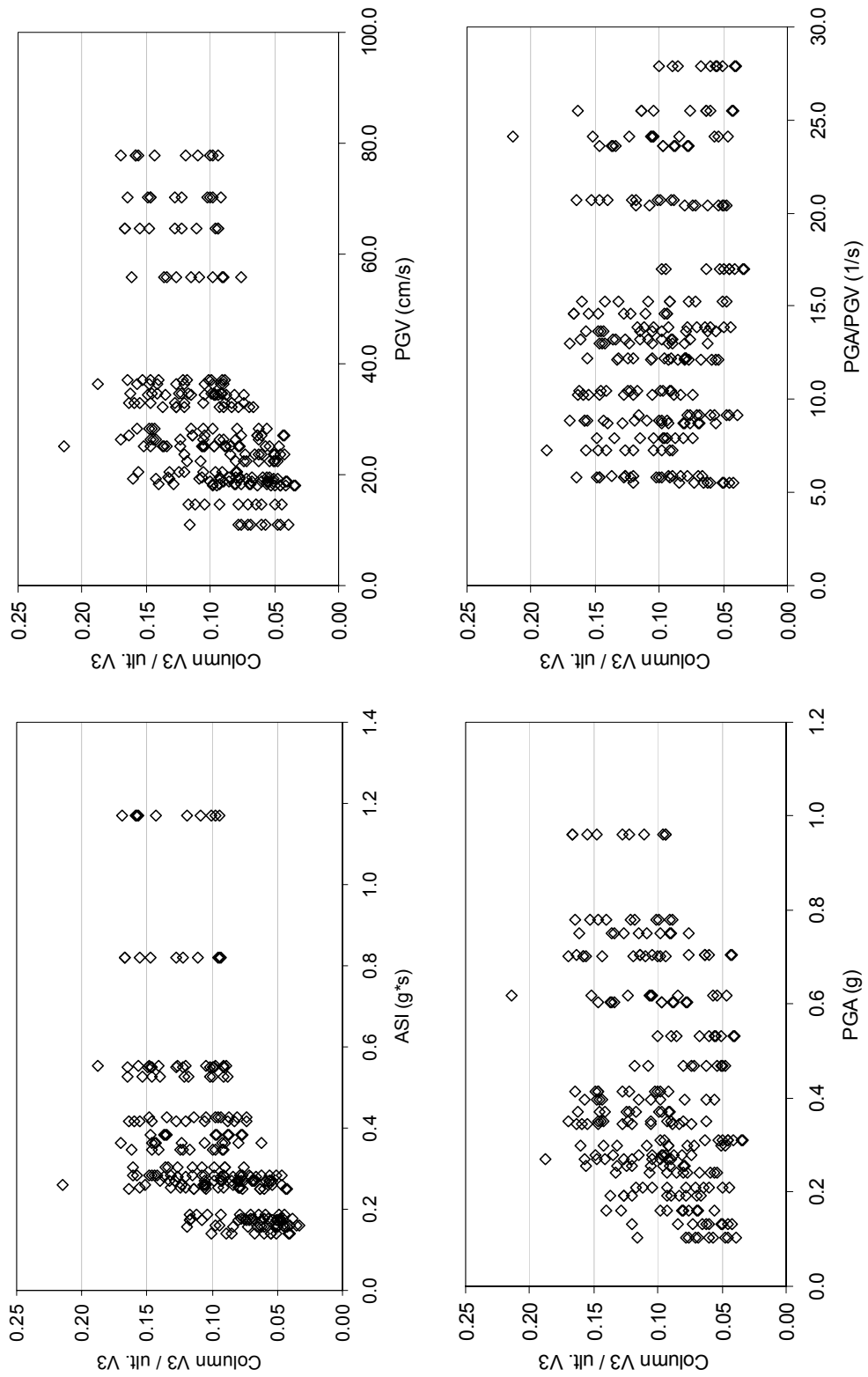
Figure A.2 Normalized column shear-3 demand for MS_MC_SL30
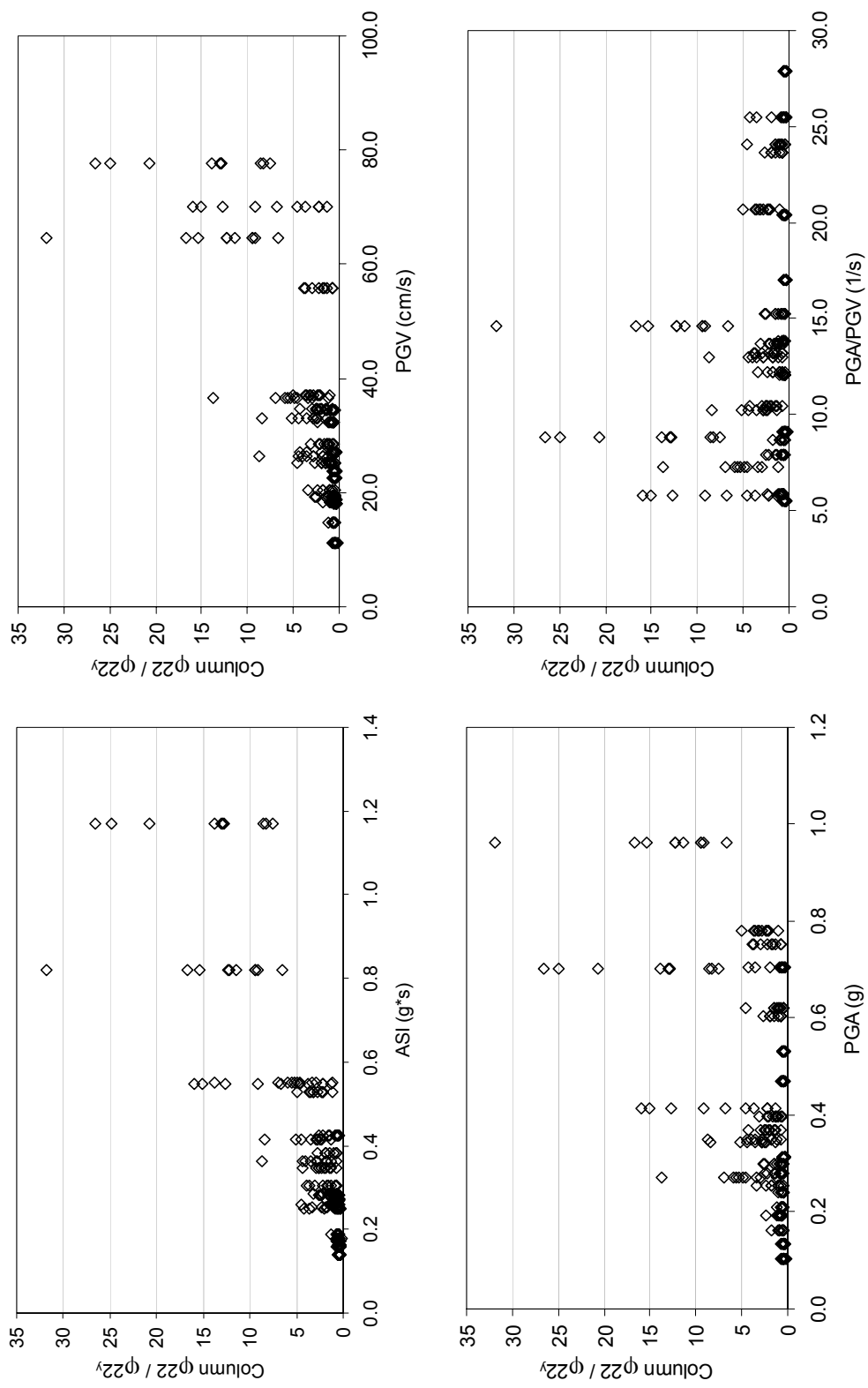
Figure A.3 Normalized column curvature-22 demand for MS_MC_SL30

209
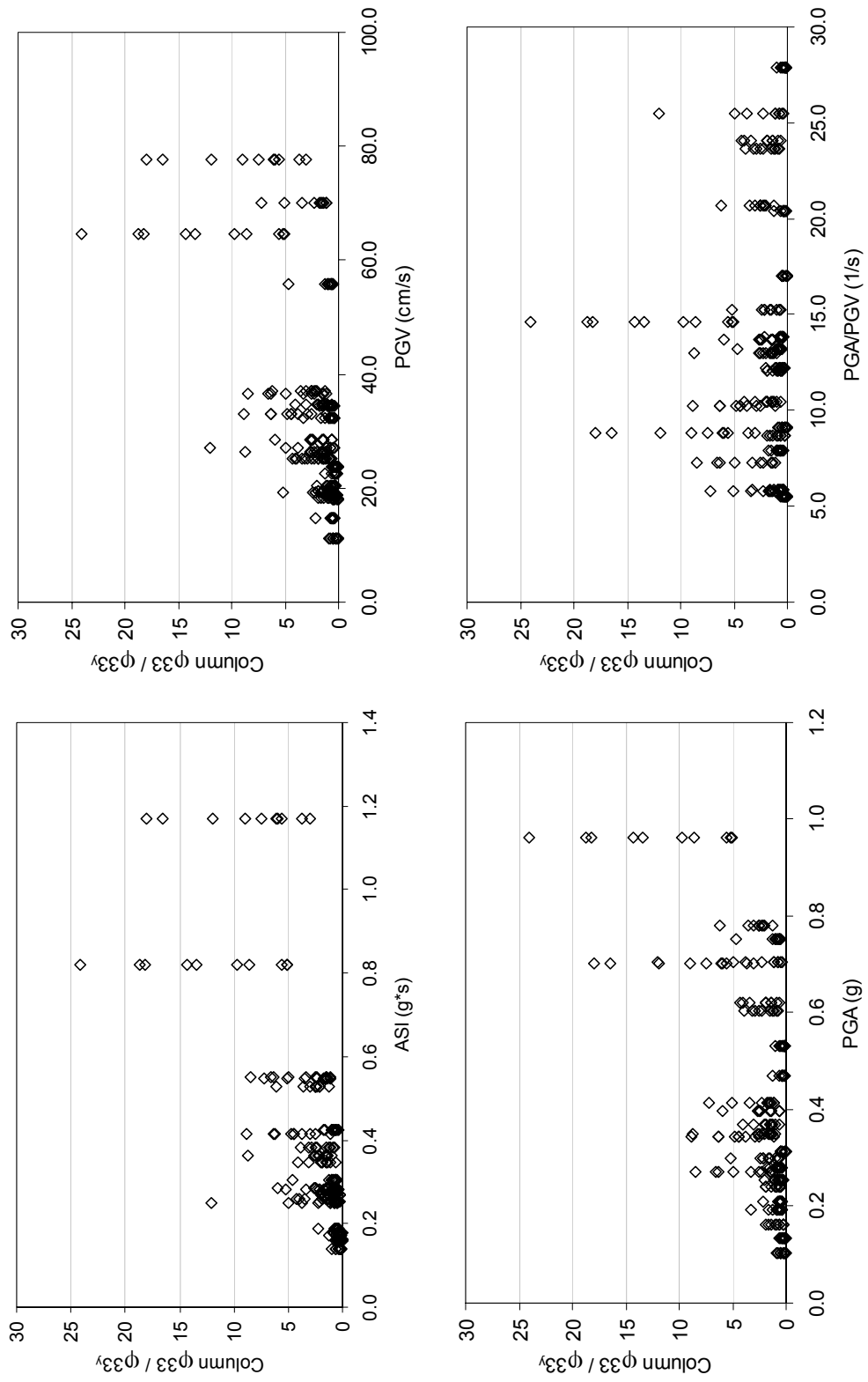
Figure A.4 Normalized column curvature-33 demand for MS_MC_SL30
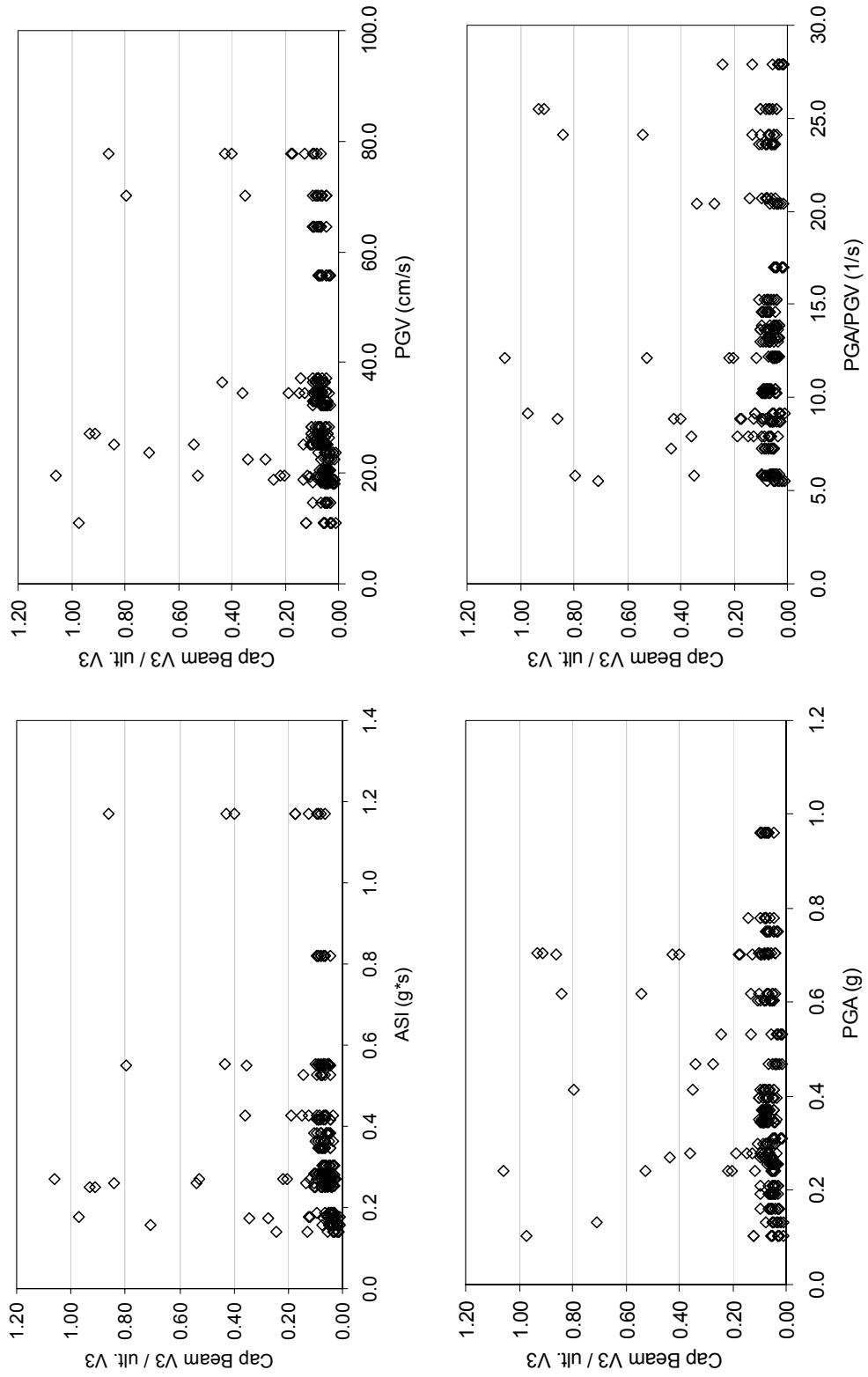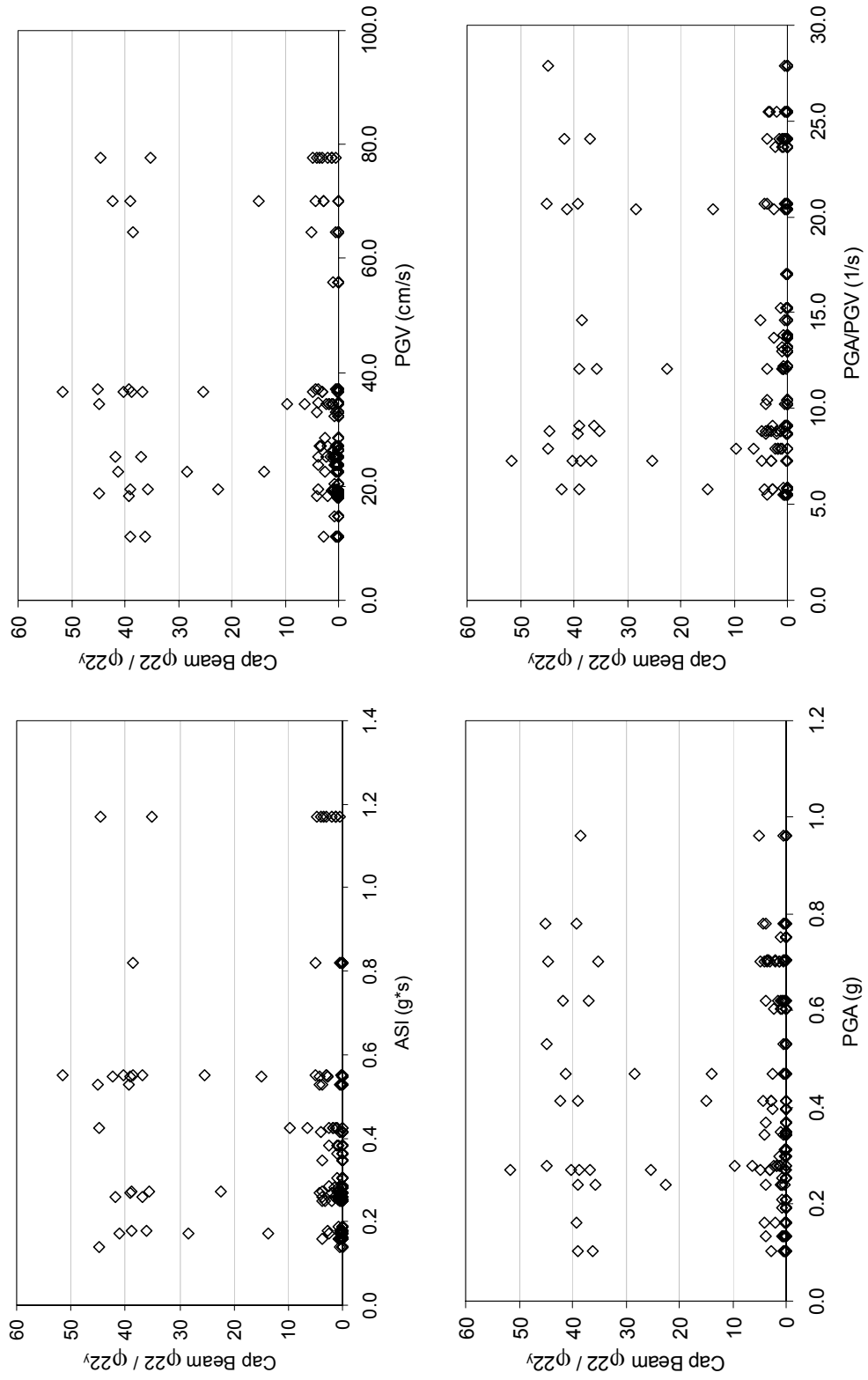
Figure A.5 Normalized cap beam shear-3 demand for MS_MC_SL30

211
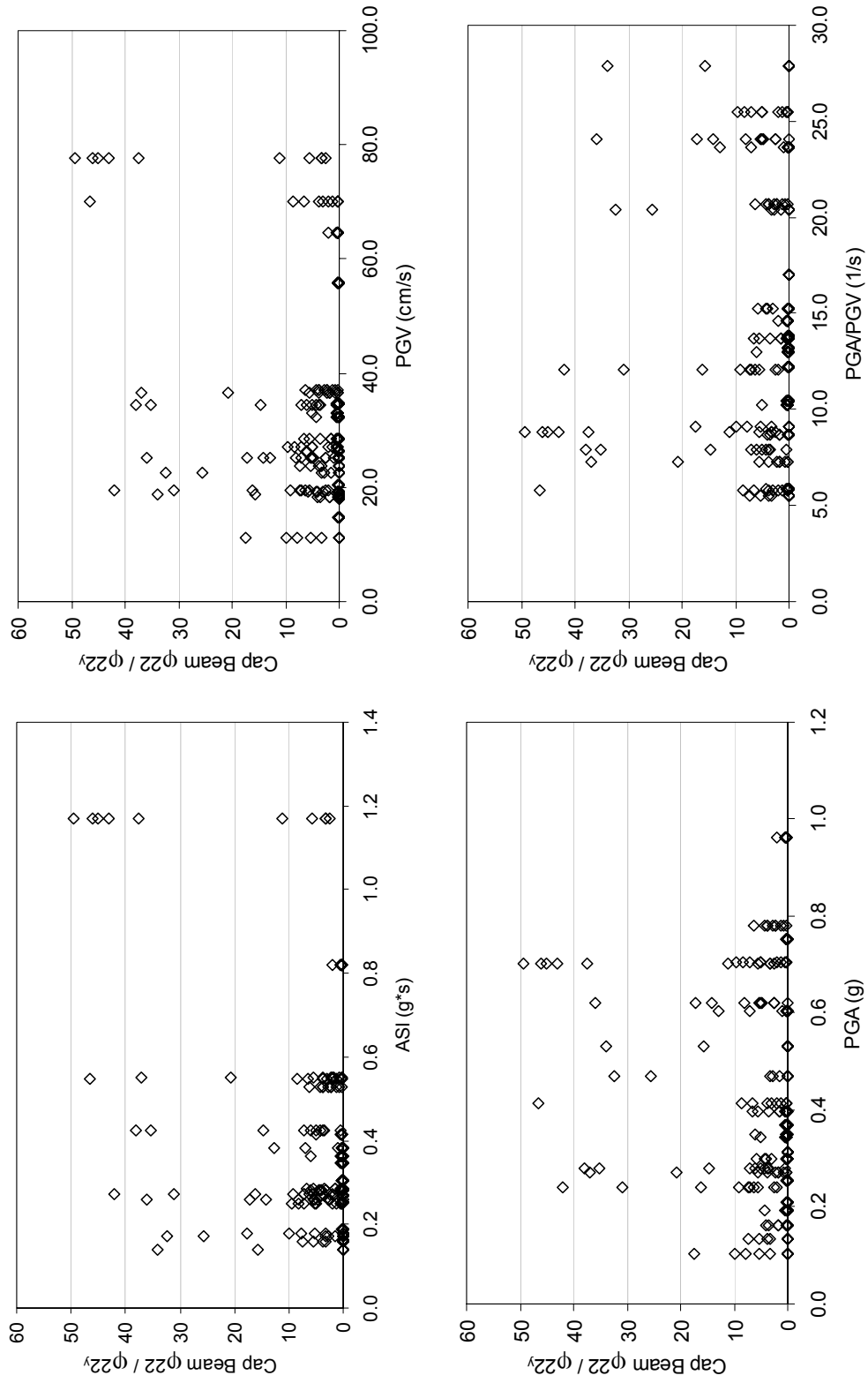
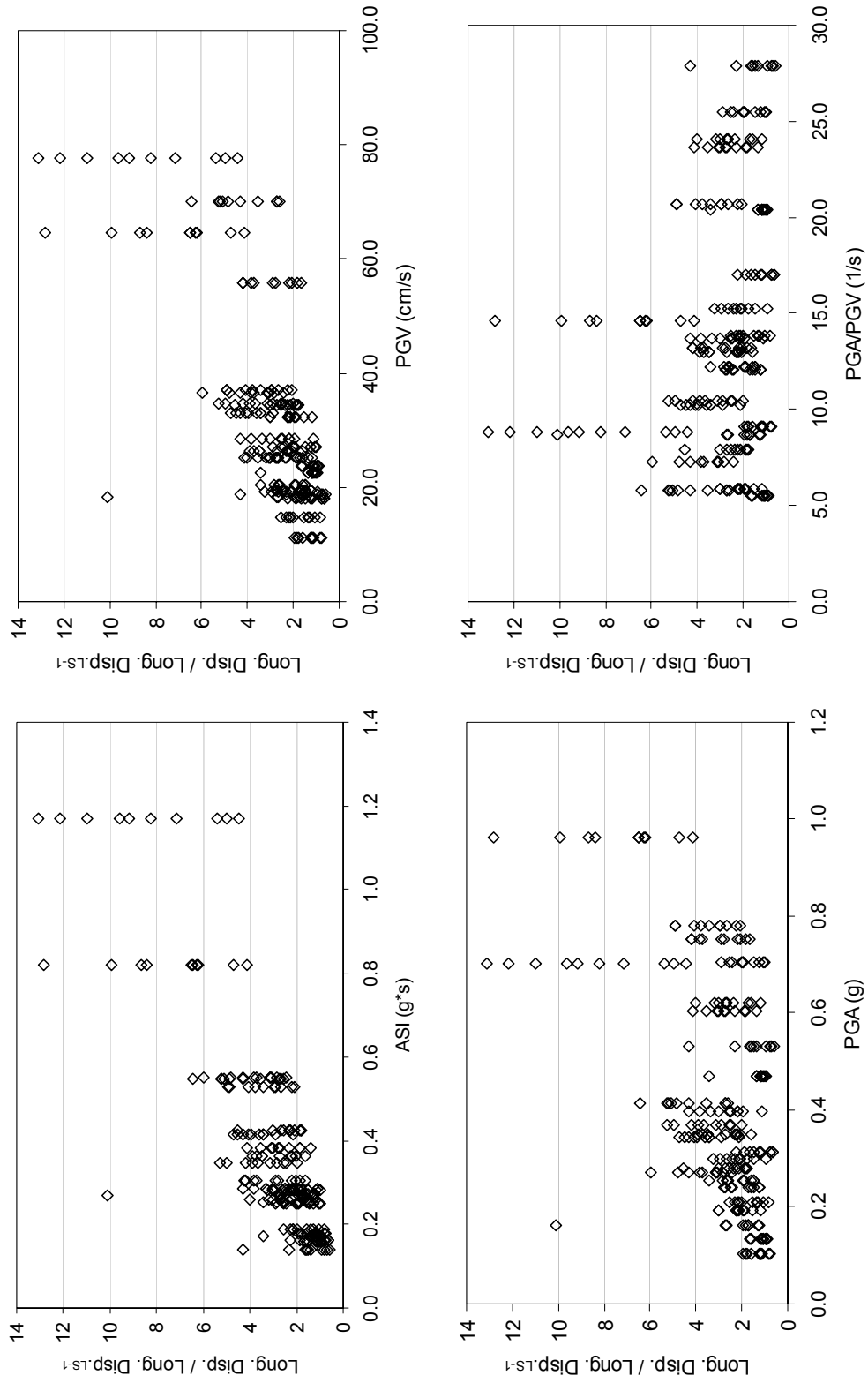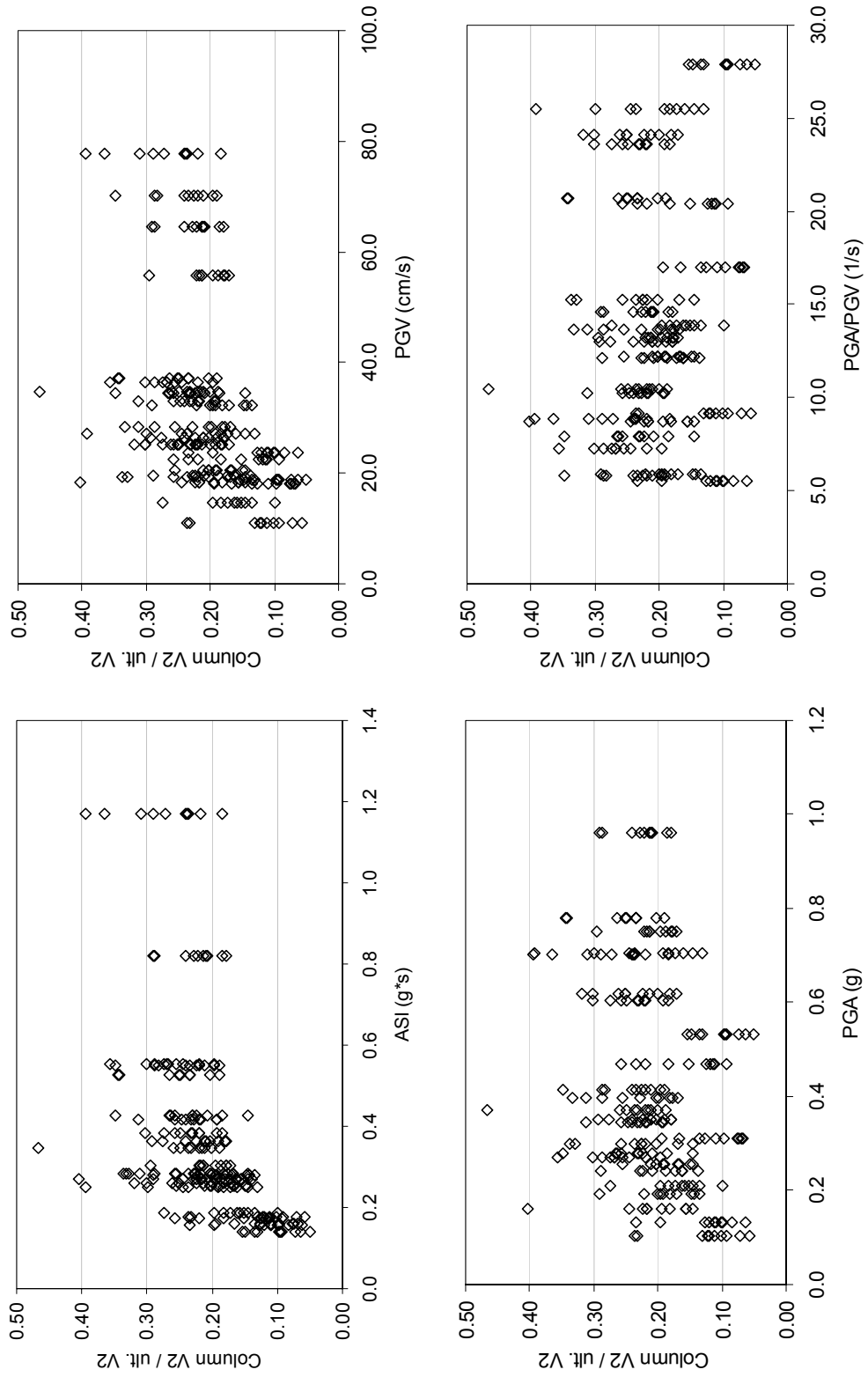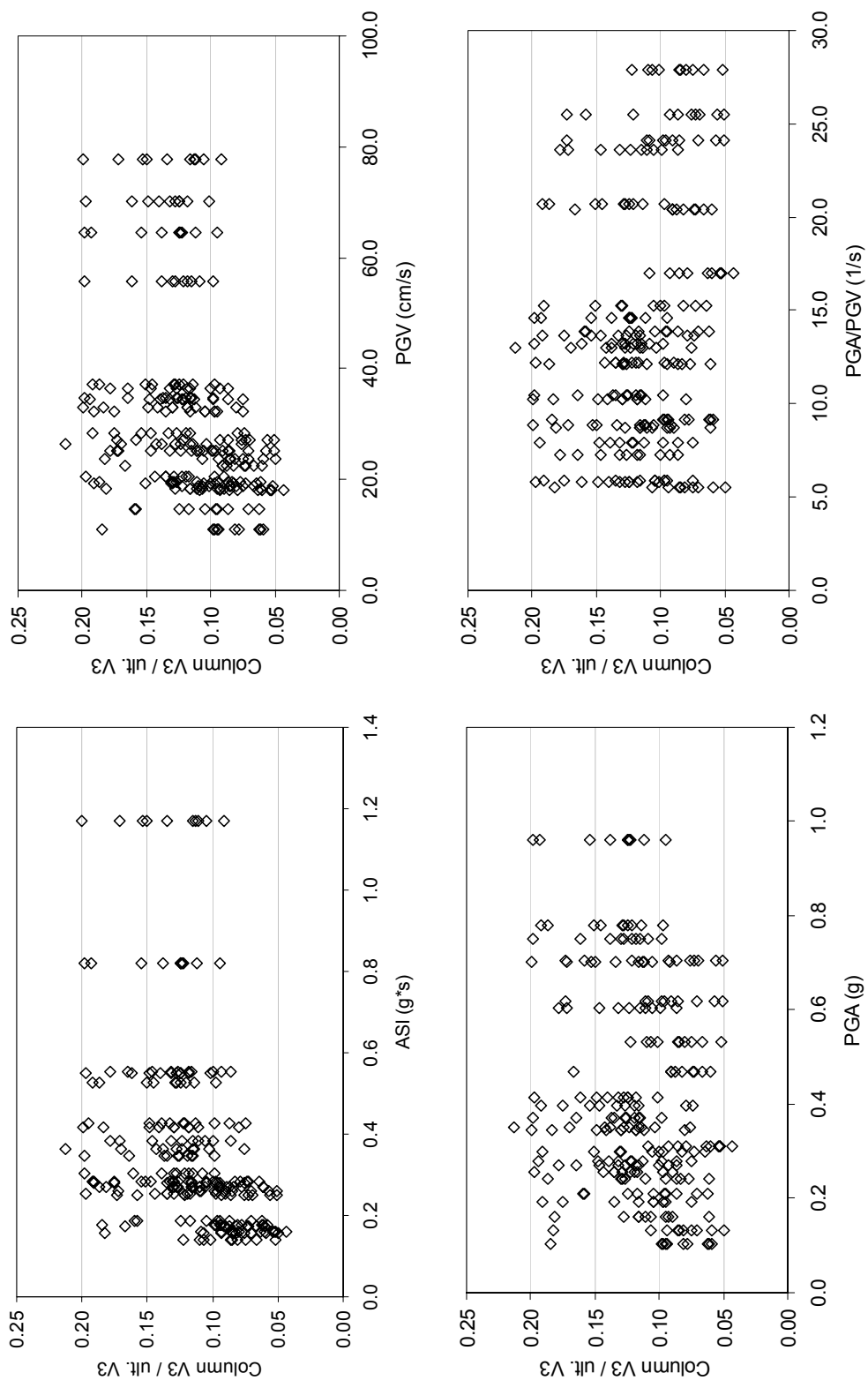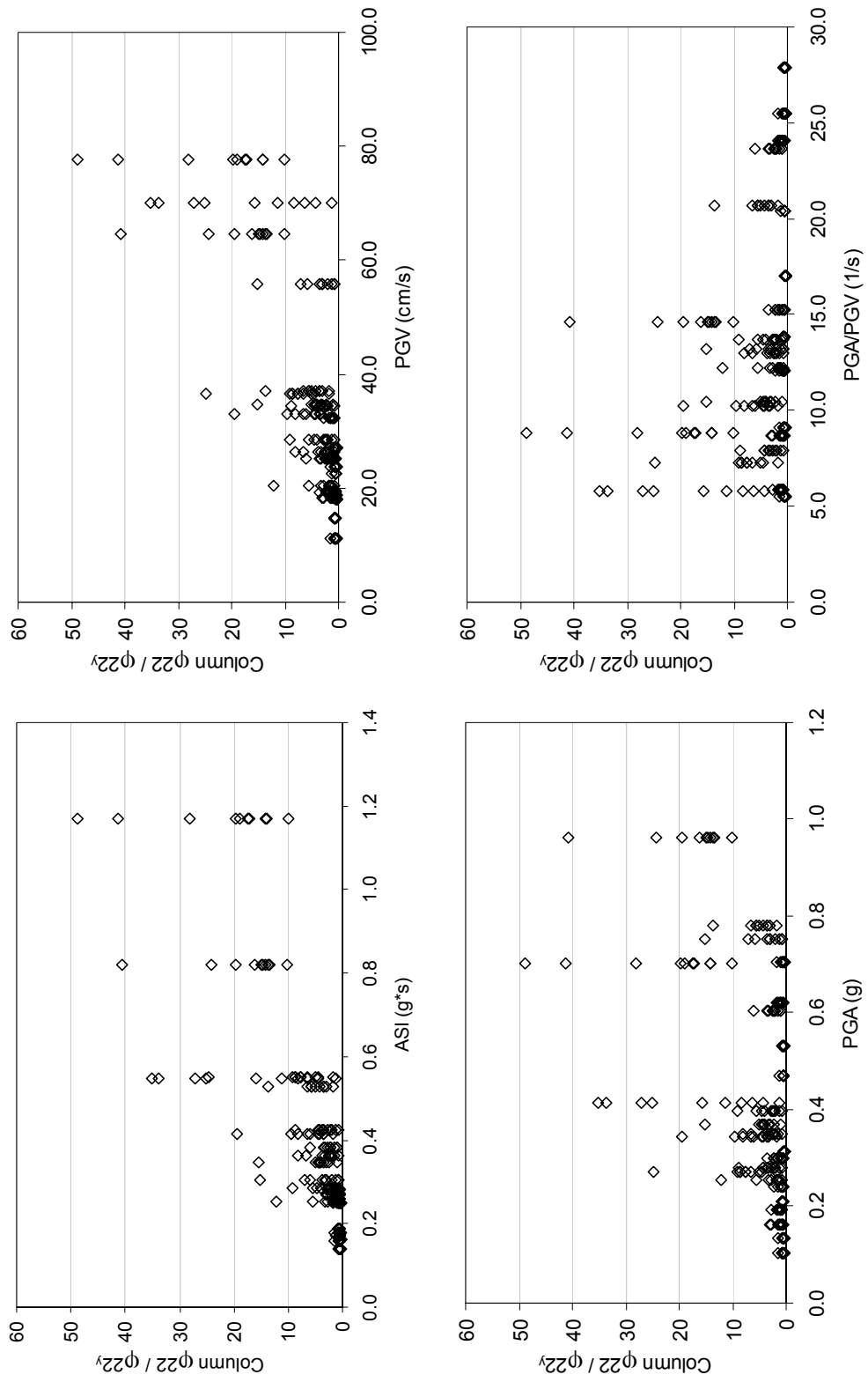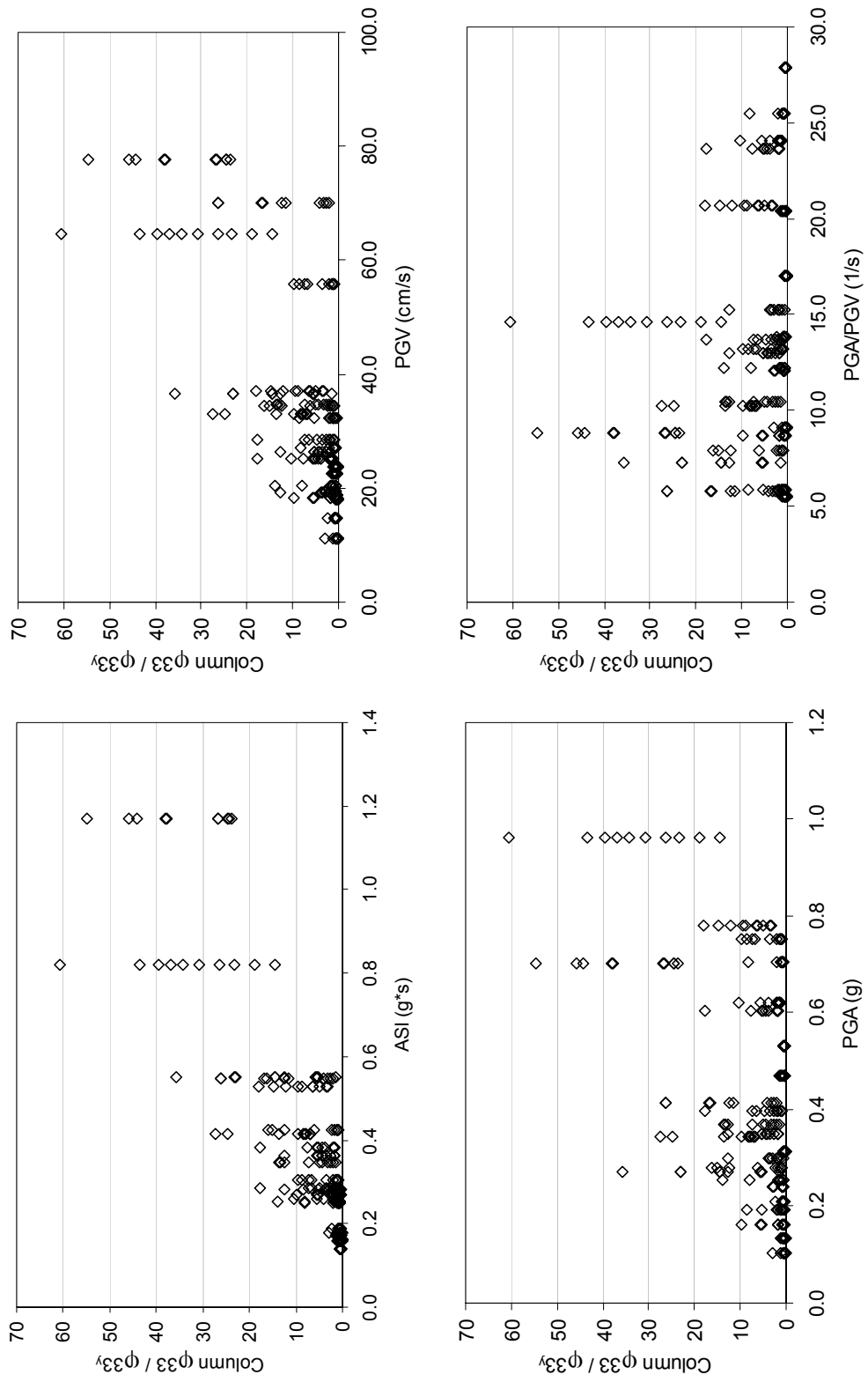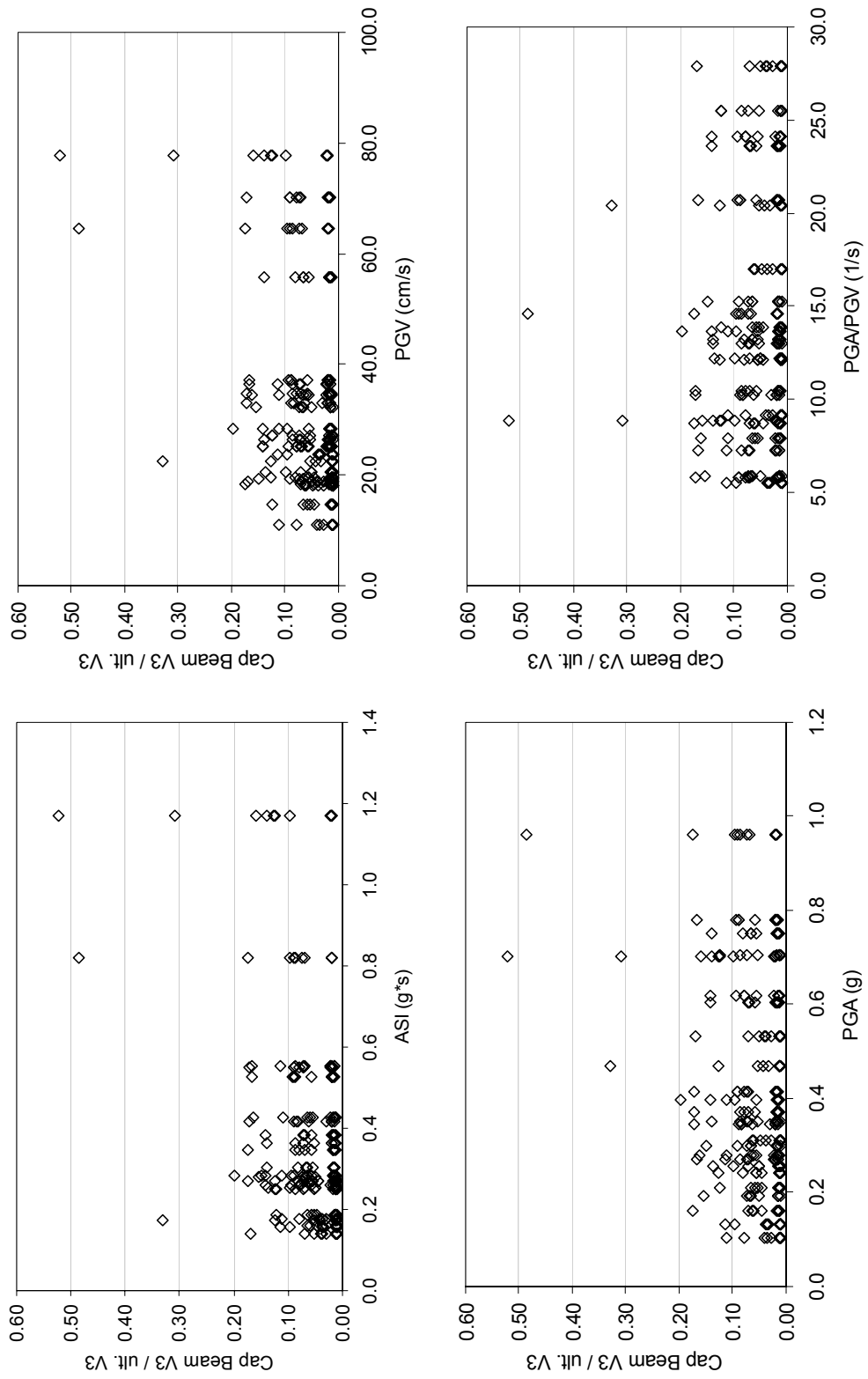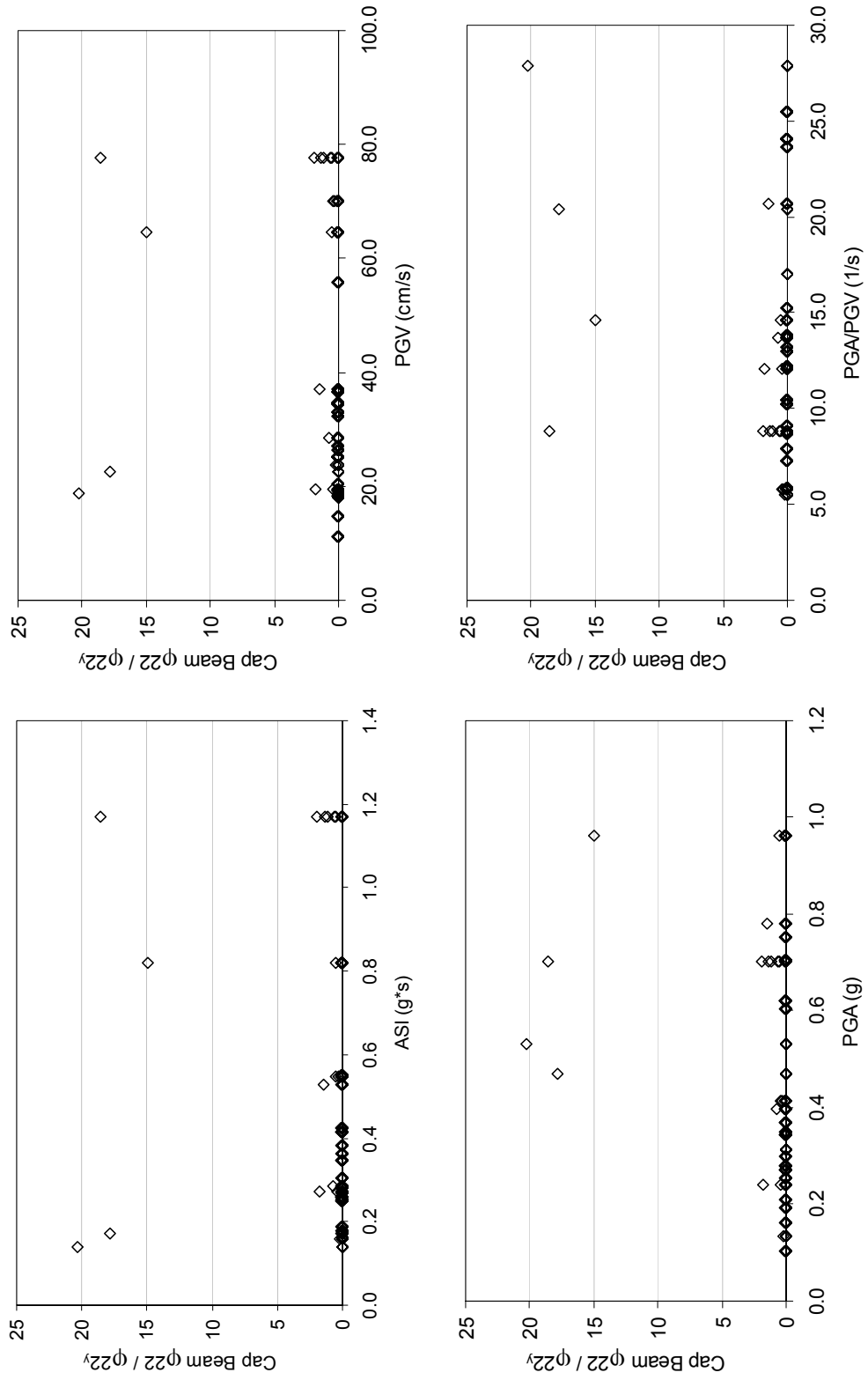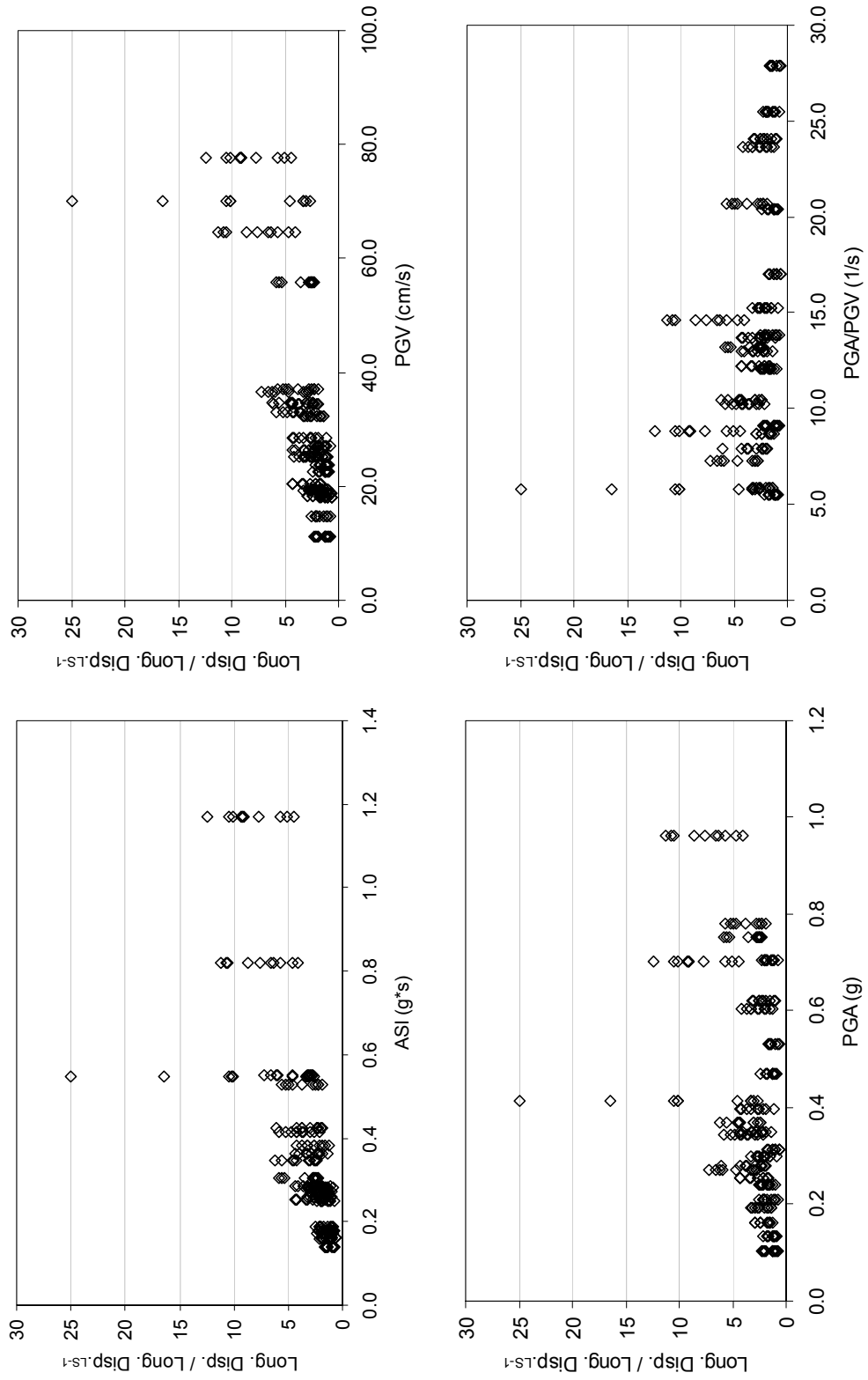Figure A.6 Normalized cap beam curvature-22 demand for MS_MC_SL30
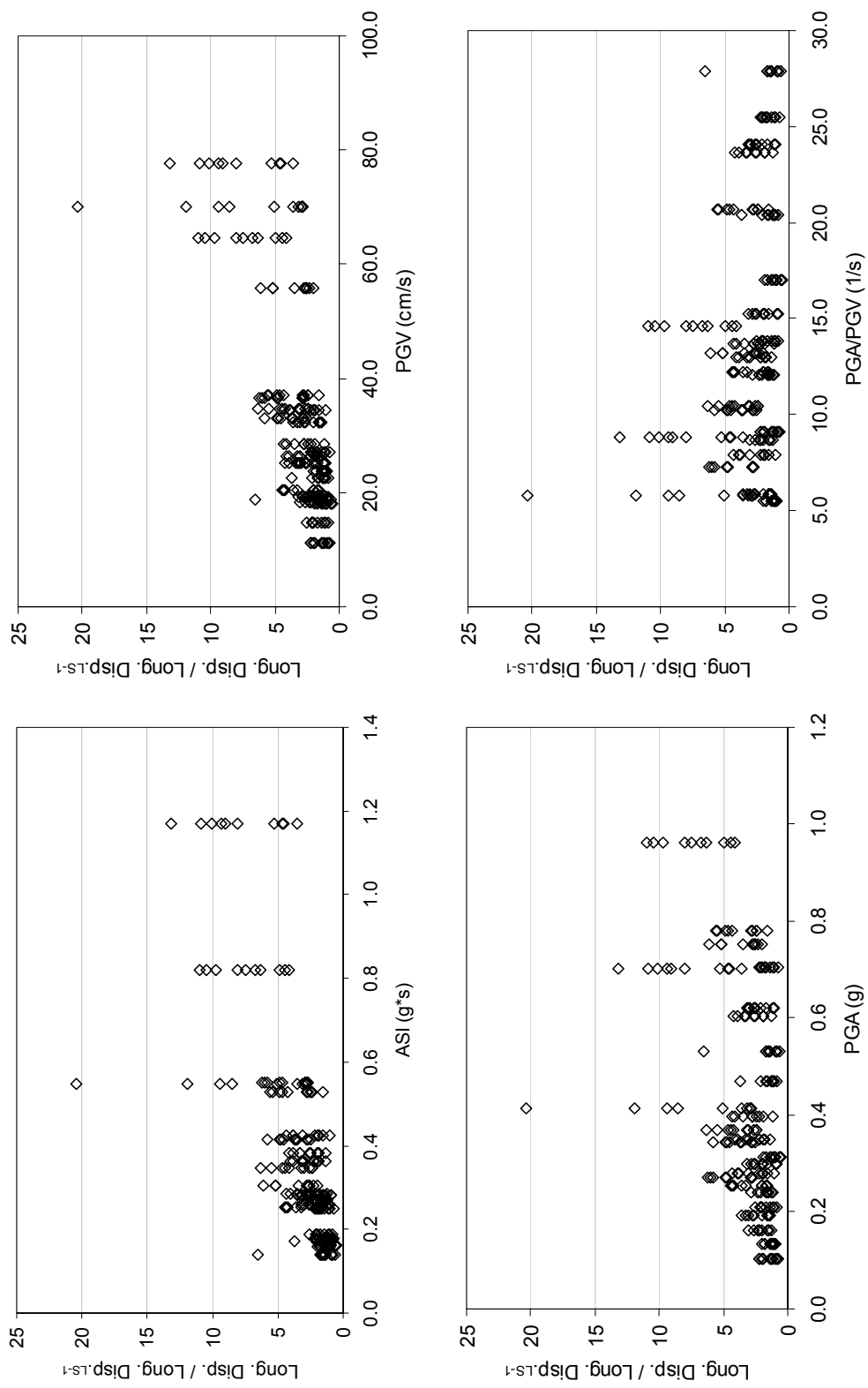
Figure A.7 Normalized superstructure longitudinal displacement demand for MS_MC_SL30
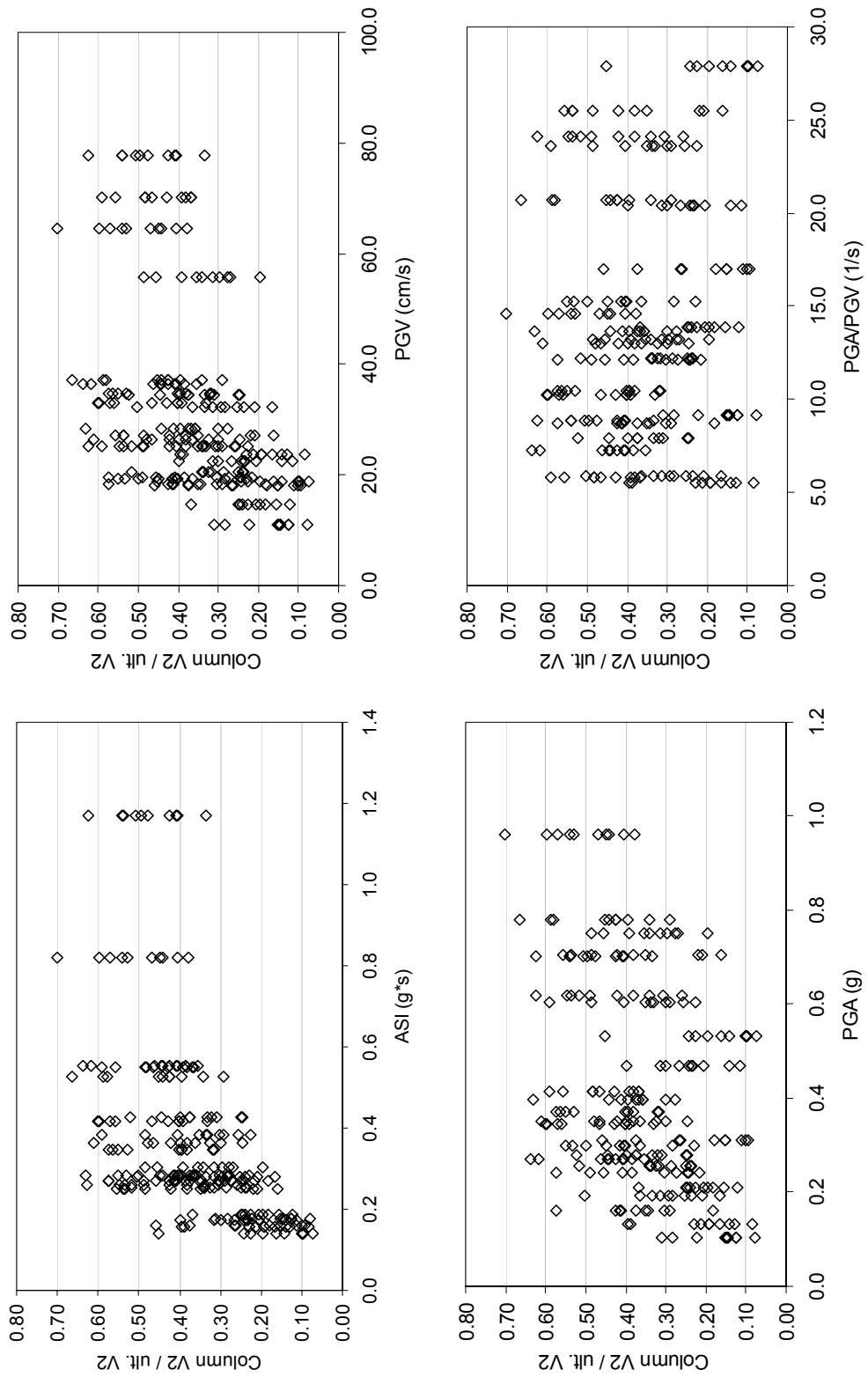
Figure A.8 Normalized column shear-2 demand for MS_MC_SG30
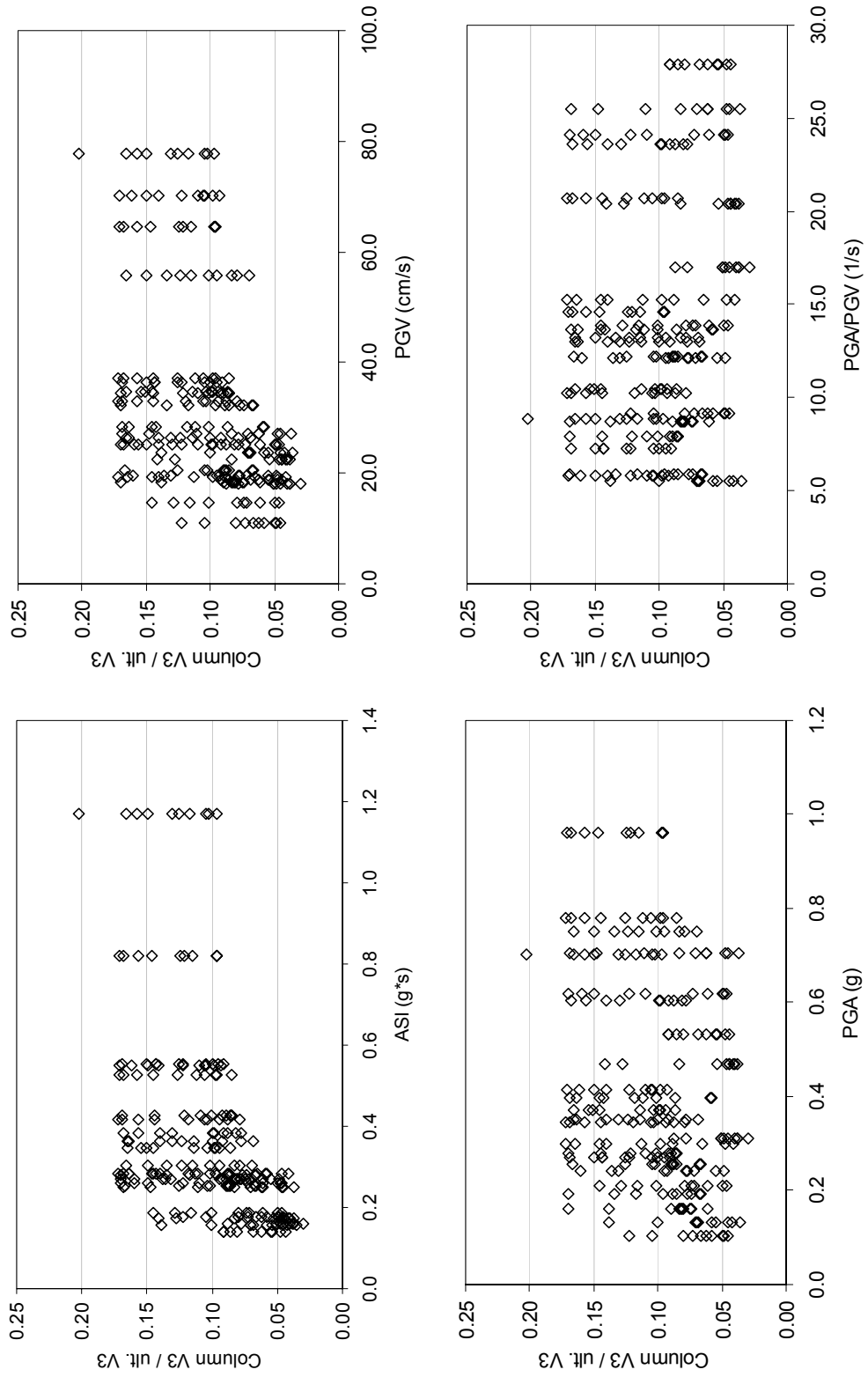
Figure A.9 Normalized column shear-3 demand for MS_MC_SG30
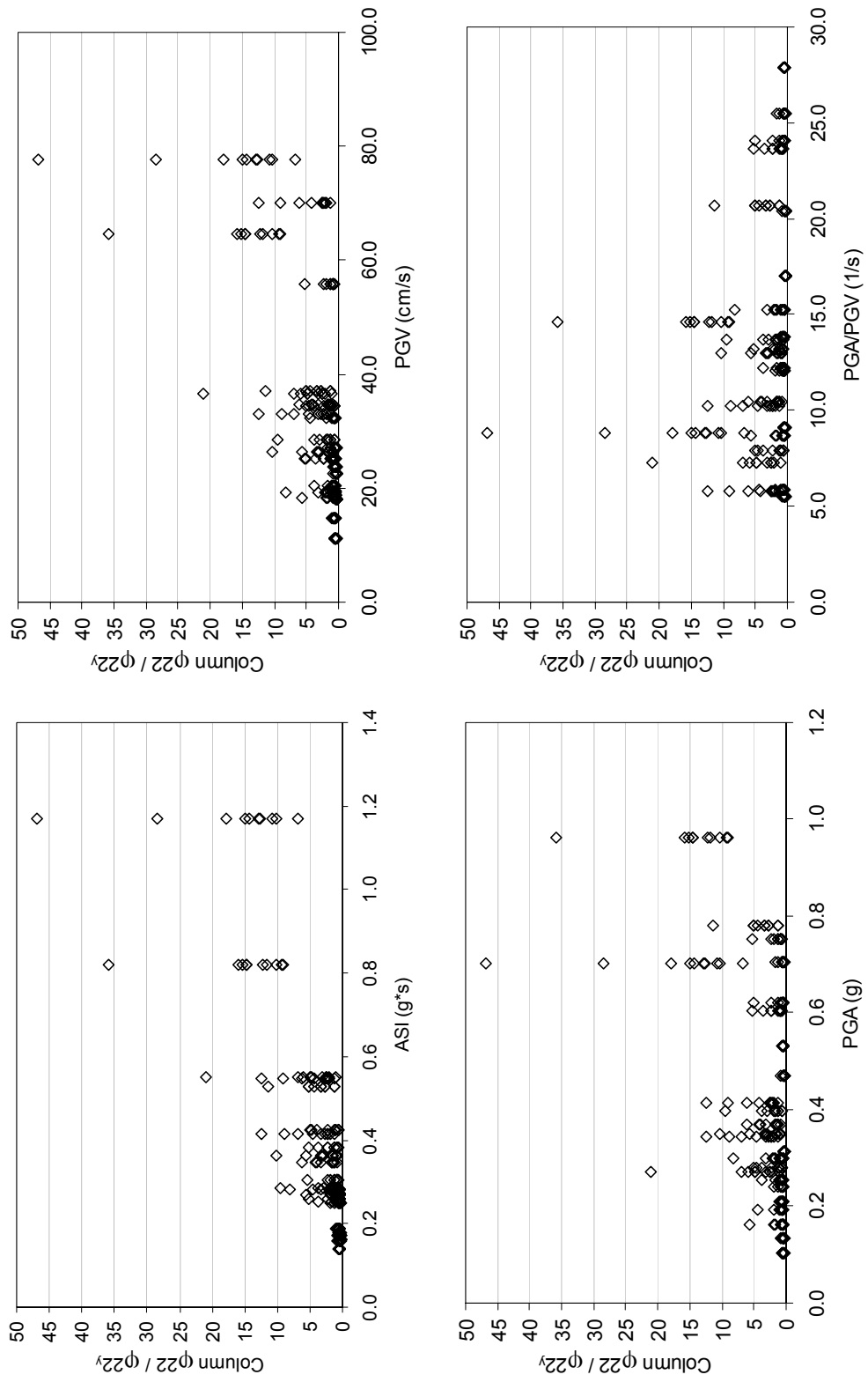
Figure A.10 Normalized column curvature-22 demand for MS_MC_SG30

216
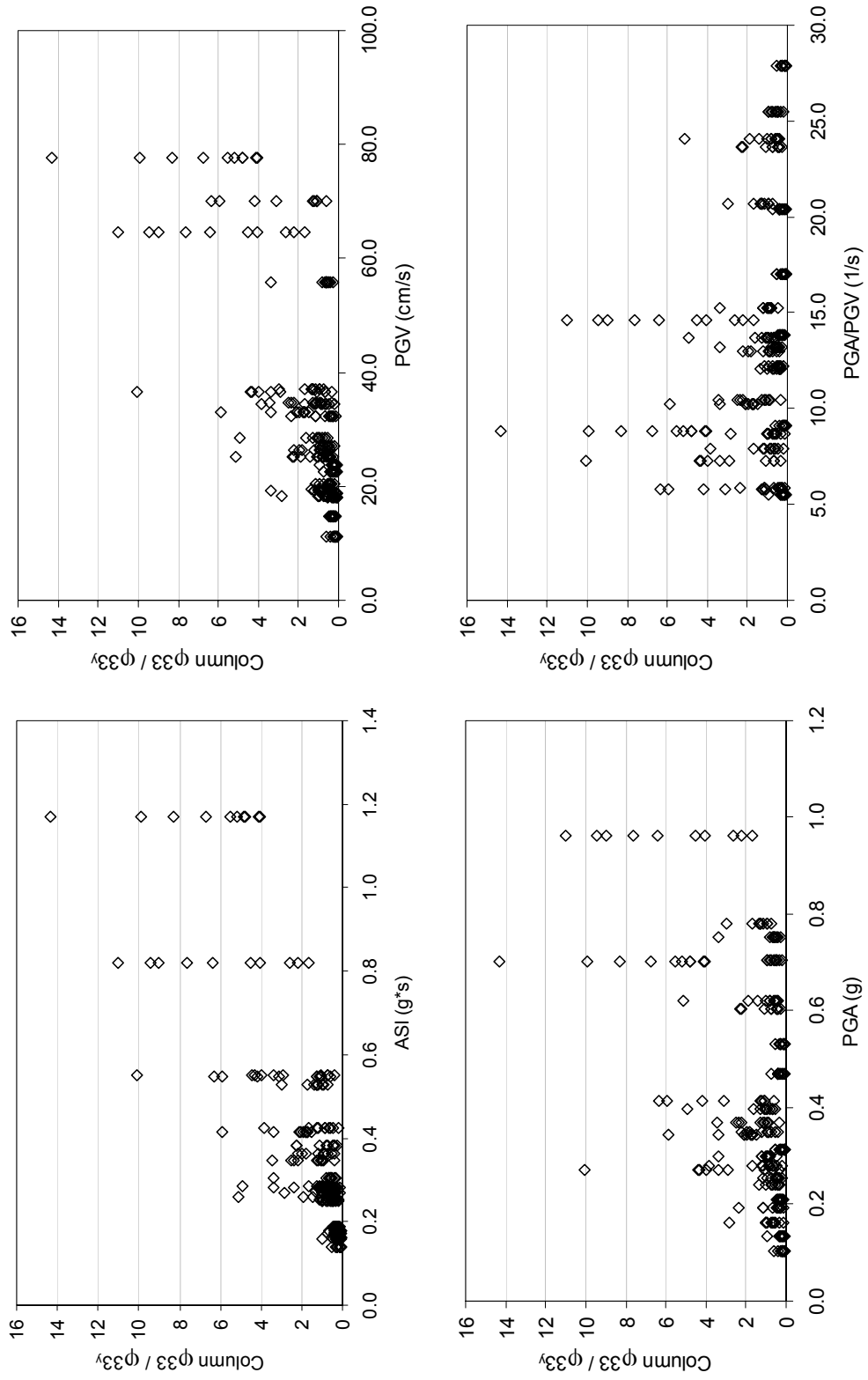
Figure A.11 Normalized column curvature-33 demand for MS_MC_SG30
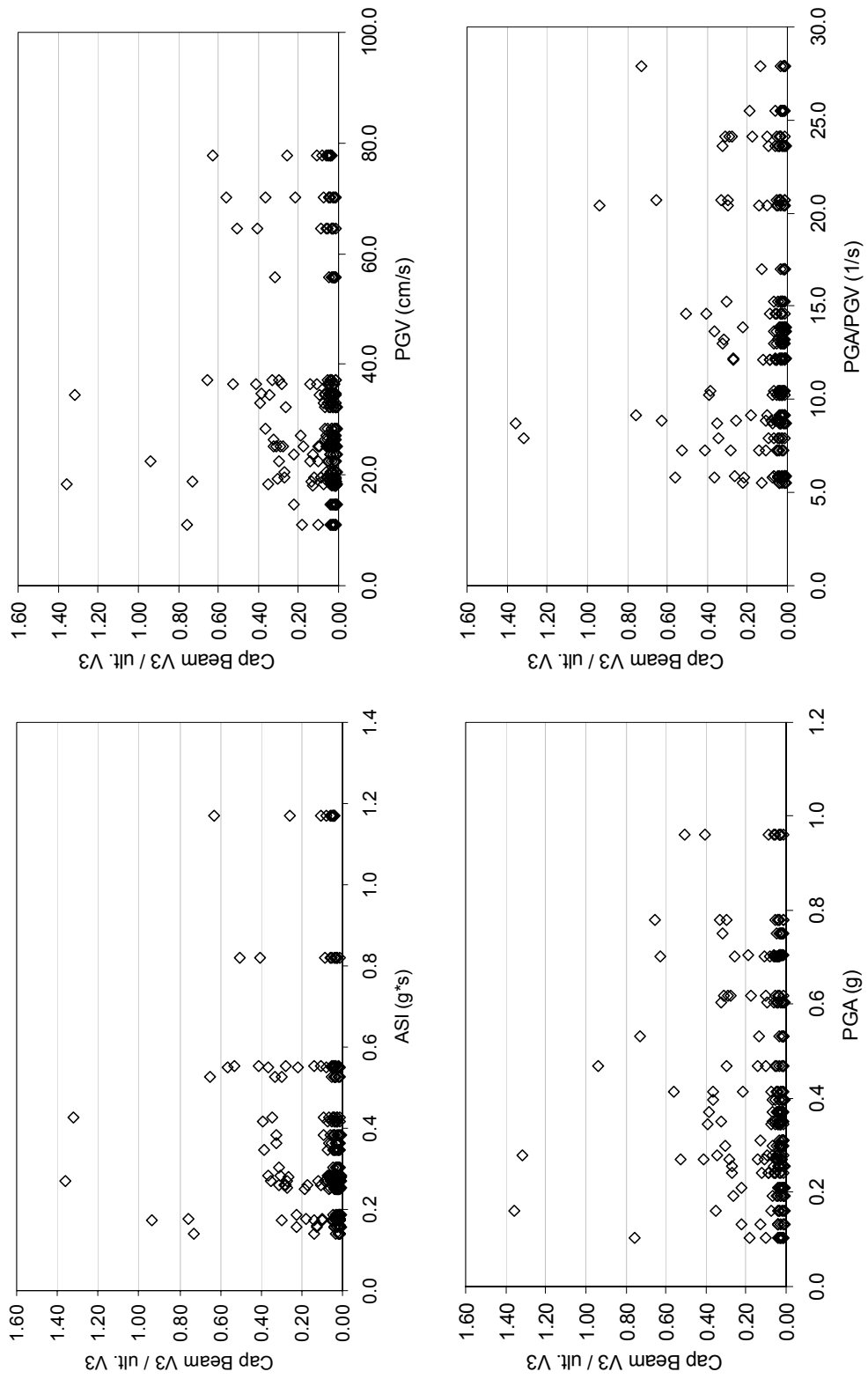
Figure A.12 Normalized cap beam shear-3 demand for MS_MC_SG30

Figure A.13 Normalized cap beam curvature-22 demand for MS_MC_SG30

Figure A.14 Normalized superstructure longitudinal displacement demand for MS_MC_SG30
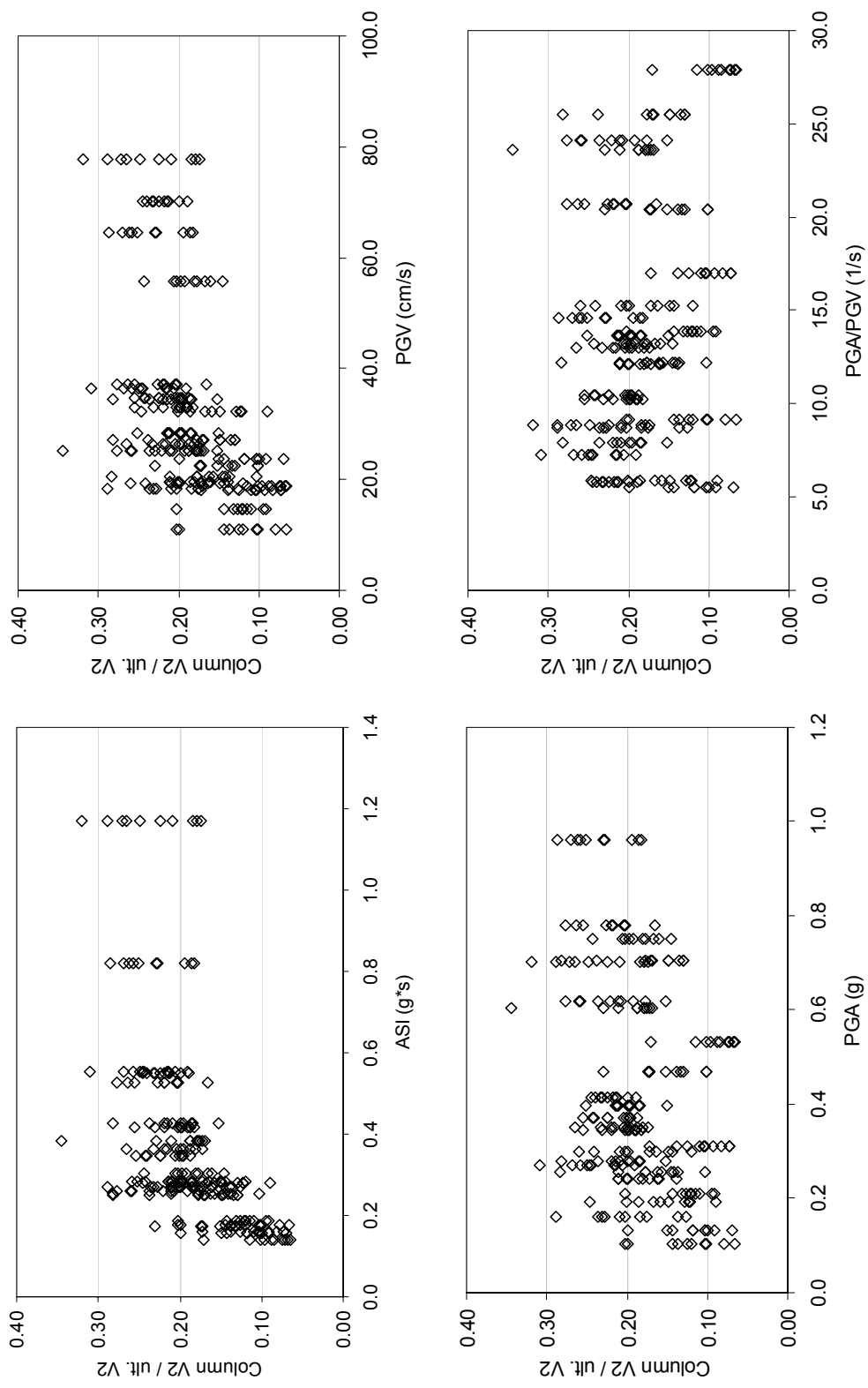
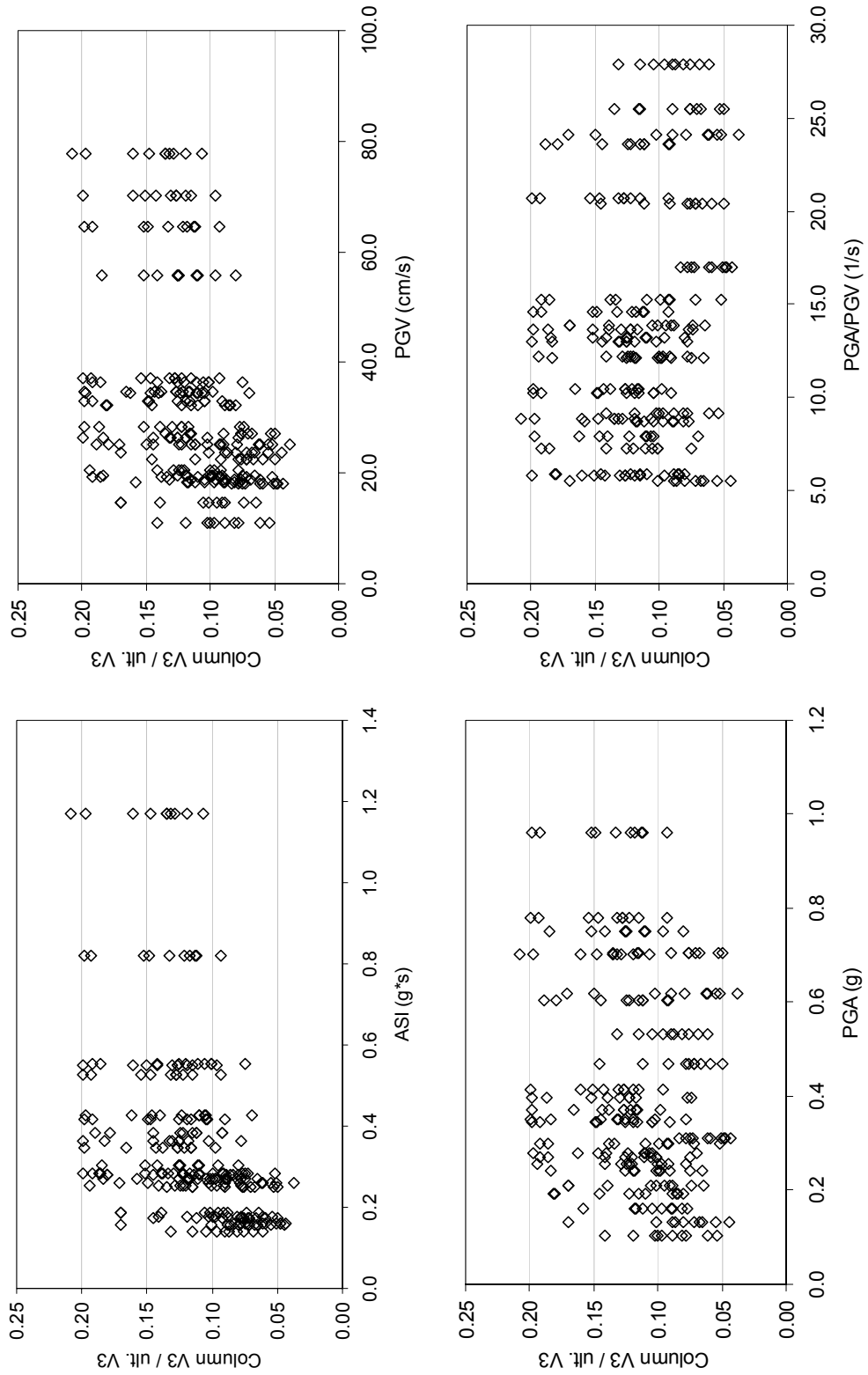Figure A.15 Normalized column shear-2 demand for MS_SC_SL30

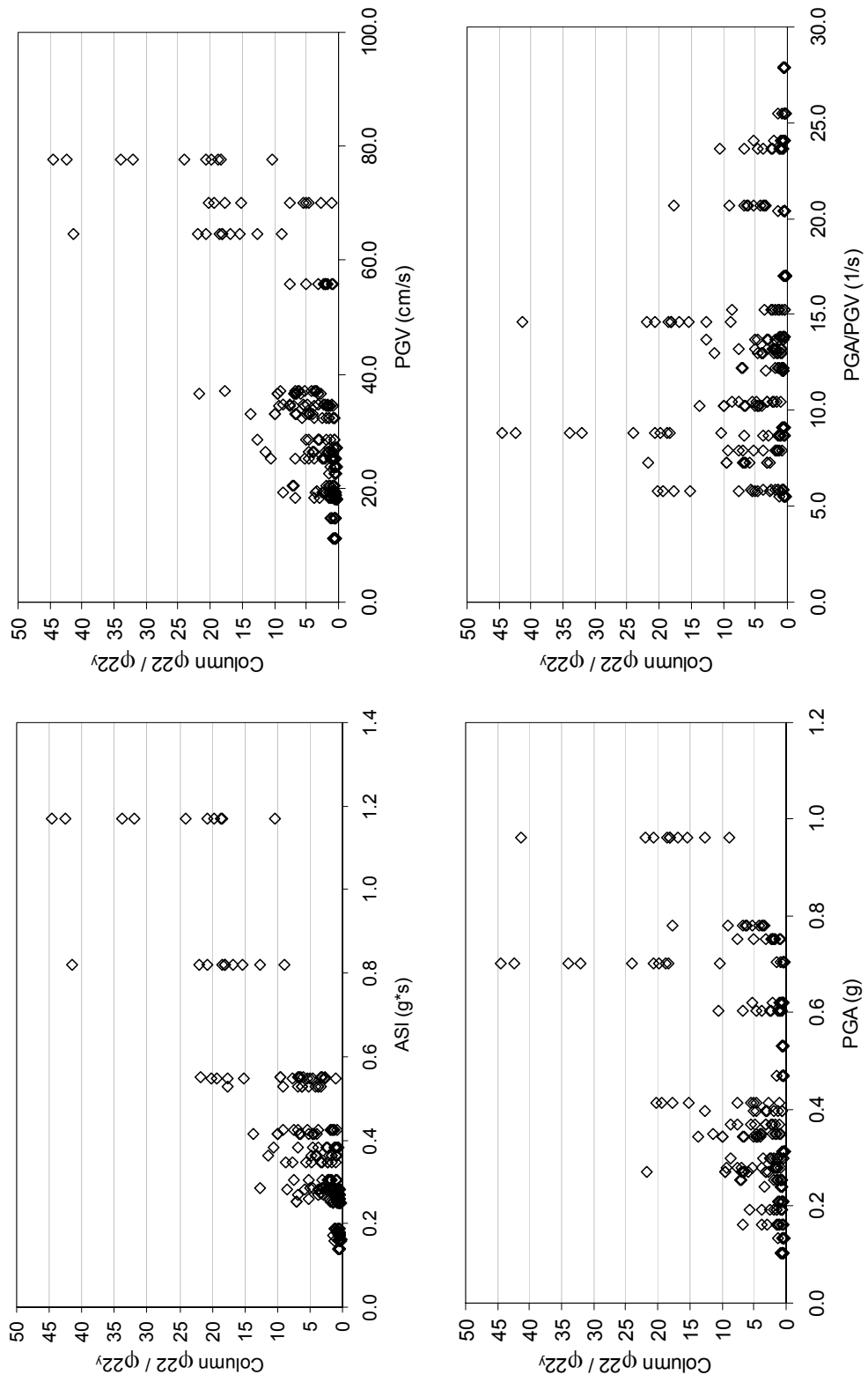Figure A.16 Normalized column shear-3 demand for MS_SC_SL30

Figure A.17 Normalized column curvature-22 demand for MS_SC_SL30

Figure A.18 Normalized column curvature-33 demand for MS_SC_SL30

Figure A.19 Normalized cap beam shear-3 demand for MS_SC_SL30

Figure A.20 Normalized cap beam curvature-22 demand for MS_SC_SL30

226

Figure A.21 Normalized superstructure longitudinal displacement demand for MS_SC_SL30

227

Figure A.22 Normalized column shear-2 demand for MS_SC_SG30

228

Figure A.23 Normalized column shear-3 demand for MS_SC_SG30

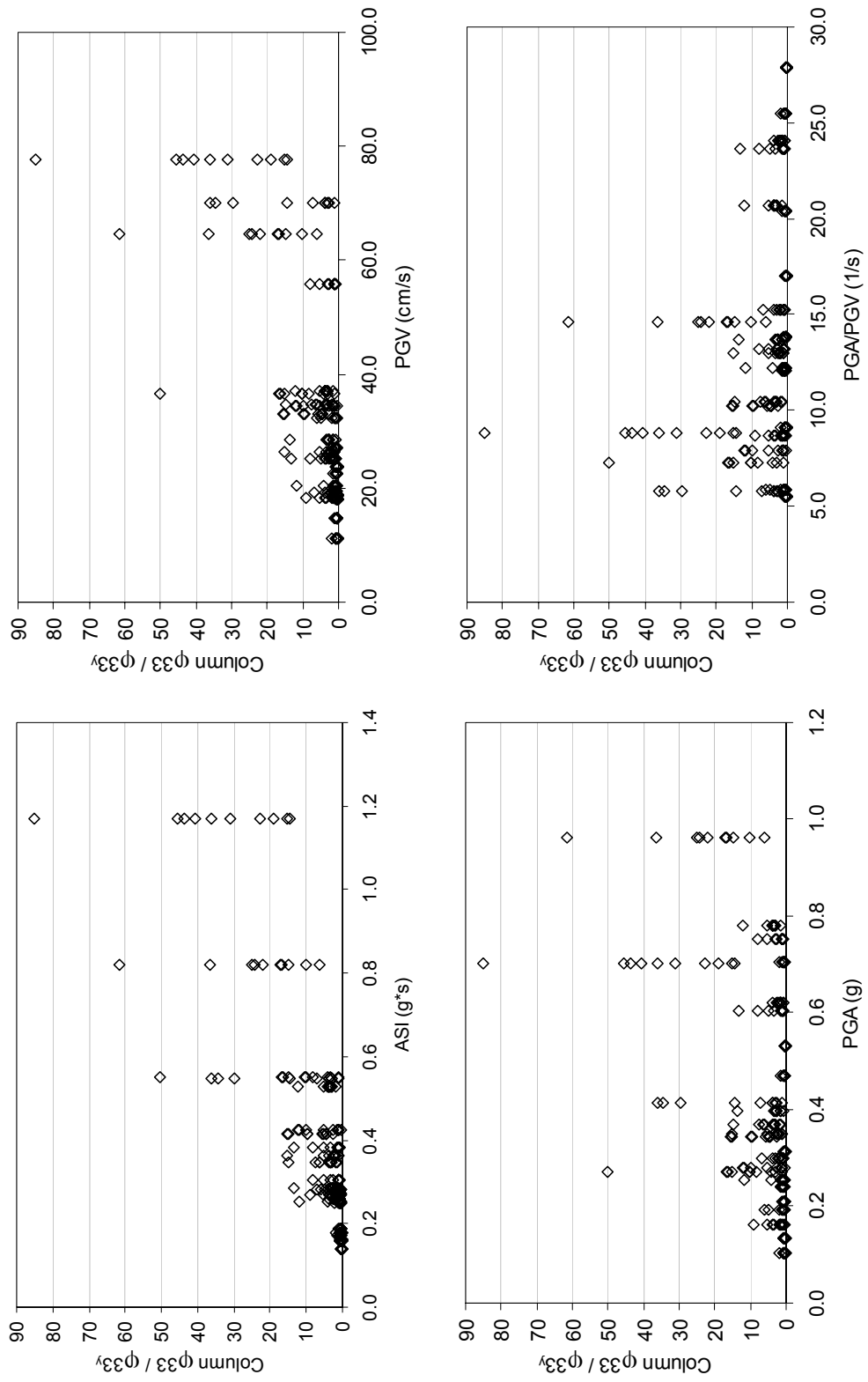Figure A.24 Normalized column curvature-22 demand for MS_SC_SG30

230

Figure A.25 Normalized column curvature-33 demand for MS_SC_SG30
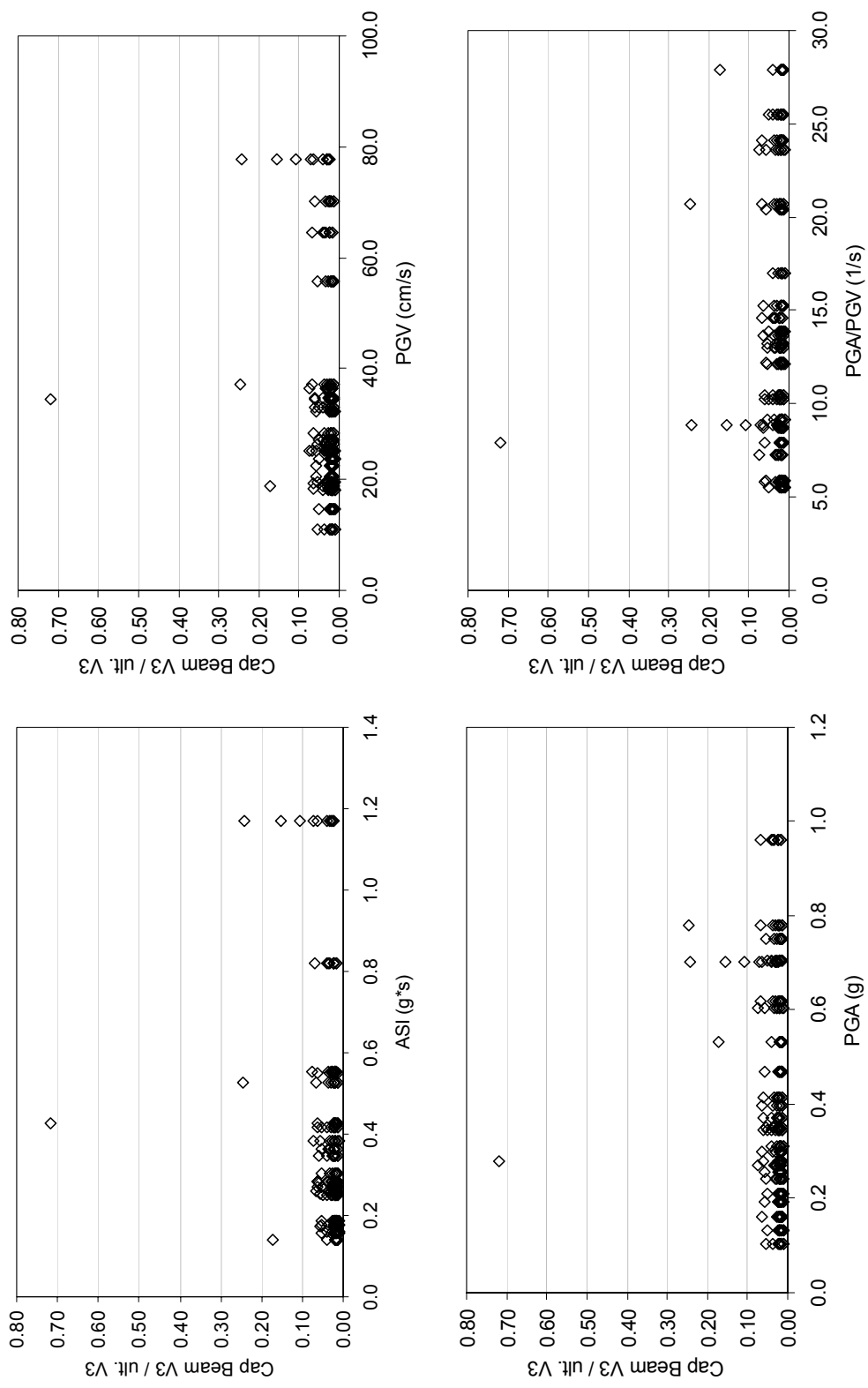
231

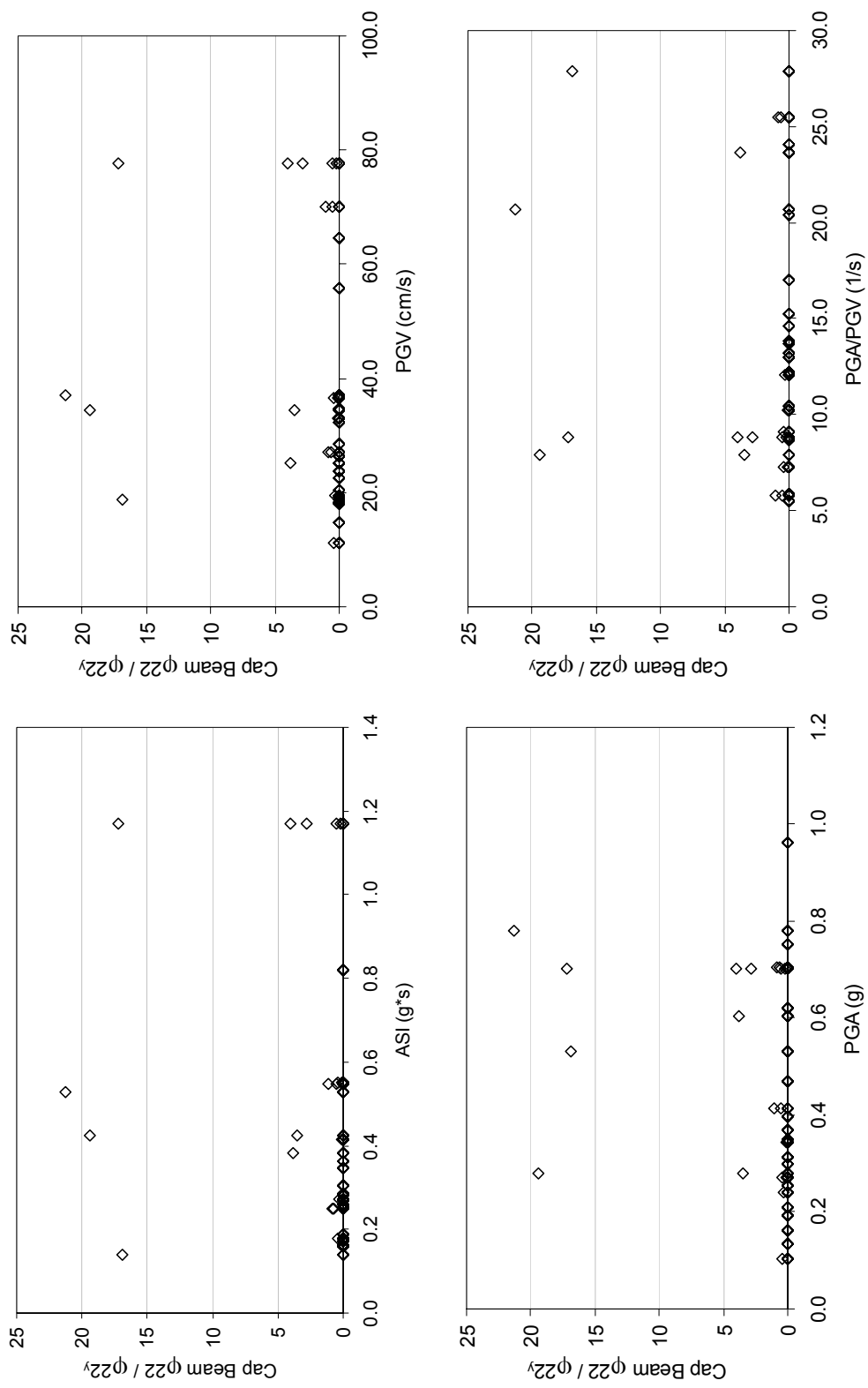Figure A.26 Normalized cap beam shear-3 demand for MS_SC_SG30

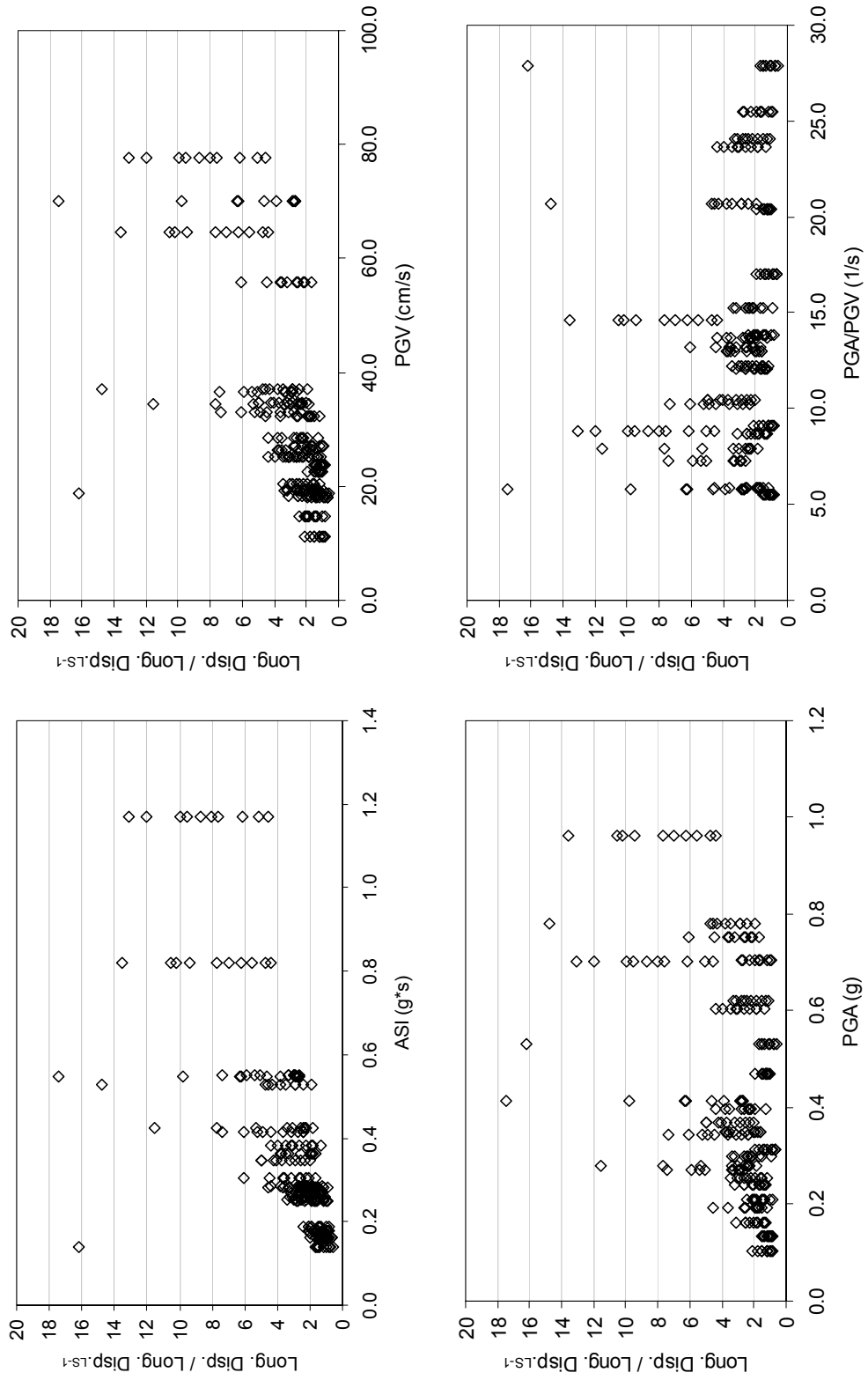Figure A.27 Normalized cap beam curvature-22 demand for MS_SC_SG30

Figure A.28 Normalized superstructure longitudinal displacement demand for MS_SC_SG30

CURRICULUM VITAE

PERSONAL INFORMATION

Surname, Name: Avşar, Özgür
Nationality: Turkish (TC)
Date and Place of Birth: 10.10.1977, Erzurum
Marital Status: Married
Phone: +90 (312) 287 2680/1545
Fax: +90 (312) 287 8951
Email: ozgur.avsar@afet.gov.tr

EDUCATION

2003-2009   Ph.D., Civil Engineering, METU

2001-2003   MS, Structural Engineering, Technical University Hamburg-Harburg

1996-2001   BS, Civil Engineering, METU

1993-1996   Eskişehir Fatih Science School

WORK EXPERIENCE

2008-2009   Civil Engineer, General Directorate of Disaster Affairs, Earthquake Research Department

2005-2008   Research Assistant, Department of Civil Engineering, METU

2003-2004   Design Engineer, Mitaş Madeni İnşaat A.Ş.

PUBLICATIONS

1. Caner A., Yanmaz A. M., Yakut A., **Avsar O.** and Yilmaz T., "Service Life Assessment of Existing Highway Bridges with No Planned Regular Inspections", *ASCE Journal of Performance of Constructed Facilities*, Vol. 22, No. 2, pp. 108-114, 2008.

2. **Avşar Ö.**, Kuran F., Bal İ.E. and Kocaman C., "Deprem Yönetmeliğindeki Doğrusal Elastik Olmayan Hesap Yöntemleri için Tanımlanan Betonarme Elemanların Kesit Birim Şekil Değiştirmelerinin İrdelenmesi", Sakarya International Symposium of Earthquake Engineering, "The Learning Outcomes of Marmara Earthquake in the First Decade", October 2009, Sakarya. (abstract accepted)

3. **Avsar O.**, Caner A. and Yakut A., "Effect of Cap Beam to Column Inertia Ratio on Transverse Seismic Response of Multi Column Bridge Bents", The 14th World Conference on Earthquake Engineering, Paper No. 06-0024, October 2008, Beijing.

4. **Avsar O.**, Yakut A. and Gulkan P., "Influence of Seismic Isolation Level on a Building Response", The 14th World Conference on Earthquake Engineering, Paper No. S15-009, October 2008, Beijing.

5. **Avsar O.**, Bayhan B. and Yakut A., "Section Based Determination of Effective Rigidities for RC Beams and Columns", The 8th Pasific Conference on Earthquake Engineering, Paper No. 37, December 2007, Singapore.

6. Caner A., Yanmaz A. M., Yakut A., Yıldırım O., **Avşar Ö.** ve Yılmaz T., "Çanakkale-Bursa Arasındaki Mevcut Köprülerin Ekonomik Ömürlerinin İstatiksel Olarak Hesaplanması", 1. Köprü ve Viyadükler Sempozyumu , Kasım 2007, Antalya, Türkiye.

7. **Avsar O.**, Yakut A., Sevgili G., and Caner A., "Preliminary Seismic Evaluation of Highway Bridges", 7th International Conference on Short&Meduim Span Bridges, RE-021, August 2006, Montreal, Canada.

8. Yakut A. ve **Avşar Ö.**, "Türkiyedeki Standart Karayolu Köprülerinin Sismik Performans Değerlendirilmesi ve Hasar Görebilirliklerinin Belirlenmesi", BAP No. 2007-03-03-02 Temmuz 2008, ODTÜ Ankara.

9. **Avşar Ö.**, "Determination of Flutter Derivatives from Free Vibration Test Results", Master Thesis, Technical University Hamburg-Harburg, Hamburg, Germany, 2003.